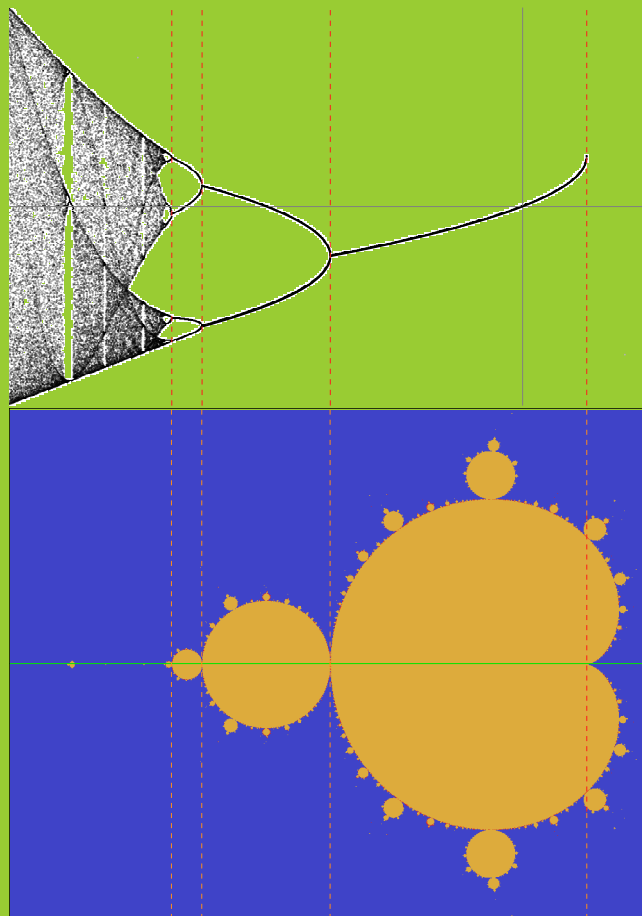


# Difference Equations and Fractals



Hans Montanus  
Ron Westdijk

Difference Equations  
and  
Fractals

Hans Montanus

Ron Westdijk



# Preface

Differential equations form a very large subject of mathematics. For many ordinary differential equations and some partial differential equations there exist methods to find solutions. The discrete counterparts of differential equations are difference equations. Difference equations are recurrence relations. Solutions can be found for simple linear difference equations. For non-linear difference equations solutions can not be found in general. However one can investigate the stability properties of fixed points and periodic limit cycles in order to gain insight in the dynamics. The latter can give rise to bifurcations. For a stable periodic limit cycle the orbit does not diverge to infinity. There also exists orbits which do not diverge to infinity and which are not periodic. Such orbits are chaotic and often attracted to a strange attractor. Whether or not an orbit diverges to infinity depends on its starting values and on the values of the constants in the difference equations. Investigation of dependency of orbits on starting values leads to basins of attraction and the investigation of dependency of orbits on constants of the difference equations leads to Lyapunov images. In these images fractals can occur. Within this brief overview we already meet terms as difference equations, recurrence relations, orbits, chaotic dynamics, periodic limit cycles, fixed points, bifurcations, basins of attraction, Lyapunov images, fractals, etc. Moreover, a fixed point can be a node, a saddle, a spiral or a center dependent on its stability behaviour. So, if, for example, somebody with a technical background wants to learn something about dynamics of non-linear difference equations or, as another example, a high school student wants to write a practical assignment on fractals, they are forced to study the whole area including all kinds of terms which may be new to them.

The present book is intended to be a simple and informal introduction to dynamical systems and properties as fixed points, bifurcations, Feigenbaum constants, chaotic orbits, Julia sets, the Mandelbrot set and Misiurewicz points. With simple is meant that a high school level of mathematics (together with the willingness to study) suffices to understand the contents. With informal is meant that the book is not organised as an enumeration of theorems and proofs. Instead it rather is a random walk through famous dynamical systems. In general, proofs are omitted, formal language is avoided and citations are restricted to a few occasions.

The present book has just been written for educational purposes. It is intended for high school students with talent for mathematics and for readers with (a little more than) a high school level mathematical background.

may 2020, Hans Montanus, Ron Westdijk

ISBN 978-90-829889-2-5

© 2020, Hans Montanus and Ron Westdijk

# Contents

<b>1 Stability</b>	<b>5</b>
1.1 Stability of one dimensional systems	5
1.2 Mathematical terms	11
1.3 Stability analysis for two dimensional systems	12
1.4 One dimensional, first order, linear difference equations	14
1.5 One dimensional, second order, linear difference equations	15
<b>2 One dimensional difference equations</b>	<b>19</b>
2.1 Introduction	19
2.2 Logistic equation	22
2.3 Feigenbaum constants	25
2.4 Chaos	27
2.5 Starting points	29
2.6 Other difference equations	30
<b>3 Two dimensional difference equations</b>	<b>35</b>
3.1 Lotka-Volterra model	35
3.2 Modified Lotka-Volterra model	40
3.3 Hénon map	44
3.4 Lyapunov exponents for two dimensional maps	45
3.5 Orbits for the Hénon map	55
3.6 Single fixed points of the Hénon map	57
3.7 Period 2 limit cycles of the Hénon map	59
3.8 Three dimensional plots for the Hénon map	61
3.9 Hénon map for $b \approx 1$	63
<b>4 Lyapunov images.</b>	<b>67</b>
4.1 Images of dynamical systems	67
4.2 Markus-Lyapunov images	68
4.3 Lyapunov image for the Hénon map	75

4.4 Basins of attraction for the Hénon map . . . . .	77
4.5 The $z^2 + c$ map . . . . .	81
4.6 Analytical solutions for the $z^2 + c$ map . . . . .	87
4.7 Number of period $n$ solutions of the $z^2 + c$ map . . . . .	90
4.8 Mandelbrot set and Fibonacci . . . . .	92
<b>5 Fractals</b>	<b>93</b>
5.1 Koch snowflake . . . . .	93
5.2 Designing fractals . . . . .	94
5.3 Two dimensional fractals . . . . .	96
5.4 Fractal dimension . . . . .	103
5.5 Julia fractals . . . . .	104
5.6 Mandelbrot fractal . . . . .	113
<b>6 Misiurewicz points</b>	<b>115</b>
6.1 Polynomials for $x_0 = 1/2$ . . . . .	115
6.2 Points of intersection . . . . .	118
6.3 Misiurewicz points . . . . .	120
6.4 Misiurewicz points for the $z^2 + c$ map . . . . .	122
<b>A A series solution</b>	<b>127</b>
<b>B A binomial identity</b>	<b>131</b>
<b>C Another binomial identity</b>	<b>135</b>
<b>D A Hénon eigenvalue inequality</b>	<b>139</b>
<b>Bibliography</b>	<b>140</b>

# Chapter 1

## Stability

### 1.1 Stability of one dimensional systems

The modelling of a process (biological, chemical, physical, economical or whatever) often leads to a differential equation or to a difference equation. Although our goal is to consider difference equations, we will occasionally also consider differential equations for comparison. For instance, the absolute growth of waterlilies in a pond will initially be proportional with the number of waterlilies. The growth will be damped when the pond becomes full of waterlilies. This can be casted in a differential equation:

$$\frac{dw}{dt} = \alpha w - \beta w^2, \quad (1.1)$$

where  $w$  is the number of waterlilies, where time  $t$  is the evolution parameter and where  $\alpha$  and  $\beta$  are constants. Since  $w$  is a function of  $t$  we should actually write  $w(t)$  instead of  $w$ . However, we just write  $w$  and keep in mind it actually is  $w(t)$ . In reality the number of waterlilies will be counted in the summer and not in the winter. A biologist may argue that the evolution of waterlilies has to be considered from year to year. This can be casted in a difference equation:

$$w_{n+1} = aw_n - bw_n^2, \quad (1.2)$$

where  $w_n$  is the number of waterlilies in year  $n$  and  $w_{n+1}$  is the number of waterlilies one year later. Here  $a$  and  $b$  are the constants. We will use greek symbols for constants in differential equations and roman symbols for constants in difference equations.

In the foregoing equations the right hand side is a function of solely  $w$  respectively  $w_n$ . That is,  $\dot{w} = f(w)$  where the dot represents the derivative  $d/dt$  and where  $f(w) = \alpha w - \beta w^2$ , and  $w_{n+1} = f(w_n)$  where  $f(w_n) = aw_n - bw_n^2$ . Differential equations such as  $\dot{w} = \alpha w - \beta w^2 - 2e^{-t}$  and difference equations such as  $w_{n+1} = aw_n - bw_n^2 + 3t$  can not be written as  $\dot{w} = f(w)$  or  $w_{n+1} = f(w_n)$ .

For a general quantity  $x$  we consider hereafter only differential equations and difference equations of the type  $\dot{x} = f(x)$  respectively  $x_{n+1} = f(x_n)$ .

We start with the stability analysis for a differential equation of the type  $\dot{x} = f(x)$ . A point of equilibrium is a point where the quantity  $x$  does not change in time:  $\dot{x}(t) = 0$ . The equilibrium points  $x_*$  therefore follow from  $f(x_*) = 0$ . For  $x$  close to  $x_*$ , that is, for  $x = x_* + \delta$  with  $\delta$  small, we have

$$\dot{x} = f(x) \quad \rightarrow \quad \dot{\delta} = f(x_* + \delta) \approx f(x_*) + \left. \frac{\partial f(x)}{\partial x} \right|_{x_*} \delta \quad \rightarrow \quad \dot{\delta} = f'(x_*)\delta, \quad (1.3)$$

where  $f'(x_*)$  is the derivative of  $f$  with respect to  $x$  evaluated at  $x_*$ . Thus  $f'(x_*) = \left. \frac{\partial f(x)}{\partial x} \right|_{x_*}$ . From the equation above for  $\delta$  it follows that an equilibrium point is stable if  $f'(x_*) < 0$  and unstable if  $f'(x_*) > 0$ .

We give an example by means of the following differential equation:

$$\dot{x} = \alpha x, \quad (1.4)$$

where  $\alpha \neq 0$  is a constant. The equilibrium point is  $x_* = 0$ . Since  $f'(x) = \alpha$  the equilibrium point is stable if  $\alpha < 0$  and unstable if  $\alpha > 0$ .

Writing the initial condition as  $x(0) = x_0$  we obtain by means of integration the solution

$$x(t) = x_0 e^{\alpha t}. \quad (1.5)$$

If  $\alpha > 0$  then  $|x(t)|$  increases exponentially for increasing  $t$ . If  $\alpha < 0$  then  $|x(t)|$  decreases exponentially for increasing  $t$ . Alternatively,  $\lim_{t \rightarrow -\infty} x(t) = 0$  if  $\alpha > 0$  and  $\lim_{t \rightarrow \infty} x(t) = 0$  if  $\alpha < 0$ . Indeed for  $\alpha > 0$  the point  $x(-\infty) = 0$  is an unstable equilibrium point (a source), the larger  $\alpha$  the faster the divergence from the source. For  $\alpha < 0$  the point  $x(\infty) = 0$  is a stable equilibrium point (a sink), the larger  $-\alpha$  the faster the convergence towards the sink. The situation is schematically illustrated in figure [1.1](#).

Suppose we wish to integrate equation [\(1.4\)](#) numerically. According to the *Euler method* we write  $x$  as  $x_n$  and  $\dot{x}$  as  $(x_{n+1} - x_n)/\Delta t$ . The result is a difference equation:

$$x_{n+1} = x_n + \alpha \cdot \Delta t \cdot x_n = (1 + a)x_n, \quad (1.6)$$

where  $a = \alpha \cdot \Delta t$ . Starting with  $x_0$  we then successively obtain  $x_1 = (1+a)x_0$ ,  $x_2 = (1+a)x_1 = (1+a)^2 x_0$ , ...,  $x_n = (1+a)^n x_0$ . Stability requires  $-\infty < \lim_{n \rightarrow \infty} (1+a)^n < \infty$ , which is, for  $a \neq 0$ , satisfied if  $-1 \leq 1+a < 1$  or  $-2 \leq a < 0$ . That is, the stability region has shrunk from  $(-\infty, 0)$  to  $(-2, 0)$  with respect to the continuous differential equation, see figure [1.2](#).

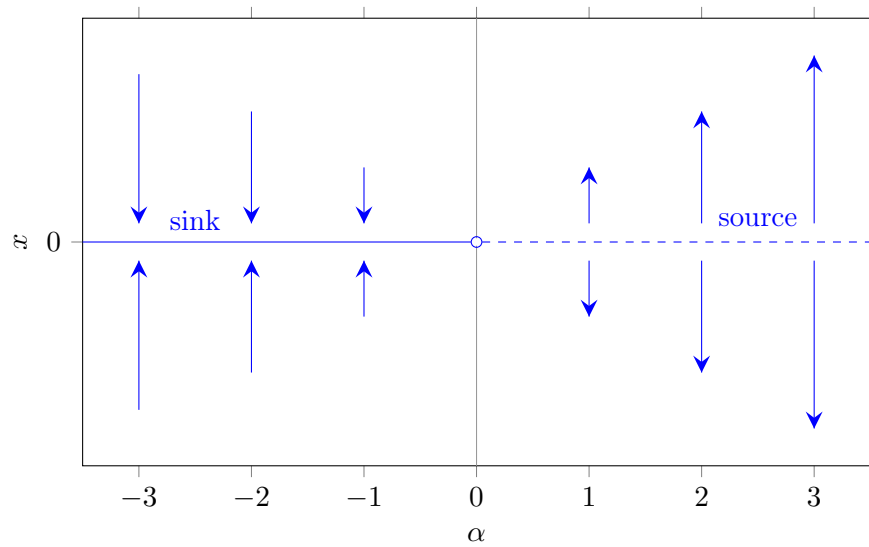


Figure 1.1: Sink and source structure of  $\dot{x} = \alpha x$ .

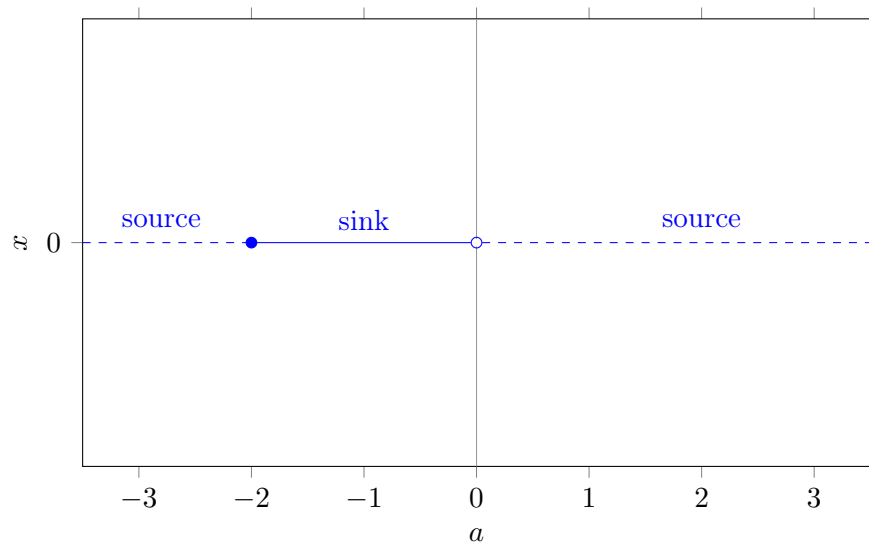


Figure 1.2: Sink and source structure of  $x_{n+1} = (1+a)x_n$ .

As another example we consider the differential equation

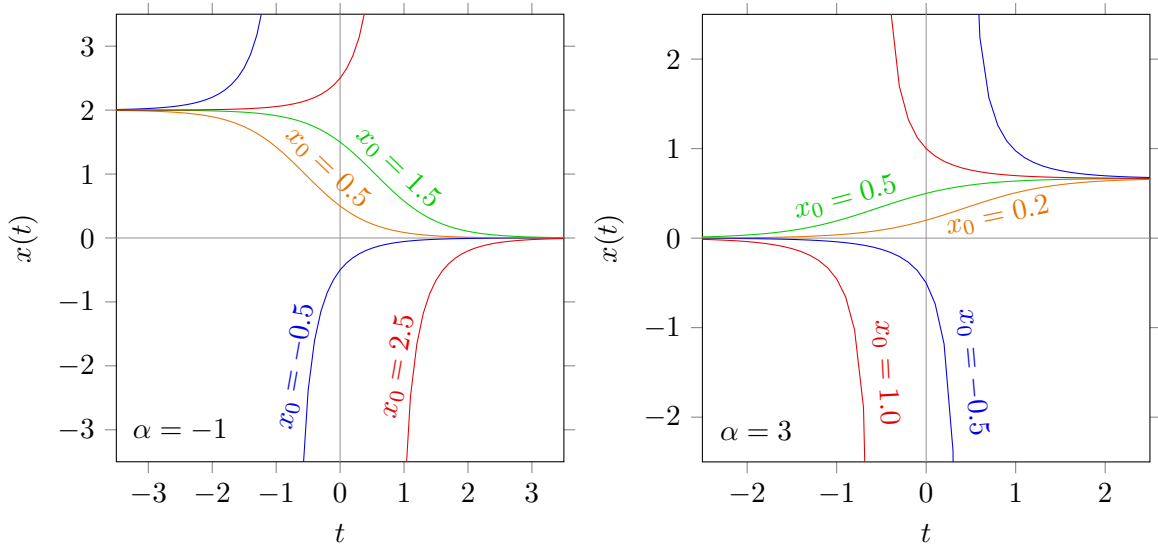
$$\dot{x} = (\alpha - 1)x - \alpha x^2, \quad (1.7)$$

where  $\alpha \neq 0$  is a constant. The differential equation is non-linear because of the  $x^2$ . The equilibrium points are  $x_* = 1 - 1/\alpha$  and  $x_{**} = 0$ . Since  $f'(x) = \alpha - 1 - 2\alpha x$  we have  $f'(x_*) = 1 - \alpha$ . So, the equilibrium point  $x_* = 1 - 1/\alpha$  is stable if  $\alpha > 1$  and unstable if  $\alpha < 1$ . Since  $f'(x_{**}) = \alpha - 1$  the equilibrium point  $x_{**} = 0$  is stable if  $\alpha < 1$  and unstable if  $\alpha > 1$ .

Writing the initial condition as  $x(0) = x_0$ , the analytical solution reads

$$x(t) = \frac{(1 - 1/\alpha)x_0}{x_0 + (1 - 1/\alpha - x_0)e^{-(\alpha-1)t}}. \quad (1.8)$$

The solution is known as the logistic function. If  $\alpha < 1$  then  $\lim_{t \rightarrow -\infty} x(t) = 1 - 1/\alpha$  and  $\lim_{t \rightarrow \infty} x(t) = 0$ . If  $\alpha = 1$  then  $x(t) = x_0$ . If  $\alpha > 1$  then  $\lim_{t \rightarrow -\infty} x(t) = 0$  and  $\lim_{t \rightarrow \infty} x(t) = 1 - 1/\alpha$ . For various  $x_0$  values the evolution of  $x(t)$  is shown in the next figure for  $\alpha = -1$  (left panel) and  $\alpha = 3$  (right panel).

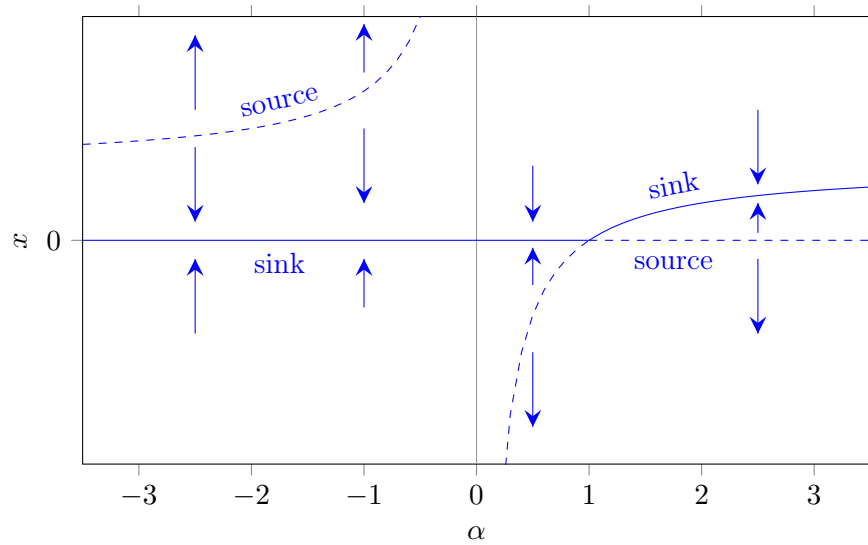


For  $\alpha < 1$  the curves  $x(t)$  depart from  $1 - 1/\alpha$  and arrive at 0, while for  $\alpha > 1$  the curves  $x(t)$  depart from 0 and arrive at  $1 - 1/\alpha$ . The curves have an *S*-shape (Sigmoid curve) if  $x_0$  is between 0 and  $1 - 1/\alpha$ , the curves are horizontal lines if  $x_0 = 0$  or  $x_0 = 1 - 1/\alpha$  and the curves have a discontinuity otherwise. The sink and source structure is schematically illustrated in the next figure.

Suppose we wish to integrate equation (1.7) numerically. The Euler method then leads to the following discrete difference equation:

$$x_{n+1} = x_n + (\alpha - 1)\Delta t \cdot x_n - \alpha \cdot \Delta t \cdot x_n^2. \quad (1.9)$$





For the choice  $\Delta t = 1$  and writing  $\alpha$  as  $a$  we have:

$$x_{n+1} = ax_n - ax_n^2. \quad (1.10)$$

The latter difference equation is known as the logistic equation. The equilibrium points or fixed points  $L$  follow from  $L = aL - aL^2$ . It follows directly that  $L = 0$  or  $L = 1 - 1/a$ . The curves of the fixed points as a function of  $a$  are the same as in the previous figure.

The stability analysis for the fixed points of a difference equation is somewhat different than for differential equation. For a first order difference equation  $x_{n+1} = f(x_n)$  a fixed point  $L$  is a solution of the equation

$$L = f(L). \quad (1.11)$$

A fixed point  $L$  is stable if

$$-1 < \left. \frac{\partial f}{\partial x} \right|_L < 1. \quad (1.12)$$

It can be seen from a first order Taylor expansion of  $f(x_n)$  in the neighborhood of  $L$ :

$$f(x_n) \approx f(L) + \left. \frac{\partial f}{\partial x_n} \right|_L (x_n - L) \quad (1.13)$$

or

$$f(x_n) - f(L) \approx \left. \frac{\partial f}{\partial x_n} \right|_L (x_n - L). \quad (1.14)$$

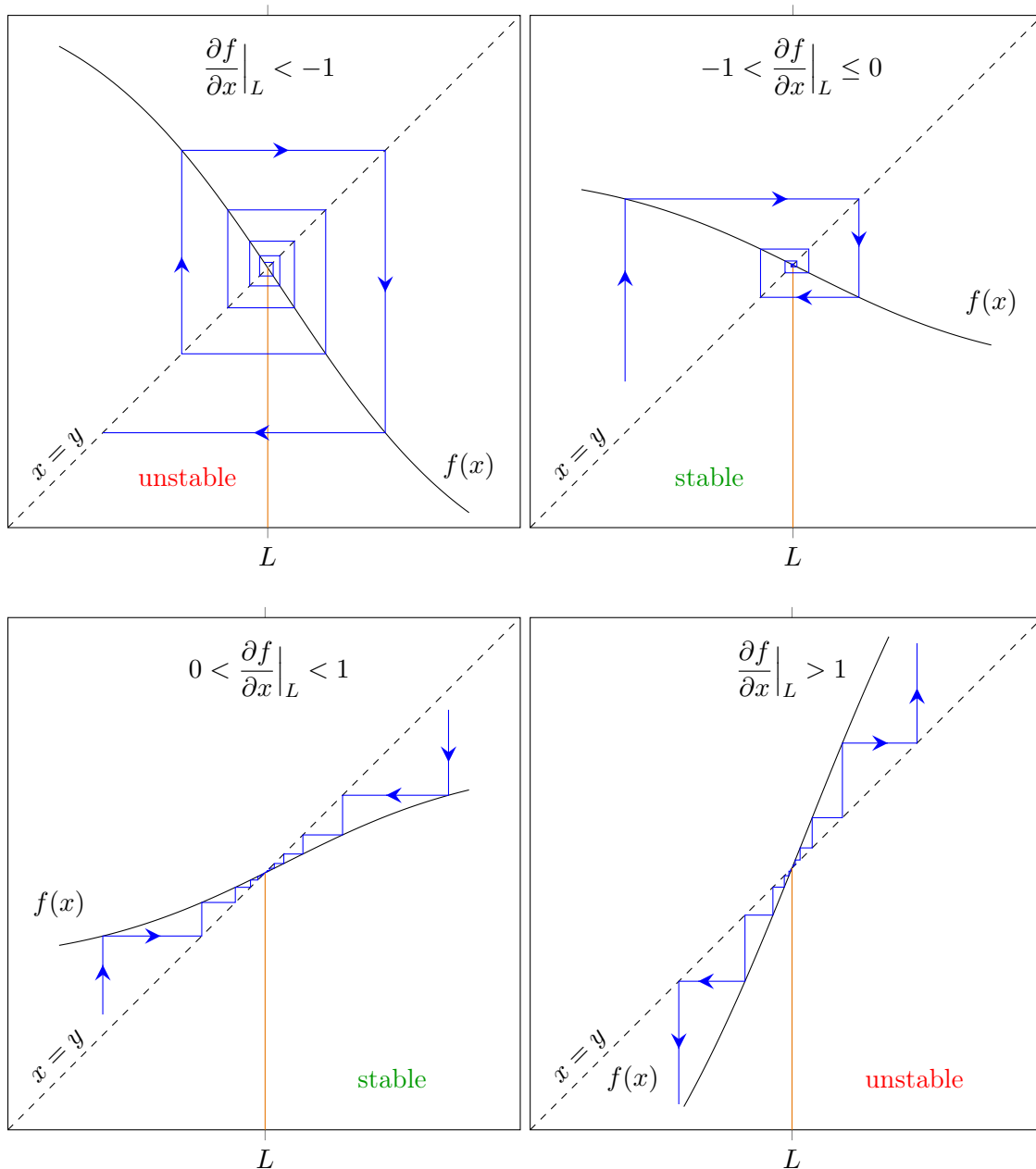
Since  $f(x_n) = x_{n+1}$  and  $f(L) = L$  we have

$$x_{n+1} - L \approx \left. \frac{\partial f}{\partial x_n} \right|_L (x_n - L). \quad (1.15)$$

The stability condition  $|x_{n+1} - L| < |x_n - L|$  is satisfied if

$$\left| \frac{\partial f}{\partial x} \Big|_L \right| < 1. \quad (1.16)$$

The latter will be briefly written as  $|f'(L)| < 1$ . The following diagrams illustrate the stability condition.



A stable fixed point  $L$  for which  $L = f(L)$  can be regarded as a limit cycle with period 1. A period 2 limit cycle occurs if both the conditions  $L = f(f(L))$  and  $-1 < \frac{\partial f(f(x))}{\partial x} \Big|_L < 1$

are satisfied. A period 3 limit cycle occurs if the conditions  $L = f(f(f(L)))$  and  $-1 < \left. \frac{\partial f(f(f(x)))}{\partial x} \right|_L < 1$  are both satisfied, and so on.

For the logistic equation  $x_{n+1} = ax_n - ax_n^2$  we have  $f'(L) = a - 2aL$ . For  $L = 0$  this is  $f'(0) = a$  and for  $L = 1 - 1/a$  this is  $f'(1 - 1/a) = 2 - a$ . So,  $L = 0$  is stable if  $-1 < a < 1$  and  $L = 1 - 1/a$  if  $1 < a < 3$ . What happens for  $L = 0$  at  $a = -1$  and for  $L = 1 - 1/a$  at  $a = 3$  is that two fixed points come into existence, a *bifurcation*. For other values of  $a$  new bifurcations can occur (multiple fixed points) or the dynamics can become chaotic (no stable fixed points at all). Bifurcations and chaos will be considered in chapter 2.

## 1.2 Mathematical terms

We already met some terms: differential equation, difference equation, non-linear, first order. It may be clarifying to make a list of terms with small explanations.

- For a differential equation the evolution is **continuous**. For example, the variable is a function of time  $t$ :  $x(t)$ .
- For a difference equation the evolution is evaluated only for fixed increments. The number of increments is counted by an integer  $n$ :  $x_n$ . A difference equation is also called a **discrete equation** and a **recursion equation**.
- A differential equation and a difference equation is **one dimensional** if there is one variable,  $x$  for instance.
- A differential equation and a difference equation is **two dimensional** if there are two variables,  $x$  and  $y$  for instance.
- A differential equation and a difference equation is **linear** if it contains only linear terms of the variables, such as  $x$ ,  $y$ , etc.
- A differential equation and a difference equation is **non-linear** if it contains non-linear terms of the variables, such as  $x^2$ ,  $xy$ ,  $y^3$ , etc.
- A differential equation is **first order** if it contains only the first derivative,  $\dot{x}$ . It is  **$n$ -th order** if there is a  $n$ -th derivative in the equation. For example,  $\ddot{x} + \alpha\dot{x} + \beta = 0$  is second order.
- A difference equation is **first order** if it contains only the maximum difference in subscripts is only 1, as for  $x_{n+1} = ax_n + b$ . It is  **$n$ -th order** if the maximum difference in subscripts is  $n$ . For example,  $x_{n+1} = ax_n + bx_{n-1}$  is second order.

### 1.3 Stability analysis for two dimensional systems

In the previous section we considered stability analyses for one dimensional systems. An example of a (non-linear, first order) two dimensional system of differential equations is

$$\begin{aligned}\dot{v} &= \alpha v - \beta v^2 - \gamma vw \\ \dot{w} &= \rho w - \kappa w^2 + \mu wv,\end{aligned}\tag{1.17}$$

where the greek symbols are constants. It will be written as

$$\begin{aligned}\dot{v} &= f(v, w) \\ \dot{w} &= g(v, w).\end{aligned}\tag{1.18}$$

The equilibrium point is the point where both  $\dot{v} = 0$  and  $\dot{w} = 0$ . Let  $(v_*, w_*)$  be a point of equilibrium, then for  $v = v_* + \delta$  and  $w = w_* + \epsilon$  with  $\delta$  and  $\epsilon$  small the system becomes

$$\begin{aligned}\dot{\delta} &\approx \left. \frac{\partial f(v, w)}{\partial v} \right|_{(v_*, w_*)} \delta + \left. \frac{\partial f(v, w)}{\partial w} \right|_{(v_*, w_*)} \epsilon \\ \dot{\epsilon} &\approx \left. \frac{\partial g(v, w)}{\partial v} \right|_{(v_*, w_*)} \delta + \left. \frac{\partial g(v, w)}{\partial w} \right|_{(v_*, w_*)} \epsilon.\end{aligned}\tag{1.19}$$

In matrix notation this is

$$\begin{pmatrix} \dot{\delta} \\ \dot{\epsilon} \end{pmatrix} \approx \begin{pmatrix} \frac{\partial f}{\partial v} & \frac{\partial f}{\partial w} \\ \frac{\partial g}{\partial v} & \frac{\partial g}{\partial w} \end{pmatrix} \Big|_{(v_*, w_*)} \cdot \begin{pmatrix} \delta \\ \epsilon \end{pmatrix}\tag{1.20}$$

The matrix with the derivatives is the *Jacobian*. The Jacobian evaluated at  $(v_*, w_*)$  will be denoted as  $J(v_*, w_*)$ . Thus

$$\begin{pmatrix} \dot{\delta} \\ \dot{\epsilon} \end{pmatrix} \approx J(v_*, w_*) \cdot \begin{pmatrix} \delta \\ \epsilon \end{pmatrix}\tag{1.21}$$

The stability of an equilibrium point  $(v_*, w_*)$  depends on the eigenvalues of  $J(v_*, w_*)$ . The eigenvalues follow from

$$\begin{vmatrix} J_{11} - \lambda & J_{12} \\ J_{21} & J_{22} - \lambda \end{vmatrix} = 0 \quad \rightarrow \quad \lambda^2 - (J_{11} + J_{22})\lambda + J_{11}J_{22} - J_{12}J_{21} = 0.\tag{1.22}$$

The equation can be written shortly as

$$\lambda^2 - T\lambda + D = 0,\tag{1.23}$$

where  $T$  is the trace of the Jacobian (the trace is the sum of the elements of the main diagonal) and where  $D$  is the determinant of the Jacobian. The solutions are

$$\lambda_{\pm} = \frac{T \pm \sqrt{T^2 - 4D}}{2}.\tag{1.24}$$

An equilibrium point is a

- **stable node** or **sink** if both eigenvalues are real and negative.
- **unstable node** or **source** if both eigenvalues are real and positive.
- **saddle** if both eigenvalues are real and have opposite sign.
- **stable focus** or **spiral sink** if both eigenvalues have an imaginary part and a negative real part.
- **unstable focus** or **spiral source** if both eigenvalues have an imaginary part and a positive real part.
- **center** if both eigenvalues are pure imaginary.

An example of a (first order, non-linear) two dimensional system of difference equations is

$$\begin{aligned} v_{n+1} &= av_n - bv_n^2 - cv_nw_n \\ w_{n+1} &= rw_n - kw_n^2 + mw_nv_n, \end{aligned} \quad (1.25)$$

where the roman symbols without subscripts are constants. In general it is

$$\begin{aligned} v_{n+1} &= f(v_n, w_n) \\ w_{n+1} &= g(v_n, w_n). \end{aligned} \quad (1.26)$$

The equilibrium point is the point where both  $v_{n+1} = v_n$  and  $w_{n+1} = w_n$ . Let  $(L, K)$  be a point of equilibrium:

$$\begin{aligned} L &= f(L, K) \\ K &= g(L, K). \end{aligned} \quad (1.27)$$

A first order Taylor expansion with respect to  $(L, K)$  gives

$$\begin{aligned} f(v_n, w_n) &= f(L, K) + \left. \frac{\partial f}{\partial v} \right|_{(L,K)} (v_n - L) + \left. \frac{\partial f}{\partial w} \right|_{(L,K)} (w_n - K) \\ g(v_n, w_n) &= g(L, K) + \left. \frac{\partial g}{\partial v} \right|_{(L,K)} (v_n - L) + \left. \frac{\partial g}{\partial w} \right|_{(L,K)} (w_n - K). \end{aligned} \quad (1.28)$$

Substituting  $f(v_n, w_n) = v_{n+1}$ ,  $f(L, K) = L$ ,  $g(v_n, w_n) = w_{n+1}$  and  $g(L, K) = K$  we have

$$\begin{aligned} v_{n+1} - L &= \left. \frac{\partial f}{\partial v} \right|_{(L,K)} (v_n - L) + \left. \frac{\partial f}{\partial w} \right|_{(L,K)} (w_n - K) \\ w_{n+1} - K &= \left. \frac{\partial g}{\partial v} \right|_{(L,K)} (v_n - L) + \left. \frac{\partial g}{\partial w} \right|_{(L,K)} (w_n - K). \end{aligned} \quad (1.29)$$

In matrix notation this is

$$\begin{pmatrix} v_{n+1} - L \\ w_{n+1} - K \end{pmatrix} \approx \left. \begin{pmatrix} \frac{\partial f}{\partial v} & \frac{\partial f}{\partial w} \\ \frac{\partial g}{\partial v} & \frac{\partial g}{\partial w} \end{pmatrix} \right|_{(L,K)} \cdot \begin{pmatrix} v_n - L \\ w_n - K \end{pmatrix} \quad (1.30)$$

The Jacobian evaluated at  $(L, K)$  will be denoted as  $J(L, K)$ . Thus

$$\begin{pmatrix} v_{n+1} - L \\ w_{n+1} - K \end{pmatrix} \approx J(L, K) \cdot \begin{pmatrix} v_n - L \\ w_n - K \end{pmatrix} \quad (1.31)$$

The stability of an equilibrium point  $(L, K)$  depends on the eigenvalues of  $J(L, K)$ . For this the modulus of a complex eigenvalue is important. The modulus is the square root of the sum of the real part squared and the imaginary part squared, thus the modulus of  $x + iy$  is  $\sqrt{x^2 + y^2}$ . An equilibrium point is a

- **stable node** if both eigenvalues are real and both moduli smaller than 1.
- **unstable node** if both eigenvalues are real and both moduli larger than 1.
- **saddle** if both eigenvalues are real and just one modulus is smaller than 1.
- **stable focus or stable spiral point** if both eigenvalues have a non-zero imaginary part and a modulus smaller than 1.
- **unstable focus or unstable spiral point** if both eigenvalues have a non-zero imaginary part and a modulus larger than 1.
- **center** if both eigenvalues have a non-zero imaginary part and a modulus equal to 1.

The stability analysis and classification of equilibrium points can be extended to three and more dimensional systems, but that is beyond our scope.

## 1.4 One dimensional, first order, linear difference equations

A recursion formula of the type  $u_{n+1} = au_n + b$ , with  $a \neq 0$  and  $b$  constants, is a one dimensional, first order, linear difference equation. The equation (1.6) is an example.

The difference equation  $u_{n+1} = au_n + b$  has a fixed point  $L = \frac{b}{1-a}$  as follows from  $L = aL + b$ . The fixed point is stable if  $-1 < a < 1$ .

Starting with  $u_0$  we successively obtain

$$\begin{aligned} u_1 &= au_0 + b, \\ u_2 &= au_1 + b = a^2u_0 + b(1 + a), \\ u_3 &= au_2 + b = a^3u_0 + b(1 + a + a^2), \\ &\dots \\ u_n &= a^n u_0 + b(1 + a + a^2 + \dots + a^{n-1}) \quad . \end{aligned}$$

The latter is equal to  $u_n = a^n u_0 + b \frac{a^n - 1}{a - 1}$ . Hence, a direct equation for  $u_n$  is  $u_n = (u_0 - L)a^n + L$ , where  $L = \frac{b}{1-a}$ .

In case  $a = 1$  there is no equilibrium,  $u_n$  grows forever:  $u_n = u_0 + nb$ .

An alternative way is to substitute  $u_n = v_n + L$  where  $L = \frac{b}{1-a}$  is the fixed point. Then  $u_{n+1} = au_n + b$  is reduced to

$$v_{n+1} + L = a(v_n + L) + b \quad \rightarrow \quad v_{n+1} = av_n - L + aL + b \quad \rightarrow \quad v_{n+1} = av_n. \quad (1.32)$$

Hence,  $v_n = a^n v_0$  and thus  $u_n - L = a^n u_0 - a^n L$ . The latter also gives  $u_n = a^n u_0 + b \frac{a^n - 1}{a - 1}$ .

First order linear difference equations,  $u_{n+1} = au_n + b$ , have simple sum rules:

If  $a \neq 1$  there holds 
$$\sum_{k=0}^m u_k = \frac{a^{m+1} - 1}{a - 1} \left( u_0 - \frac{b}{1-a} \right) + \frac{(m+1)b}{1-a}.$$

If  $a = 1$  there holds 
$$\sum_{k=0}^m u_k = (m+1) \left( u_0 + \frac{1}{2}mb \right).$$

## 1.5 One dimensional, second order, linear difference equations

A recursion formula of the type  $u_{n+1} = au_n + bu_{n-1} + c$ , with  $a, b \neq 0$  and  $c$  constants is a one dimensional, second order, linear difference equation. As follows from  $L = aL + bL + c$  it has a fixed point  $L = \frac{c}{1-a-b}$ . Here it is advantageous to substitute  $u_n = v_n + L$  with  $L = \frac{c}{1-a-b}$ . Then the equation  $u_{n+1} = au_n + bu_{n-1} + c$  is reduced to

$$v_{n+1} = av_n + bv_{n-1}. \quad (1.33)$$

Starting with  $v_0$  and  $v_1$  we successively obtain

$$v_2 = av_1 + bv_0,$$

$$v_3 = av_2 + bv_1 = (a^2 + b)v_1 + abv_0,$$

$$v_4 = av_3 + bv_2 = (a^3 + 2ab)v_1 + (a^2 + b)bv_0,$$

etc. As shown in appendix A for arbitrary  $n \geq 2$  this is

$$v_n = v_1 \sum_{k=0}^{\lfloor n/2-1/2 \rfloor} \binom{n-1-k}{k} a^{n-1-2k} b^k + bv_0 \sum_{k=0}^{\lfloor n/2-1 \rfloor} \binom{n-2-k}{k} a^{n-2-2k} b^k. \quad (1.34)$$

When we substitute  $v_n = g^n$ , with  $g$  a constant, the equation (1.33) reduces to the *characteristic equation*:

$$g^2 - ag - b = 0. \quad (1.35)$$

It has two solutions:

$$g_+ = \frac{1}{2} \left( a + \sqrt{a^2 + 4b} \right) \quad , \quad g_- = \frac{1}{2} \left( a - \sqrt{a^2 + 4b} \right). \quad (1.36)$$

It is shown in appendix B that for  $a^2 + 4b \neq 0$  the equation (1.34) is identical to the equation

$$v_n = \frac{v_0 g_+ - v_1}{g_+ - g_-} g_-^n - \frac{v_0 g_- - v_1}{g_+ - g_-} g_+^n. \quad (1.37)$$

If  $a^2 + 4b = 0$  then  $g_+ = g_- = a/2$ . For this situation we will write both  $g_+$  and  $g_-$  as  $g$ . So,  $g = a/2$  and  $g^2 = a^2/4 = -b$ . It is shown in appendix C that for  $a^2 + 4b = 0$  the equation (1.34) is identical to the equation

$$v_n = n v_1 g^{n-1} - (n-1) v_0 g^n. \quad (1.38)$$

As a result we have two expressions for the solution of linear second order difference equations. The first one is the equation (1.34). The second equation is the equation (1.37) if  $a^2 + 4b \neq 0$  and the equation (1.38) if  $a^2 + 4b = 0$ .

For the stability analysis we write  $v_n$  as  $w_{n+1}$ . Then the equation (1.33) becomes a two dimensional system:

$$\begin{aligned} v_{n+1} &= a v_n + b w_n \\ w_{n+1} &= v_n. \end{aligned} \quad (1.39)$$

In matrix form this is

$$\begin{pmatrix} v_{n+1} \\ w_{n+1} \end{pmatrix} \approx \begin{pmatrix} a & b \\ 1 & 0 \end{pmatrix} \Big|_{(L,K)} \cdot \begin{pmatrix} v_n \\ w_n \end{pmatrix}. \quad (1.40)$$

The fixed point is  $(L, K) = (0, 0)$ . The equation for the eigenvalues of the Jacobian is equation  $\lambda^2 - a\lambda - b = 0$ . This is equal to the characteristic equation. The eigenvalues are

$$\lambda_+ = \frac{1}{2} \left( a + \sqrt{a^2 + 4b} \right) \quad , \quad \lambda_- = \frac{1}{2} \left( a - \sqrt{a^2 + 4b} \right). \quad (1.41)$$

Obviously,  $g_{\pm}$  is identical to  $\lambda_{\pm}$ .

We distinguish three cases:

1.  $a^2 + 4b > 0$ , then  $g_+$  and  $g_-$  are real. As an example we consider the difference equation

$$F_{n+1} = F_n + F_{n-1}, \quad (1.42)$$

with  $F_0 = 0$  and  $F_1 = 1$ . That is,  $a = 1$  and  $b = 1$ . According to the equation (1.34) we therefore have

$$F_n = \sum_{k=0}^{\lfloor n/2 - 1/2 \rfloor} \binom{n-1-k}{k} \quad (1.43)$$

and according to the equation (1.37) we have

$$F_n = \frac{g_+^n - g_-^n}{g_+ - g_-} = \frac{(1 + \sqrt{5})^n - (1 - \sqrt{5})^n}{2^n \sqrt{5}}. \quad (1.44)$$



1.5. ONE DIMENSIONAL, SECOND ORDER, LINEAR DIFFERENCE EQUATIONS 17

Both lead to the Fibonacci series 0, 1, 1, 2, 3, 5, 8, 13, 21, 34, 55, 89, .... For increasing  $n$  the Fibonacci numbers diverge to infinity, while their ratio  $F_n/F_{n-1}$  converges to  $\phi = (1 + \sqrt{5})/2$ ; the *golden ratio*.

As another example we consider the difference equation is

$$v_{n+1} = \frac{1}{2}v_n + \frac{1}{4}v_{n-1}, \quad (1.45)$$

with  $v_0 = 0$  and  $v_1 = 4$ . That is,  $a = 1/2$  and  $b = 1/4$ . According to the equation (1.34) we obtain

$$v_n = 2^{3-n} \sum_{k=0}^{\lfloor n/2-1/2 \rfloor} \binom{n-1-k}{k} \quad (1.46)$$

and according to the equation (1.37) we obtain

$$v_n = 4 \frac{g_+^n - g_-^n}{g_+ - g_-} = 2^{3-n} \frac{(1 + \sqrt{5})^n - (1 - \sqrt{5})^n}{2^n \sqrt{5}}. \quad (1.47)$$

Both lead to the series 0, 4, 2, 2,  $\frac{3}{2}$ ,  $\frac{5}{4}$ , 1,  $\frac{13}{16}$ ,  $\frac{21}{32}$ ,  $\frac{17}{32}$ , .... The series converge to 0. Notice the connection with the Fibonacci numbers:  $v_n = 2^{3-n}F_n$ .

2.  $a^2 + 4b = 0$ , then  $g = a/2$  and  $g^2 = -b$ . Expressed in the constant  $a$  the equation (1.38) reads

$$v_n = \left(\frac{a}{2}\right)^n \left(v_0 + n \left(\frac{2v_1}{a} - v_0\right)\right). \quad (1.48)$$

For  $|a| > 2$  the series diverges. If  $a = 2$  the series grows linear with  $n$ :

$$v_n = v_0 + n(v_1 - v_0). \quad (1.49)$$

For  $|a| < 2$  the series converges.

3.  $a^2 + 4b < 0$ , then  $g_+$  and  $g_-$  are complex numbers. As an example we consider the difference equation

$$v_{n+1} = v_n - v_{n-1}, \quad (1.50)$$

with  $v_0 = 0$  and  $v_1 = 1$ . That is,  $a = 1$  and  $b = -1$ . According to the equation (1.34) we therefore have

$$v_n = \sum_{k=0}^{\lfloor n/2-1/2 \rfloor} \binom{n-1-k}{k} (-1)^k \quad (1.51)$$

and according to the equation (1.37) we have

$$v_n = \frac{g_+^n - g_-^n}{g_+ - g_-} = \frac{(1 + i\sqrt{3})^n - (1 - i\sqrt{3})^n}{2^n i\sqrt{3}}. \quad (1.52)$$

The latter can also be written as

$$v_n = \frac{1}{i\sqrt{3}} \left( \left( \cos \frac{\pi}{3} + i \sin \frac{\pi}{3} \right)^n - \left( \cos \frac{\pi}{3} - i \sin \frac{\pi}{3} \right)^n \right). \quad (1.53)$$

By means of the *de Moivre's theorem* this is equal to

$$\begin{aligned} v_n &= \frac{1}{i\sqrt{3}} \left( \left( \cos \frac{n\pi}{3} + i \sin \frac{n\pi}{3} \right) - \left( \cos \frac{n\pi}{3} - i \sin \frac{n\pi}{3} \right) \right) \\ &= \frac{1}{i\sqrt{3}} \left( \cos \frac{n\pi}{3} + i \sin \frac{n\pi}{3} - \cos \frac{n\pi}{3} + i \sin \frac{n\pi}{3} \right) \\ &= \frac{2}{\sqrt{3}} \sin \frac{n\pi}{3} \end{aligned} \quad (1.54)$$

All expressions lead to the series  $0, 1, 1, 0, -1, -1, 0, 1, 1, 0, -1, -1, 0, 1, 1, 0, \dots$ . From a two dimensional perspective this is  $(0, 1), (1, 1), (1, 0), (0, -1), (-1, -1), (-1, 0), (0, 1), \dots$

Since the modulus is of  $\lambda_{\pm}$  is 1 the fixed point  $(0, 0)$  is a center of clockwise rotation.

As another example we consider the difference equation

$$v_{n+1} = v_n - \frac{1}{2}v_{n-1}, \quad (1.55)$$

with  $v_0 = 0$  and  $v_1 = 1$ . That is,  $a = 1$  and  $b = -1/2$ . According to the equation (1.37) we have  $g_{\pm} = (1 \pm i)/2$  and

$$v_n = \frac{g_+^n - g_-^n}{g_+ - g_-} = \frac{(1+i)^n - (1-i)^n}{2^n i} = \frac{2}{(\sqrt{2})^n} \sin \frac{n\pi}{4}. \quad (1.56)$$

It leads to the series  $0, 1, 1, 1/2, 0, -1/4, -1/4, -1/8, 0, 1/16, 1/16, 1/32, 0, \dots$ . From a two dimensional perspective this is  $(0, 1), (1, 1), (1, 1/2), (1/2, 0), (0, -1/4), \dots$ . Since the modulus is of  $g_{\pm}$  is  $\frac{1}{2}\sqrt{2} < 1$  the fixed point  $(0, 0)$  is a stable focus. The successive points spiralize (clockwise rotation) towards the fixed point.

## Chapter 2

# One dimensional difference equations

### 2.1 Introduction

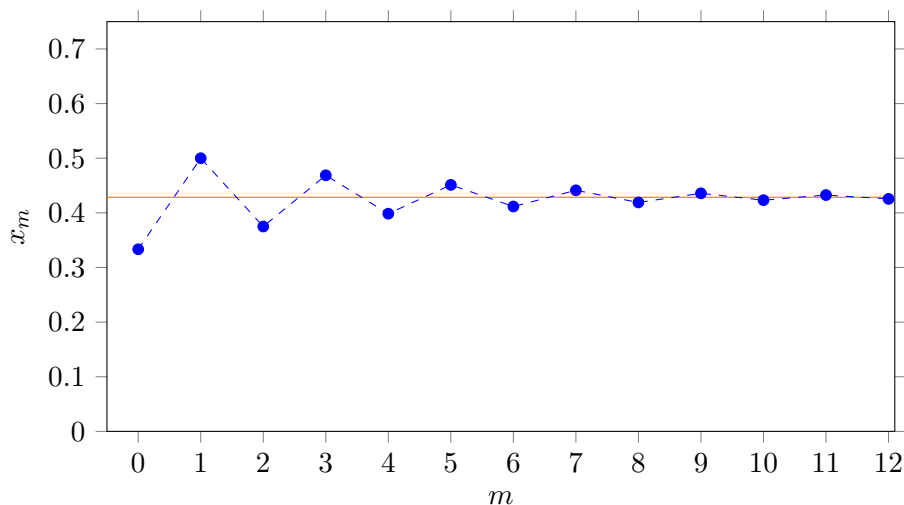
In this chapter we will consider difference equations of the type

$$x_{m+1} = f(x_m), \quad (2.1)$$

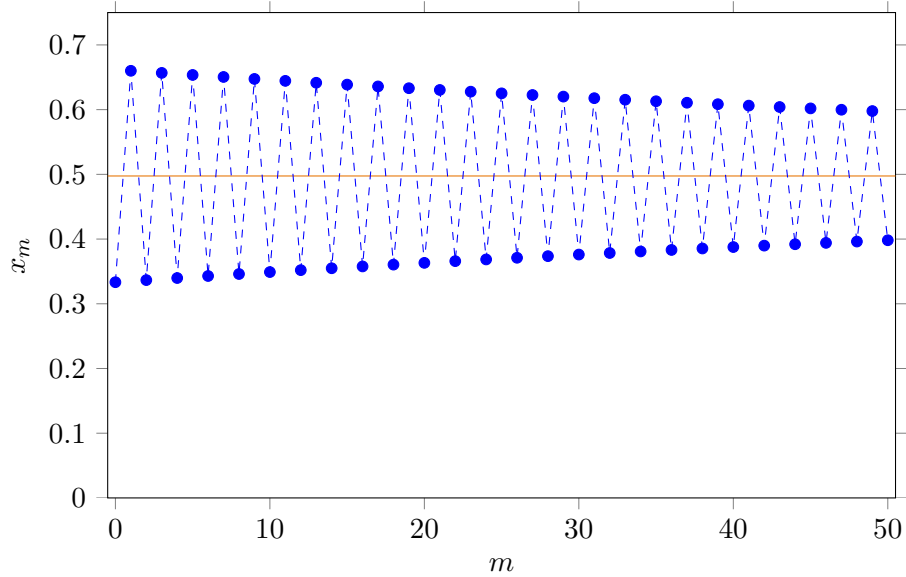
where  $f$  may depend on one or more parameters. For instance, for  $f(x) = a(1 - x)$  with  $a$  a parameter, the difference equation is as follows:

$$x_{m+1} = a(1 - x_m). \quad (2.2)$$

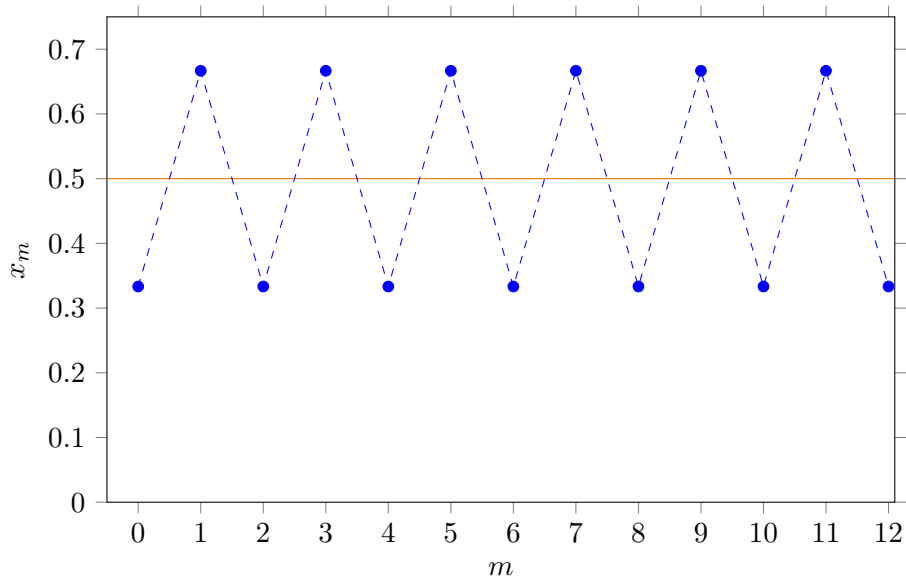
An equilibrium point,  $L$ , also called a fixed point, follows from  $L = a(1 - L)$ . The fixed point is  $L = \frac{a}{a+1}$ . For  $a = 3/4$ , for instance, the fixed point is  $L = 3/7$  and it is stable. To illustrate it we take  $a = 3/4$  and start with  $x_0 = 1/3$ . Then  $x_1 = 1/2$ ,  $x_2 = 3/8$ ,  $x_3 = 15/32$ ,  $x_4 = 51/128$ , etc. In the long run the values of  $x_m$  converge to  $3/7$ , see the next figure.



For  $a = 0.99$  and  $x_0 = 1/3$  the successive  $x_m$  slowly converge to  $99/199 \approx 0.4974874$ , see the next figure.

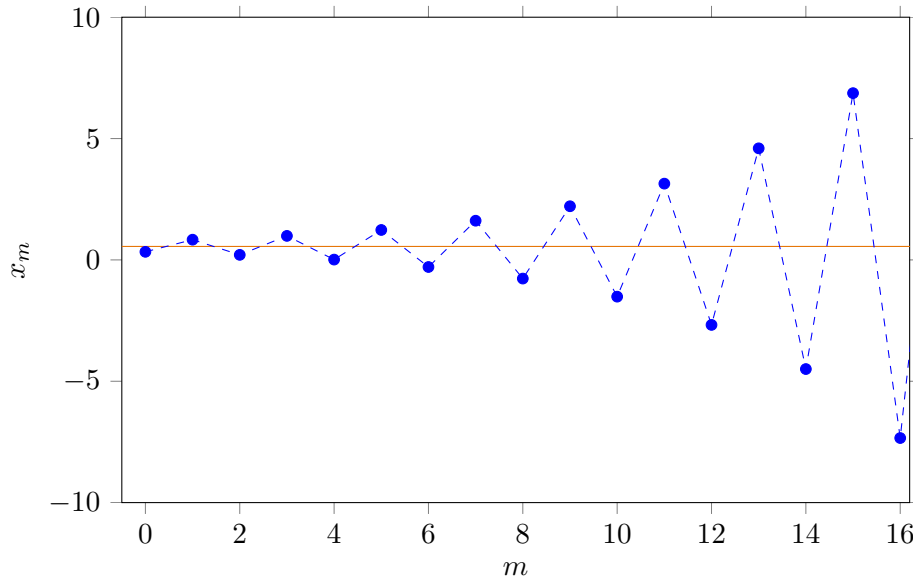


For  $a = 1$  and  $x_0 = 1/3$ , we obtain  $x_1 = 2/3$ ,  $x_2 = 1/3$ ,  $x_3 = 2/3$ ,  $x_4 = 1/3$ , etc. That is, the  $x_m$  alternate are  $1/3$  and  $2/3$ , see next figure.



There is neither convergence nor divergence. Of course, for all  $x_0$  we will obtain  $x_1 = 1 - x_0$ ,  $x_2 = 1 - (1 - x_0) = x_0$ ,  $x_3 = 1 - x_0$ ,  $x_4 = x_0$ , etc. For  $a = 1$  and  $x_0 \neq 1/2$  we obtain an alternating sequence. For  $a = 1$  and  $x_0 = 1/2$  we have  $x_m = x_0 = 1/2$  for all  $m$ .

For  $a = 5/4$  and  $x_0 = 1/3$  the successive  $x_m$  diverge from  $5/9$ , see the next figure.



In a similar manner it is found for  $a < 0$  that subsequent  $x_m$  converge if  $-1 < a < 0$ , and diverge if  $a < -1$ .

The foregoing mapping function was linear: the power of  $x$  in  $f(x)$  is 1. Things become more of interest when we consider more general functions with larger powers of  $x$ , such as  $f(x) = x^2 + a$  or  $f(x) = a \sin(x)$ . For a general function  $f(x)$  a fixed point  $L$  is a solution of the equation

$$L = f(L). \quad (2.3)$$

As shown in chapter 1 a fixed point  $L$  is stable if

$$-1 < \left. \frac{\partial f}{\partial x} \right|_L < 1. \quad (2.4)$$

A stable fixed point  $L$  for which  $L = f(L)$  can be regarded as a limit cycle with period 1.

A period 2 limit cycle occurs if both the conditions  $L = f(f(L))$  and  $-1 < \left. \frac{\partial f(f(x))}{\partial x} \right|_L < 1$  are satisfied.

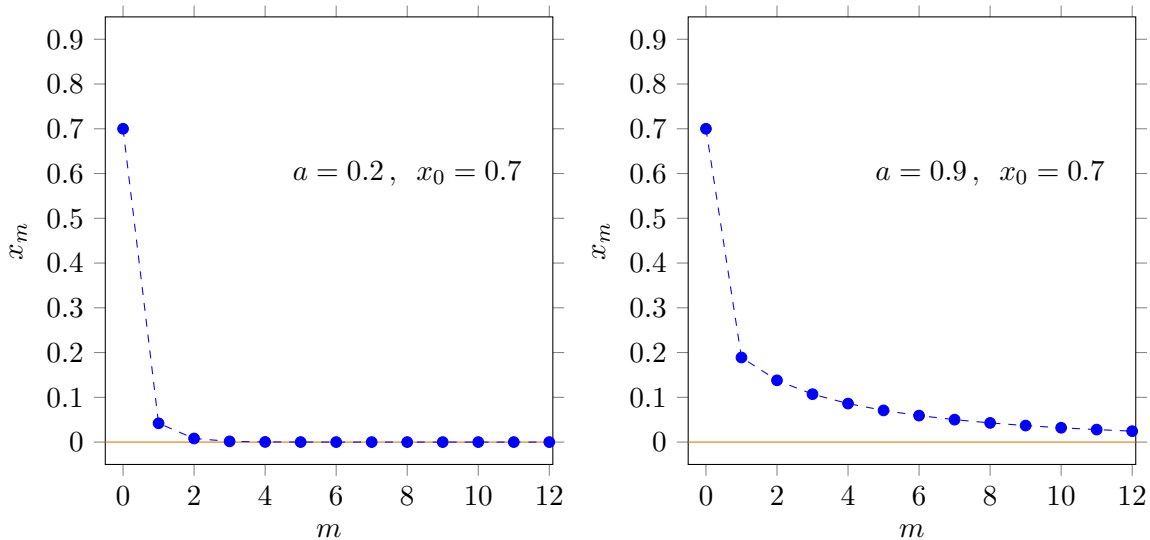
A period 3 limit cycle occurs if the conditions  $L = f(f(f(L)))$  and  $-1 < \left. \frac{\partial f(f(f(x)))}{\partial x} \right|_L < 1$  are both satisfied, and so on.

## 2.2 Logistic equation

A one dimensional, first order, non-linear difference equation is the logistic equation:

$$x_{m+1} = ax_m(1 - x_m). \quad (2.5)$$

The function  $f(x) = ax - ax^2$  is the logistic function. The additional condition  $0 \leq a \leq 4$  guarantees  $0 \leq x_{m+1} \leq 1$  for  $x_m \in [0, 1]$ . A fixed point  $L$  occurs if  $L = aL - aL^2$ . There are two solutions:  $L = 0$  and  $L = \frac{a-1}{a}$ . Since  $\left. \frac{\partial f}{\partial x} \right|_L = a - 2aL$ , the stability requires  $-1 < a - 2aL < 1$ . Substituting  $L = 0$  into the stability requirement leads to  $0 \leq a < 1$  and substituting  $L = \frac{a-1}{a}$  into the stability requirement leads to  $1 < a < 3$ . So, this is what happens: for  $a$  close to 0 the sequence  $x_0, x_1, x_2, \dots$  quickly converges to 0. It is illustrated in the left panel of the next figure.

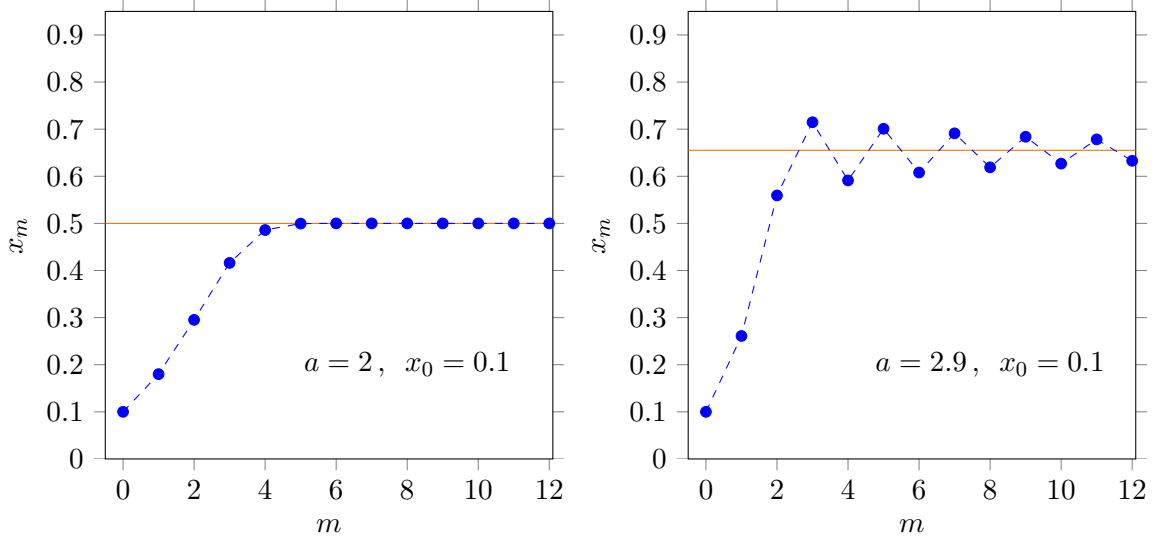


For  $a$  a little smaller than 1 the sequence  $x_0, x_1, x_2, \dots$  slowly converges to 0, see right panel of previous figure. For  $a$  a little larger than 1 the sequence  $x_0, x_1, x_2, \dots$  slowly converges to  $\frac{a-1}{a}$ . For  $a$  close to 2 the sequence  $x_0, x_1, x_2, \dots$  quickly converges to  $\frac{a-1}{a}$ , see the left panel of next figure. For  $a$  a little smaller than 3 the sequence  $x_0, x_1, x_2, \dots$  slowly converges to  $\frac{a-1}{a}$ , see the right panel of next figure.

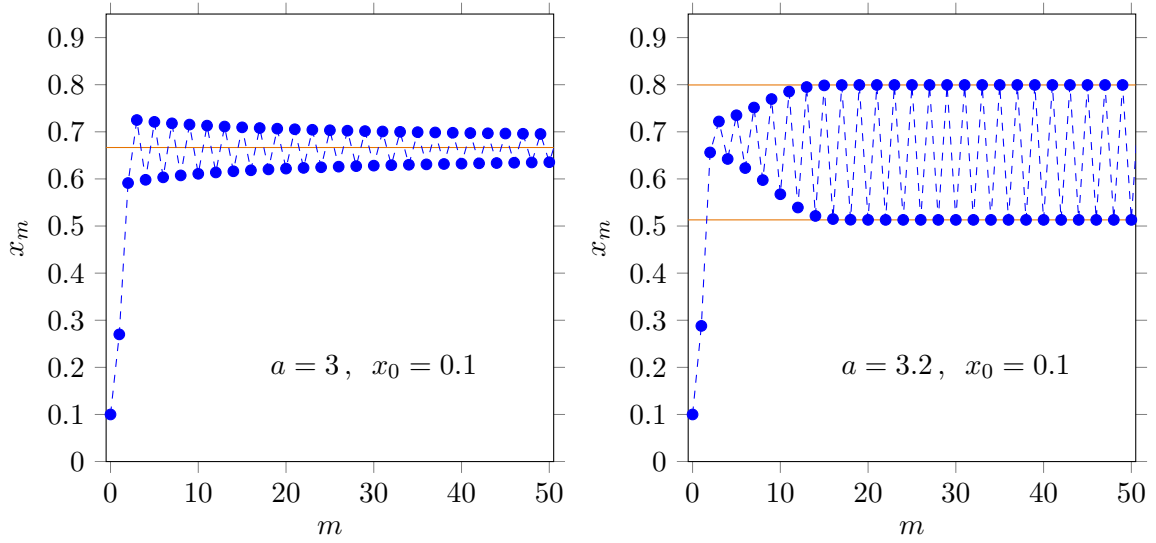
The speed with which the sequence  $x_0, x_1, x_2, \dots$  converges to a stable fixed point  $L$  is determined by  $\left. \frac{\partial f}{\partial x} \right|_{x_m}$  at this point. If, for instance,  $\left. \frac{\partial f}{\partial x} \right|_{x_m} = \frac{1}{8}$  the speed of convergence is three times larger in comparison to the situation where  $\left. \frac{\partial f}{\partial x} \right|_{x_m} = \frac{1}{2}$ . Actually,

$$|x_{m+1} - L| \approx e^{\kappa_m} |x_m - L|, \quad (2.6)$$

where  $\kappa_m = \ln \left| \left. \frac{\partial f}{\partial x} \right|_{x_m} \right|$ , as will be derived in section 2.4.



In particular for  $a = 3$  and  $x_m = 2/3$  we have  $\kappa_m = 0$ : no convergence. Beyond  $a = 3$  a period 2 limit cycle sets in, see next figure.



Alternatively, for  $a = 3$  there is a *bifurcation* to two fixed points. The fixed points follow from

$$L = f(f(L)) \quad \rightarrow \quad L = af(L) - af^2(L) \quad \rightarrow \quad L = a(aL - aL^2) - a(aL - aL^2)^2. \quad (2.7)$$

The latter equation can be elaborated to

$$a^3L^4 - 2a^3L^3 + (a^2 + a^3)L^2 - a^2L + L = 0. \quad (2.8)$$

This polynomial for  $L$  can be reduced to

$$(aL^2 + (1 - a)L) (a^2L^2 - (a + a^2)L + 1 + a) = 0. \quad (2.9)$$

The expression between the first pair of brackets is the 1 limit cycle. This is not a surprise since a 2 limit cycle contains a 1 limit cycle. The expression between the second pair of brackets is for a 2 limit cycle with two different limit values. The two limit values follow from

$$a^2 L^2 - (a + a^2)L + 1 + a = 0. \quad (2.10)$$

The two solutions are

$$L_{\pm} = \frac{a + 1 \pm \sqrt{(a + 1)(a - 3)}}{2a}. \quad (2.11)$$

We also find

$$\frac{\partial f(f(L))}{\partial L} = a^2 - 2a^2(1 + a)L + 6a^3L^2 - 4a^3L^3. \quad (2.12)$$

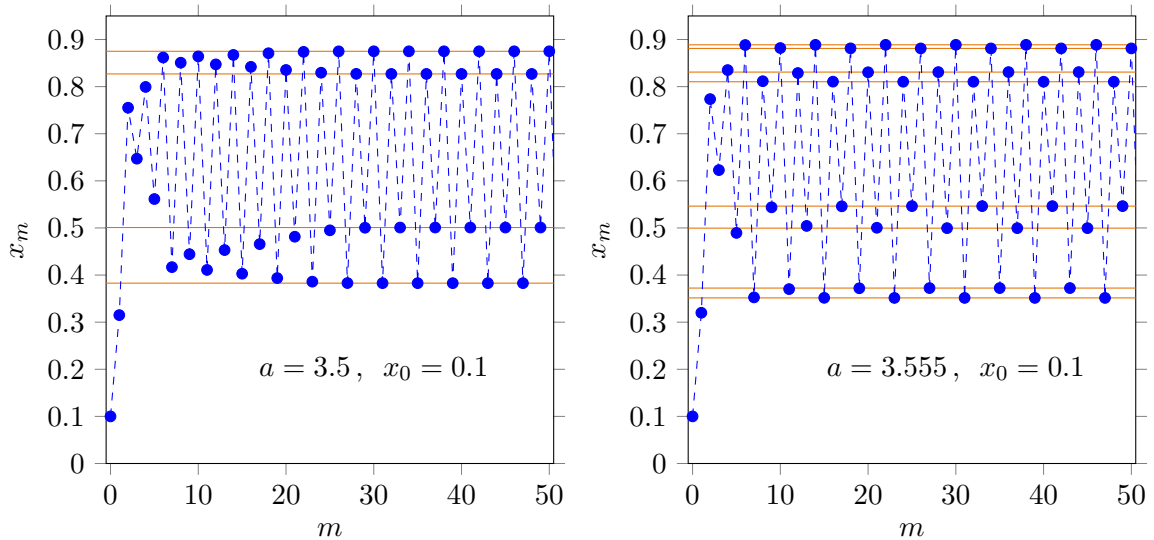
for  $L = L_{\pm}$  it is reduced to

$$\left. \frac{\partial f(f(L))}{\partial L} \right|_{L_{\pm}} = a^2 - 2a - 4. \quad (2.13)$$

The requirement for stability therefore is

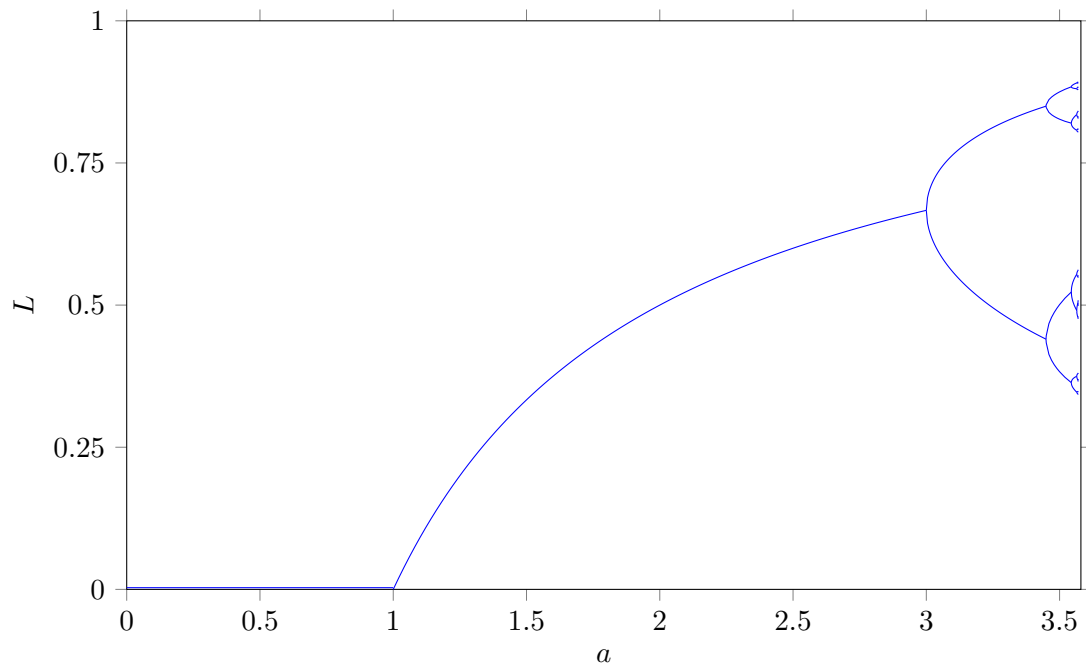
$$-1 < a^2 - 2a - 4 < 1 \quad \rightarrow \quad 3 < a < 1 + \sqrt{6}. \quad (2.14)$$

At  $a = 1 + \sqrt{6} \approx 3.449\dots$  a new bifurcation occurs. The two limit values for  $a = 1 + \sqrt{6}$  are  $\frac{1}{5} \left( 2 + \sqrt{3} + \sqrt{2 - \sqrt{3}} \right)$  and  $\frac{1}{5} \left( 2 - \sqrt{3} + \sqrt{2 + \sqrt{3}} \right)$ . As a result there will be a 4 limit cycle for values of  $a$  slightly larger than  $a = 1 + \sqrt{6}$ , see the left panel of next figure. At  $a \approx 3.544090\dots$  a new bifurcation occurs and an 8 limit cycle comes into existence, see right panel of next figure.



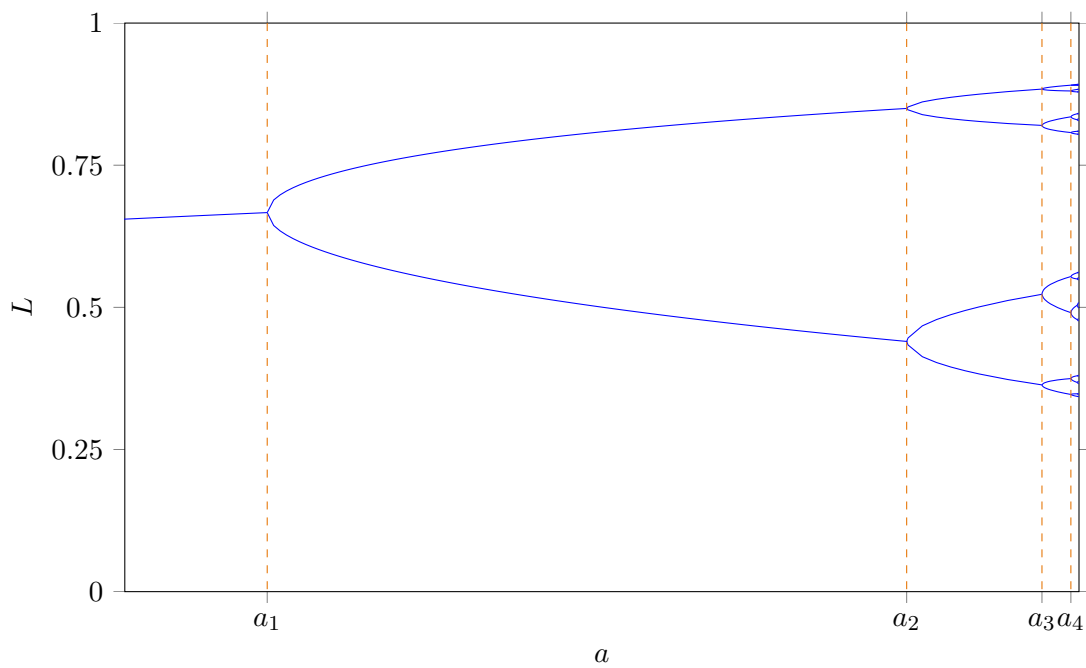
At  $a \approx 3.564\dots$  the 8 limit cycle turns into a  $2^4$  limit cycle, etc. The sequence of  $2^n$  limit cycles for  $n \rightarrow \infty$  ends at  $a \approx 3.56994567\dots$ . In the next diagram the limit values are plotted against  $a$ . It visualizes the bifurcations. It is called a bifurcation diagram.





### 2.3 Feigenbaum constants

The value of  $a$  where a limit cycle with period  $2^n$  changes in a limit cycle with period  $2^{n+1}$  is denoted as  $a_n$ , see next figure.



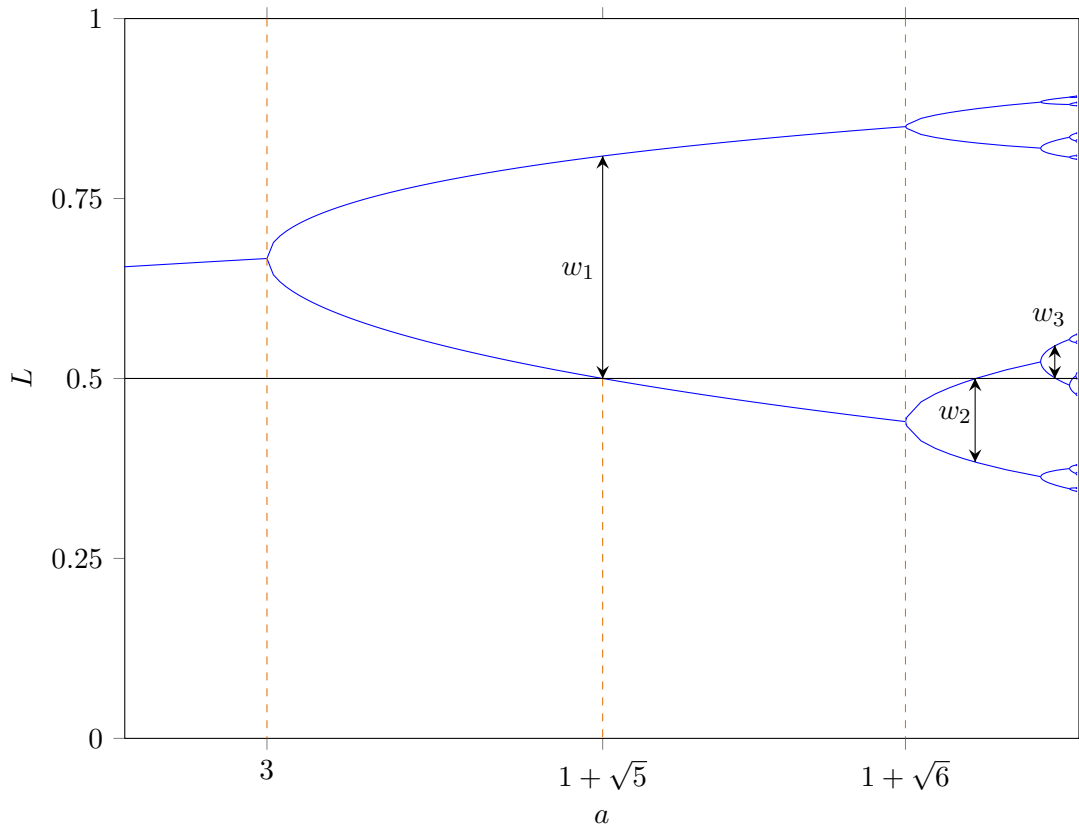
The ratio of differences between two successive  $a_n$  values is:

$$\frac{a_n - a_{n-1}}{a_{n+1} - a_n}. \quad (2.15)$$

In the limit where  $n \rightarrow \infty$  the series of ratios converges to a constant value  $\delta$  which is known as a Feigenbaum constant:

$$\delta := \lim_{n \rightarrow \infty} \frac{a_n - a_{n-1}}{a_{n+1} - a_n} = 4.6692016091\dots \quad (2.16)$$

We denote the width of a  $2^n$  bifurcation at the value of  $a$  where  $L = 1/2$  as  $w_n$ , see next figure.



In the limit where  $n \rightarrow \infty$  this series of ratios of successive widths

$$\frac{w_{n-1}}{w_n}. \quad (2.17)$$

converges to a constant value  $\alpha$ :

$$\alpha = \lim_{n \rightarrow \infty} \frac{w_{n-1}}{w_n} = 2.502907875\dots \quad (2.18)$$

The latter also is a Feigenbaum constant.

## 2.4 Chaos

For the logistic equation the  $2^n$  limit cycle ends for  $n \rightarrow \infty$  at  $a \approx 3.5699\dots$ . So far we only considered the situation for  $a$  smaller than this value. For a slightly larger value of  $a$ , say 3.57, the sequence of  $x_m$ 's, the *orbit*, does not converge to a limit cycle. Instead, the sequence shows chaotic behaviour. From every starting point  $0 < x_0 < 1$  the orbit is quite irregular. The orbit never passes twice through the same point since then one would have periodic behaviour. For increasing  $a$  'windows' with chaotic behaviour and windows with periodic limit cycles alternate. To visualize the chaotic behaviour and periodic limit values one can for every  $a$  iterate the starting value  $x_0$  for instance 20 000 times and plot the final 50 values of the  $x_m$  sequence. The result is shown in the next figure.

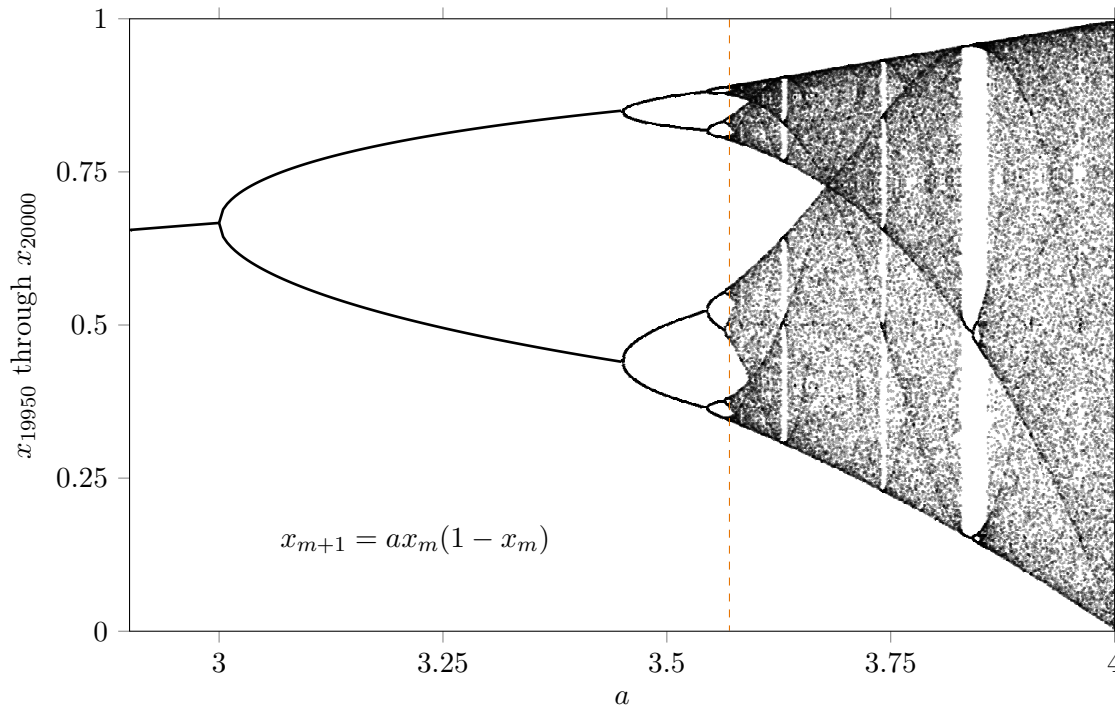


Figure 2.1: Orbit diagram for the logistic equation. The dashed, orange line is where the  $2^n$  limit cycles end and where the first chaos sets in.

There are several windows of periodic cycles present. An obvious window is for the  $3 \times 2^n$  limit cycle. It is a 3 limit cycle for  $n = 0$ . From  $L = f(f(f(L)))$  it follows, after factoring out  $L = f(L)$ , that  $1 + a + a^2 - (a + 2a^2 + 2a^3 + a^4)L + (a^2 + 3a^3 + 3a^4 + 2a^5)L^2 - (a^3 + 3a^4 + 5a^5 + a^6)L^3 + (a^4 + 4a^5 + 3a^6)L^4 - (a^5 + 3a^6)L^5 + a^6L^6 = 0$ . Together with the condition  $\left. \frac{\partial f(f(f(x)))}{\partial x} \right|_L = 1$  we obtain  $-49 - 28a - 18a^2 + 24a^3 + 4a^4 - 6a^5 + a^6 = 0$ . It factorizes into  $(7 - 5a + a^2)(-7 - 2a + a^2)(1 + a + a^2) = 0$ . The factor  $(-7 - 2a + a^2) = 0$  has the analytical solution  $a = 1 + 2\sqrt{2}$ . Hence, a 3 limit cycle sets in at  $a = 1 + 2\sqrt{2} \approx 3.8284\dots$

A less obvious window is a 4 limit cycle for  $a$  close to 4. From  $L = f(f(f(f(L))))$  together with the condition  $\left. \frac{\partial f(f(f(f(x))))}{\partial x} \right|_L = 1$  we obtain  $(1 + a^2)(5 - 4a + a^2)(-5 - 2a + a^2)(-135 - 54a - 9a^2 + 28a^3 + 3a^4 - 6a^5 + a^6) = 0$ . The factor  $-5 - 2a + a^2$  has a root  $a = 1 + \sqrt{6}$  as we already met before. The factor  $-135 - 54a - 9a^2 + 28a^3 + 3a^4 - 6a^5 + a^6$  has a root  $1 + \sqrt{4 + 3 \times \sqrt[3]{4}} \approx 3.96010188\dots$ . It turns into an 8 limit cycle at  $a \approx 3.96076\dots$ . The sequence of  $4 \times 2^n$  limit cycles ends at  $a \approx 3.9612\dots$ . The window for this cycle is very narrow;  $\Delta a \approx 0.001$ .

In between the windows of limit cycles there is chaotic behaviour: the sequence of  $x_m$ 's is sensitive for the initial value  $x_0$ . A slightly different  $x_0$  may lead to a completely different orbit. Starting with  $x_0$  we are after one step at  $x_1 = f(x_0)$ . Starting with  $x_0 + \delta_0$  we arrive after one step at  $x_1 + \delta_1 = f(x_0 + \delta_0)$ . Taking a first order Taylor expansion of  $f$  the latter is  $x_1 + \delta_1 \approx f(x_0) + \delta_0 \left. \frac{\partial f}{\partial x} \right|_{x_0}$ . Since  $x_1 = f(x_0)$  it is reduced to  $\frac{\delta_1}{\delta_0} \approx \left. \frac{\partial f}{\partial x} \right|_{x_0}$ . The rate of change is  $\left| \frac{\delta_1}{\delta_0} \right| \approx \left| \left. \frac{\partial f}{\partial x} \right|_{x_0} \right|$ . Calculating  $\delta_2$  from  $\delta_1$ ,  $\delta_3$  from  $\delta_2$ , etc. through  $\delta_n$  leads to the equation

$$\left| \frac{\delta_n}{\delta_0} \right| = \left| \frac{\delta_n}{\delta_{n-1}} \right| \cdot \left| \frac{\delta_{n-1}}{\delta_{n-2}} \right| \cdot \dots \cdot \left| \frac{\delta_2}{\delta_1} \right| \cdot \left| \frac{\delta_1}{\delta_0} \right| \approx \left| \frac{\partial f}{\partial x} \right|_{x_{n-1}} \cdot \dots \cdot \left| \frac{\partial f}{\partial x} \right|_{x_1} \cdot \left| \frac{\partial f}{\partial x} \right|_{x_0}, \quad (2.19)$$

or

$$\left| \frac{\delta_n}{\delta_0} \right| \approx e^{\kappa_{n-1} + \dots + \kappa_1 + \kappa_0}, \quad (2.20)$$

where

$$\kappa_m = \ln \left| \left. \frac{\partial f}{\partial x} \right|_{x_m} \right|. \quad (2.21)$$

It can be written as

$$|\delta_n| \approx e^{n\bar{\kappa}} |\delta_0|, \quad (2.22)$$

where

$$\bar{\kappa} := \frac{1}{n} \sum_{m=0}^{n-1} \kappa_m. \quad (2.23)$$

In the limit where  $n$  goes to infinity it is known as the Lyapunov exponent  $\lambda$ :

$$\lambda = \lim_{n \rightarrow \infty} \bar{\kappa}. \quad (2.24)$$

In case of a convergence to a periodic limit cycle the Lyapunov exponent is smaller than 0. In case of chaotic behaviour the Lyapunov exponent is larger than 0: small differences initially grow each step. In the next figure the Lyapunov exponent is plotted against the parameter  $a$  for the logistic equation.

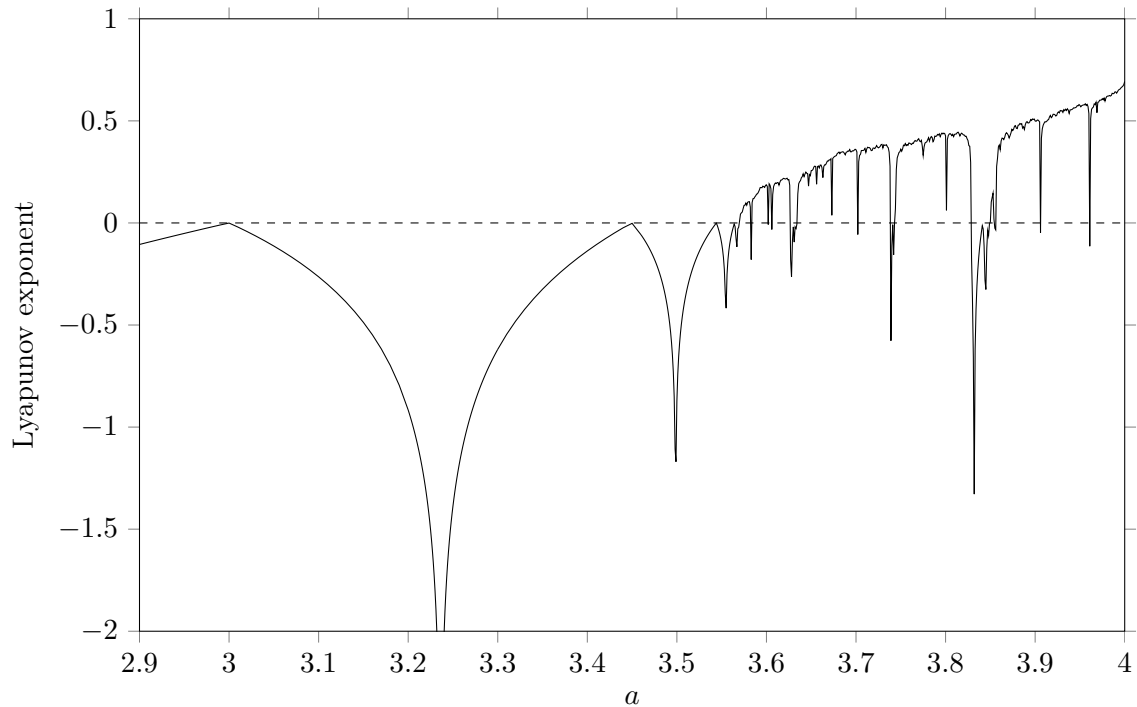
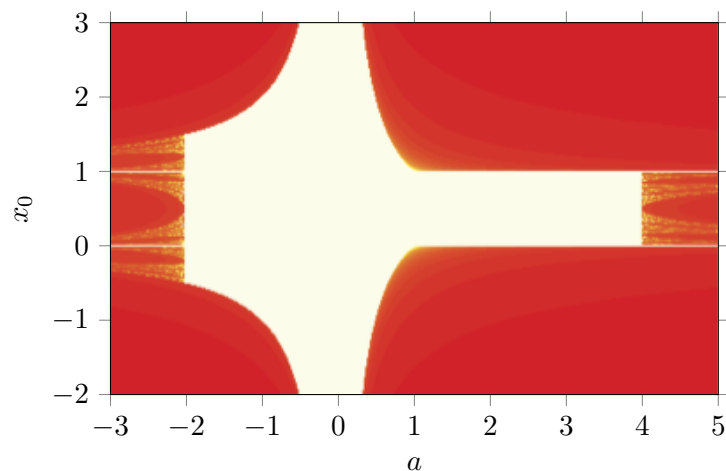


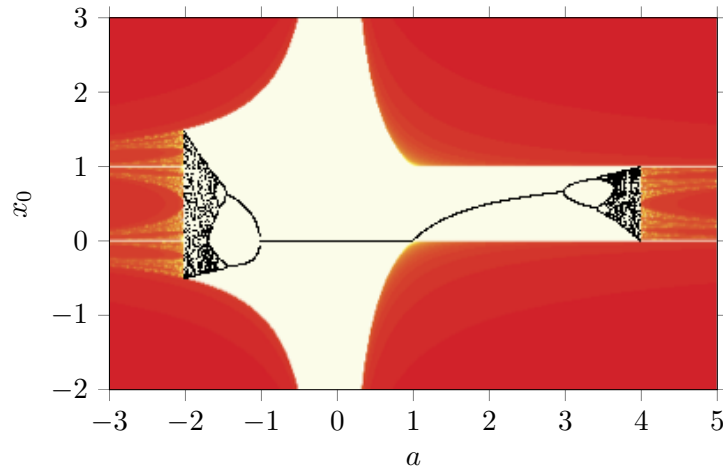
Figure 2.2: Lyapunov exponent for the logistic equation.

## 2.5 Starting points

So far we only considered  $0 \leq a \leq 4$  and starting values  $x_0$  between 0 and 1 for the logistic equation, since the orbit either is periodic or chaotic for  $0 \leq a \leq 4$  and  $0 \leq x_0 \leq 1$ . For other starting values  $x_0$  and other values for  $a$  the orbit may either be attracted to a periodic limit cycle, diverge, stay in a chaotic region or diverge to infinity. The situation is shown in the next figure. If the orbit tends to infinity the pixel at  $(a, x_0)$  is coloured yellow, orange through red



dependent on a slow, intermediate through fast velocity with which the orbit goes to infinity. If the orbit ends in a stable periodic limit cycle or is at an unstable fixed point (as  $x_0 = 0$  or  $x_0 = 1$ ) or stays in a chaotic region, that is, if the orbit does not diverge to infinity, the pixel at  $(a, x_0)$  is coloured white. The region of  $x_0$ 's which do not lead to divergence to infinity has the borders  $\frac{1}{a} \leq x_0 \leq \frac{a-1}{a}$  if  $-2 \leq a \leq 0$ ,  $\frac{a-1}{a} \leq x_0 \leq \frac{1}{a}$  if  $0 \leq a \leq 1$  and  $0 \leq x_0 \leq 1$  if  $1 \leq a \leq 4$ . In the next figure the orbit diagram is shown on top of the previous figure.



## 2.6 Other difference equations

In this section we will investigate how the orbit diagrams look for other difference equations. First we consider the sine map:

$$x_{m+1} = b \sin(\pi x_m). \quad (2.25)$$

The additional condition  $0 \leq b \leq 1$  guarantees  $0 \leq x_{m+1} \leq 1$  for  $x_m \in [0, 1]$ . The orbit diagram for the sine map is shown in the figure [2.3](#). Although the logistic map differs from the sine map, their orbit diagrams look almost identical. The Feigenbaum numbers  $\delta$  and  $\alpha$  for the sine map are identical to the ones for the logistic equation. This suggests that the Feigenbaum numbers are universal constants. Except for some scaling effects, power sine maps such as  $b \sin^c(\pi x)$  have a comparable orbit diagram.

With the linear transformation  $x \rightarrow \left(\frac{1}{4}a - \frac{1}{2}\right)x + \frac{1}{2}$  the logistic equation takes the form  $f(x) = 1 - \mu x^2$  with  $\mu = \frac{1}{4}a(a-2)$ . The iterations

$$x_{m+1} = 1 - \mu x_m^2, \quad 0 \leq \mu \leq 2 \quad (2.26)$$

lead to the diagram in figure [2.4](#). Also here the Feigenbaum numbers  $\delta$  and  $\alpha$  are identical to the ones for the logistic equation.

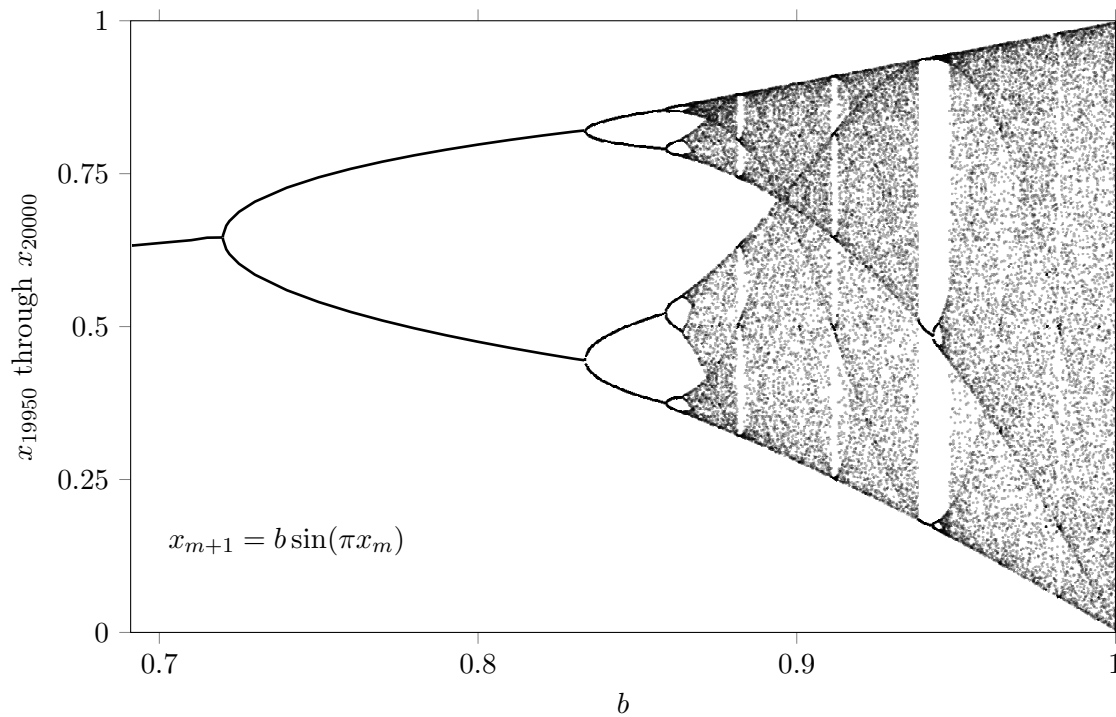
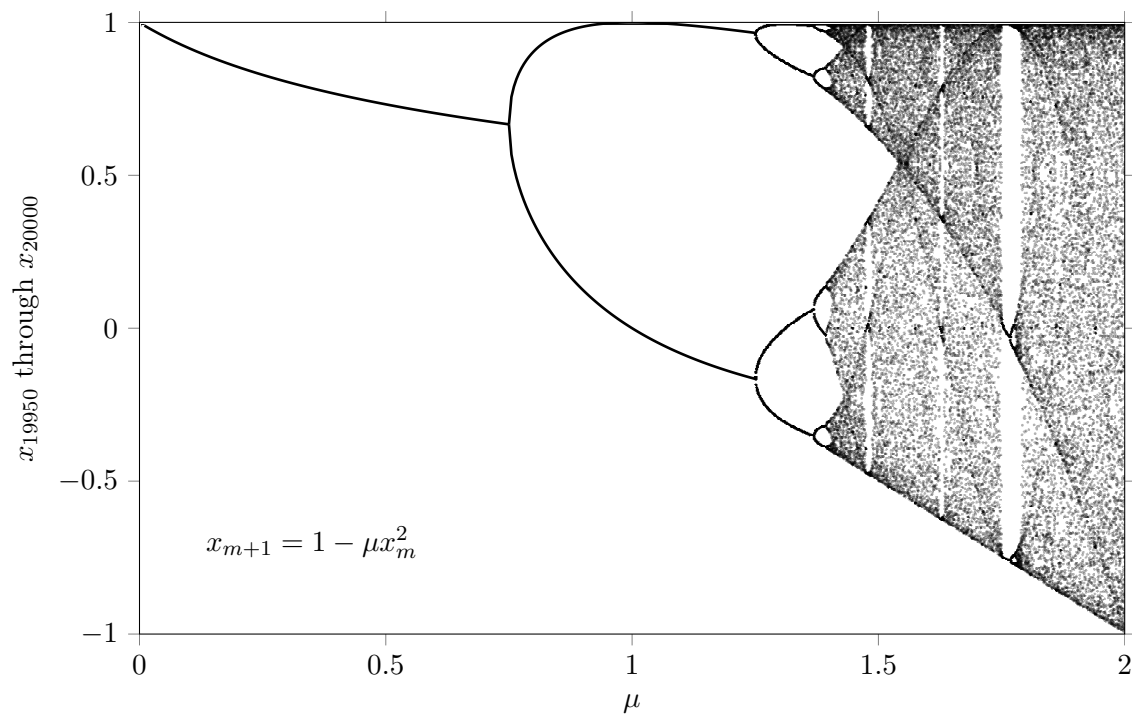


Figure 2.3: Orbit diagram for the sine map.

Figure 2.4: Orbit diagram for the map  $f(x) = 1 - \mu x^2$ .

Another often used example is the hyperbolic tangent map:  $f(x) = gx(1 - \tanh x)$ . The iterations  $x_{m+1} = gx_m(1 - \tanh x_m)$ , with  $g \geq 1$ , lead to the orbit diagram and Lyapunov diagram as shown in figure 2.5 and figure 2.6 respectively.

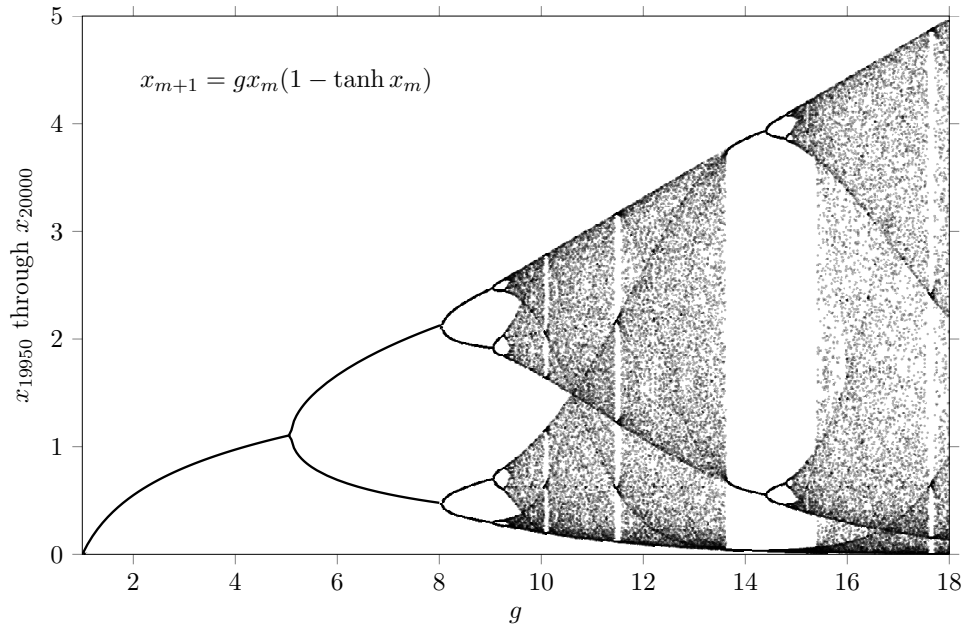


Figure 2.5: Orbit diagram for the hyperbolic tangent map  $f(x) = gx(1 - \tanh x)$ .

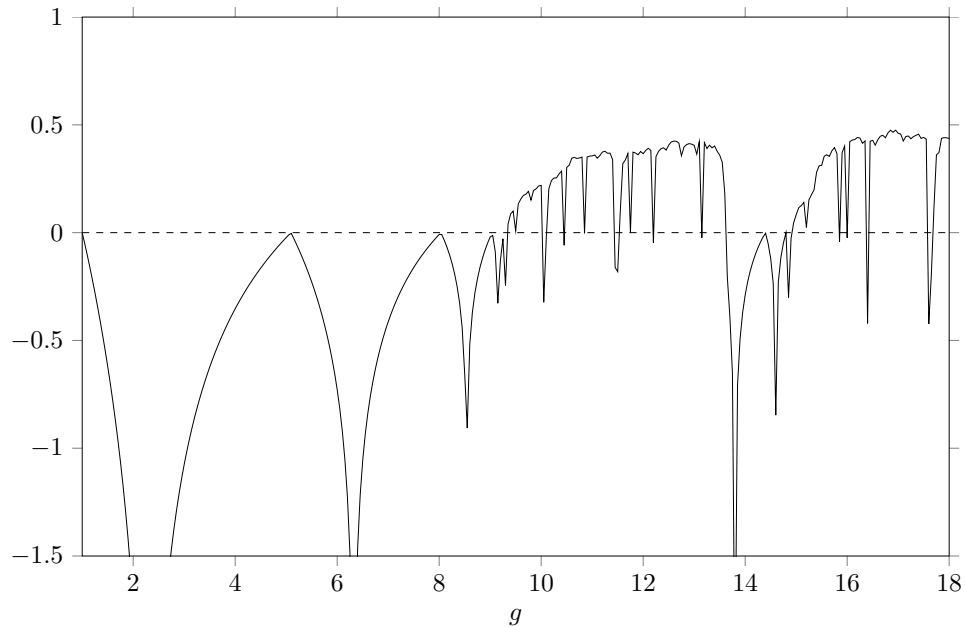


Figure 2.6: Lyapunov exponent for the hyperbolic tangent map.



Of course, one can create an arbitrary smooth function with a maximum value on its domain. Let us try, for instance,  $f(x) = hxe^{-x}$ . The iterations  $x_{m+1} = hx_me^{x_m}$ , with  $h \geq 1$ , lead to the orbit diagram and Lyapunov diagram as shown in figure 2.7 and figure 2.8 respectively..

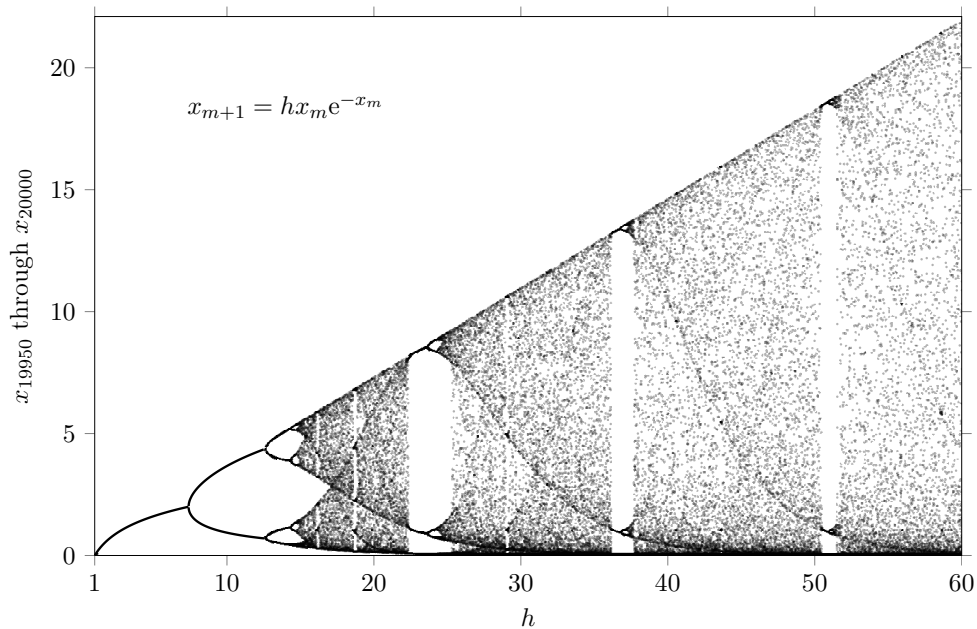


Figure 2.7: Orbit diagram for the map  $f(x) = hxe^{-x}$ .

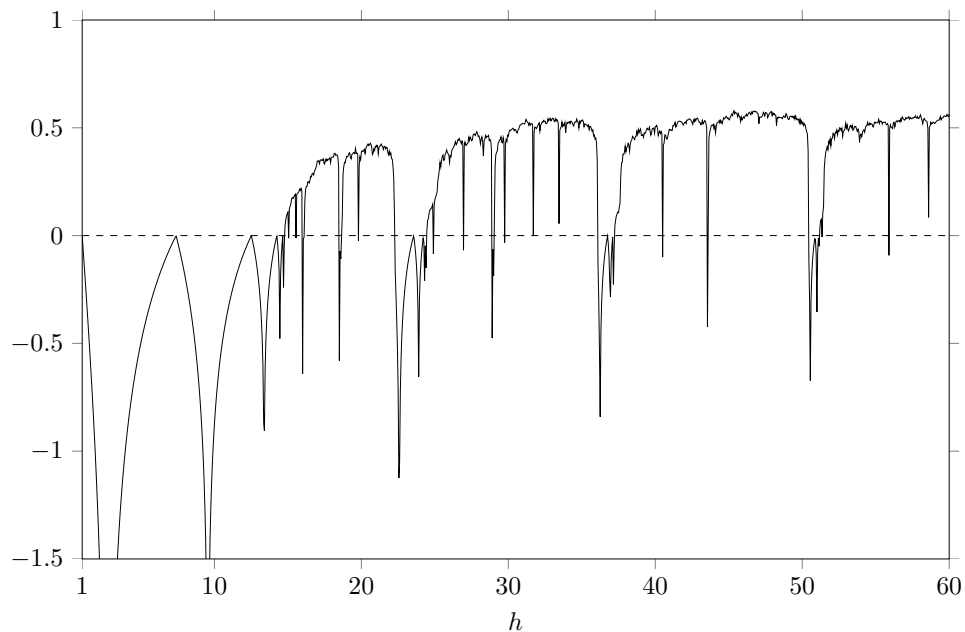


Figure 2.8: Lyapunov exponent for the map  $f(x) = hxe^{-x}$ .

For all these examples the Feigenbaum numbers  $\delta$  and  $\alpha$  are identical to the ones for the original logistic map. For one-dimensional maps  $f(x)$  the Feigenbaum numbers are universal if the Schwarzian derivative of  $f(x)$ ,

$$D_{\text{Schwarzian}} = \left( \frac{f''(x)}{f'(x)} \right)' - \frac{1}{2} \left( \frac{f''(x)}{f'(x)} \right)^2 = \frac{f'''(x)}{f'(x)} - \frac{3}{2} \left( \frac{f''(x)}{f'(x)} \right)^2, \quad (2.27)$$

is negative on the given domain.

An example of a one-dimensional difference equation whose Schwarzian derivative is not negative is the tent map  $f(x) = d \min(x, 1 - x)$ . The iterations  $x_{m+1} = d \min(x_m, 1 - x_m)$  on the domain  $[0, 1]$  lead to the diagram of figure [2.9](#).

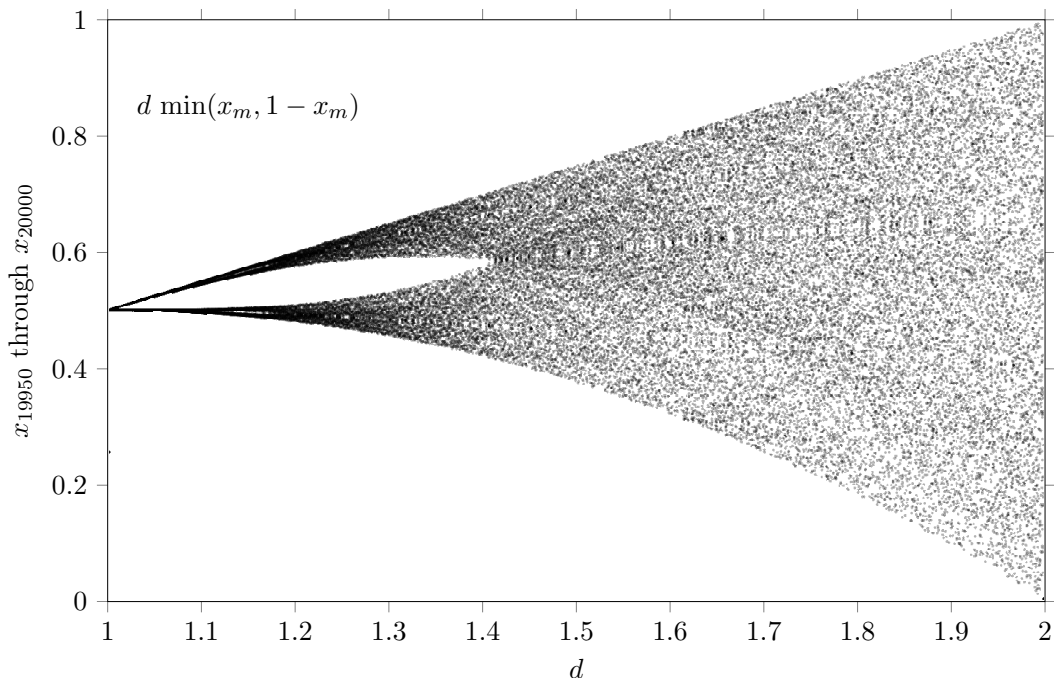


Figure 2.9: Orbit diagram for the tent map  $f(x) = d \min(x_m, 1 - x_m)$ .

The diagram for the tent map contains unstable periodic orbits and chaotic orbits. Cascades of bifurcations are not present.

## Chapter 3

# Two dimensional difference equations

In this chapter the main characteristics of non-linear, two dimensional systems will be explained by means of the Lotka-Volterra model and the Hénon map. We start with the Lotka-Volterra model.

### 3.1 Lotka-Volterra model

The Lotka-Volterra model describes the evolution of the size of the population of two interacting species, predators and prey. For concreteness we take stoats as the predators and rabbits as the prey. If  $s$  is the number of stoats and  $r$  the number of rabbits then the Lotka-Volterra system in differential form is [1, 2]

$$\dot{r} = \frac{dr}{dt} = \alpha r - \beta r s \quad , \quad \dot{s} = \frac{ds}{dt} = -\gamma s + \delta s r, \quad (3.1)$$

where  $t$  is the time parameter and where the constants are defined by:

$\alpha$  is the growth rate of rabbits in the absence of stoats,

$\beta$  is the death rate of rabbits due to the presence of stoats,

$\gamma$  is the natural death rate of stoats in the absence of rabbits,

$\delta$  is the growth rate of stoats in the presence of rabbits.

All four constants are larger than 0.

The equilibrium points of the system follow from  $\dot{r} = 0$  and  $\dot{s} = 0$ . They are  $(r_*, s_*) = \left(\frac{\gamma}{\delta}, \frac{\alpha}{\beta}\right)$  and  $(r_{**}, s_{**}) = (0, 0)$ . For the stability analysis we write the system as

$$\dot{r} = f(r, s) \quad , \quad \dot{s} = g(r, s), \quad (3.2)$$

where  $f(r, s) = \alpha r - \beta r s$  and  $g(r, s) = -\gamma s + \delta s r$ . The Jacobian is

$$J(r, s) = \begin{pmatrix} \frac{\partial f}{\partial r} & \frac{\partial f}{\partial s} \\ \frac{\partial g}{\partial r} & \frac{\partial g}{\partial s} \end{pmatrix} = \begin{pmatrix} \alpha - \beta s & -\beta r \\ \delta s & -\gamma + \delta r \end{pmatrix} \quad (3.3)$$

At the equilibrium point  $(r_{**}, s_{**}) = (0, 0)$  this is

$$J(r_{**}, s_{**}) = \begin{pmatrix} \alpha & 0 \\ 0 & -\gamma \end{pmatrix} \quad (3.4)$$

The eigenvalues are  $\lambda_+ = \alpha$  and  $\lambda_- = -\gamma$ . Since  $\lambda_+ > 0$  and  $\lambda_- < 0$  the equilibrium point  $(r_{**}, s_{**}) = (0, 0)$  is a saddle point.

At the equilibrium point  $(r_*, s_*) = \left(\frac{\gamma}{\delta}, \frac{\alpha}{\beta}\right)$  the Jacobian is

$$J(r_*, s_*) = \begin{pmatrix} 0 & -\frac{\beta\gamma}{\delta} \\ \frac{\delta\alpha}{\beta} & 0 \end{pmatrix} \quad (3.5)$$

The eigenvalues follow from

$$\begin{vmatrix} -\lambda & -\frac{\beta\gamma}{\delta} \\ \frac{\delta\alpha}{\beta} & -\lambda \end{vmatrix} = 0 \quad \rightarrow \quad \lambda^2 + \alpha\gamma = 0. \quad (3.6)$$

The eigenvalues are  $\lambda_+ = i\sqrt{\alpha\gamma}$  and  $\lambda_- = -i\sqrt{\alpha\gamma}$ . Since the eigenvalues are pure imaginary the equilibrium point  $(r_*, s_*) = (\gamma/\delta, \alpha/\beta)$  is a center. The solutions near this center are periodic. We consider the dynamics close to the equilibrium point  $(r_*, s_*)$ . That is, we take  $r(t) = r_* + \eta(t)$  and  $s(t) = s_* + \epsilon(t)$ . Then we have the system

$$\frac{d\eta}{dt} = -\frac{\beta\gamma}{\delta}\epsilon - \beta\epsilon\eta \quad , \quad \frac{d\epsilon}{dt} = \frac{\delta\alpha}{\beta}\eta + \delta\eta\epsilon. \quad (3.7)$$

For  $\eta$  and  $\epsilon$  very small we have the approximation

$$\frac{d\eta}{dt} \approx -\frac{\beta\gamma}{\delta}\epsilon \quad , \quad \frac{d\epsilon}{dt} \approx \frac{\delta\alpha}{\beta}\eta, \quad (3.8)$$

from which it follows that  $\ddot{\eta} \approx -\alpha\gamma\eta$  and  $\ddot{\epsilon} \approx -\alpha\gamma\epsilon$ . The solutions are  $\eta(t) \approx \chi \sin(\sqrt{\alpha\gamma}t + \theta)$  and  $\epsilon(t) \approx \xi \sin(\sqrt{\alpha\gamma}t + \phi)$ , where  $\theta = \arcsin(\eta(0)/\chi)$  and  $\phi = \arcsin(\epsilon(0)/\xi)$ .

There is no analytical solution for  $r(t)$  and  $s(t)$ . One can eliminate  $t$  by dividing the two equations of motion:

$$\frac{dr}{ds} = \frac{\alpha r - \beta r s}{-\gamma s + \delta r} = \frac{(\alpha - \beta s)r}{(-\gamma + \delta r)s}. \quad (3.9)$$

Separation of variables gives

$$\frac{(-\gamma + \delta r)}{r} dr = \frac{(\alpha - \beta s)}{s} ds \quad \rightarrow \quad \left(\frac{-\gamma}{r} + \delta\right) dr = \left(\frac{\alpha}{s} - \beta\right) ds. \quad (3.10)$$

Integration gives

$$\int \left(\frac{-\gamma}{r} + \delta\right) dr = \int \left(\frac{\alpha}{s} - \beta\right) ds \quad \rightarrow \quad -\gamma \ln r + \delta r + c = \alpha \ln s - \beta s, \quad (3.11)$$

where  $c$  is the constant of integration. Exponentiation of both sides leads to

$$K = r^\gamma s^\alpha e^{-\delta r - \beta s}, \quad (3.12)$$

where  $K = e^c$  is a constant of motion:  $\dot{K} = 0$ . Its value is therefore determined by the initial conditions:

$$K = r_0^\gamma s_0^\alpha e^{-\delta r_0 - \beta s_0}. \quad (3.13)$$

For a given  $r$  the equation (3.12) delivers two values for  $s$ . If after a while the number of rabbits is again the earlier  $r$ , the values for  $s$  will be the earlier values since  $K$  is a constant of motion. As a consequence the parametric plot of  $(r(t), s(t))$  is a closed curve.

As an example we consider the situation for  $\alpha = 0.05$ ,  $\beta = 0.005$ ,  $\gamma = 0.025$  and  $\delta = 0.00025$ . The equilibrium point  $\left(\frac{\gamma}{\delta}, \frac{\alpha}{\beta}\right)$  is the point  $(100, 10)$ . For the initial condition  $r_0 = 50$  and  $s_0 = 10$  the evolution of  $r$  and  $s$  is shown in the left panel of figure 3.1. The parametric plot is shown in the right panel of figure 3.1. The arrow in the parametric curve indicates the evolution in forward time. The time unit is arbitrary, something like days or weeks or so.

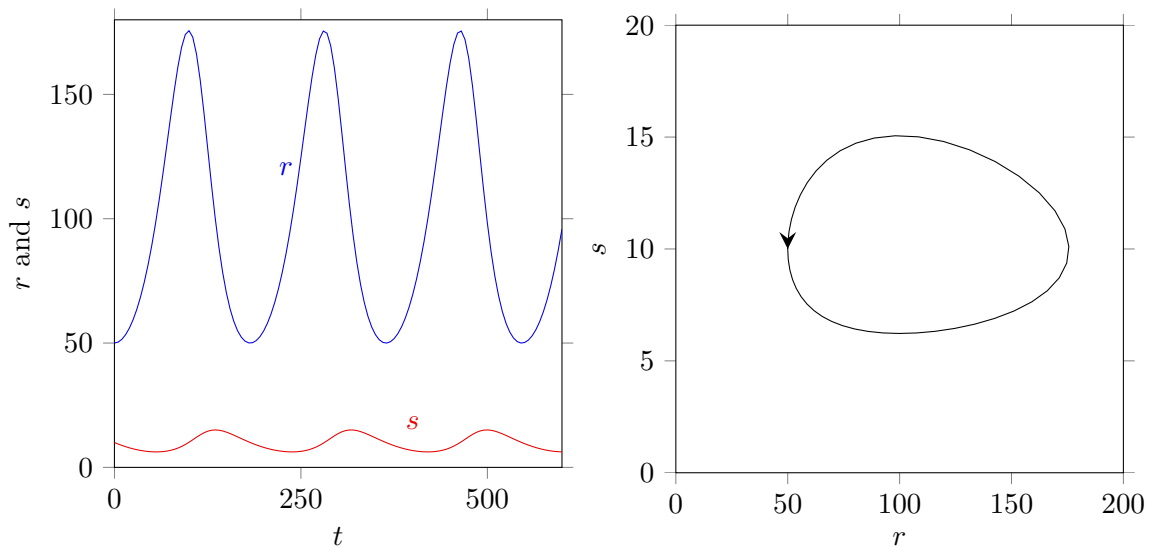


Figure 3.1: Evolution of the population size of rabbits  $r$  and stoats  $s$  (left panel) and the parametric plot (right panel). See the text for the initial conditions and the constants.

Next we consider the population dynamics close to the equilibrium point  $(100, 10)$ . To be specific, we take the initial conditions  $r_0 = 90$  and  $s_0 = 10$ . The result is shown in figure 3.2. As expected, the closer the populations are to the equilibrium point  $(100, 10)$ , the more the parametric plot looks like an ellipse. And the closer the populations are to the equilibrium point  $(100, 10)$ , the closer is the period of the oscillation to  $2\pi/\sqrt{\alpha\gamma} = 177.7$ . Indeed, in figure 3.2 the period is approximately 177.7, while in figure 3.1 the period is approximately 182.

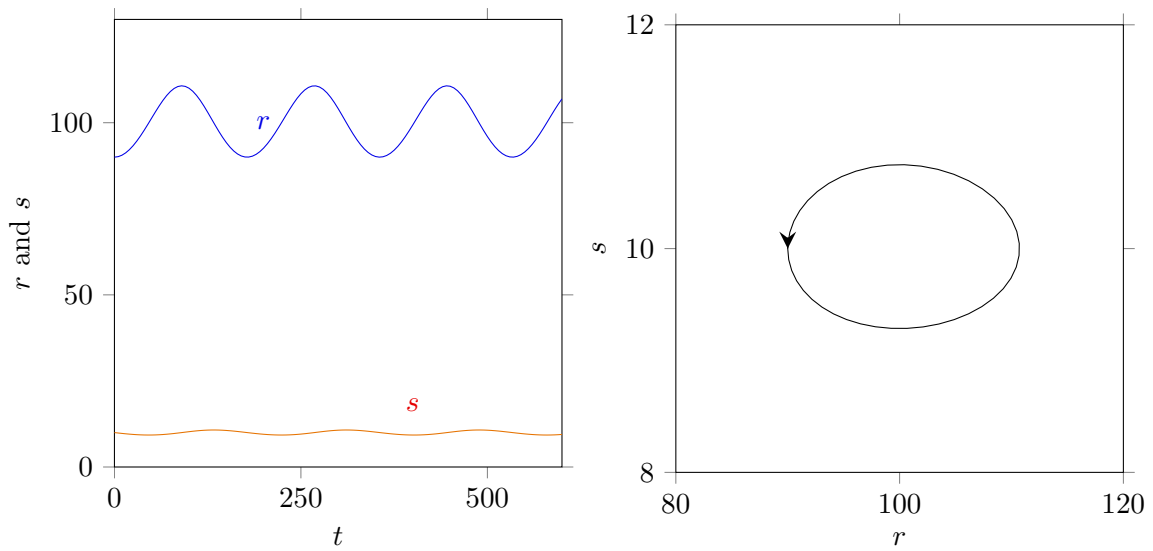


Figure 3.2: Evolution of the population size of rabbits  $r$  and stoats  $s$  (left panel) and the parametric plot (right panel). See the text for the initial conditions and the constants.

If we take the equilibrium point  $(100, 10)$  as the initial populations, then the  $r(t)$  and  $s(t)$  curves are horizontal lines and the parametric plot is the single point  $(100, 10)$ . From the figures [3.1](#) and [3.2](#) we see the shape of the parametric curve depends on the initial condition. Parametric curves are drawn for  $s_0 = 10$  and  $r_0 = 10$  through 100 in steps of 10 in figure [3.3](#).

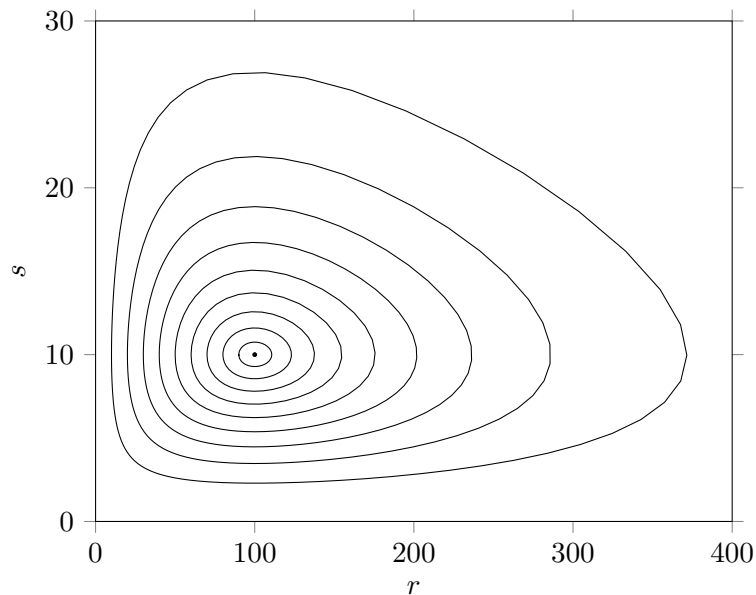


Figure 3.3: Parametric plots for various initial conditions. The rotation is anti-clockwise.

Close to the equilibrium point  $(100, 10)$  the parametric curve is almost an ellipse, while far away from the equilibrium point  $(100, 10)$  it rather is a triangle with rounded corners.

Since we do not have an analytical solution for  $r(t)$  and  $s(t)$  we have to resort to numerical methods for the plots. To this end we write  $\dot{r}$  as  $\frac{r_{n+1} - r_n}{\Delta t}$  and  $\dot{s}$  as  $\frac{s_{n+1} - s_n}{\Delta t}$ . Then

$$\begin{aligned} r_{n+1} &= r_n + \alpha \Delta t r_n - \beta \Delta t r_n s_n \\ s_{n+1} &= s_n - \gamma \Delta t s_n + \delta \Delta t s_n r_n, \end{aligned} \quad (3.14)$$

with  $r_0$  and  $s_0$  as the starting values. Absorbing  $\Delta t$  in the constants, thus  $a = \alpha \Delta t$ ,  $b = \beta \Delta t$ , etc., we obtain

$$\begin{aligned} r_{n+1} &= r_n + a r_n - b r_n s_n \\ s_{n+1} &= s_n - c s_n + d s_n r_n, \end{aligned} \quad (3.15)$$

The latter is a discrete system of difference equations. It often is considered as a more appropriate model for the prey-predator system than the continuous system.

The equilibrium points of the discrete system follow from  $r_{n+1} = r_n = L$  and  $s_{n+1} = s_n = K$ . They are  $(L, K) = (0, 0)$  and  $(L, K) = \left(\frac{c}{d}, \frac{a}{b}\right)$ . For the stability analysis of the equilibrium points we write the system of equations as  $r_{n+1} = f(r_n, s_n)$  and  $s_{n+1} = g(r_n, s_n)$ , where  $f(r, s) = r + a r - b r s$  and  $g(r, s) = s - c s + d s r$ . The Jacobian of the system is

$$J(r, s) = \begin{pmatrix} \frac{\partial f}{\partial r} & \frac{\partial f}{\partial s} \\ \frac{\partial g}{\partial r} & \frac{\partial g}{\partial s} \end{pmatrix} = \begin{pmatrix} 1 + a - b s & -b r \\ d s & 1 - c + d r \end{pmatrix} \quad (3.16)$$

At the equilibrium point  $(0, 0)$  the Jacobian is

$$J(0, 0) = \begin{pmatrix} 1 + a & 0 \\ 0 & 1 - c \end{pmatrix} \quad (3.17)$$

The eigenvalues are  $\lambda_+ = 1 + a$  and  $\lambda_- = 1 - c$ . For  $a > 0$  and  $0 < c < 2$  there holds  $|\lambda_+| > 1$  and  $|\lambda_-| < 1$ . That is, for  $a > 0$  and  $0 < c < 2$  the equilibrium point  $(0, 0)$  is a saddle.

At the equilibrium point  $\left(\frac{c}{d}, \frac{a}{b}\right)$  the Jacobian is

$$J\left(\frac{c}{d}, \frac{a}{b}\right) = \begin{pmatrix} 1 & -\frac{bc}{d} \\ \frac{ad}{b} & 1 \end{pmatrix} \quad (3.18)$$

The eigenvalues follow from

$$\begin{vmatrix} 1 - \lambda & -\frac{bc}{d} \\ \frac{ad}{b} & 1 - \lambda \end{vmatrix} = 0 \quad \rightarrow \quad (\lambda - 1)^2 + ac = 0. \quad (3.19)$$

The eigenvalues are  $\lambda_+ = 1 + i\sqrt{ac}$  and  $\lambda_- = 1 - i\sqrt{ac}$ . Since the eigenvalues are complex the solutions are periodic. Since the moduli of the complex eigenvalues are larger than 1

the equilibrium point  $\left(\frac{c}{d}, \frac{a}{b}\right)$  is an unstable focus. The curve is spiraling outwards. For  $a = 0.05$ ,  $b = 0.005$ ,  $c = 0.025$ ,  $d = 0.00025$ ,  $r_0 = 50$  and  $s_0 = 10$  the evolution of  $r$  and  $s$  and the parametric plot is shown in figure 3.4.

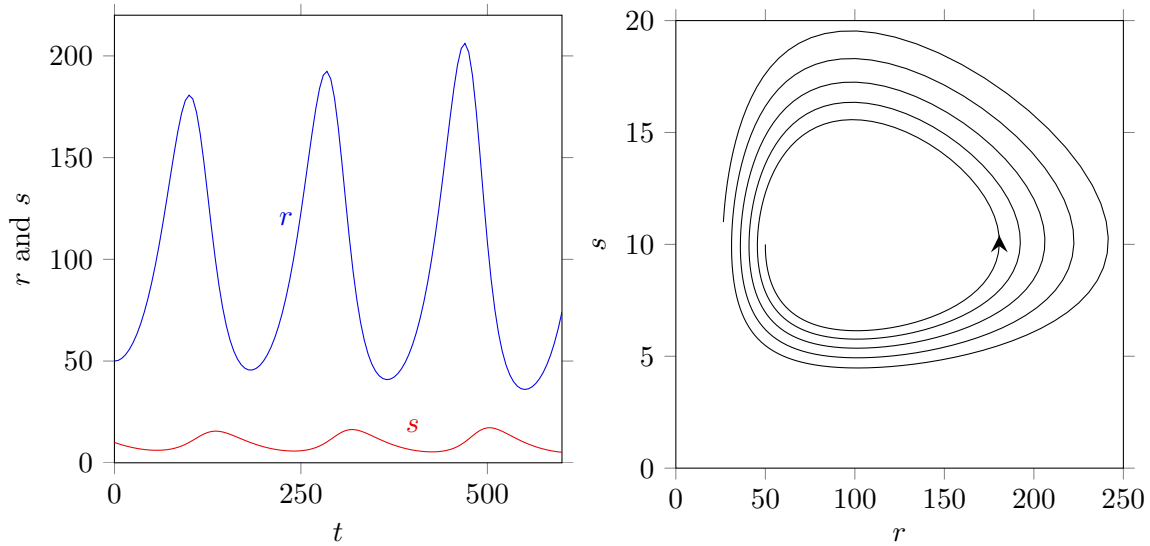


Figure 3.4: Evolution of the population size of rabbits  $r$  and stoats  $s$  (left panel) and the parametric plot (right panel) according to the difference equations as given in the text.

### 3.2 Modified Lotka-Volterra model

According to the system of equations (3.22) the population of rabbits will grow to infinity when stoats are absent. Of course this is not realistic. In reality the population of rabbits can not grow to infinity because of the limited amount of food. When stoats (and other predators) are absent the evolution of rabbits will be rather something like the logistic equation:

$$\dot{r} = \frac{dr}{dt} = \alpha r - \mu r^2, \quad (3.20)$$

where  $\alpha > 0$  and  $\mu > 0$  are constants. The equilibrium points are  $r_* = \frac{\alpha}{\mu}$  (stable) and  $r_{**} = 0$  (unstable). Writing the initial condition as  $r(0) = r_0$ , the analytical solution reads

$$r(t) = \frac{\alpha r_0}{\mu r_0 + (\alpha - \mu r_0)e^{-\alpha t}}. \quad (3.21)$$

The solution has the property:  $\lim_{t \rightarrow \infty} r(t) = \frac{\alpha}{\mu}$  as required.



If we do take the limited growth of the rabbit population into account the rabbit-stoat system is modified to

$$\dot{r} = \frac{dr}{dt} = \alpha r - \mu r^2 - \beta r s \quad , \quad \dot{s} = \frac{ds}{dt} = -\gamma s + \delta s r . \quad (3.22)$$

The modified Lotka-Volterra system has the equilibrium points  $(0, 0)$ ,  $\left(\frac{\alpha}{\mu}, 0\right)$  and  $\left(\frac{\gamma}{\delta}, \frac{\alpha\delta - \gamma\mu}{\beta\delta}\right)$ . The Jacobian of the system is

$$J(r, s) = \begin{pmatrix} \alpha - 2\mu r - \beta s & -\beta r \\ \delta s & -\gamma + \delta r \end{pmatrix} \quad (3.23)$$

At the equilibrium point  $(0, 0)$  the Jacobian is

$$J(0, 0) = \begin{pmatrix} \alpha & 0 \\ 0 & -\gamma \end{pmatrix} \quad (3.24)$$

with eigenvalues  $\lambda_+ = \alpha > 0$  and  $\lambda_- = -\gamma < 0$ . The equilibrium point  $(0, 0)$  therefore is a saddle.

At the equilibrium point  $\left(\frac{\alpha}{\mu}, 0\right)$  the Jacobian is

$$J\left(\frac{\alpha}{\mu}, 0\right) = \begin{pmatrix} -\alpha & -\frac{\alpha\beta}{\mu} \\ 0 & -\gamma + \frac{\alpha\delta}{\mu} \end{pmatrix} \quad (3.25)$$

The eigenvalues are  $\lambda_+ = -\alpha$  and  $\lambda_- = -\gamma + \frac{\alpha\delta}{\mu}$ . Now  $\lambda_+ < 0$  while  $\lambda_- > 0$  if  $\alpha\delta > \gamma\mu$  and  $\lambda_- < 0$  if  $\alpha\delta < \gamma\mu$ . Thus  $\left(\frac{\alpha}{\mu}, 0\right)$  is a stable node if  $\alpha\delta < \gamma\mu$  and a saddle if  $\alpha\delta > \gamma\mu$ .

At the equilibrium point  $\left(\frac{\gamma}{\delta}, \frac{\alpha\delta - \gamma\mu}{\beta\delta}\right)$  the Jacobian is

$$J\left(\frac{\gamma}{\delta}, \frac{\alpha\delta - \gamma\mu}{\beta\delta}\right) = \begin{pmatrix} -\frac{\gamma\mu}{\delta} & -\frac{\beta\gamma}{\delta} \\ \frac{\alpha\delta - \gamma\mu}{\beta} & 0 \end{pmatrix} \quad (3.26)$$

The eigenvalues are

$$\lambda_{\pm} = -\frac{\gamma\mu}{2\delta} \pm \sqrt{\left(\frac{\gamma\mu}{2\delta}\right)^2 + \frac{\gamma^2\mu}{\delta} - \alpha\gamma} \quad (3.27)$$

Also for the modified Lotka-Volterra model we consider the situation for  $\alpha = 0.05$ ,  $\beta = 0.005$ ,  $\gamma = 0.025$  and  $\delta = 0.00025$ . Suppose we take  $\mu = 0.0001$ . For these numerical values of the constants the equilibrium point  $\left(\frac{\gamma}{\delta}, \frac{\alpha\delta - \gamma\mu}{\beta\delta}\right)$  is the point  $(100, 8)$  and the eigenvalues of the Jacobian at this point are  $\lambda_{\pm} \approx -0.005 \pm i 0.031225$ . So,  $(100, 8)$  is a stable focus. The equilibrium point  $\left(\frac{\alpha}{\mu}, 0\right)$  is  $(500, 0)$  and the eigenvalues of the Jacobian at this point are  $-0.05$  and  $0.1$ . So,  $(500, 0)$  is a saddle for these constants. For the initial condition  $r_0 = 20$  and  $s_0 = 5$  the evolution of  $r$  and  $s$  is shown in the left panel of figure [3.5](#). The parametric plot is shown in the right panel of figure [3.5](#).

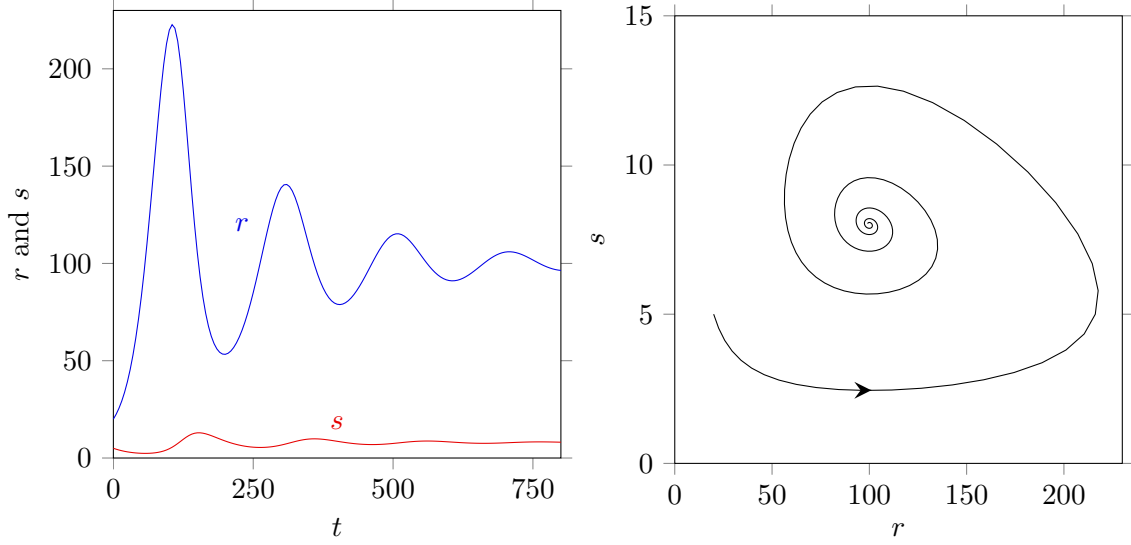


Figure 3.5: Evolution of the population size of rabbits  $r$  and stoats  $s$  (left panel) and the parametric plot (right panel). See the text for the initial conditions and the constants.

Applying Euler's method we obtain the discrete equivalent of the modified system of equations:

$$\begin{aligned} r_{n+1} &= r_n + \alpha \Delta t r_n - \mu \Delta t r_n^2 - \beta \Delta t r_n s_n \\ s_{n+1} &= s_n - \gamma \Delta t s_n + \delta \Delta t s_n r_n, \end{aligned} \quad (3.28)$$

with  $r_0$  and  $s_0$  as the starting values. Absorbing  $\Delta t$  in the constants, thus  $a = \alpha \Delta t$ ,  $b = \beta \Delta t$ , etc., we obtain

$$\begin{aligned} r_{n+1} &= r_n + a r_n - m r_n^2 - b r_n s_n \\ s_{n+1} &= s_n - c s_n + d s_n r_n. \end{aligned} \quad (3.29)$$

The equilibrium points  $(L, K)$  of the discrete system follow from  $r_{n+1} = r_n = L$  and  $s_{n+1} = s_n = K$ . Thus  $L = L + aL - mL^2 - bLK$  and  $K = K - cK + dKL$ . Solving for  $L$  and  $K$  we obtain the following three equilibrium points:  $(0, 0)$ ,  $(\frac{a}{m}, 0)$  and  $(\frac{c}{d}, \frac{ad - cm}{bd})$ . For the stability analysis of the equilibrium points we write the system as  $r_{n+1} = f(r_n, s_n)$  and  $s_{n+1} = g(r_n, s_n)$ , where  $f(r, s) = r + ar - mr^2 - brs$  and  $g(r, s) = s - cs + dsr$ . The Jacobian of the system is

$$J(r, s) = \begin{pmatrix} \frac{\partial f}{\partial r} & \frac{\partial f}{\partial s} \\ \frac{\partial g}{\partial r} & \frac{\partial g}{\partial s} \end{pmatrix} = \begin{pmatrix} 1 + a - 2mr - bs & -br \\ ds & 1 - c + dr \end{pmatrix} \quad (3.30)$$

At the equilibrium point  $(0, 0)$  the Jacobian is

$$J(0, 0) = \begin{pmatrix} 1 + a & 0 \\ 0 & 1 - c \end{pmatrix}. \quad (3.31)$$

The eigenvalues are  $\lambda_+ = 1 + a$  and  $\lambda_- = 1 - c$ . For  $a > 0$  and  $0 < c < 2$  we have  $|\lambda_+| > 1$  and  $|\lambda_-| < 1$  and the equilibrium point  $(0, 0)$  is a saddle.

At the equilibrium point  $\left(\frac{a}{m}, 0\right)$  the Jacobian is

$$J\left(\frac{a}{m}, 0\right) = \begin{pmatrix} 1 - a & -\frac{ab}{m} \\ 0 & 1 - c + \frac{ad}{m} \end{pmatrix}. \quad (3.32)$$

The eigenvalues are  $\lambda_+ = 1 - a$  and  $\lambda_- = 1 - c + \frac{ad}{m}$ . Depending on the values of  $a$ ,  $c$ ,  $d$  and  $m$  the equilibrium point  $\left(\frac{a}{m}, 0\right)$  is a stable node or an unstable node.

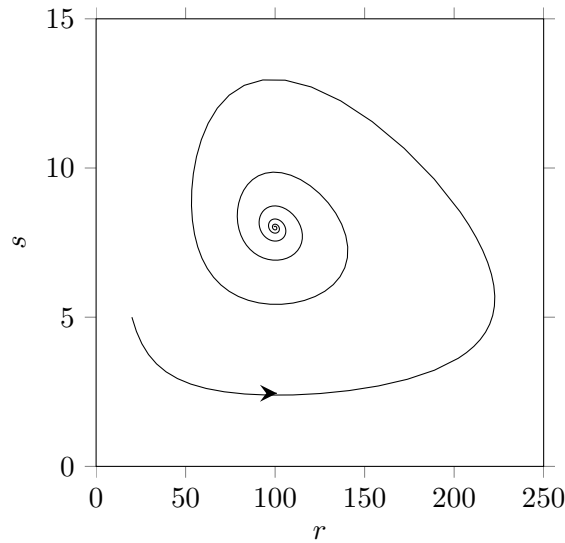
At the equilibrium point  $\left(\frac{c}{d}, \frac{ad - cm}{bd}\right)$  the Jacobian is

$$J\left(\frac{c}{d}, \frac{ad - cm}{bd}\right) = \begin{pmatrix} 1 - \frac{cm}{d} & -\frac{bc}{d} \\ \frac{ad - cm}{b} & 1 \end{pmatrix}. \quad (3.33)$$

The eigenvalues are

$$\lambda_{\pm} = 1 - \frac{cm}{2d} \pm \sqrt{\left(\frac{cm}{2d}\right)^2 + \frac{c^2m}{2d} - ac}. \quad (3.34)$$

For  $a = 0.05$ ,  $b = 0.005$ ,  $c = 0.025$ ,  $d = 0.00025$  and  $m = 0.0001$  the latter is  $\lambda_{\pm} \approx 0.995 \pm i0.031225$  and the equilibrium point  $\left(\frac{c}{d}, \frac{ad - cm}{bd}\right) = (100, 8)$ . Since the modulus of  $0.995 \pm i0.031225$  is smaller than 1 the equilibrium point  $(100, 8)$  is a stable focus. The node  $\left(\frac{a}{m}, 0\right) = (500, 0)$  and the eigenvalues of the Jacobian at this node are  $\lambda_+ = 1 - a = 0.95$  and  $\lambda_- = 1 - c + \frac{ad}{m} = 1.1$ . So,  $(500, 0)$  is a saddle. For  $r_0 = 20$  and  $s_0 = 5$  the parametric plot, see next figure, is quite similar to the parametric plot in figure [3.5](#).



### 3.3 Hénon map

The Hénon map is non-linear map. The two dimensional first order Hénon map reads

$$\begin{aligned}x_{m+1} &= 1 - ax_m^2 + y_m \\ y_{m+1} &= bx_m,\end{aligned}\tag{3.35}$$

where  $a$  and  $b$  are constants and where  $(x_0, y_0)$  is the starting position. For  $a = 1.4$  and  $b = 0.3$  the points  $(x_m, y_m)$  are attracted to a so called strange attractor, see next figure.

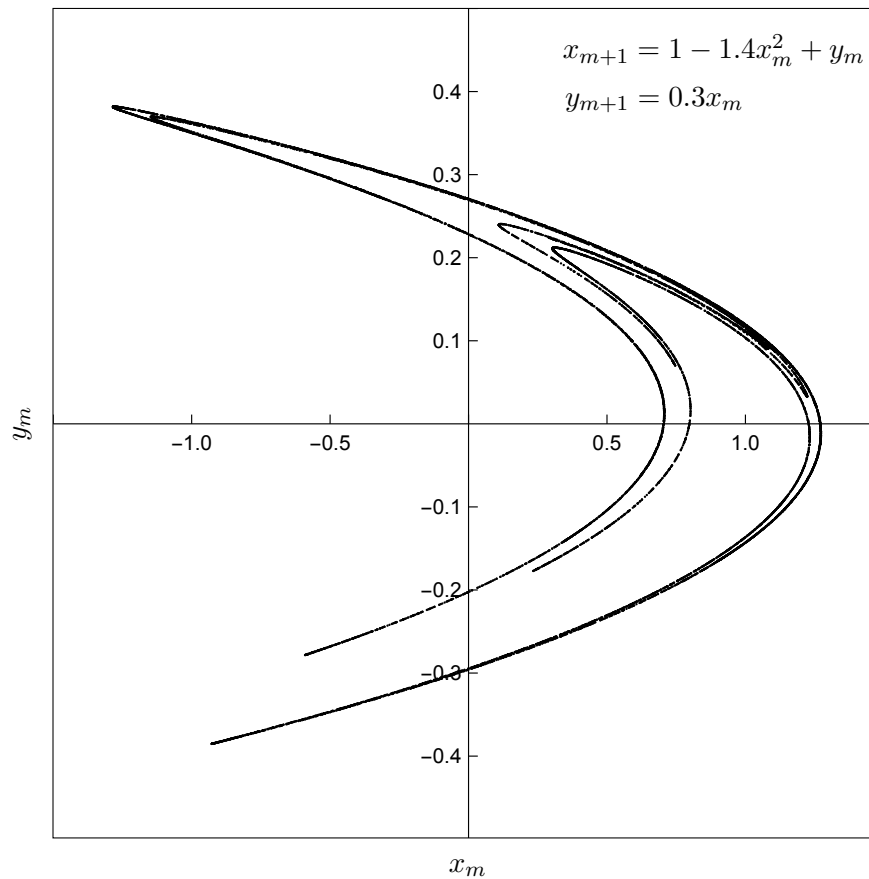
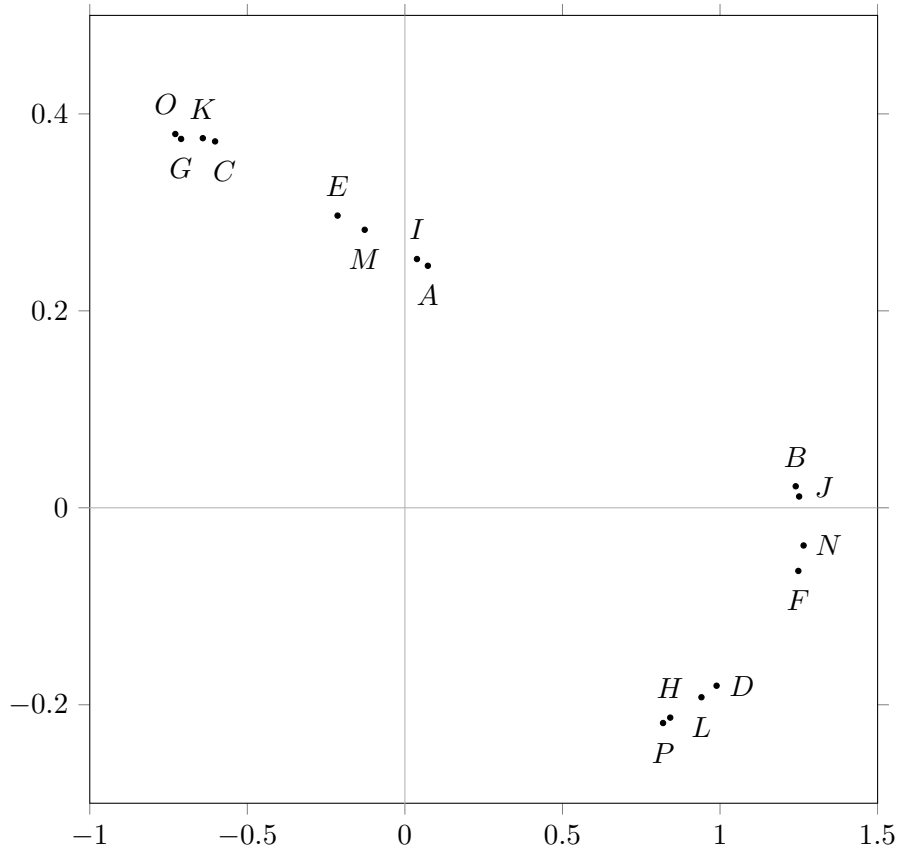


Figure 3.6: Attractor of the map  $x_{m+1} = 1 - ax_m^2 + y_m$ ,  $y_{m+1} = bx_m$  for  $a = 1.4$  and  $b = 0.3$ .

Periodic limit cycli are also possible. For  $b = 0.3$  a period 1 limit changes to a period 2 limit when  $a = 0.3675$ . The period 2 limit changes to a period 4 limit when  $a = 0.9125$ , which in turn changes to a period 8 limit when  $a \approx 1.026$ , etc. A period 16 limit is shown in the next figure. The period 16 limit cycle is depicted by the symbols  $A$  through  $P$ . For instance, starting the cycle in point  $N$  the next point is  $O$ , then  $P$ , then  $A$ , then  $B$  etc., through  $M$ . The larger  $n$  the more the  $n$  points of the period  $2^n$  limit cycle approaches the strange attractor of figure [3.6](#).



The two dimensional first order Hénon map (3.35) can also be written in the form of a one dimensional second order map:

$$x_{m+1} = 1 - ax_m^2 + bx_{m-1} \quad (3.36)$$

with  $x_0$  and  $x_1$  as the initial values.

Linear, one dimensional, second order difference equations, such as  $x_{m+1} = c - ax_m + bx_{m-1}$ , can be solved analytically, as we saw in chapter 1. It is the square in the one dimensional, second order difference equation (3.36), or in general the non-linearity, which makes the situation complicated: bifurcations and chaotic behaviour. Before we proceed we first have to outline the calculation of the Lyapunov exponent for two dimensional maps.

### 3.4 Lyapunov exponents for two dimensional maps

For a one dimensional map we already met the concept of a Lyapunov exponent when we considered the logistic equation. For a one dimensional iterative function  $f(x)$ ,  $x_{m+1} = f(x_m)$ , the Lyapunov exponent  $\lambda$  is given by

$$\lambda = \lim_{n \rightarrow \infty} \frac{1}{n} \sum_{m=0}^n \ln \left| \frac{\partial f}{\partial x} \right|_{x_m}. \quad (3.37)$$

For a two dimensional map  $x_{m+1} = f(x_m, y_m)$  and  $y_{m+1} = g(x_m, y_m)$ , we have to first order

$$\begin{aligned} x_1 + \delta_1 &= f(x_0 + \delta_0, y_0 + \epsilon_0) \approx f(x_0, y_0) + \delta_0 \left| \frac{\partial f}{\partial x} \right|_{(x_0, y_0)} + \epsilon_0 \left| \frac{\partial f}{\partial y} \right|_{(x_0, y_0)} \\ y_1 + \epsilon_1 &= g(x_0 + \delta_0, y_0 + \epsilon_0) \approx g(x_0, y_0) + \delta_0 \left| \frac{\partial g}{\partial x} \right|_{(x_0, y_0)} + \epsilon_0 \left| \frac{\partial g}{\partial y} \right|_{(x_0, y_0)}. \end{aligned} \quad (3.38)$$

Since  $x_1 = f(x_0, y_0)$  and  $y_1 = g(x_0, y_0)$  there holds

$$\begin{pmatrix} \delta_1 \\ \epsilon_1 \end{pmatrix} = \begin{pmatrix} \partial f(x, y)/\partial x & \partial f(x, y)/\partial y \\ \partial g(x, y)/\partial x & \partial g(x, y)/\partial y \end{pmatrix}_{[0]} \begin{pmatrix} \delta_0 \\ \epsilon_0 \end{pmatrix}, \quad (3.39)$$

where  $_{[0]}$  expresses that the derivatives are evaluated at  $(x_0, y_0)$ . The matrix with derivatives is the *Jacobian*:  $J_{[0]}$ . From  $(x_1, y_1)$  to  $(x_2, y_2)$  the errors go as

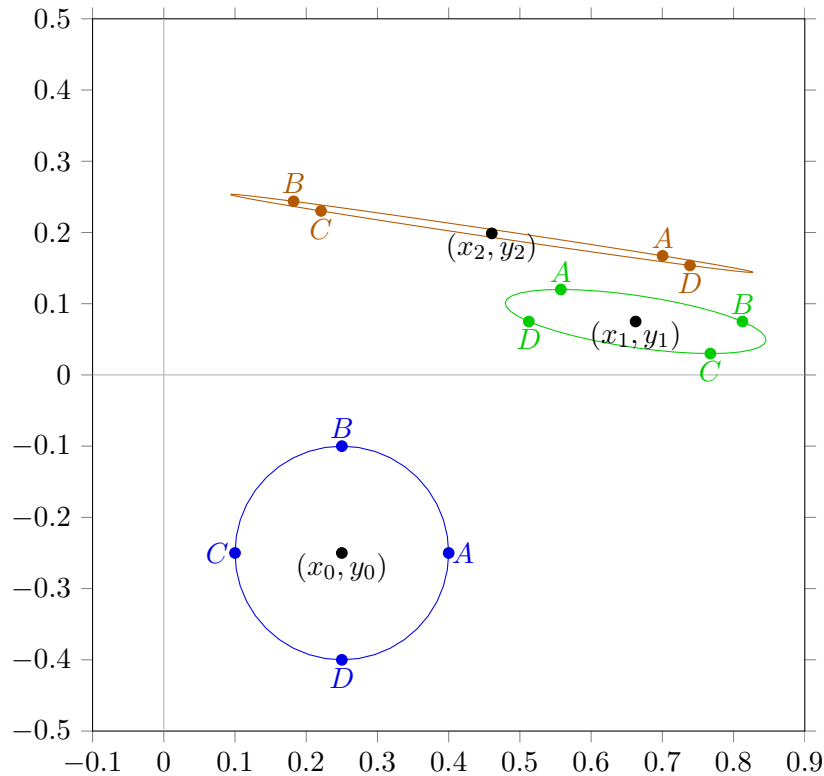
$$\begin{pmatrix} \delta_2 \\ \epsilon_2 \end{pmatrix} = \begin{pmatrix} \partial f(x, y)/\partial x & \partial f(x, y)/\partial y \\ \partial g(x, y)/\partial x & \partial g(x, y)/\partial y \end{pmatrix}_{[1]} \begin{pmatrix} \delta_1 \\ \epsilon_1 \end{pmatrix}, \quad (3.40)$$

where  $_{[1]}$  expresses that the derivatives are evaluated at  $(x_1, y_1)$ . The matrix with derivatives is the Jacobian:  $J_{[1]}$ . For  $2 \times 2$  matrices there are 2 eigenvalues and therefore 2 Lyapunov exponents. We are interested in the largest Lyapunov exponent. For the situation after two steps we have the product of 1 step Jacobians  $J_{[1]}$  and  $J_{[0]}$ :

$$\begin{pmatrix} \delta_2 \\ \epsilon_2 \end{pmatrix} = \begin{pmatrix} \partial f(x, y)/\partial x & \partial f(x, y)/\partial y \\ \partial g(x, y)/\partial x & \partial g(x, y)/\partial y \end{pmatrix}_{[1]} \begin{pmatrix} \partial f(x, y)/\partial x & \partial f(x, y)/\partial y \\ \partial g(x, y)/\partial x & \partial g(x, y)/\partial y \end{pmatrix}_{[0]} \begin{pmatrix} \delta_0 \\ \epsilon_0 \end{pmatrix}. \quad (3.41)$$

For increasing  $n$  the resulting product matrix becomes almost singular: determinant  $\rightarrow 0$ . Because of limited machine precision an almost singular matrix leads to large inaccuracies in the numerical calculation of the eigenvalues. For this reason the product of Jacobians is not used. Instead, the largest Lyapunov exponent will be extracted from the single step Jacobians.

To illustrate the method we follow the dynamics of the Hénon map a few steps. For the constants we take  $a = 1.4$  and  $b = 0.3$ . For these values the orbit is chaotic. For the present purpose we take  $(x_0, y_0) = (0.25, -0.25)$  as the initial point. We will follow the evolution of a circle with a small enough radius,  $r = 0.00015$ , with the initial point as its center. Then  $(x_1, y_1) = (0.6625, 0.075)$  and  $(x_2, y_2) = (0.46053125, 0.19875)$ . The evolution of the circle is shown in the next figure. For educational purposes the circle and its evolutionary curves are shown thousand times too large.



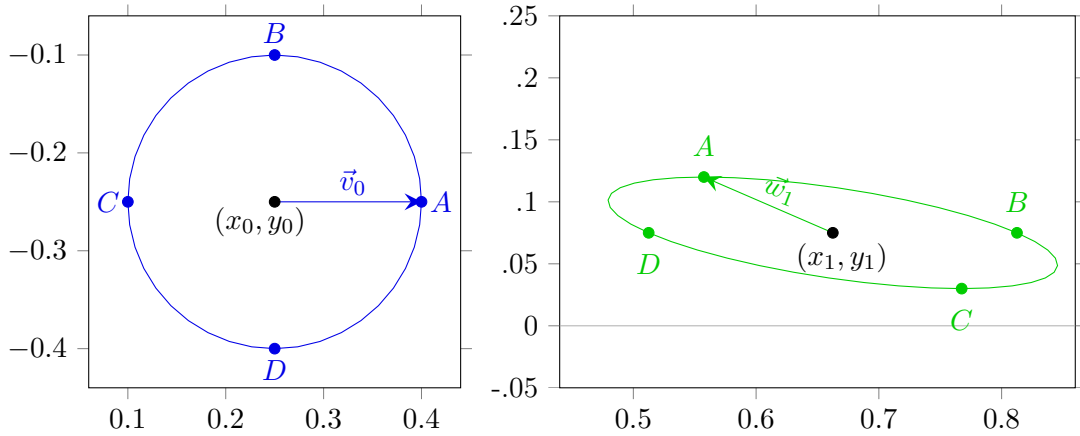
We see the initial blue circle has transformed into the green elliptic shape after the first step and to the brown elliptic shape after the second step. The blue points  $A$  through  $D$  have transformed in the green points  $A$  through  $D$  and brown points  $A$  through  $D$  respectively. The distance between brown point  $A$  and  $(x_2, y_2)$  is grown with respect to the distance between the blue point  $A$  and  $(x_0, y_0)$ . In case of a positive Lyapunov exponent the distance will grow and grow. After about hundred steps the distance is such large that second order effects are no longer negligible. To avoid a situation where second order effects are no longer negligible, the distance is resized after every step. We will outline the procedure step by step. For the blue circle the difference between the blue point  $A$  and  $(x_0, y_0)$  is the error vector  $\vec{v}_0$ :

$$\vec{v}_0 = \begin{pmatrix} \delta_0 \\ \epsilon_0 \end{pmatrix} = \begin{pmatrix} 0.00015 \\ 0 \end{pmatrix} \quad (3.42)$$

The vector  $\vec{v}_0$  is shown 1000 times too large in the left panel of the next figure. If we let the Jacobian for starting point  $(x_0, y_0)$  act on  $\vec{v}_0$  we get the vector  $\vec{w}_1$ . Explicitly

$$\vec{w}_1 = J_{[0]}\vec{v}_0 = \begin{pmatrix} -0.7 & 1 \\ 0.3 & 0 \end{pmatrix} \begin{pmatrix} 0.00015 \\ 0 \end{pmatrix} = \begin{pmatrix} -0.000105 \\ 0.000045 \end{pmatrix}. \quad (3.43)$$

The vector  $\vec{w}_1$  is with respect to point  $(x_1, y_1)$ . Together with the transformed circle it is drawn, 1000 times magnified, in the right panel of the next figure.



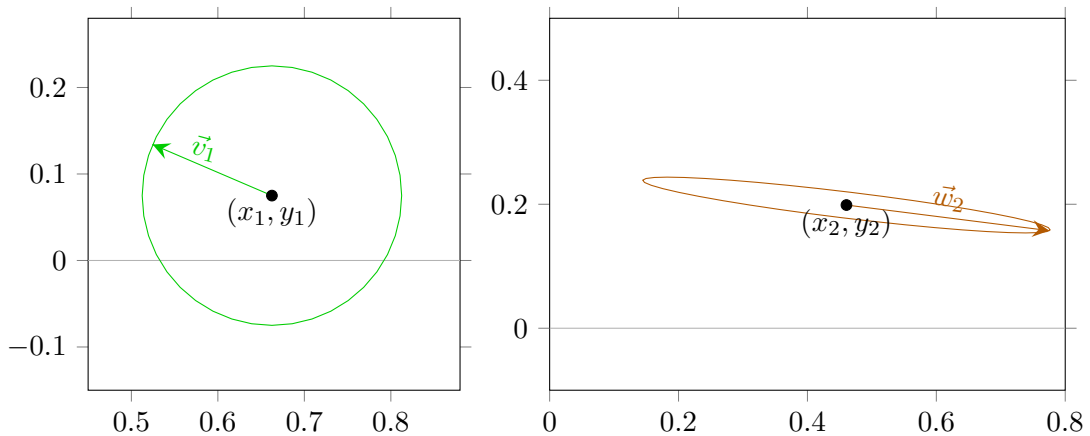
Now we proceed with a circle of radius 0.00015 with  $(x_1, y_1)$  as the center. From  $\vec{w}_1$  we construct a new vector  $\vec{v}_1$ , which has length 0.00015 and the same direction as  $\vec{w}_1$ :

$$\vec{v}_1 = \begin{pmatrix} -0.00013787 \\ 0.000059088 \end{pmatrix} \quad (3.44)$$

We let the Jacobian for point  $(x_1, y_1)$  act on the vector  $\vec{v}_1$  to obtain the vector  $\vec{w}_2$ :

$$\vec{w}_2 = J_{[1]} \vec{v}_1 = \begin{pmatrix} -1.855 & 1 \\ 0.3 & 0 \end{pmatrix} \begin{pmatrix} -0.00013787 \\ 0.00005908 \end{pmatrix} = \begin{pmatrix} 0.00031484 \\ -0.00004136 \end{pmatrix}. \quad (3.45)$$

The evolution of  $\vec{v}_1$  to  $\vec{w}_2$  is shown in the next figure.



From  $\vec{w}_2$  we construct a new vector  $\vec{v}_2$ , which has length 0.00015 and the same direction as  $\vec{w}_2$ . Then we let the Jacobian for point  $(x_2, y_2)$  act on the vector  $\vec{v}_2$  in order to obtain the vector  $\vec{w}_3$ . The procedure is repeated as long as desired. Often the length of  $\vec{w}_k$  is close to the length of the semi-major axis of the elliptic curve. One calculates for  $k = 0, 1, 2, 3, \dots$  the



ratio of the length of  $w_{k+1}$  and 0.00015 and take the logarithm of it in order to obtain  $\kappa_k$ :

$$\kappa_k = \ln \left( \frac{|w_{k+1}|}{0.00015} \right). \quad (3.46)$$

The results of the first 16 steps are shown in the next table.

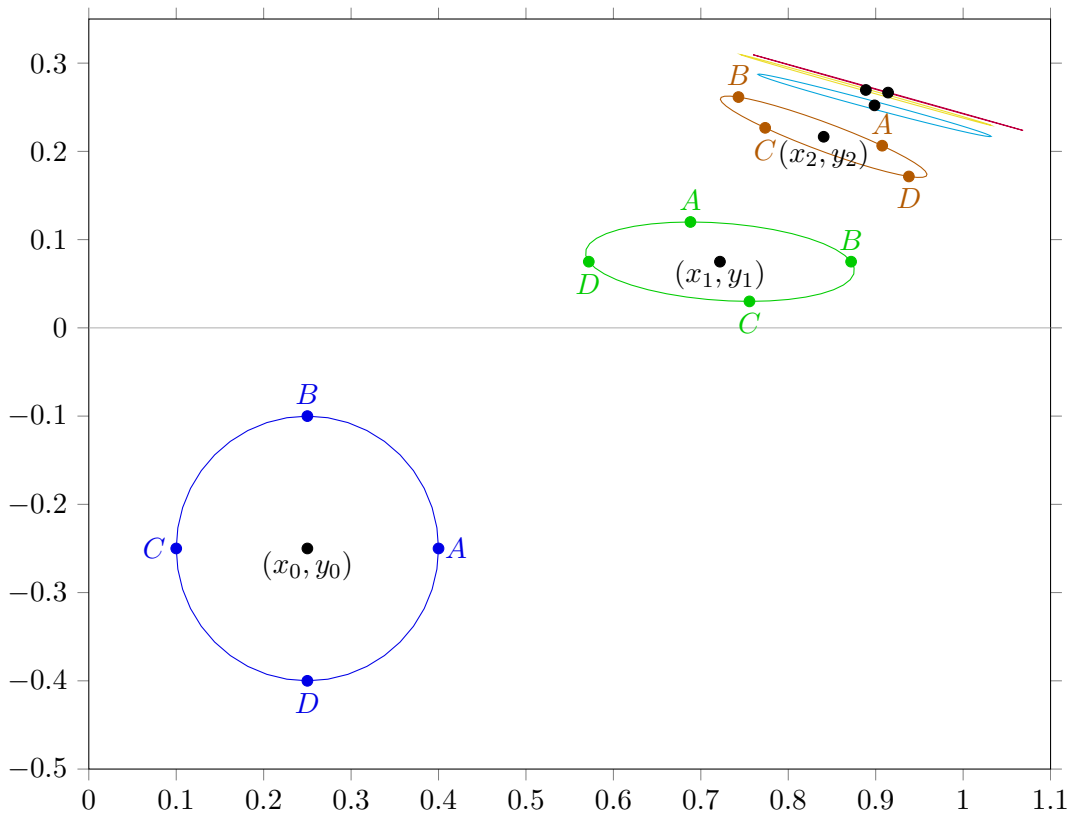
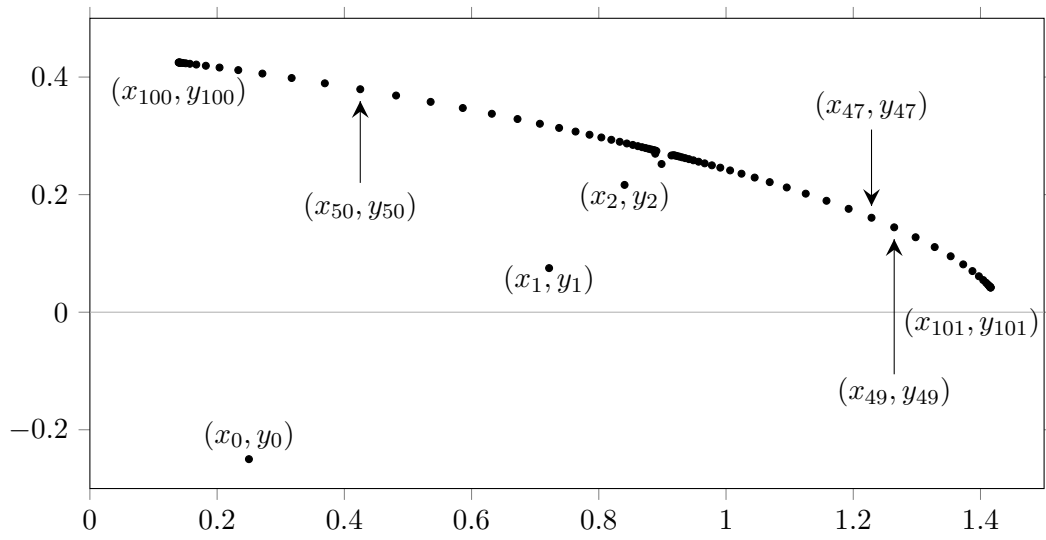
$k$	0	1	2	3	4	5	6	7
$\kappa_k$	-0.27236	0.74999	0.36451	0.99076	-1.14860	0.76630	1.24989	0.89729

$k$	8	9	10	11	12	13	14	15
$\kappa_k$	0.17350	0.25303	0.40657	0.95979	-0.85634	1.16730	1.18259	0.57448

The average value of the 16  $\kappa_k$  values shown in the table is  $\bar{\kappa} \approx 0.466$ . After 100 steps the average is  $\bar{\kappa} \approx 0.453$ , after 1000 steps  $\bar{\kappa} \approx 0.429$ , after 10 000 steps  $\bar{\kappa} \approx 0.427$  and after 100 000 steps  $\bar{\kappa} \approx 0.420$ . For the present example of the Hénon map with  $a = 1.4$  and  $b = 0.3$  the largest Lyapunov exponent found this way is 0.42.

Next we will consider the situation in case the largest Lyapunov exponent is negative. This is the case if the Hénon map converges to a limit cycle. For example, for  $a = 0.45$  and  $b = 0.3$  the Hénon map converges to a period 2 limit. The two fixed points are  $(0.13949, 0.42482)$  and  $(1.4161, 0.041848)$ . For this example we will consider the evolution. As for the previous example we start with the initial point  $(0.25, -0.25)$ . From  $(x_0, y_0) = (0.25, -0.25)$  it follows  $(x_1, y_1) = (0.721875, 0.075)$  and  $(x_2, y_2) = (0.840503, 0.216563)$ . The successive points are shown in the figure at the top of next page. We see initially big steps between successive points until the points are close to  $(0.90, 0, 27)$ . From there the points alternately jump between two branches, to the left for even  $k$  and to the right for odd  $k$ . For  $k > 100$  the points  $(x_k, y_k)$  are very close to the fixed points. The first five steps of the evolution of a circle with radius 0.00015 and center  $(x_0, y_0)$  is shown in the figure at the bottom of the next page. Also here the initial blue circle has transformed into a green elliptic shape after the first step and to a brown elliptic shape after the second step. The curve after the third step is cyan, after the fourth step yellow and after the fifth step purple. All curves are 1000 times magnified.

As for the previous example the error vector is resized at each new point. We should, because we do not know in advance whether or not the Lyapunov exponent is larger than zero.



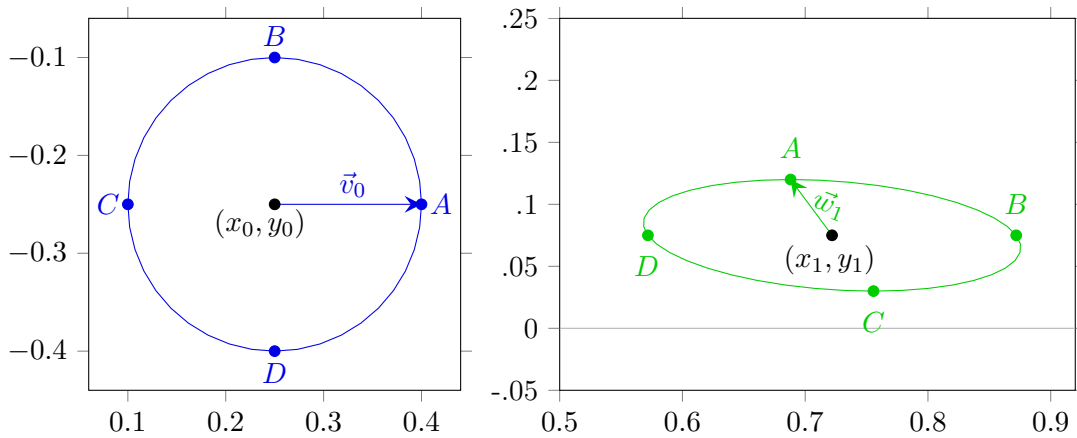
The difference between  $A(0.4, -0.25)$  and  $(x_0, y_0) = (0.25, -0.25)$  is the error vector  $\vec{v}_0$ :

$$\vec{v}_0 = \begin{pmatrix} \delta_0 \\ \epsilon_0 \end{pmatrix} = \begin{pmatrix} 0.00015 \\ 0 \end{pmatrix} \tag{3.47}$$

The vector  $\vec{v}_0$  is shown in the left panel of the next figure. If we let the Jacobian for starting point  $(x_0, y_0)$  act on  $\vec{v}_0$  we get the vector  $\vec{w}_1$ :

$$\vec{w}_1 = J_{[0]}\vec{v}_0 = \begin{pmatrix} -0.225 & 1 \\ 0.3 & 0 \end{pmatrix} \begin{pmatrix} 0.00015 \\ 0 \end{pmatrix} = \begin{pmatrix} -0.00003375 \\ 0.000045 \end{pmatrix}. \tag{3.48}$$

The vector  $\vec{w}_1$  and the transformed circle are drawn in the right panel of the next figure.



Again  $\vec{w}_1$  is resized to vector  $\vec{v}_1$ . Then  $\vec{w}_2$  is obtained from  $\vec{v}_1$  via  $\vec{w}_2 = J_{[1]}\vec{v}_1$ , and so on.

The  $\kappa$  values of the first 16 steps are shown in the next table.

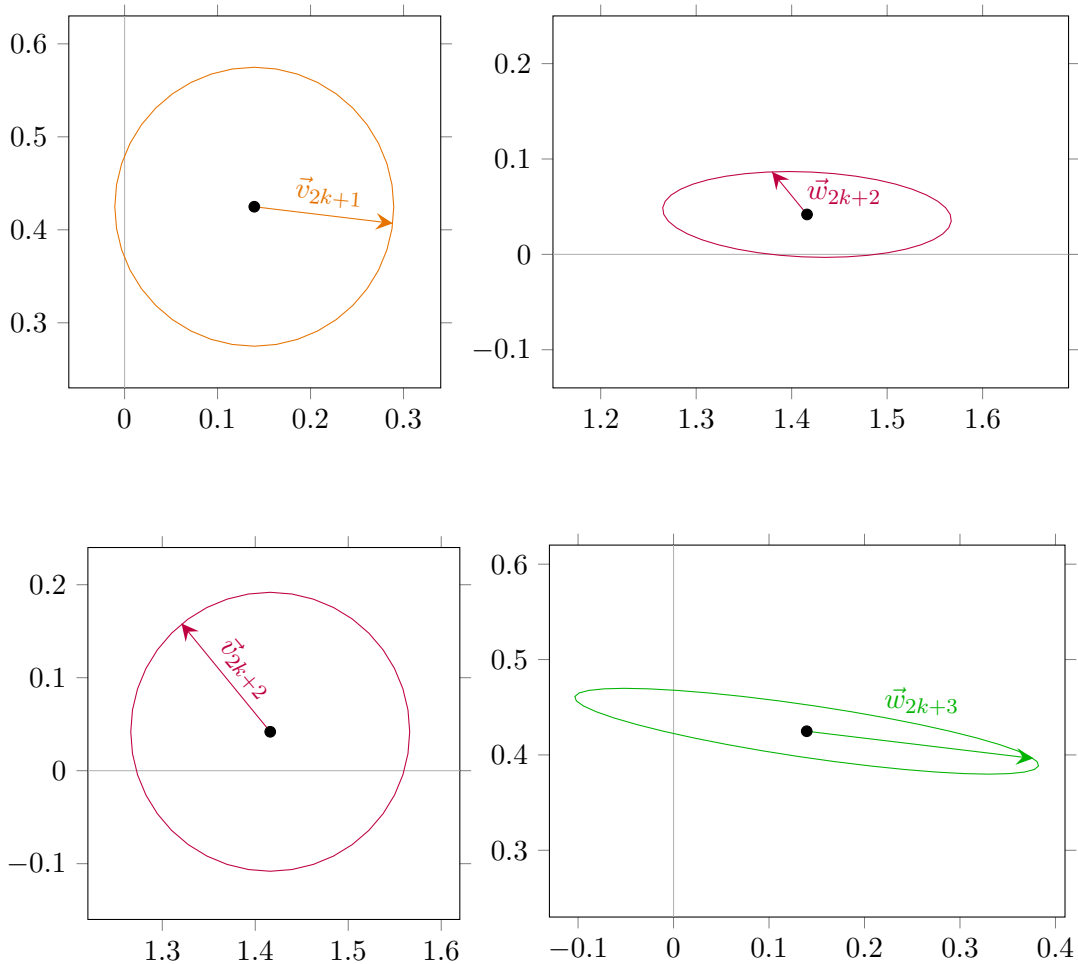
$k$	0	1	2	3	4	5	6	7
$\kappa_k$	-0.98083	0.18511	-0.05628	0.11209	0.06605	0.09703	0.07254	0.09795

$k$	8	9	10	11	12	13	14	15
$\kappa_k$	0.07087	0.10024	0.06825	0.10301	0.06510	0.10629	0.06134	0.11016

For the first 16 steps we find for the average value of the  $\kappa_k$ :  $\bar{\kappa} \approx 0.017$ . So, initially there is a little growth of the error. After 100 steps this is  $\bar{\kappa} \approx -0.083$ , after 1000 steps  $\bar{\kappa} \approx -0.228$ , after 10 000 steps  $\bar{\kappa} \approx -0.243$  and after 100 000 steps  $\bar{\kappa} \approx -0.244$ . For the Hénon map with

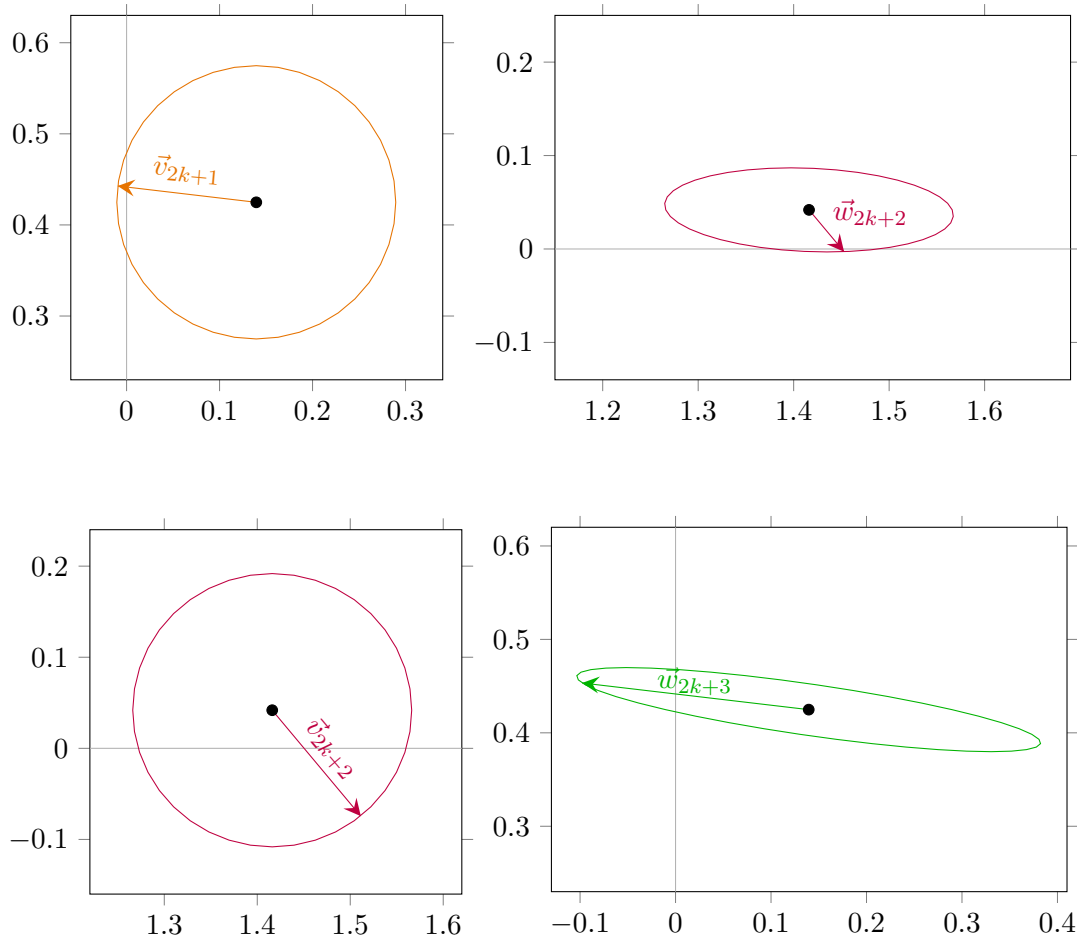
$a = 0.45$  and  $b = 0.3$  the largest Lyapunov exponent found this way is  $-0.244$ .

When the points are close to the fixed points the situation is as shown below.

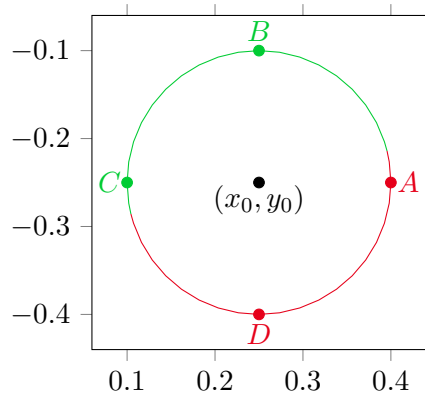


When the points alternate between the two fixed points, the errors also alternate. That is,  $w_{2k+4}$  is the same as  $w_{2k+2}$  and  $w_{2k+3}$  is the same as  $w_{2k+1}$ . For large  $k$ , say 1000 or more, the length of vector  $w_{2k+2}$  is a fraction 0.385052 of the length of  $v_{2k+1}$ , while the length of vector  $w_{2k+3}$  is a fraction 1.59261 of the length of  $v_{2k+2}$ . In effect there is a net decrease of  $\sqrt{0.385052 \cdot 1.59261} \approx .783$  per step. Taking the logarithm of it we find indeed a Lyapunov exponent of  $-0.244$ .

If we would have taken point  $B$  instead of  $A$  for the initial error, the  $\kappa_k$  will be different. When the points have arrived at the fixed points, the error vector happens to be opposite with respect to the situation for  $A$ , compare the figures on the next page with the ones above.



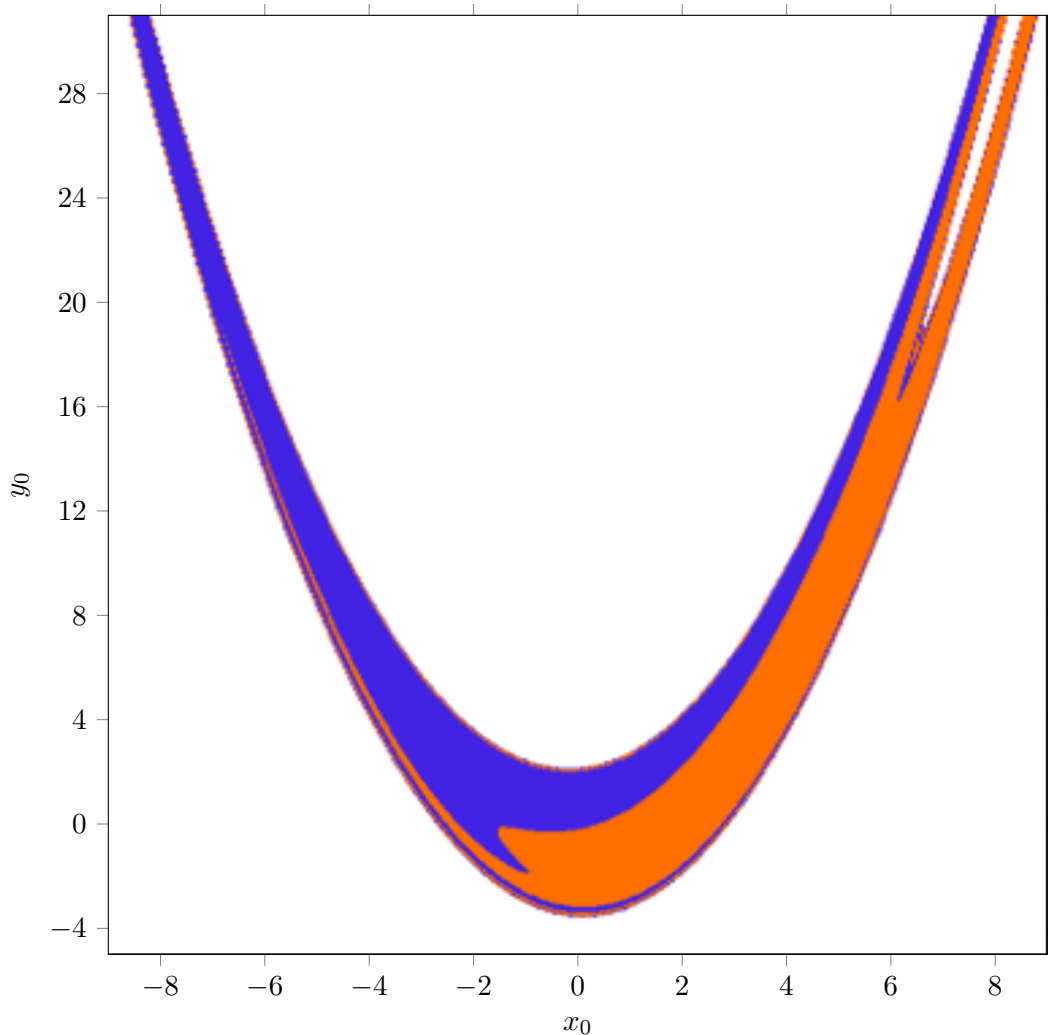
It makes clear that the Lyapunov exponent is independent of the direction of the error vector we start with. The question arises which initial errors lead, on the long run, to the same error vectors as initial error  $A$  and which to the same error vectors as initial error  $B$ . In the next diagram the part of the initial circle which leads to the same error vectors as  $A$  or  $B$  is shown red respectively green.



In case of two fixed points, say  $F_1$  and  $F_2$ , there are three possibilities:

1. for increasing  $k$  the points  $(x_{2k}, y_{2k})$  converge to  $F_1$  and the points  $(x_{2k+1}, y_{2k+1})$  converge to  $F_2$ ,
2. for increasing  $k$  the points  $(x_{2k}, y_{2k})$  converge to  $F_2$  and the points  $(x_{2k+1}, y_{2k+1})$  converge to  $F_1$ ,
3. the points  $(x_k, y_k)$  diverge to infinity.

We can colour each starting point  $(x_0, y_0)$  accordingly. As an example, for the Hénon map with  $a = 0.45$ ,  $b = 0.3$  the two fixed points are  $F_1(0.13949, 0.42482)$  and  $F_2(1.4161, 0.041848)$ . In case of possibility 1, 2 or 3 a starting point  $(x_0, y_0)$  is coloured blue, orange or white respectively. The result is shown in the next figure.



### 3.5 Orbits for the Hénon map

For  $x_0 = 0$ ,  $x_1 = 0$  and  $b = 0.3$  a plot of  $x_m$  against  $a$  for  $a = 0.3$  through  $a = 1.426$  is shown in figure 3.7. Under the same conditions the largest Lyapunov exponent is plotted against  $a$  in figure 3.8. The main period doubling cascade, the one with 1,2,4,8,... limit cycles, runs from  $a = -0.1225$  through  $a \approx 1.058$ . By inspection it is found that at  $a \approx 1.072374$  a period 12 limit cycle shows up. At  $a \approx 1.07288$  it turns into a period 24 limit cycle, a little further a period 48 cycle, etc. The whole  $3 \cdot 2^n$ ,  $n = 2, 3, 4, \dots$ , cascade takes place in a small window. A small change in  $a$  leads to a discontinuous change of the orbit at  $a \approx 1.0772$  and  $a \approx 1.0808$  and at other places. At  $a \approx 1.07878$  starts a period 18 limit cycle. Its period doubles at  $a \approx 1.07893$ . The whole  $9 \cdot 2^n$ ,  $n = 1, 2, 3, \dots$ , cascade ends at  $a \approx 1.07903$ . So, also this cascade takes place on a very small window. At  $a \approx 1.1001$  a period  $5 \cdot 2^n$ ,  $n = 1, 2, 3, \dots$ , sets in. At  $a \approx 1.1724$  a period  $9 \cdot 2^n$ ,  $n = 0, 1, 2, \dots$ , limit cycle sets in. At  $a \approx 1.17675$  a period  $5 \cdot 2^n$ ,  $n = 1, 2, 3, \dots$ , sets in. At  $a \approx 1.226$  a period  $7 \cdot 2^n$ ,  $n = 0, 1, 2, \dots$ , limit cycle sets in. The window is clearly visible in figure 3.7. At  $a \approx 1.299$  again a period  $7 \cdot 2^n$ ,  $n = 0, 1, 2, \dots$ , limit cycle sets in. Since it ends at  $a \approx 1.3065$  it also is visible in figure 3.7. At  $a \approx 1.3233$  a period  $2^n$ ,  $n = 3, 4, 5, \dots$ , limit cycle sets in and ends at  $a \approx 1.3238$ . At  $a \approx 1.3539$  a period  $13 \cdot 2^n$ ,  $n = 0, 1, 2, \dots$ , limit cycle sets in and ends at  $a \approx 1.3542$ . At  $a \approx 1.36546$  a period  $13 \cdot 2^n$ ,  $n = 0, 1, 2, \dots$ , limit cycle sets in and at  $a \approx 1.36615$  a period  $11 \cdot 2^n$ ,  $n = 0, 1, 2, \dots$ , limit cycle sets in. There exist many more periodic limit cycles, all with small windows.

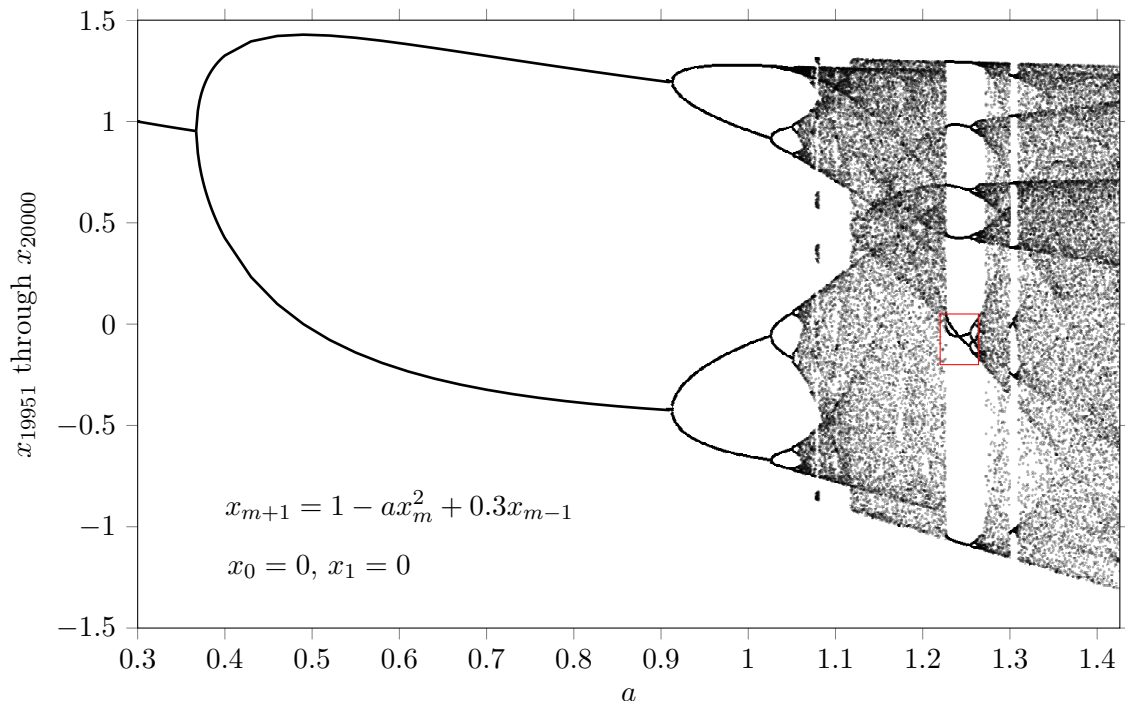


Figure 3.7: Orbit diagram for the Hénon map.

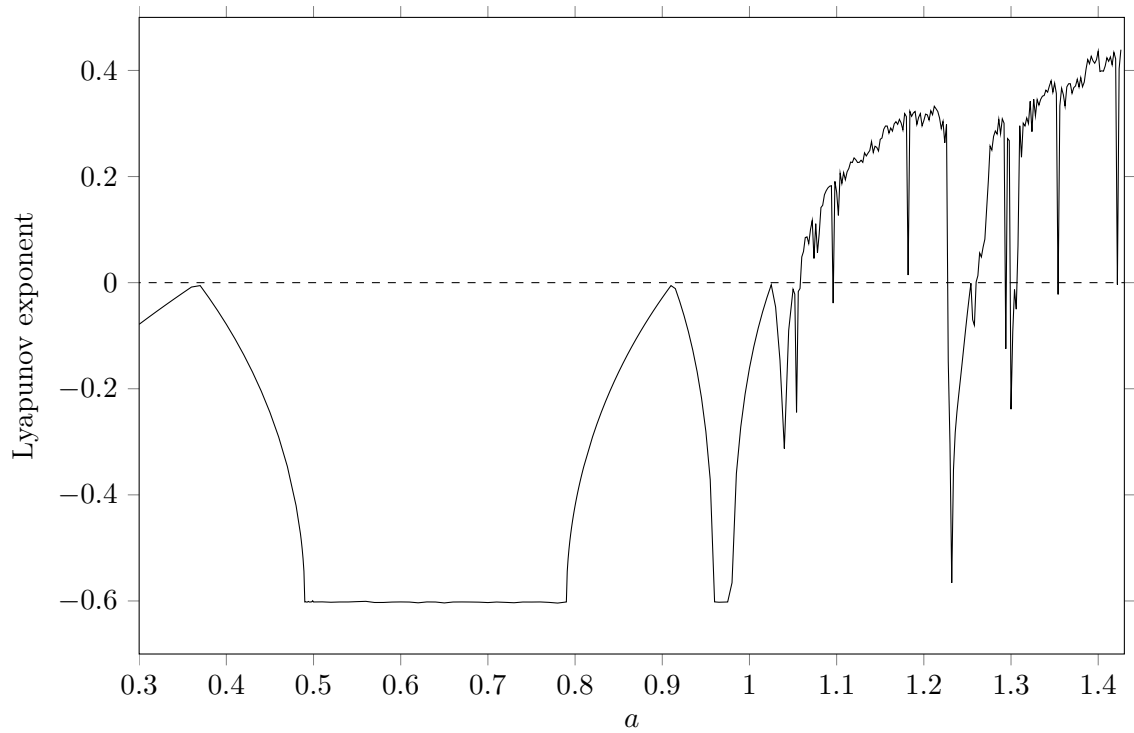


Figure 3.8: Largest Lyapunov exponent for the Hénon map, with  $b = 0.3$ .

If we zoom in on the red rectangle in figure [3.7](#) we see that bifurcation branches sometimes do intersect, see the next figure.

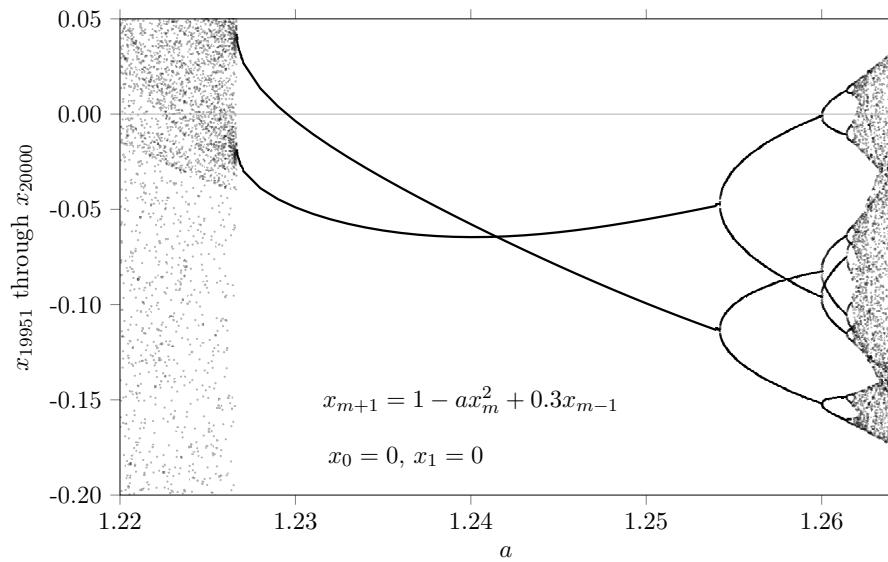


Figure 3.9: Part of the orbit diagram for the Hénon map.



Instead of varying  $a$  for a fixed value of  $b$  we can vary  $b$  for a fixed value of  $a$ . For  $x_0 = 0$ ,  $x_1 = 0$  and  $a = 1.4$  the  $x_m$  are plotted against  $b$  in the next figure.

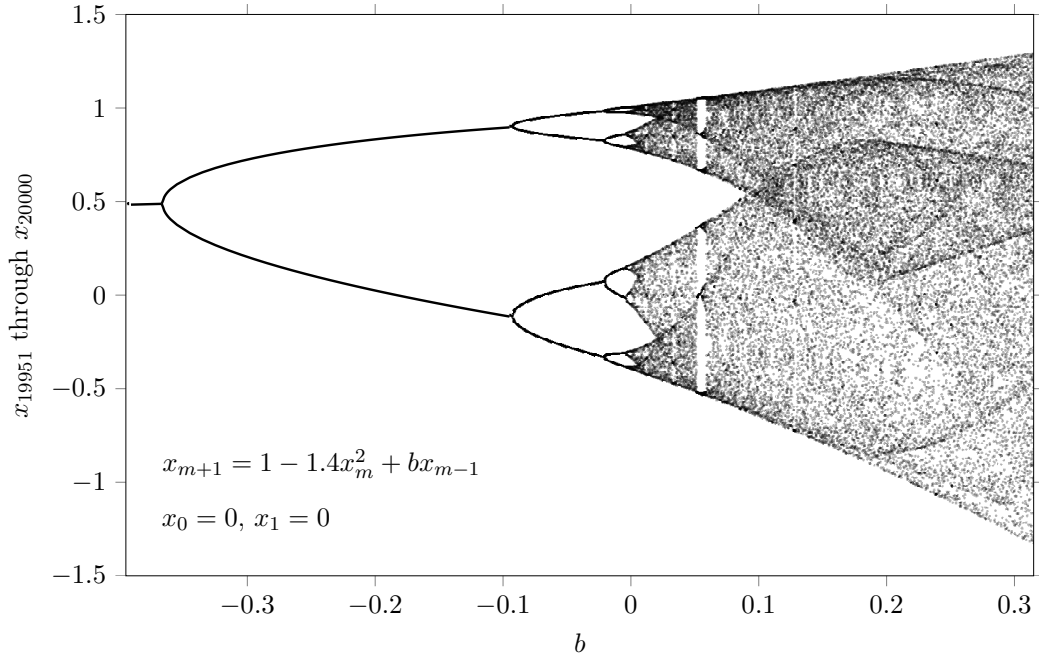


Figure 3.10: Orbit diagram for the Hénon map.

In this orbit diagram one also recognizes various limit cycles.

### 3.6 Single fixed points of the Hénon map

In order to understand the orbit diagrams we will analyse the Hénon map by means of the methods shown in the previous chapters. We start with a single fixed point  $(L, K)$ . According to the Hénon map (3.35) the point  $(L, K)$  should satisfy

$$\begin{aligned} L &= 1 - aL^2 + K \\ K &= bL. \end{aligned} \quad (3.49)$$

Elimination of  $K$  leads to  $aL^2 + (1 - b)L - 1 = 0$ . The solutions are

$$L_{\pm} = \frac{b - 1 \pm \sqrt{(b - 1)^2 + 4a}}{2a}. \quad (3.50)$$

For real solutions  $(b - 1)^2 + 4a$  has to be larger than zero. At the edge we have  $L = \frac{b - 1}{2a}$  if  $(b - 1)^2 + 4a = 0$ . That is, if  $a = -(b - 1)^2/4$ . For  $b = 0.3$  this is at  $a = -0.1225$ , see the position of green dashed line in the next figure.

For the stability of the solutions we consider the Jacobian of system (3.35):

$$\begin{pmatrix} -2ax_m & 1 \\ b & 0 \end{pmatrix}. \quad (3.51)$$

At the point  $(L, K)$  this is

$$\begin{pmatrix} -2aL & 1 \\ b & 0 \end{pmatrix}. \quad (3.52)$$

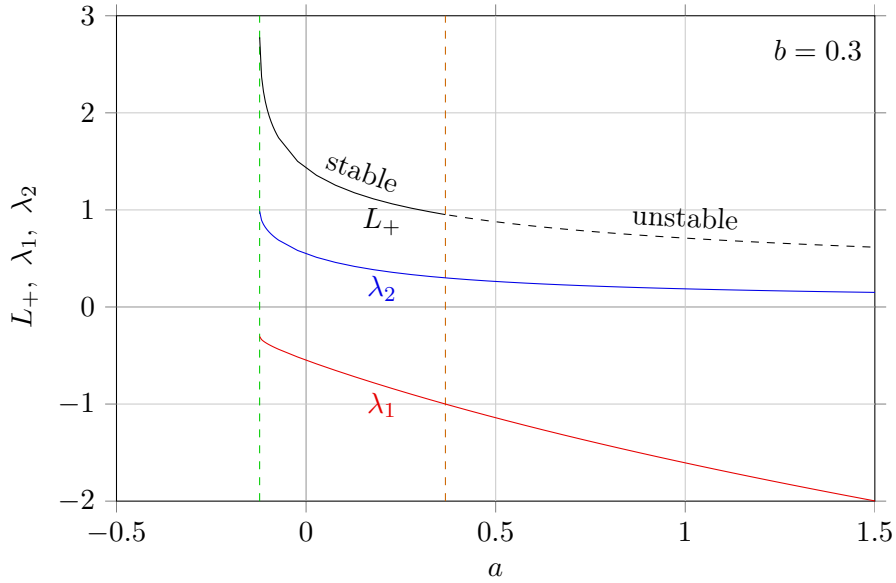
The equation for the eigenvalues is

$$\lambda^2 + 2aL\lambda - b = 0. \quad (3.53)$$

Since  $L$  can be  $L_+$  and  $L_-$  there are four solutions

$$\begin{aligned} \lambda_1 &= -aL_+ - \sqrt{a^2L_+^2 + b}, & \lambda_2 &= -aL_+ + \sqrt{a^2L_+^2 + b} \\ \lambda_3 &= -aL_- - \sqrt{a^2L_-^2 + b}, & \lambda_4 &= -aL_- + \sqrt{a^2L_-^2 + b}. \end{aligned} \quad (3.54)$$

For  $(b-1)^2 + 4a > 0$  the equilibrium  $L_-$  is unstable since  $\lambda_4 > 1$ , see appendix D. For the equilibrium  $L_+$  the stability depends on  $a$  and  $b$ . As an example we consider the case  $b = 0.3$ . In the next figure we have plotted  $L_+$  (black),  $\lambda_1$  (red) and  $\lambda_2$  (blue) against  $a$  for  $b = 0.3$ .



The fixed point  $L_+$  becomes unstable when  $\lambda_1 < -1$ . To determine the value of  $a$  for which this occurs, we substitute  $\lambda = -1$  into the equation (3.53):

$$1 - 2aL - b = 0 \quad \rightarrow \quad L = \frac{1-b}{2a}. \quad (3.55)$$

The latter is in agreement with  $L_+$  if

$$\sqrt{(b-1)^2 + 4a} = 2 - 2b. \quad (3.56)$$

Taking the square we obtain

$$(b-1)^2 + 4a = 4(1-b)^2. \quad (3.57)$$

Hence, the single fixed point bifurcates to a period 2 limit cycle at

$$a = \frac{3}{4}(1-b)^2. \quad (3.58)$$

For  $b = 0.3$  this is at  $a = 0.3675$ , see the position of orange dashed line in the previous figure.

### 3.7 Period 2 limit cycles of the Hénon map

The system (3.35) is for the single step from  $(x_m, y_m)$  to  $(x_{m+1}, y_{m+1})$ . For two steps we have

$$\begin{aligned} x_{m+2} &= 1 - ax_{m+1}^2 + y_{m+1} = 1 - a(1 - ax_m^2 + y_m)^2 + bx_m \\ y_{m+2} &= bx_{m+1} = b(1 - ax_m^2 + y_m). \end{aligned} \quad (3.59)$$

Expanding the brackets we obtain

$$\begin{aligned} x_{m+2} &= 1 - a + 2a^2x_m^2 - a^3x_m^4 - 2ay_m + 2a^2x_m^2y_m - ay_m^2 + bx_m \\ y_{m+2} &= b - abx_m^2 + by_m. \end{aligned} \quad (3.60)$$

For  $(L, K)$  to be a period 2 limit point, the other period 2 limit point has to be  $(K/b, bL)$ .

The substitution of these period 2 limits into the period 2 system gives

$$\begin{aligned} L &= 1 - a + 2a^2L^2 - a^3L^4 - 2aK + 2a^2L^2K - aK^2 + bL \\ K &= b - abL^2 + bK. \end{aligned} \quad (3.61)$$

The elimination of  $K$  leads to

$$(aL^2 + (1-b)L - 1)(a^2L^2 - a(1-b)L + (1-b)^2 - a) = 0. \quad (3.62)$$

The solution  $aL^2 + (1-b)L - 1 = 0$  with the roots

$$L_{\pm} = \frac{b-1 \pm \sqrt{(b-1)^2 + 4a}}{2a} \quad (3.63)$$

corresponds to the single fixed point we already met in the previous section. The other solution  $a^2L^2 - a(1-b)L + (1-b)^2 - a = 0$  with the roots

$$L_{\pm} = \frac{1-b \pm \sqrt{4a - 3(1-b)^2}}{2a} \quad (3.64)$$

corresponds to a period 2 cycle with two different limit points. The corresponding  $K_{\pm}$  is given by

$$K_{\pm} = b(1-b)/a - bL_{\pm}, \quad (3.65)$$

as can be derived from  $K = b - abL^2 + bK$  and  $a^2L^2 - a(1-b)L + (1-b)^2 - a = 0$ .

The bifurcation point for  $L$  is where  $L_- = L_+$ . That is at  $a = \frac{3}{4}(1-b)^2$ . The latter we already found at the end of the previous section. The value of  $L$  at the bifurcation point is:  $L = \frac{1-b}{2a}$  or, if you wish,  $L = \frac{2}{3(1-b)}$  or  $L = \frac{1}{\sqrt{3a}}$ .

To find the bifurcation point where the period 2 limit cycle converts into a period 4 limit cycle, we consider the stability of the period 2 limit by means of the Jacobian. To this end we write the system (3.60) as

$$\begin{aligned} x_{m+2} &= f(f(x_m, y_m)) \\ y_{m+2} &= g(g(x_m, y_m)), \end{aligned} \quad (3.66)$$

where

$$f(f(x, y)) = 1 - a + 2a^2x^2 - a^3x^4 - 2ay + 2a^2x^2y - ay^2 + bx \quad (3.67)$$

and

$$g(g(x, y)) = b - abx^2 + by. \quad (3.68)$$

The Jacobian for the two step system is

$$\begin{pmatrix} \frac{\partial f(f(x,y))}{\partial x} & \frac{\partial f(f(x,y))}{\partial y} \\ \frac{\partial g(g(x,y))}{\partial x} & \frac{\partial g(g(x,y))}{\partial y} \end{pmatrix} = \begin{pmatrix} 4a^2x - 4a^3x^3 + 4a^2xy + b & -2a + 2a^2x^2 - 2ay \\ -2abx & b \end{pmatrix}. \quad (3.69)$$

Evaluated at  $(L, K)$  the Jacobian is

$$\begin{pmatrix} 4a^2L - 4a^3L^3 + 4a^2LK + b & -2a + 2a^2L^2 - 2aK \\ -2abL & b \end{pmatrix}. \quad (3.70)$$

The equation for the eigenvalues  $\lambda$  of the Jacobian is

$$(4a^2L - 4a^3L^3 + 4a^2LK + b - \lambda)(b - \lambda) - (-2a + 2a^2L^2 - 2aK)(-2abL) = 0. \quad (3.71)$$

An eigenvalue is 1 if

$$(4a^2L - 4a^3L^3 + 4a^2LK + b - 1)(b - 1) - (-2a + 2a^2L^2 - 2aK)(-2abL) = 0. \quad (3.72)$$

Together with system (3.61) we obtain  $a = \frac{3}{4}(1-b)^2$ . So, this corresponds to the left side of the period 2 limit cycle. An eigenvalue is  $-1$  if

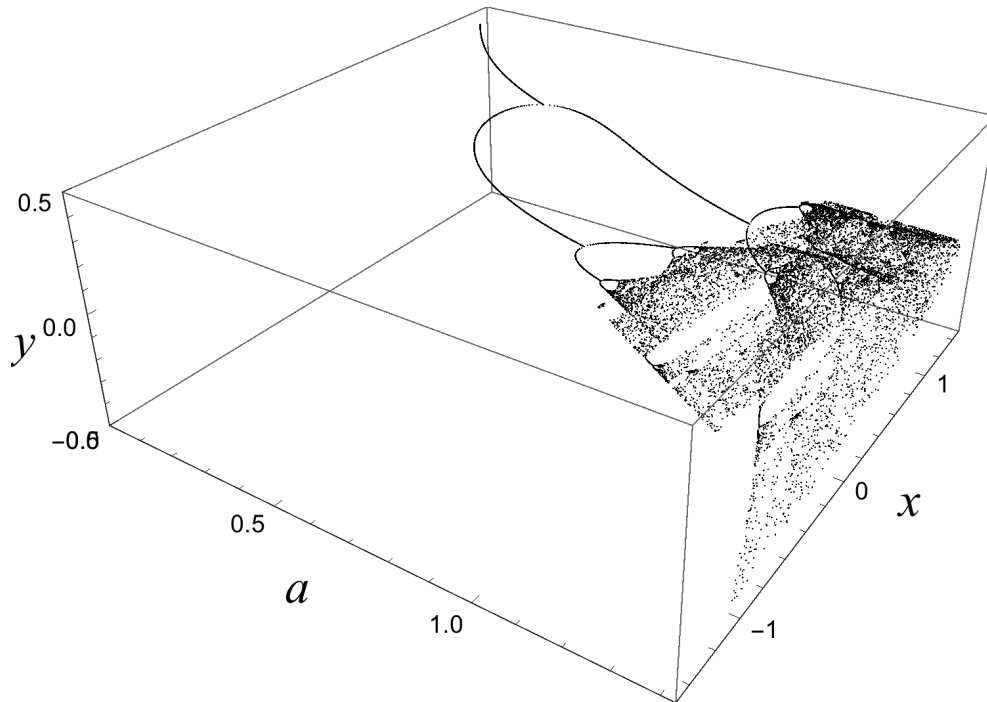
$$(4a^2L - 4a^3L^3 + 4a^2LK + b + 1)(b + 1) - (-2a + 2a^2L^2 - 2aK)(-2abL) = 0. \quad (3.73)$$

Together with system (3.61) we obtain  $a = b + \frac{5}{4}(1-b)^2 = \frac{1}{4}(5 - 6b + 5b^2)$ , which corresponds to the right side of the period 2 limit cycle. For  $b = 0.3$  this is at  $a = 0.9125$ .

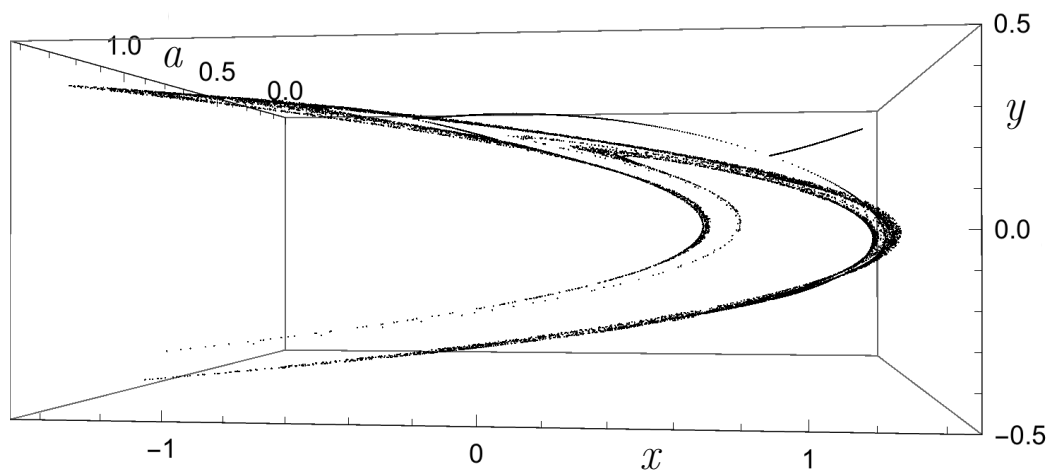
For limit cycles with period 3 and larger the method is similar. However, the algebra becomes very complicated.

### 3.8 Three dimensional plots for the Hénon map

To gain insight we will consider some three dimensional (3D) plots of orbits of the Hénon map. In the next figure the orbit of  $(x_m, y_m)$  is plotted against  $a$  for  $b = 0.3$ .

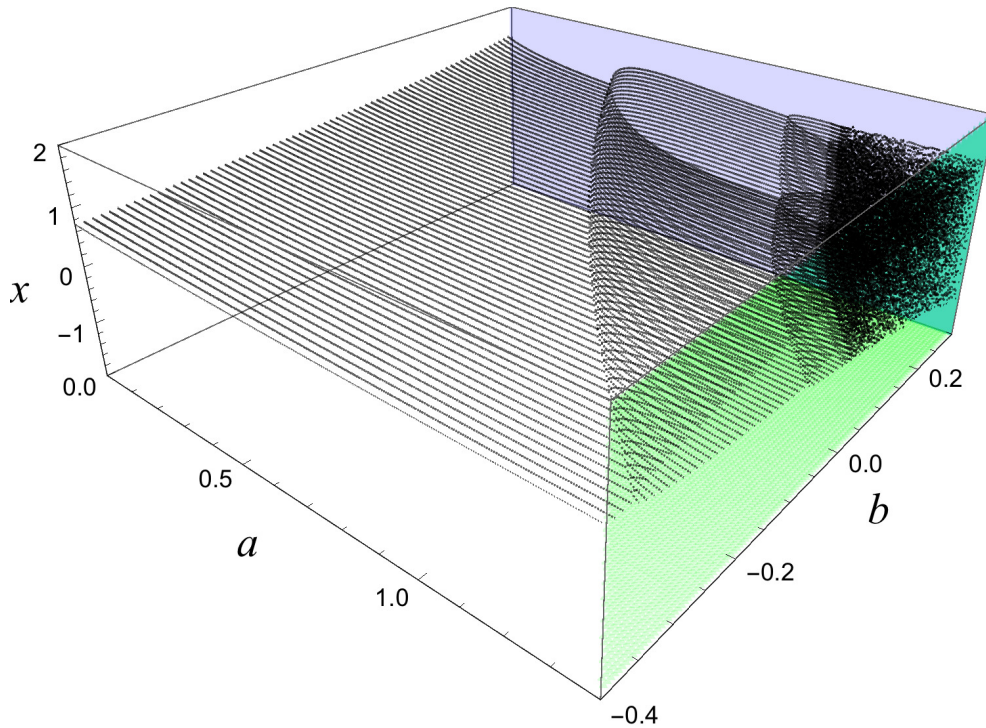


A top view of it corresponds with figure [3.7](#). A side view from the right delivers the next figure.



We see that for all  $a$  the orbits  $(x_m, y_m)$  are close to the attractor shown in figure [3.6](#).

In the following figure the orbits of  $x_m$  is shown for  $0.0 < a < 1.4$  and  $-0.4 < b < 0.3$ .



The black dots on the  $b = 0.3$  plane (the blue back side) corresponds with figure [3.7](#). The black dots on the  $a = 1.4$  plane (the green right side) corresponds with figure [3.10](#). We see planes for fixed  $b$  show bifurcations. The  $a$  values for which bifurcations take place depend on  $b$ . As a consequence bifurcations have to take place in the  $b$  direction as well.

From the analysis in the previous two sections we obtained the single fixed point is between  $a = -\frac{1}{4}(1-b)^2$  and  $a = \frac{3}{4}(1-b)^2$ . For  $b = 1$  these points coincide at  $a = 0$ . The bifurcation from a period 2 to a period 4 limit cycle is at  $a = b + \frac{5}{4}(1-b)^2$ . The smallest  $a$  value for this bifurcation is  $a = \frac{4}{5}$  and occurs for  $b = \frac{3}{5}$ . For values of  $a$  a little larger than 0.8 the orbit diagram in the  $b$  direction will therefore show a bifurcation from a period 2 to a period 4 limit cycle followed by a confinement to a period 2 limit cycle. It is illustrated in the left panel of figure [3.11](#) for  $a = 0.85$ . For  $a = 0.92$  also a bifurcation from a period 4 to a period 8 limit cycle followed by a confinement to a period 4 limit cycle occurs, see right panel of figure [3.11](#). In both panels we see the orbits become already unstable before  $b = 1$ . The value of  $b$  where the instability sets in differs more from 1 if  $a$  is relatively large. For or  $a \approx 0.9$ , as in figure [3.11](#), instabilities start already at  $b \approx 0.7$ , while for instance for  $a \approx 0.5$  instabilities start rather at  $b \approx 0.9$ . For  $a < 0.3$  the orbit is stable from  $b = -1$  through  $b \approx 1$ .

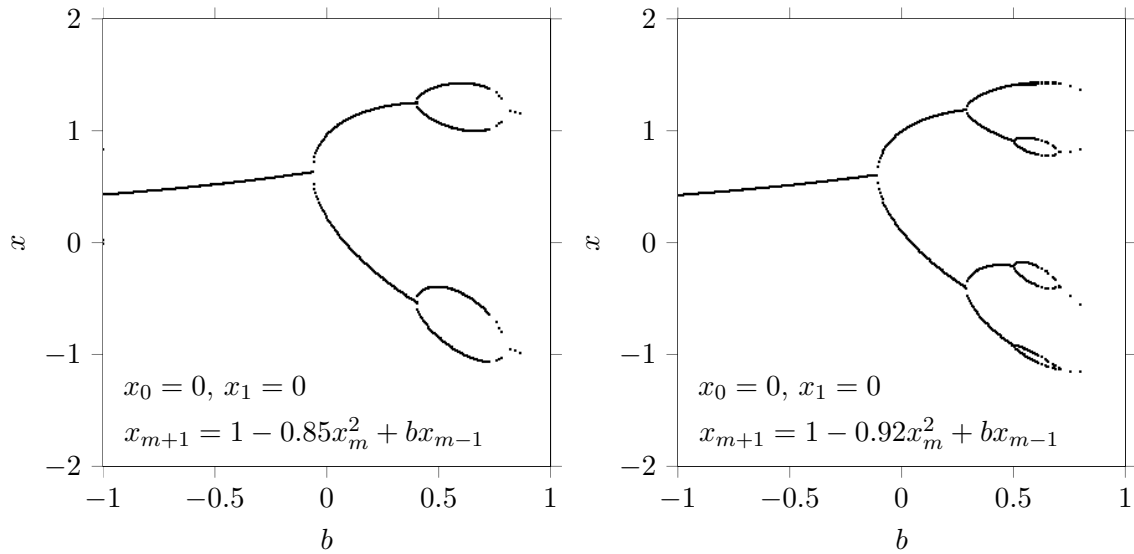


Figure 3.11: Bifurcation diagram for the Hénon map for  $a = 0.85$  (left) and  $a = 0.92$  (right).

### 3.9 Hénon map for $b \approx 1$

For  $b \approx 1$  the orbit diagrams differ completely from the ones with  $b$  smaller than, say, 0.9. In figure [3.12](#) the values of  $x_{19801}$  through  $x_{20000}$  are shown for  $b = 1$ ,  $x_0 = 0$ ,  $y_0 = 0$  and  $a$  running from 0.10 through 0.14.

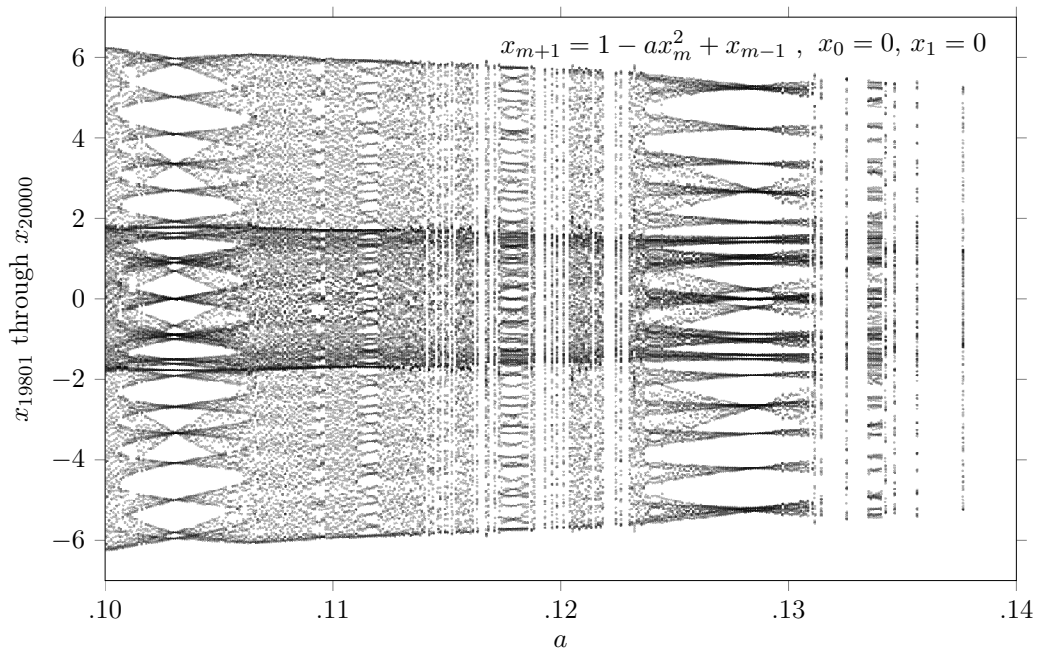
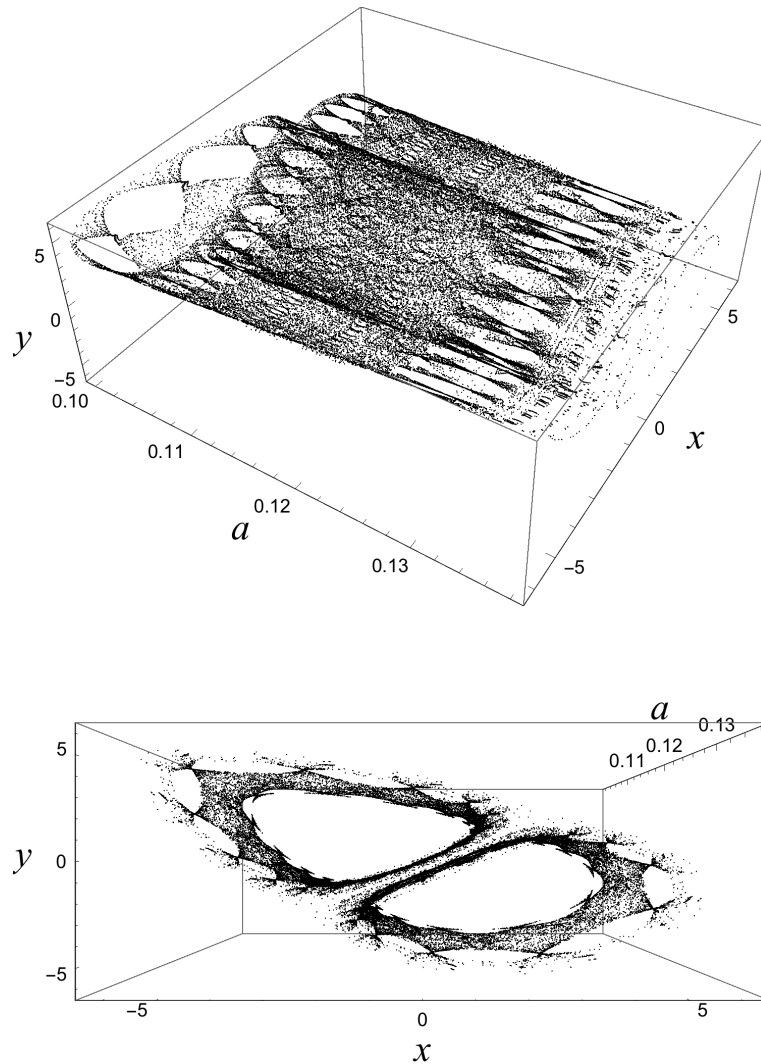


Figure 3.12: Orbit diagram for the Hénon map for  $b = 1$ .



We see periodic structures which are not related to a period doubling cascade. For instance, for  $b = 1$  and  $a \approx 0.1031$  the points of the orbit seem confined to 32 values. To see what is actually going on we consider a 3D plot of the orbit  $(x_m, y_m)$  against  $a$ , see next three figures. The counter  $m$  is taken sufficiently large:  $9850 < m \leq 10000$ . A projection of the first figure on the  $a, x$ -plane gives figure 3.12. The three figures show the orbit diagrams from different points of view. It is clear that the orbits are divided in two regions. The size of the regions shrinks for increasing  $a$ .



The two regions are a sort of rolls each with 16 holes for  $a \approx 0.103$ . The projection on the  $a, x$ -plane therefore shows a confinement to 32 values if  $a \approx 0.103$ . Such periodic structures also occur for other values of  $a$ . Unstabilities lead to void windows such as for  $a \approx 0.14$ .



For  $b = 1$ ,  $x_0 = 0$  and  $x_1 = 0$  the attractor is separated in two regions as shown in the next figure for  $a = 0.05$  (left panel) and  $a = 0.1$  (right panel).

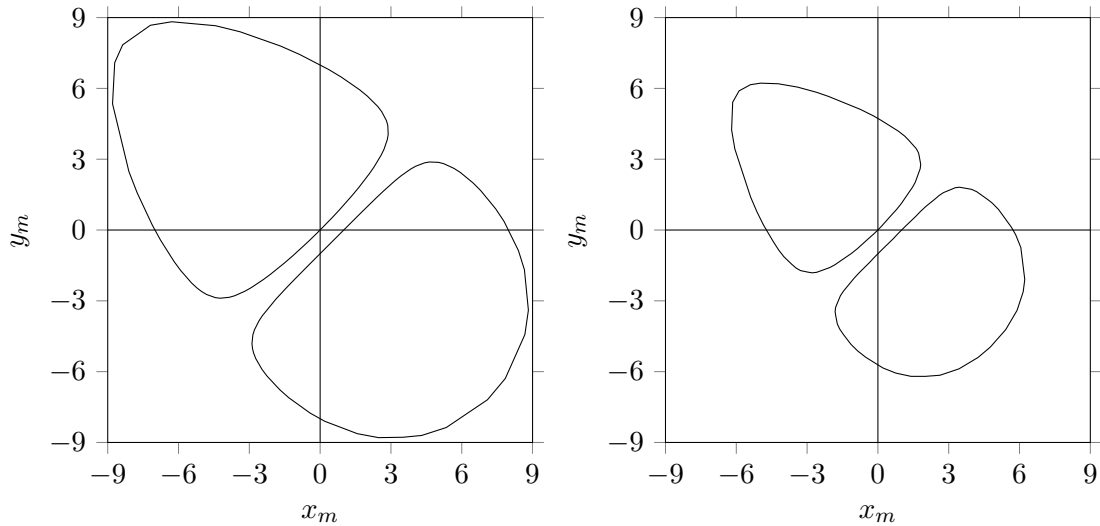
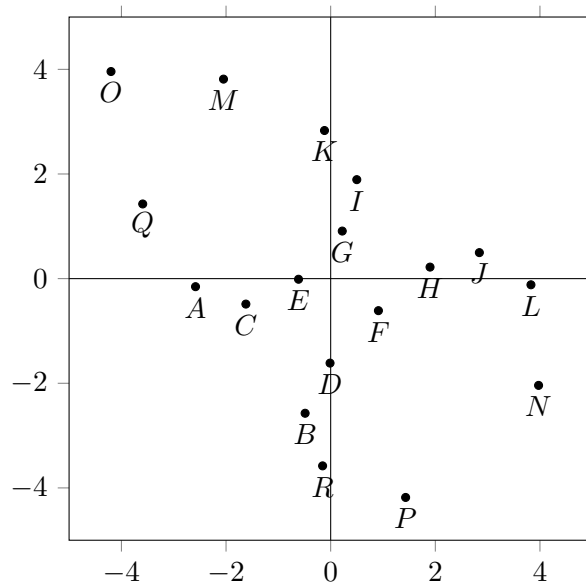


Figure 3.13: Hénon attractor for  $b = 1$ ,  $x_0 = 0$ ,  $y_0 = 0$  and  $a = 0.05$  (left) and  $a = 0.1$  (right).

The size of the attractor shrinks for increasing  $a$ . For  $a$  small and  $b$  close to 1 the orbit either converges to two points or to a two region kind of attractor as shown in the previous figure. For instance, for  $a = 0.2$  and  $b = .99608128679148016938$  the orbit converges to two points:  $(2.2458, -2.21748)$  and  $(-2.22621, 2.237)$ , while for  $a = 0.2$  and  $b = .99608128679148016937$  the orbit converges to a period 18 limit cycle, see the next figure.



The orbit of the period 18 limit cycle is depicted by the symbols  $A$  through  $R$ . For instance, starting the cycle in point  $P$  the next point is  $Q$ , then  $R$ , then  $A$ , then  $B$  etc., through  $O$ . So, the orbit alternately jumps from one region to the other region.

Extreme sensitivity occurs also for other values of  $a$  and  $b$ . If we look in the neighborhood of  $a = 1.4$  and  $b = 0.3$ , then one obtains a period 18 cycle for  $(a, b) = (1.3999769098975, 0.3)$  and a period 19 cycle for  $(a, b) = (1.4, 0.30009066023)$ , etc. [\[3\]](#).

## Chapter 4

# Lyapunov images.

### 4.1 Images of dynamical systems

There are many ways to create images which illustrate the dynamics of systems of difference equations. One way is by plotting the orbits as we have seen before. Another way is by plotting Lyapunov exponents. For a two dimensional system with  $x$  and  $y$  as the variables the plot of Lyapunov exponents against  $(x, y)$  results in a two dimensional Lyapunov image for a particular choice of the constants. For a system with two constants  $a$  and  $b$  the plot of Lyapunov exponents against  $(a, b)$  results in a two dimensional Lyapunov image for a particular choice of the initial values  $(x_0, y_0)$ . A two dimensional Lyapunov image against one variable and one constant is also possible, see the figures in section 2.5.

In Lyapunov images different regions can be distinguished: regions for which the system tend to infinity, regions for which the system shows chaotic behaviour and regions for which the system is attracted to a limit cycle.

Regions for which the system is attracted to a limit cycle with period  $n$  can be subdivided into  $n$  regions for which the points  $(x_0, y_0), (x_n, y_n), (x_{2n}, y_{2n}), \dots, (x_{kn}, y_{kn}), \dots$ , with  $k \in \mathbb{N}$ , converges to one of the  $n$  limit points. The last figure of section 3.2 is an example of a limit cycle with period 2 which can be subdivided into 2 regions for which the points  $(x_0, y_0), (x_2, y_2), (x_4, y_4), \dots, (x_{2k}, y_{2k}), \dots$ , with  $k \in \mathbb{N}$ , converges to one of the 2 limit points.

We will consider Lyapunov images for the Hénon map. Because of its interesting Lyapunov images we will consider at the end of this chapter the so called  $z^2 + c$  map. We will start however with a particular type of Lyapunov images which occur for the logistic equation if the parameter is periodically changed. Such images are called Markus-Lyapunov images.

## 4.2 Markus-Lyapunov images

For the logistic equation  $x_{m+1} = ax_m(1 - x_m)$  two dimensional Lyapunov images can be created by periodically changing the parameter  $a$  between two values  $B$  and  $A$  during the iteration process. To be specific,  $x_1 = Bx_0(1 - x_0)$ ,  $x_2 = Ax_1(1 - x_1)$ ,  $x_3 = Bx_2(1 - x_2)$ ,  $x_4 = Ax_3(1 - x_3)$ , etc. For every  $(B, A)$  pair the Lyapunov exponent is calculated as an average over the iteration process. We will look at density plots or contour plots of the Lyapunov exponents in a  $(B, A)$  plane.

For the sequence  $BABABA\dots$  with  $0 \leq A, B \leq 4$  and  $0 \leq A, B \leq 4$ , the  $(B, A)$  points are coloured dependent on the Lyapunov exponent  $\lambda$ , see next figure.

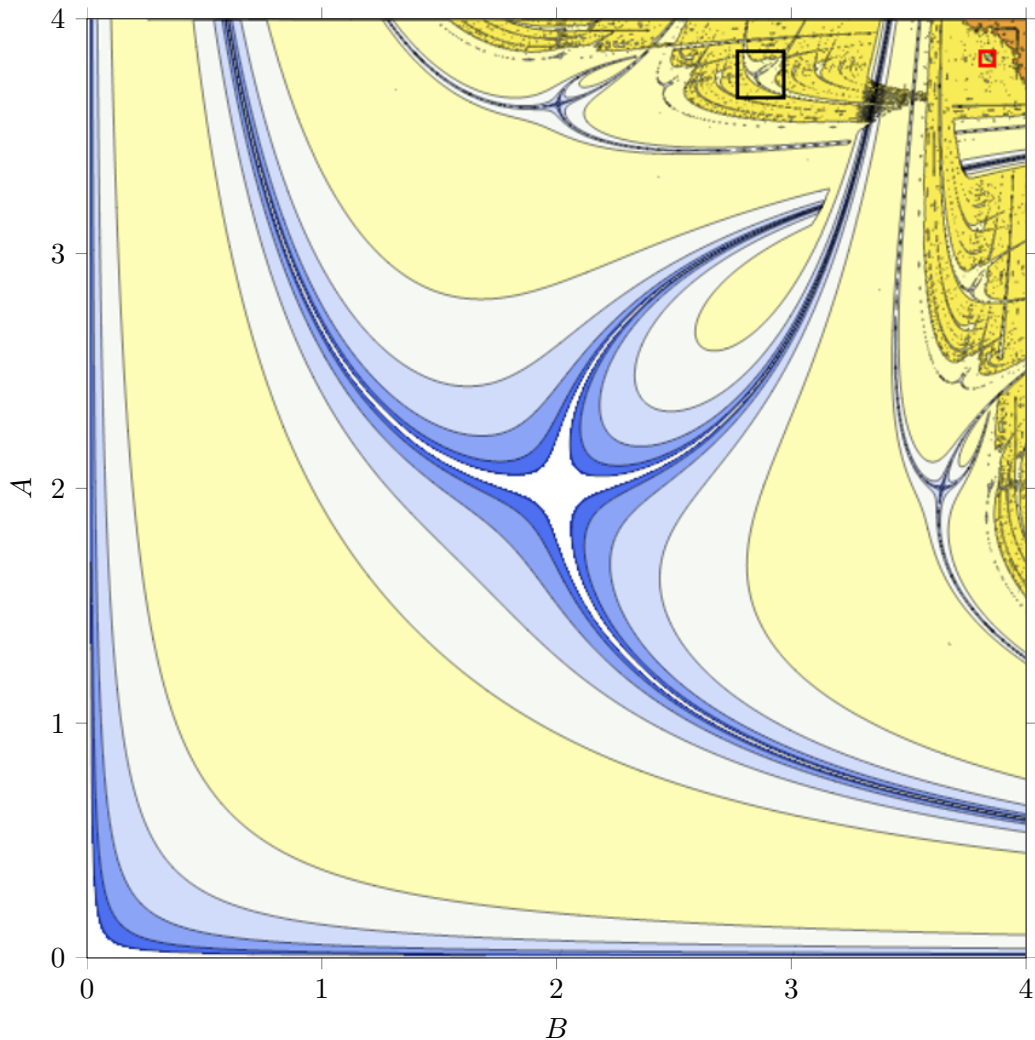


Figure 4.1: Markus-Lyapunov image for  $0 \leq A, B \leq 4$ . The black square and the red square are the boundaries of two areas that will be zoomed in further on.

In the previous figure the colouring is as follows: the  $\lambda = 0.5$  contour is between brown and dark yellow, the  $\lambda = 0.0$  contour is between dark yellow and light yellow, the  $\lambda = -0.5$  contour is between light yellow and white-blue, the  $\lambda = -1.0$  contour is between white blue and light blue, the  $\lambda = -1.5$  contour is between light blue and blue, the  $\lambda = -2.0$  contour is between blue and dark blue, the  $\lambda = -2.5$  contour is between dark blue and very dark blue and the  $\lambda = -3.0$  contour is between very dark blue and white. The dark yellow and brown colours in the upper right corner of the contour plot indicate a more chaotic behaviour.

The previous figure contains repeating self-similar structures. To illustrate the self-similarity the structure within the black square,  $2.772 \leq B \leq 2.965$  and  $3.672 \leq A \leq 3.865$ , of figure 4.1 is shown in the next figure with a slightly different colouring.

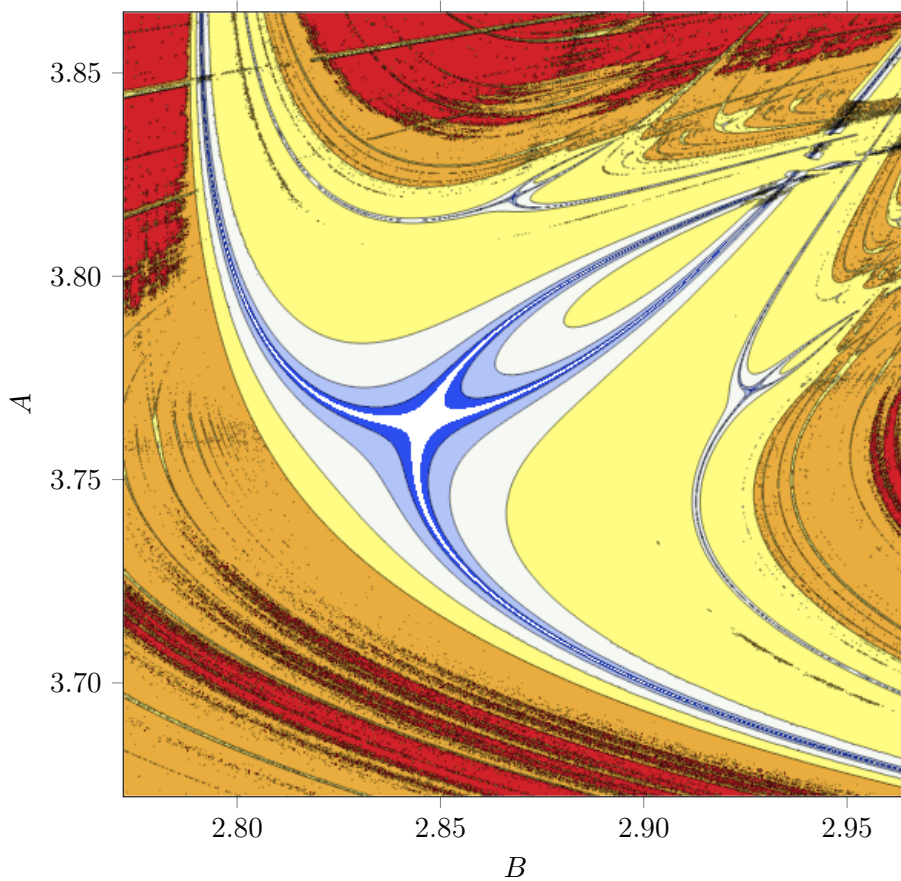


Figure 4.2: Zoom of the black square of figure 4.1. Brown and red are for positive Lyapunov exponents while yellow, light blue, blue, etc. are for negative Lyapunov exponents.

Completely different colouring schemes may lead to aesthetically beautiful pictures and more pronounced repetitive self-similar structures. The figures 4.3 and 4.4 are the Markus-Lyapunov images of figures 4.1 and 4.2 with a different colouring method.

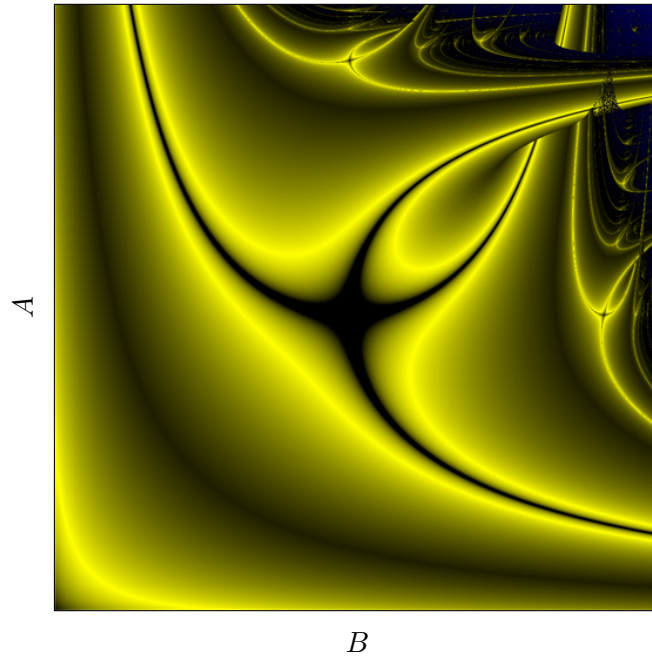


Figure 4.3: Different colouring of figure [4.1](#).

The structure within the black square,  $2.772 \leq B \leq 2.965$  and  $3.672 \leq A \leq 3.865$ , of figure [4.1](#), with a different colouring method:

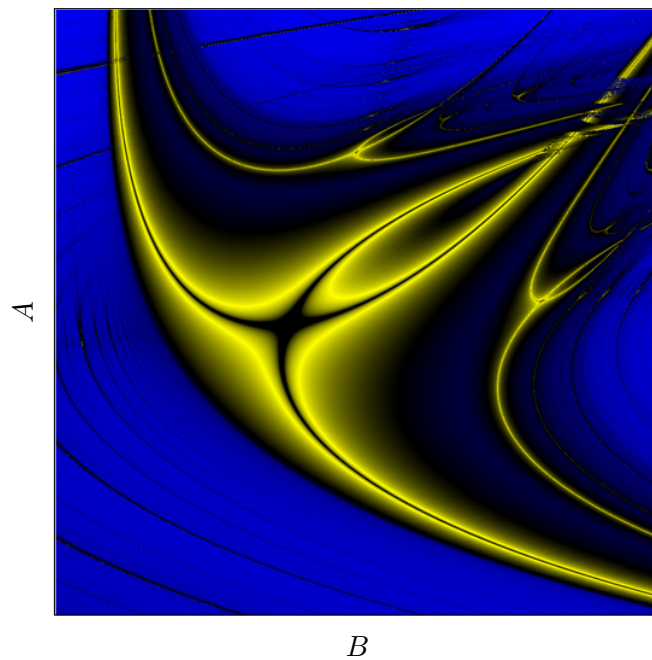


Figure 4.4: Different colouring of figure [4.2](#).

The main structure in the previous figures is determined by intersecting parabola's. With a little fantasy it reminds us of swallows.

Lyapunov images in the  $(B, A)$  plane for two values  $B$  and  $A$  of the periodically changing parameter of the logistic equation were first described by M. Markus and B. Hess [6] [7]. In both references a picture is presented for the  $BABA\dots$  sequence for  $3.808 \leq A, B \leq 3.867$ . This  $B, A$  region is shown as the red square in figure 4.1. A zoom of this region is shown in the figure below:

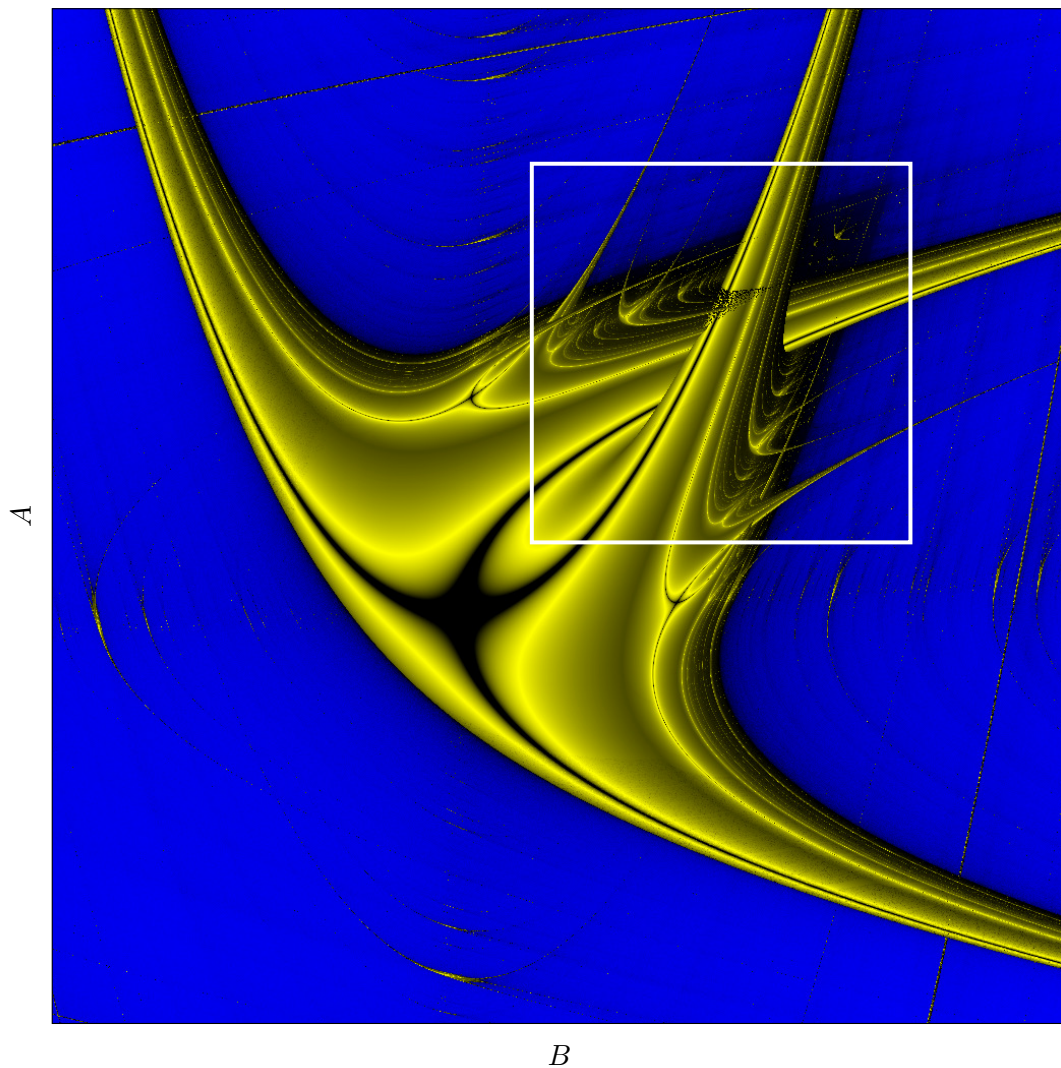


Figure 4.5: Zoom of the red square of figure 4.1 in different colours.

At many positions 'swallows' are present.



Enlargement of the white square region of figure [4.5](#),  $3.836 \leq A, B \leq 3.858$ , delivers similar structures as in figures [4.4](#) and [4.5](#):

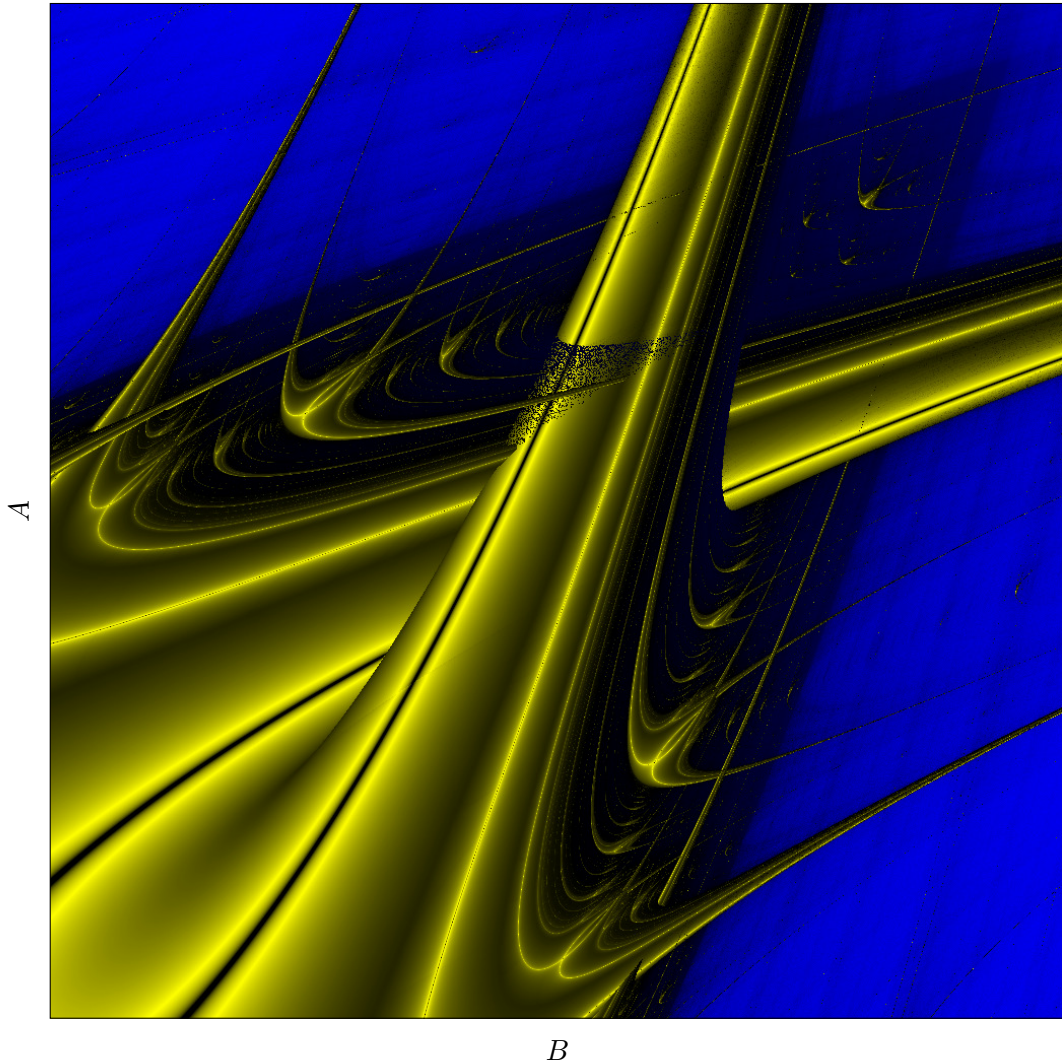


Figure 4.6: Zoom of white square region of figure [4.5](#).

No matter how much one zooms in, at every level ‘swallows’ are present.



One can also take other repetitive sequences like  $AAB$  or  $AABB$  etc. For the repetitive sequence  $BBABABA$  with  $3.212 \leq A \leq 4.0$  and  $2.759 \leq B \leq 3.744$  the next figure is obtained. Again, similar structures as in figures [4.4](#) and [4.5](#) can be seen.

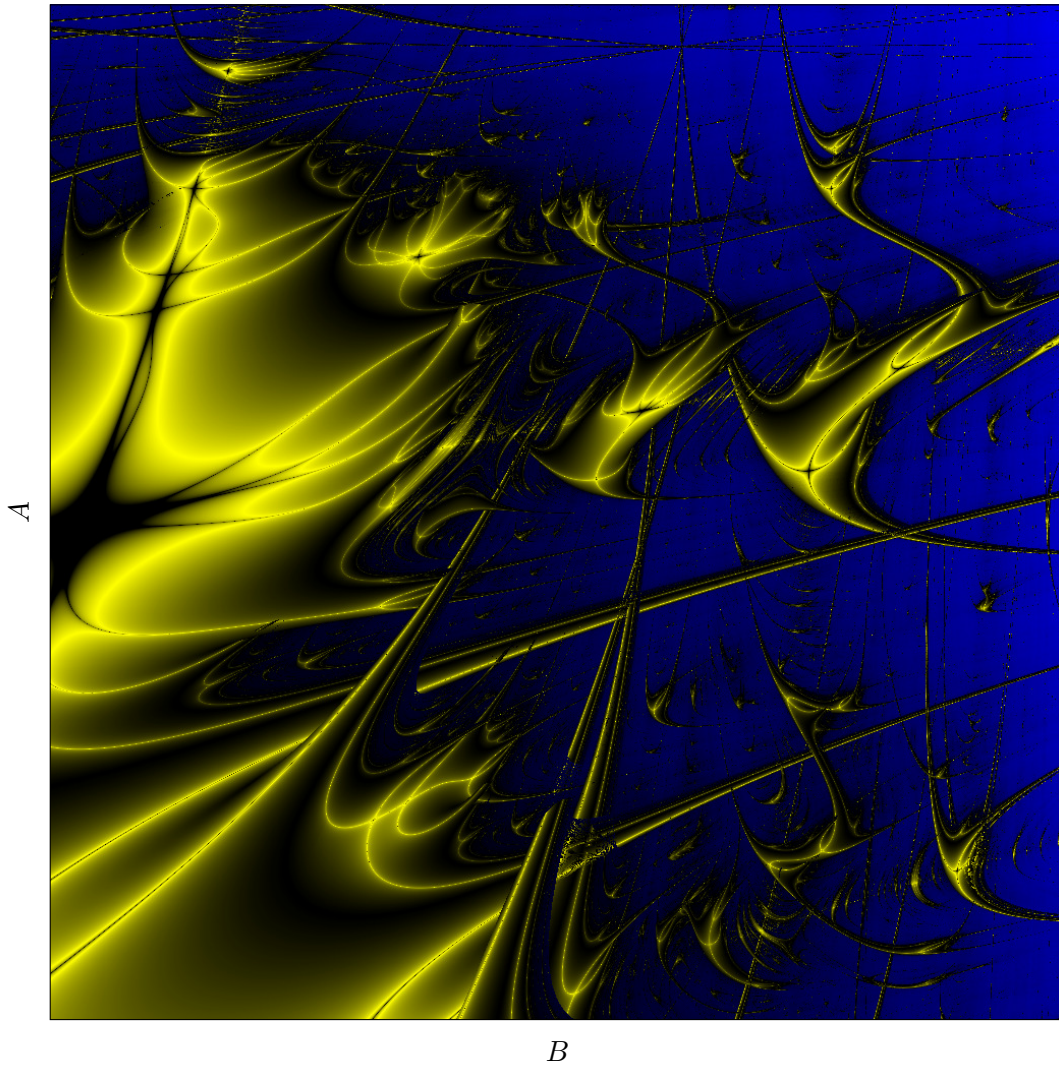


Figure 4.7: Markus-Lyapunov image for repetitive  $BBABABA$  sequence.

Another often used sequence is the repetition of  $BBBBBAAAAAA$  for  $0 \leq A, B \leq 4$ . On the next page we see a contour plot and a density plot of the of the Lyapunov exponents.

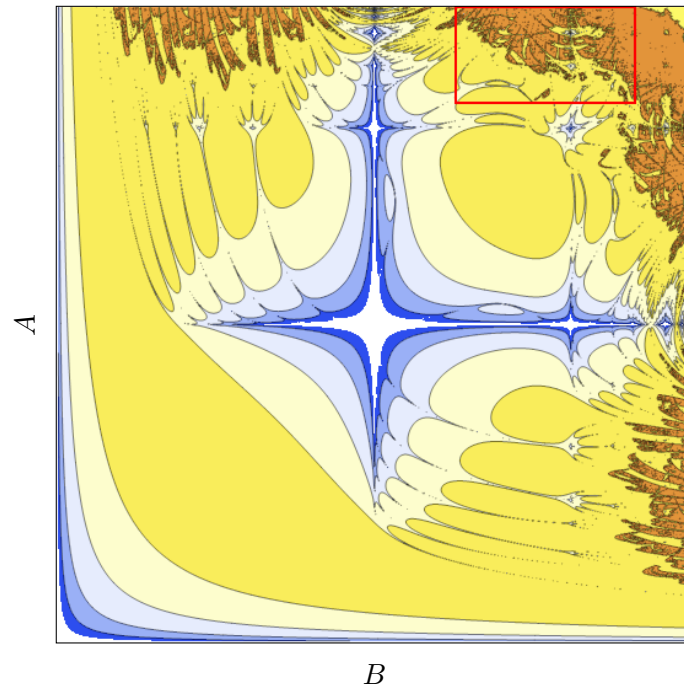


Figure 4.8: Markus-Lyapunov image for repetitive  $BBBBBBAAAAA$  sequence.

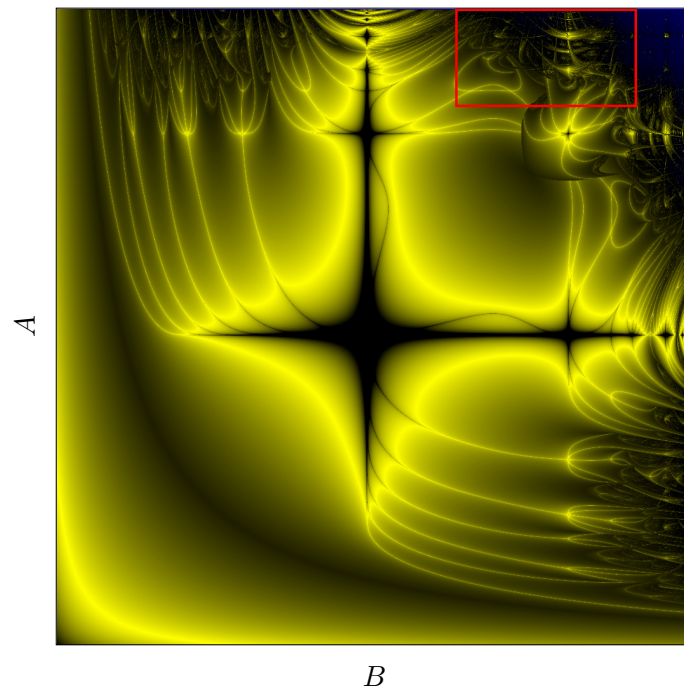


Figure 4.9: Different colouring of figure [4.8](#).

The red area in figures [4.8](#) and [4.9](#) with  $3.394 \leq A \leq 4.0$  and  $2.516 \leq B \leq 3.647$  has a very rich structure, see the figure below. It is known as Zircon Zity.

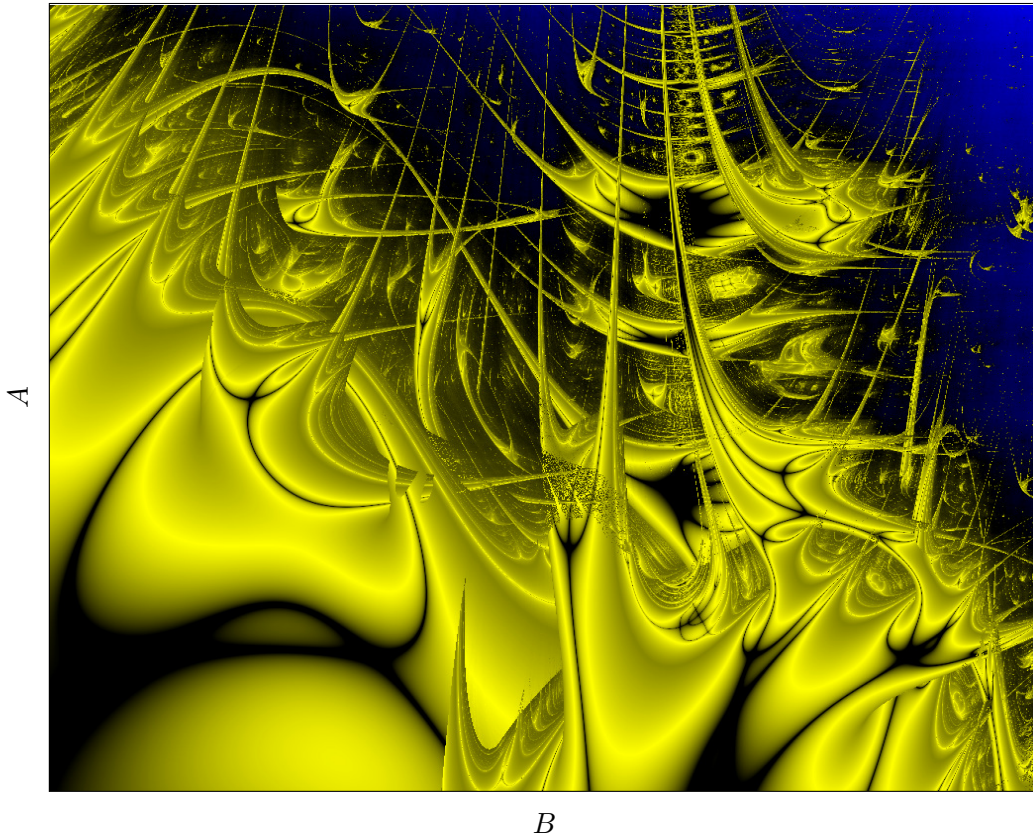


Figure 4.10: Zircon Zity.

### 4.3 Lyapunov image for the Hénon map

The largest Lyapunov exponent of the Hénon map for each pair of constants  $(a, b)$  can be created by assigning a color to each pixel with coordinates  $(a, b)$ . The color depends on the largest Lyapunov exponent. An example is shown in figure [4.11](#). In figure [4.11](#) a pixel is yellow or red if the Lyapunov exponent is negative respectively positive, and blue if the orbit runs to infinity. Notice the presence of ‘swallows’ in the red region.

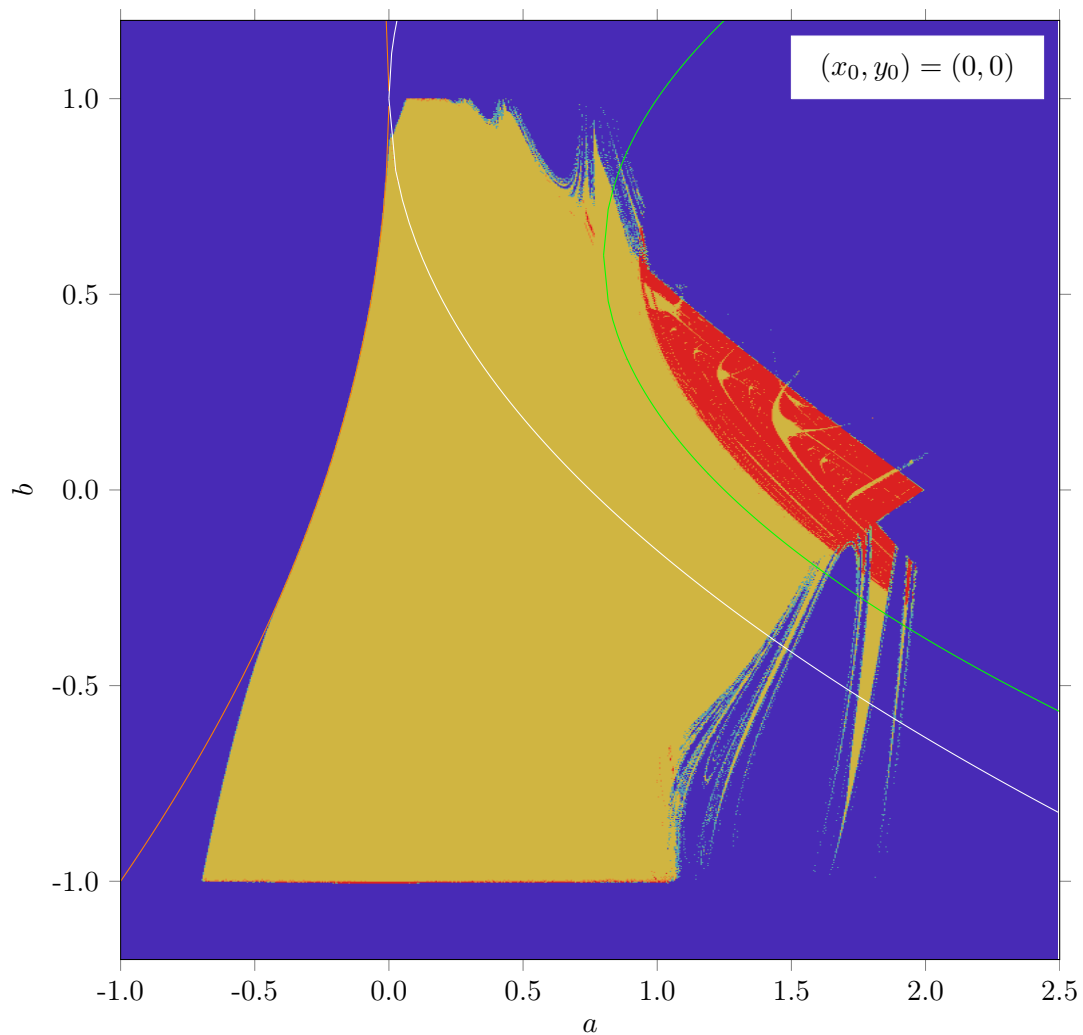


Figure 4.11: A Lyapunov image for the Hénon map. See the text for the coloring.

In the previous chapter we already obtained that a single fixed point is between the curves  $a = -\frac{1}{4}(1-b)^2$  and  $a = \frac{3}{4}(1-b)^2$ . In figure 4.11 they are shown as an orange curve and a white curve respectively.

The period 2 limit cycle is between the curves  $a = \frac{3}{4}(1-b)^2$  and  $a = b + \frac{5}{4}(1-b)^2$ .

In figure 4.11 the curve  $a = b + \frac{5}{4}(1-b)^2$  is shown as a green curve.

The period 4 limit cycle will be between the green curve and the border between red and yellow regions.

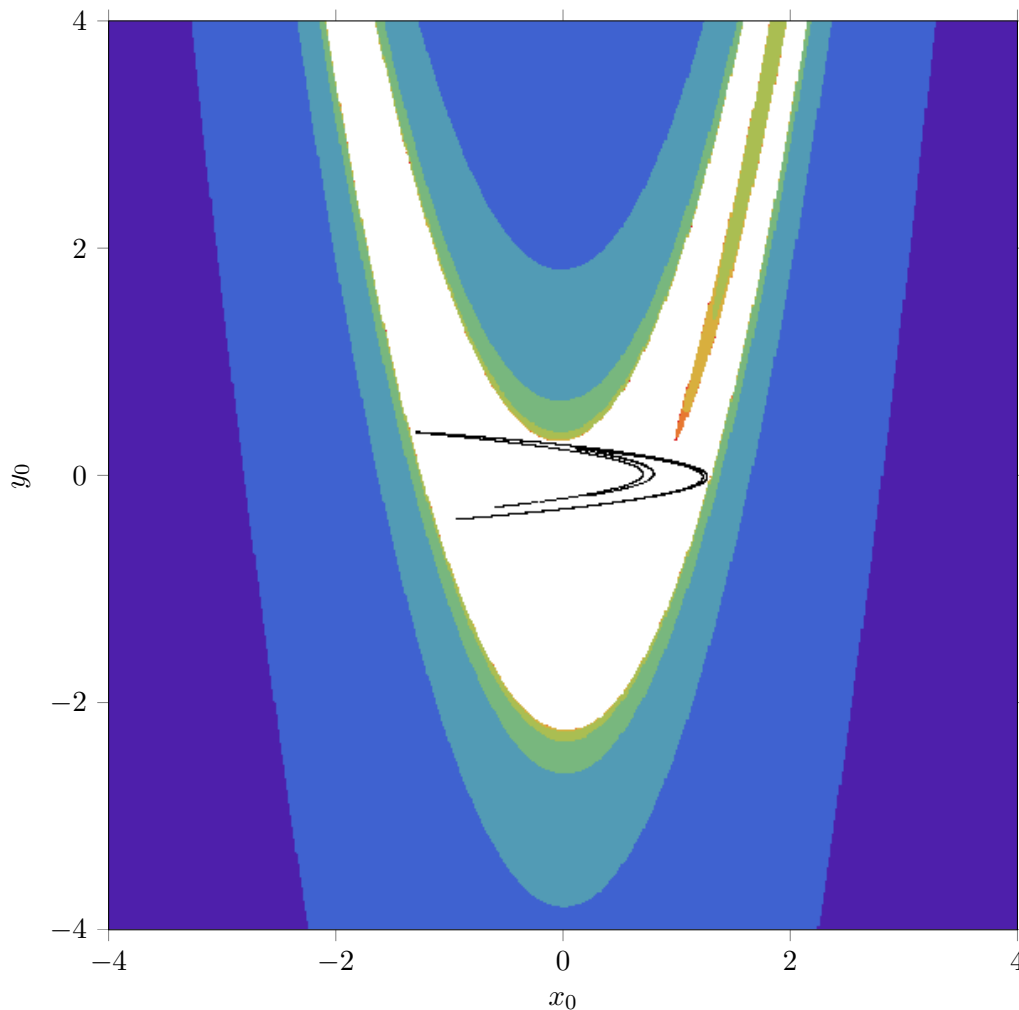
The end of the period  $2^n$  limit cycle bifurcations is at the border between red and yellow regions.



## 4.4 Basins of attraction for the Hénon map

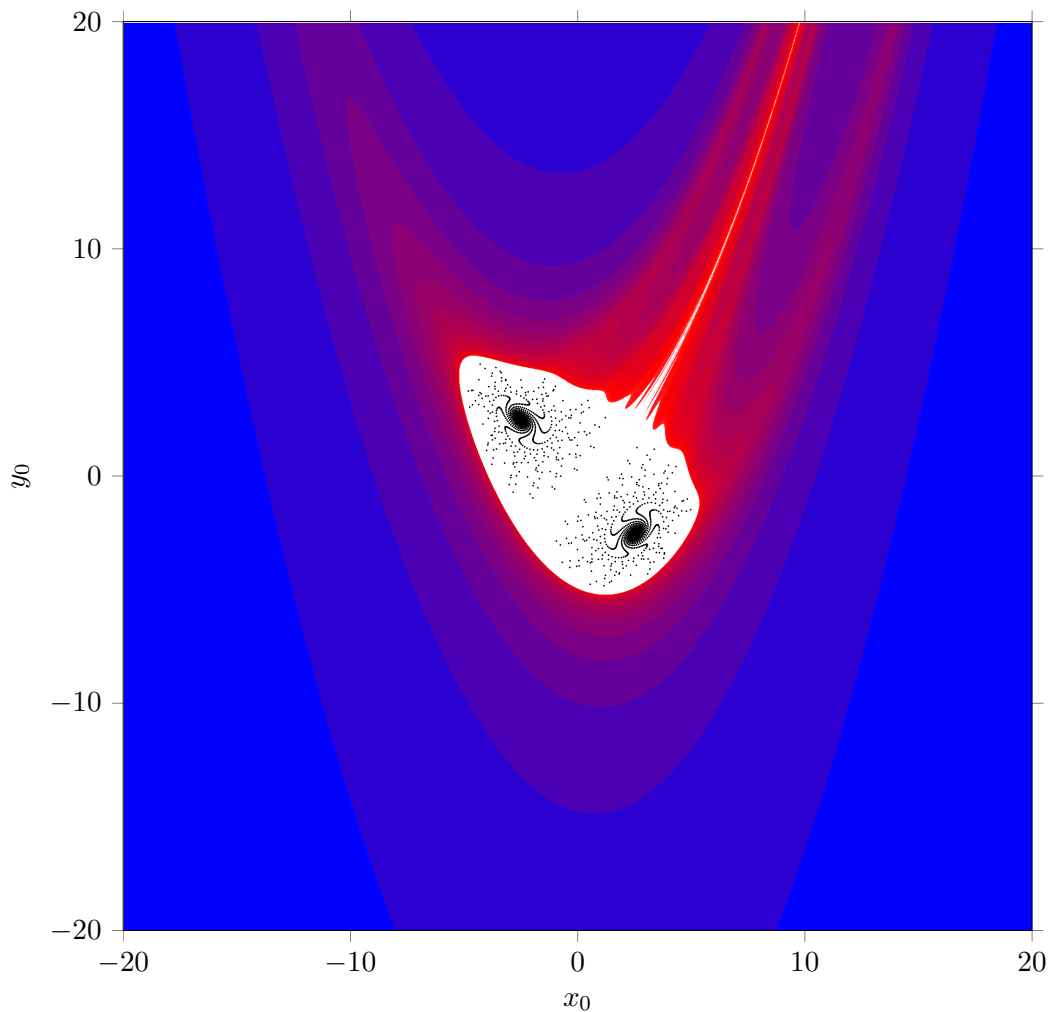
If, for a certain map, one follows the orbit for a given starting point, it either diverges to infinity or is attracted to a stable fixed point or a limit cycle or a strange attractor. All starting points that do not diverge to infinity form the basins of attraction. In the case of the Hénon map, points in the real plane are either attracted to the Hénon attractor or escape to infinity. The larger the Lyapunov exponent, the faster it escapes to infinity.

In the next figure the starting points  $(x_0, y_0)$  with  $-4.0 \leq x_0 \leq 4.0$ ,  $-4.0 \leq y_0 \leq 4.0$ ,  $a = 1.4$  and  $b = 0.3$ , are coloured depending on how quickly they go to ‘infinity’. Here we simply consider a point  $(x_n, y_n)$  to be at ‘infinity’ if  $x_n^2 + y_n^2 > 20\,000$ . Take for example  $(x_0, y_0) = (4.0, 4.0)$  then  $(x_1, y_1) = (-17.4, 1.2)$  and  $x_1^2 + y_1^2 = 304.2$ . A further step leads to  $(x_2, y_2) = (-421.664, -5.22)$  and  $x_2^2 + y_2^2 = 177\,828$ . So, already after 2 iterations ‘infinity’ is reached.

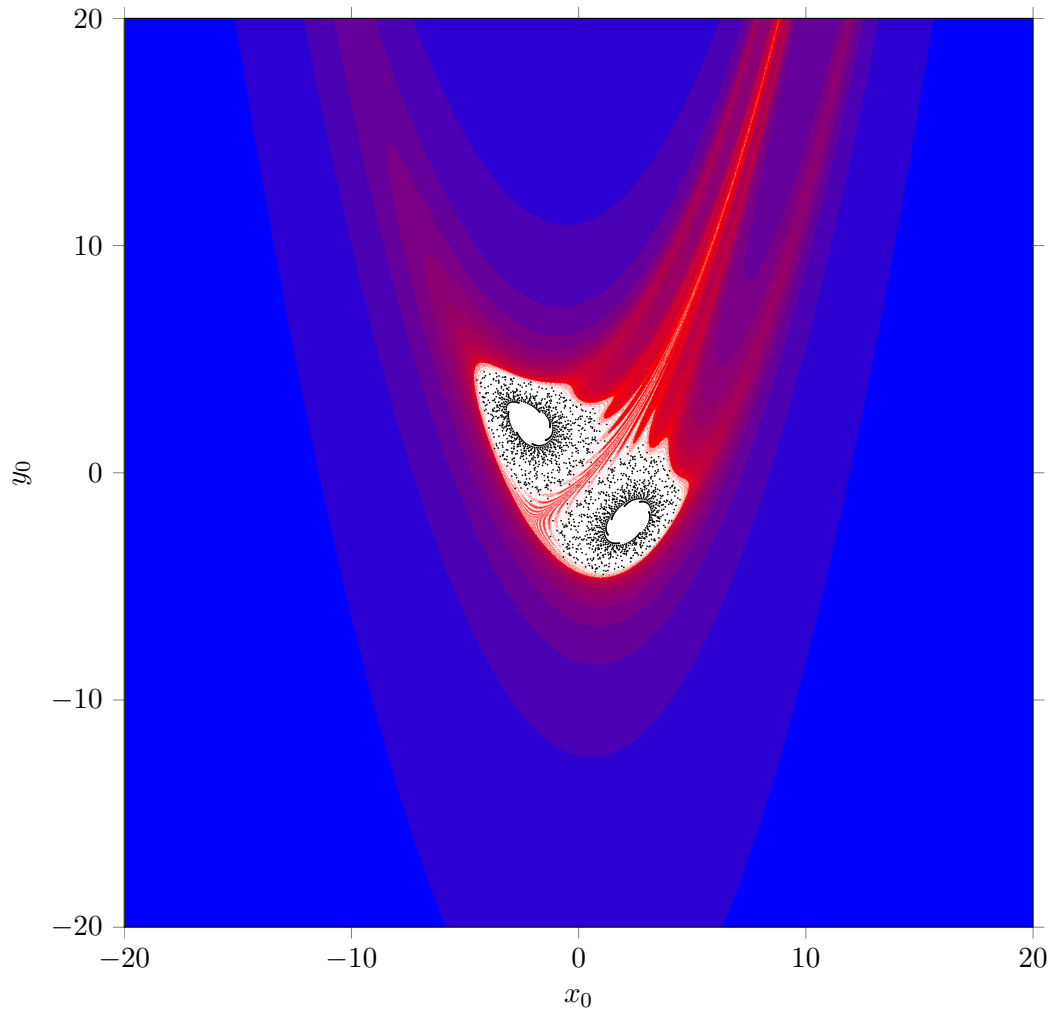


In the latter figure the Hénon attractor for  $(x_0, y_0) = (0, 0)$  is drawn in black. All white starting points  $(x_0, y_0)$  iterate towards the Hénon attractor, so they form the basin of attraction for the Hénon map. The other colours indicate the number of iterations needed before  $x_n^2 + y_n^2 > 20\,000$ : from orange (close to the white basin) for 7 iterations through purple (more in the outer parts) for 2 iterations.

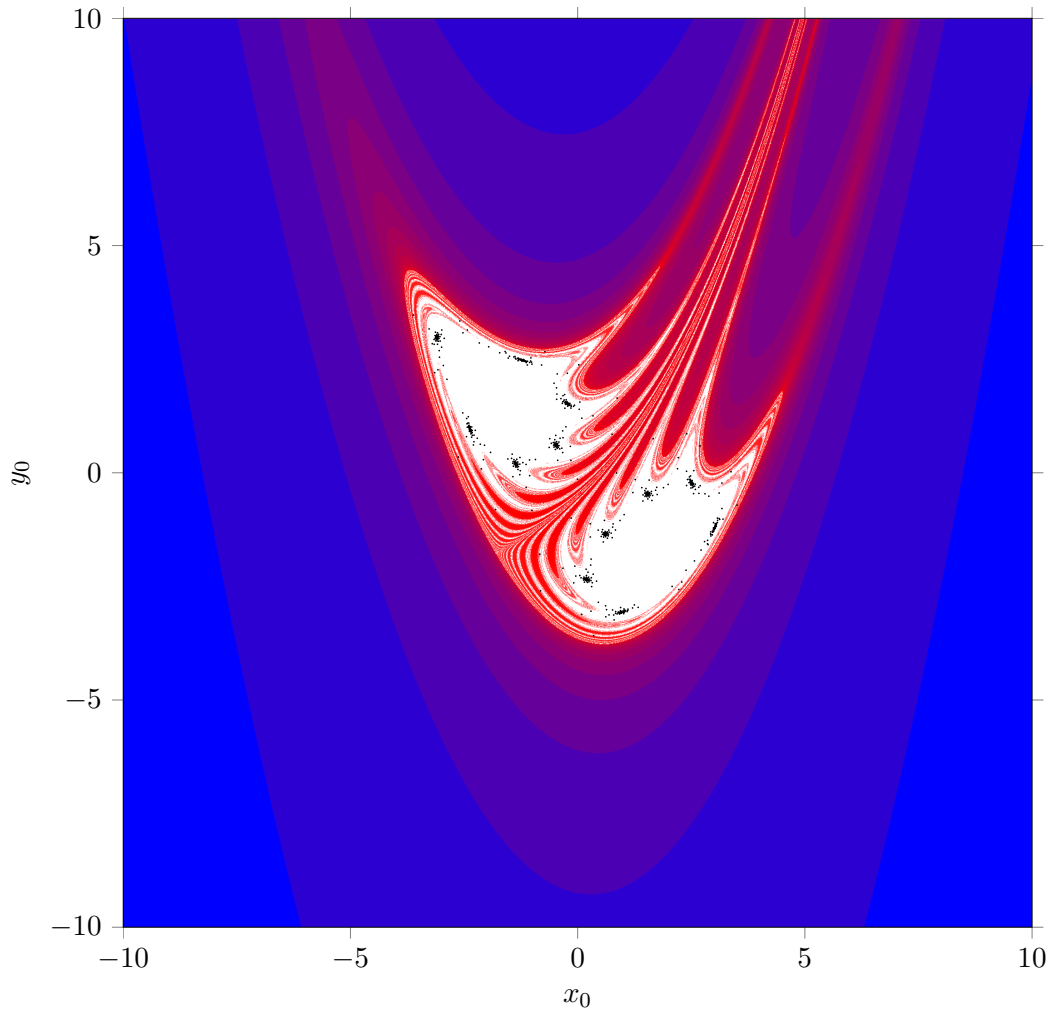
A similar picture for the Hénon map with  $a = 0.155$  and  $b = 0.996$  is shown in the next figure. Again the Hénon attractor for  $(x_0, y_0) = (0, 0)$  is drawn in black. For the escape to ‘infinity’ the colouring is different: from pink (close to the white basin) in 5 steps through blue (outer parts) in 1 step.



For  $a = 0.2$  and  $b = 0.999$  the result is shown in the next figure. Also here the Hénon attractor for  $(x_0, y_0) = (0, 0)$  is drawn in black. As we already saw on page 65, the attractor is split in two regions.

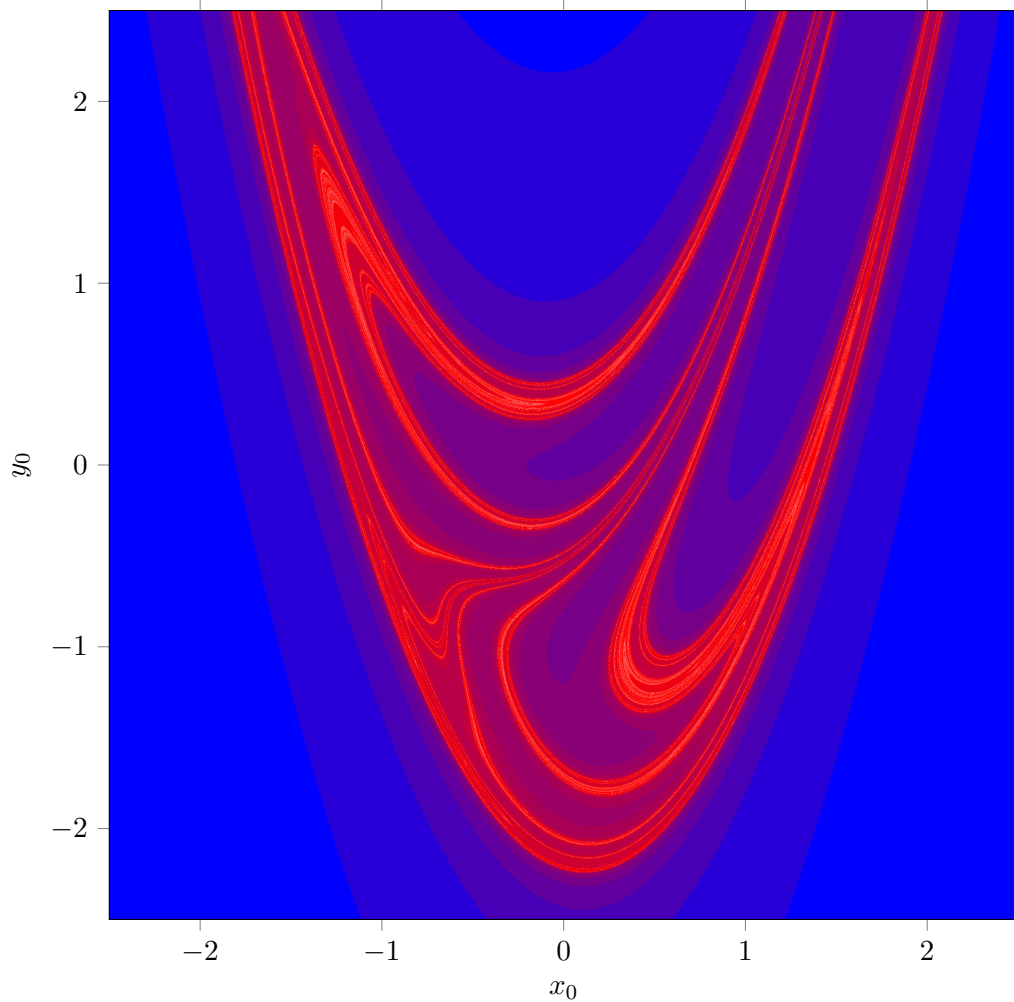


For  $a = 0.31552$  and  $b = 0.99004$  the result is shown in the next figure. In comparison with the previous figure, the attractor seems to ‘evaporate’: in each of the two regions there only is a clustering to 6 small ‘clouds’ away from the center.





For  $a = 1.2$  and  $b = 0.99$  the attractor is completely vanished, all points go to ‘infinity’, but with different ‘speed’.



## 4.5 The $z^2 + c$ map

Here we will consider the following map:

$$\begin{aligned} x_{m+1} &= x_m^2 - y_m^2 + a \\ y_{m+1} &= 2x_my_m + b, \end{aligned} \tag{4.1}$$

where  $a$  and  $b$  are constants. With  $z = x + iy$  and  $c = a + ib$  it takes the simple form  $z^2 + c$ . For this reason it is known as the  $z^2 + c$  map.

For many values of  $a$  and  $b$  the orbit end in a periodic cycle. For  $a = 0.2$ ,  $b = 0.541$  and  $(x_0, y_0) = (0, 0)$  the evolution of points  $(x_m, y_m)$  is as shown in the next figure.

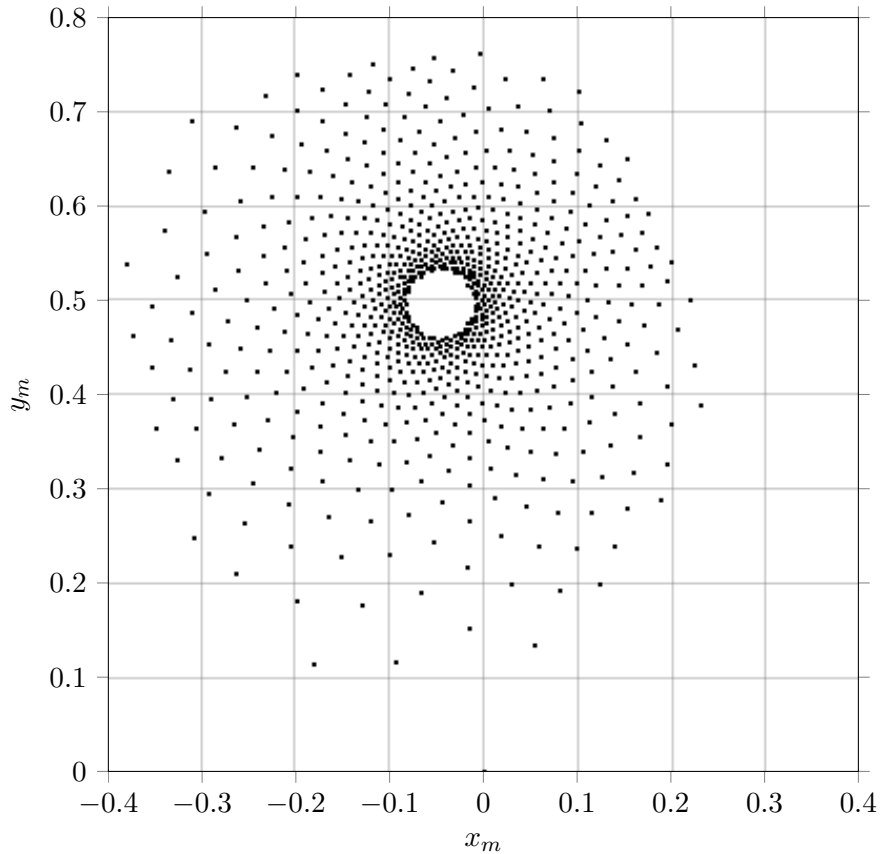


Figure 4.12: Time series of  $(x_m, y_m)$  for  $a = 0.2$ ,  $b = 0.541$  and  $(x_0, y_0) = (0, 0)$ .

We recognize 21 clockwise and 34 anti-clockwise spirals, both are Fibonacci numbers. In the long run the points tend to a single point  $(-0.044658, 0.49664)$ . For other values of  $a$  the points  $(x_m, y_m)$  may end up in a periodic limit cycle or diverge to infinity. For  $b = 0.541$  the orbits are plotted against  $a$  in figure [4.13](#). Curves are periodic cycles, points on a vertical line are part of a chaotic orbit, and the absent of points for a value of  $a$  means the orbit has diverged to infinity.

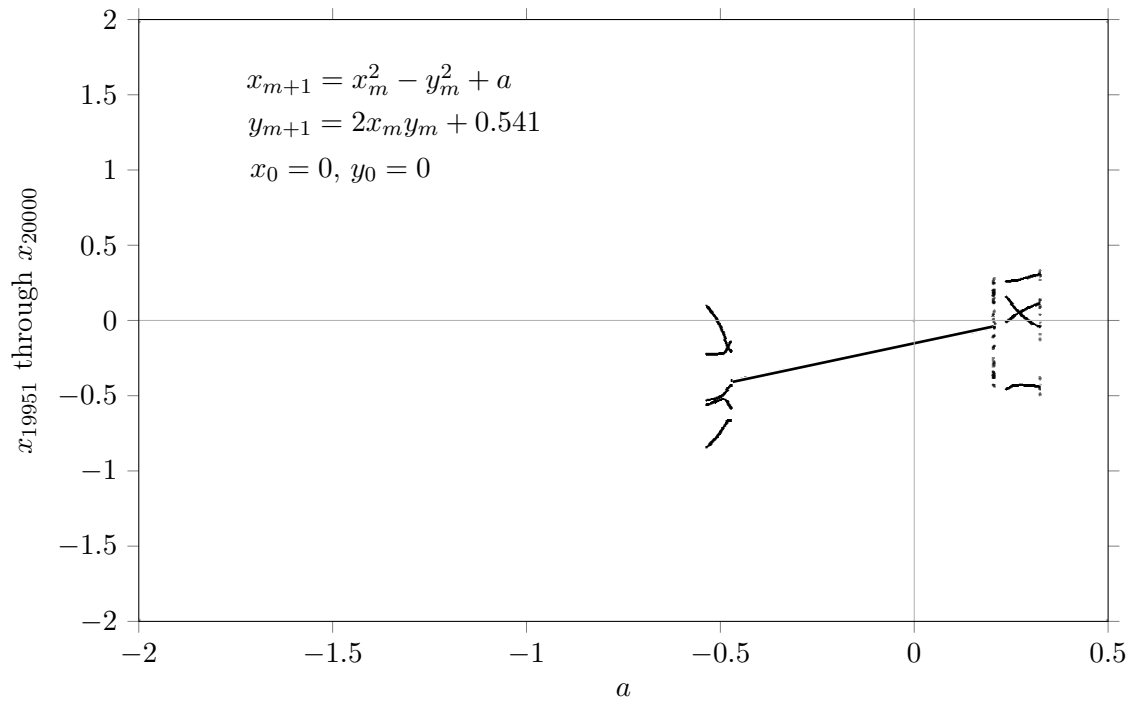


Figure 4.13: Orbit diagram for the  $z^2 + c$  map with  $b = 0.541$  and  $(x_0, y_0) = (0, 0)$ .

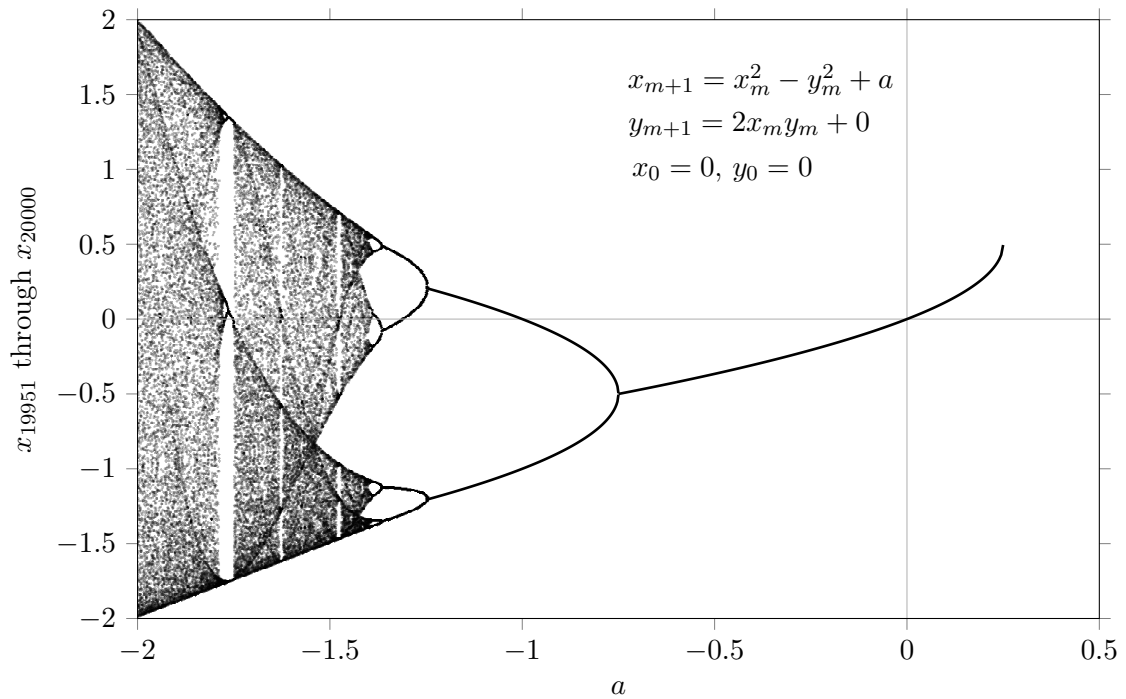


Figure 4.14: Orbit diagram for the  $z^2 + c$  map with  $b = 0$  and  $(x_0, y_0) = (0, 0)$ .

A special situation occurs for  $b = 0$  and  $y_0 = 0$ . Then  $y_m = 0$  for all  $m$ . As a consequence the system is reduced to  $x_{m+1} = x_m^2 + a$ , which is, up to a trivial transformation, equal to the logistic equation. The orbit diagram is shown in figure [4.14](#). The single fixed points start at  $a = 1/4$ , the bifurcation to two fixed points is at  $a = -3/4$ , and the bifurcation to 4 fixed points is at  $a = -5/4$ . The next bifurcation is at  $a \approx -1.3681$ , etc.

A Lyapunov image for the  $z^2 + c$  map is shown in the next figure.

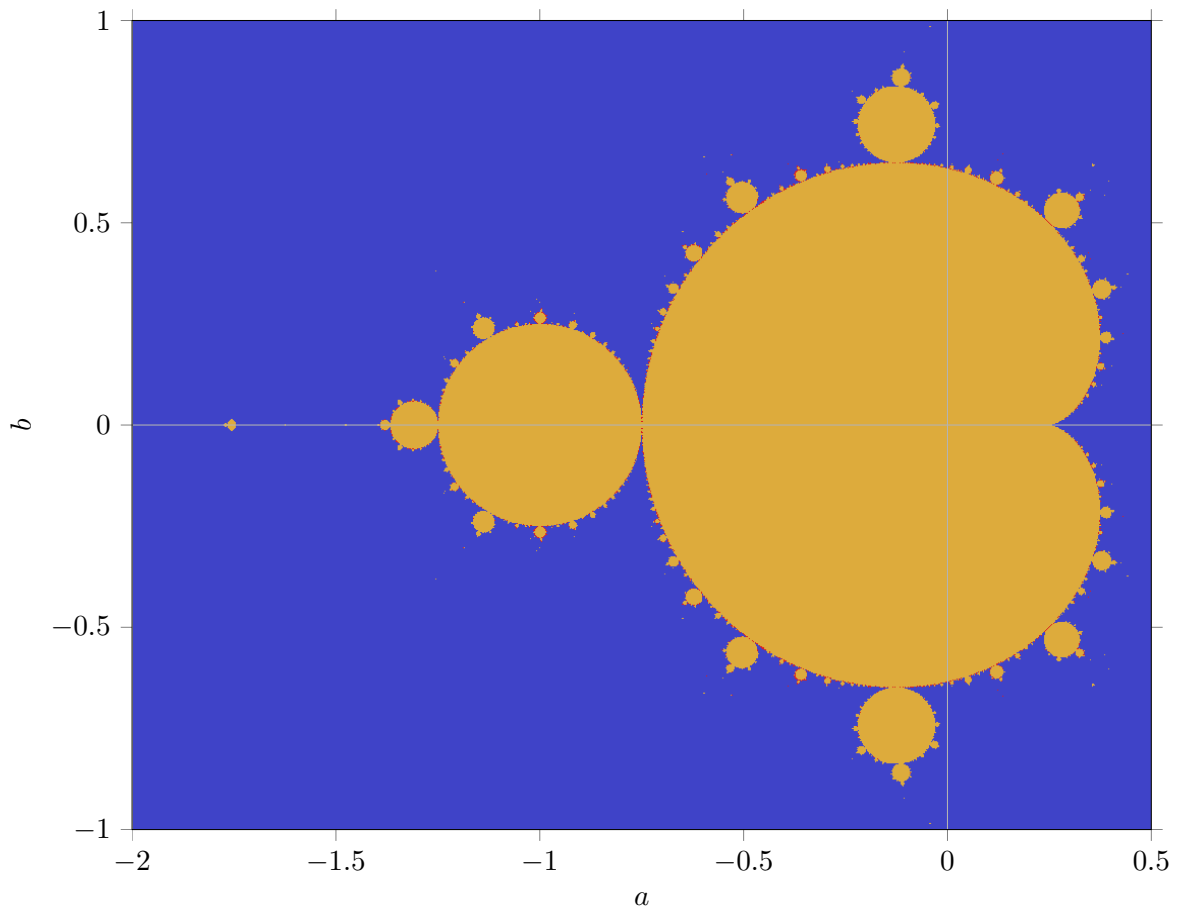
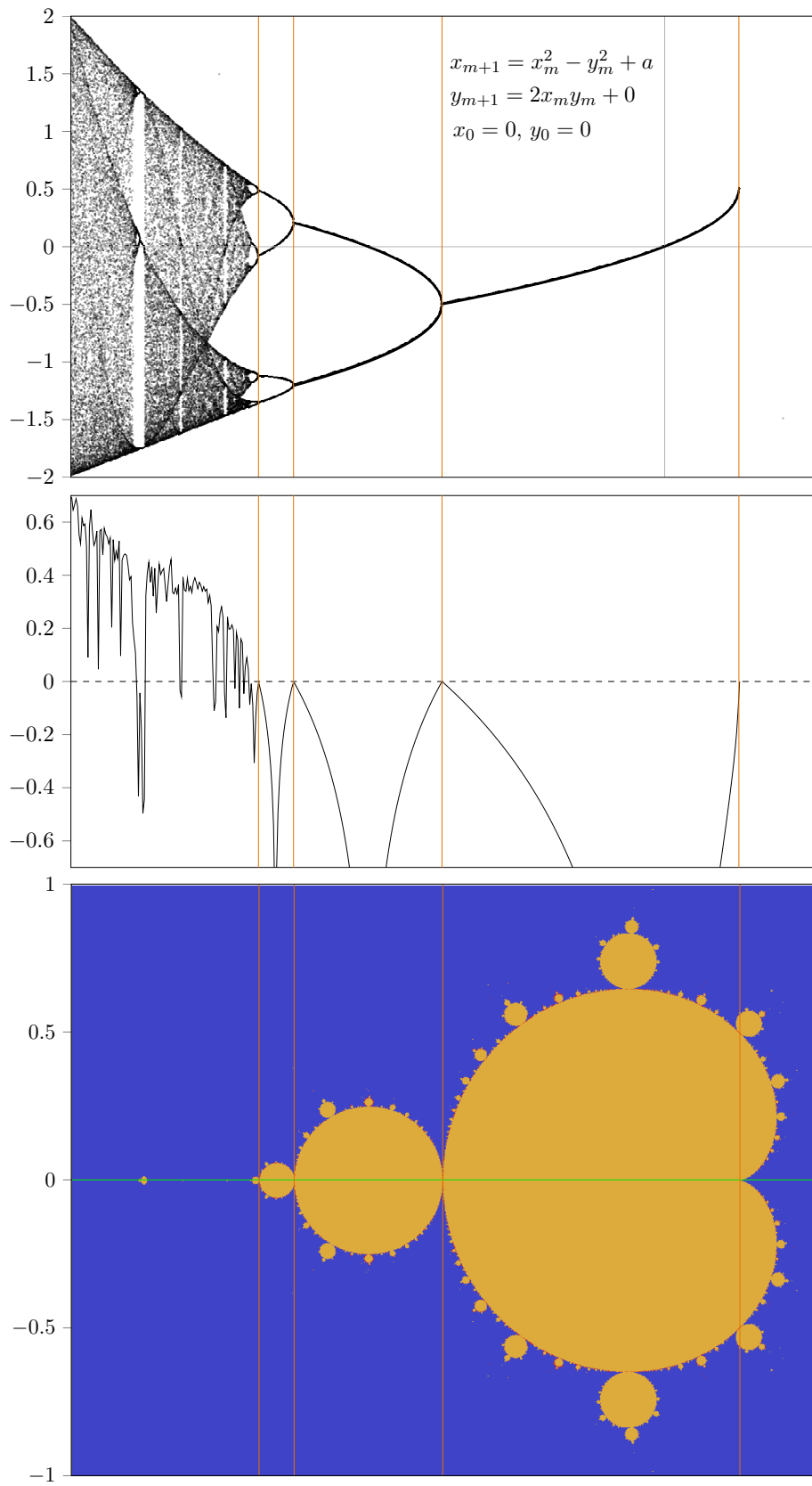
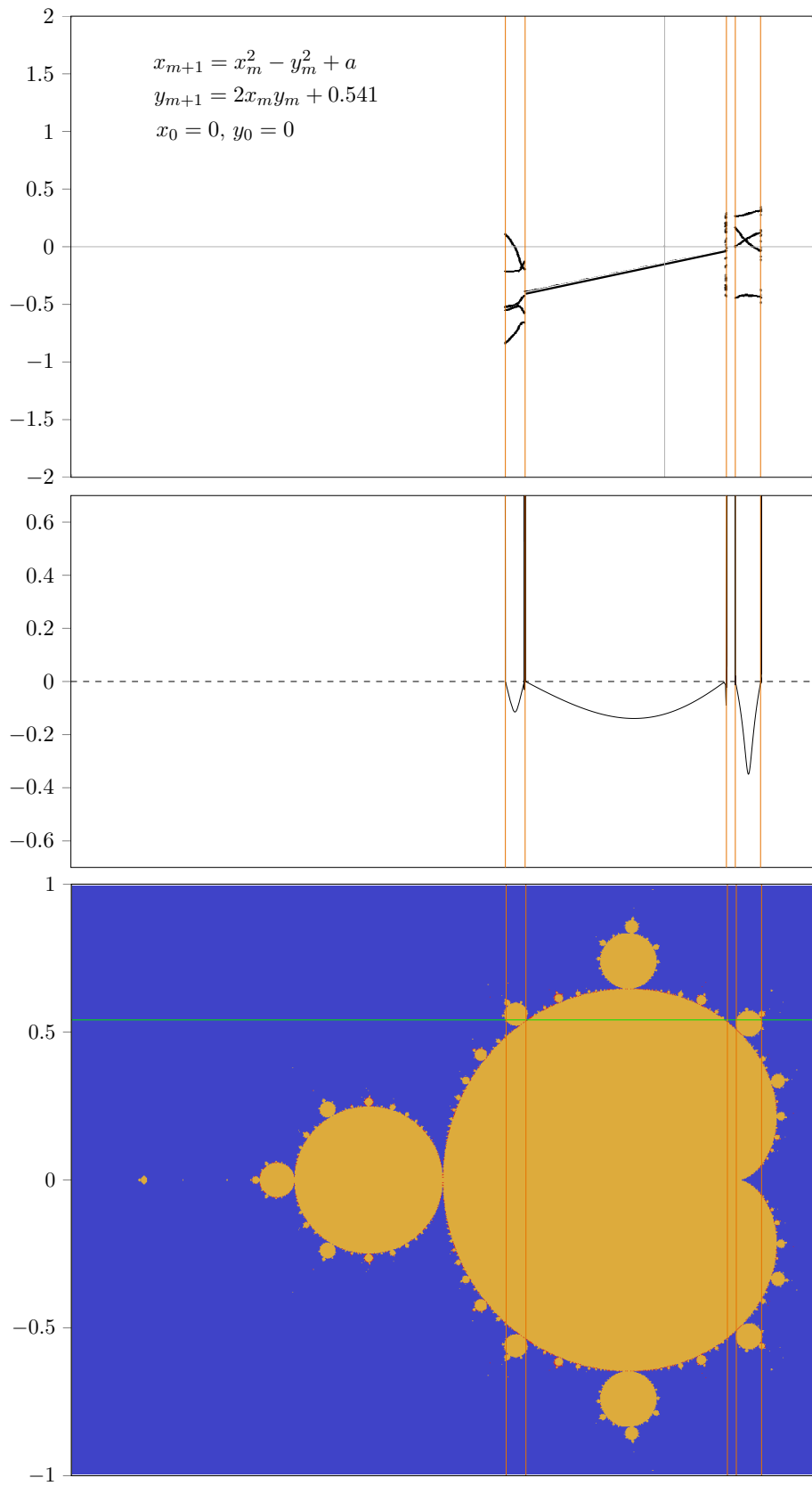


Figure 4.15: A Lyapunov image for the  $z^2 + c$  map. Pixels are colored yellow for a negative Lyapunov exponent, red for a positive Lyapunov exponent and blue in case the iterative values  $(x_m, y_m)$  run to infinity.

The yellow part in the figure is called the Mandelbrot set. The big part with a kidney shape is a cardioid with the cusp at  $a = 1/4$ . A circle touches the cardioid in  $(a, b) = (-3/4, 0)$ , which in turn is touched by a smaller circle in  $(a, b) = (-5/4, 0)$ , and so on. It is illuminating to draw the  $b = 0$  line in figure [4.15](#) and put it together with the orbit diagram [4.14](#) and the corresponding Lyapunov image in a single picture, see the next page.





The vertical brown lines show the connection between bifurcation points and the touching points. Since the ratio of the distances between successive bifurcations approach to the Feigenbaum number 4.66920..., the ratio of the radii of successive circles also approach to the Feigenbaum number.

For  $b = 0.541$  we also combine three diagrams, see the previous page. From left to right the green  $b = 0.541$  line enters at  $a \approx -0.537$  a circle which corresponds to period 5 limit cycles. For  $a \approx 0.47$  it leaves the circle and enters the main cardioid. The latter corresponds to period 1 limit cycle. It leaves the cardioid for  $a \approx 0.208$  to arrive in the blue area of divergence to infinity. The green line enters a circle for  $a \approx 0.238$ . The circle corresponds to period 4 cycles. The green line leaves this circle for  $a \approx 0.323$ .

## 4.6 Analytical solutions for the $z^2 + c$ map

So far the investigations were numerical. To a certain extent the Mandelbrot set can be investigated in an analytic way. By means of the complex variable  $z = x + iy$  and the complex constant  $c = a + ib$  the system (4.1) takes the form

$$z_{m+1} = z_m^2 + c. \quad (4.2)$$

That is,  $f(z) = z^2 + c$ . For a fixed point there holds  $f(z) = z$  and the stability requires the absolute value of the derivative to be smaller than 1:  $|\partial f/\partial z| < 1$ . At the boundary between stable and unstable regions we have  $|\partial f/\partial z| = 1 = |e^{i\theta}|$ , where the angle  $\theta$ , is from 0 through  $2\pi$ .

For  $f(z) = z^2 + c$  we therefore have the following two conditions for the boundary:  $z^2 + c = z$  and  $2z = e^{i\theta}$ . Substituting  $z = e^{i\theta}/2$  in  $c = z - z^2$  we obtain

$$c = \frac{1}{2}e^{i\theta} - \frac{1}{4}e^{2i\theta}. \quad (4.3)$$

This is the equation for a cardioid. The fixed point is stable inside this region, see the blue cardioid in figure 4.16. The equation for the cardioid can also be written as

$$\begin{aligned} a &= \frac{1}{4} + \frac{1}{2}(1 - \cos \theta) \cos \theta \\ b &= \frac{1}{2}(1 - \cos \theta) \sin \theta. \end{aligned} \quad (4.4)$$

For a period 2 cycle we have  $f(f(z)) = z \rightarrow c + c^2 - z + 2cz^2 + z^4 = 0$  and  $4z^3 + 4cz = e^{i\theta}$ . The first equation can be written as  $(c - z + z^2)(c + 1 + z + z^2) = 0$ . The solution  $(c - z + z^2) = 0$  corresponds the period 1 cycle (single fixed point). Substitution of the second solution  $c = -1 - z - z^2$  into the equation  $4z^3 + 4cz = e^{i\theta}$  gives:  $-z - z^2 = e^{i\theta}/4$ . Substituting this result back into  $c = -1 - z - z^2$  we obtain [4]

$$c = -1 + \frac{1}{4}e^{i\theta}. \quad (4.5)$$

The latter is the equation for a circle with radius  $1/4$  and center  $(-1, 0)$ . The period 2 limit is stable inside this circle, see the cyan disk in figure [4.16](#). The cyan disk touches the blue cardioid in  $(-3/4, 0)$ . The equation for the circle can also be written as

$$\begin{aligned} a &= -1 + \frac{1}{4} \cos \theta \\ b &= \frac{1}{4} \sin \theta. \end{aligned} \quad (4.6)$$

For a period 3 cycle we have  $f(f(f(z))) = z \rightarrow (c - z + z^2)(1 + c + 2c^2 + c^3 + z + 2cz + c^2z + z^2 + 3cz^2 + 3c^2z^2 + z^3 + 2cz^3 + z^4 + 3cz^4 + z^5 + z^6) = 0$  and  $c^2z + c^3z + cz^3 + 3c^2z^3 + 3cz^5 + z^7 = e^{i\theta}/8$ . Discarding the period 1 solution  $(c - z + z^2) = 0$  and eliminating  $z$  we obtain

$$64c^3 + 128c^2 + 8c(8 - e^{i\theta}) + (8 - e^{i\theta})^2 = 0. \quad (4.7)$$

It has three solutions. By means of the variable

$$w = -1600 + 288e^{i\theta} - 27e^{2i\theta} + 3\sqrt{3}\sqrt{(8 - e^{i\theta})^2(1472 - 176e^{i\theta} + 27e^{2i\theta})} \quad (4.8)$$

the solutions read

$$c = -\frac{2}{3} + \left(\frac{4}{3} + \frac{1}{2}e^{i\theta}\right) \left(\frac{w}{2}\right)^{-1/3} + \frac{1}{12} \left(\frac{w}{2}\right)^{1/3}, \quad (4.9)$$

$$c = -\frac{2}{3} - \left(\frac{4}{3} + \frac{1}{2}e^{i\theta}\right) \left(\frac{1}{2} + \frac{1}{2}i\sqrt{3}\right) \left(\frac{w}{2}\right)^{-1/3} + \frac{1}{12} \left(-\frac{1}{2} + \frac{1}{2}i\sqrt{3}\right) \left(\frac{w}{2}\right)^{1/3}, \quad (4.10)$$

$$c = -\frac{2}{3} + \left(\frac{4}{3} + \frac{1}{2}e^{i\theta}\right) \left(-\frac{1}{2} + \frac{1}{2}i\sqrt{3}\right) \left(\frac{w}{2}\right)^{-1/3} - \frac{1}{12} \left(\frac{1}{2} + \frac{1}{2}i\sqrt{3}\right) \left(\frac{w}{2}\right)^{1/3}, \quad (4.11)$$

The three solutions correspond with two circles and one cardioid. The stable regions are therefore two disks and a cardioid, see the three brown shapes in figure [4.16](#). One disk touches the cardioid at the top  $(-1 + \sqrt{3})/8$  and one disk at the bottom  $(-1 - \sqrt{3})/8$  respectively. The third brown shape is a small cardioid (same shape and same orientation as the big blue cardioid) with its cusp point at  $(-7/4, 0)$ , and it intersects the  $b = 0$  line at  $(v, 0)$ , where

$$v = -\frac{2}{3} - \frac{5}{6} \sqrt[3]{\frac{2}{1915 - 135\sqrt{201}}} - \frac{1}{12} \sqrt[3]{\frac{1915 - 135\sqrt{201}}{2}} \approx -1.76852915. \quad (4.12)$$

The latter was found by evaluating equation [\(4.9\)](#) for  $c$  at  $\theta = \pi$ . The equation [\(4.9\)](#) describes for  $0 < \theta \leq \pi$  the upper half of the small cardioid, and for  $\pi < \theta \leq 2\pi$  the left half of the circle in the upper half plane. The equation [\(4.10\)](#) describes for  $0 < \theta \leq \pi$  the left half of the circle in the lower half plane, and for  $\pi < \theta \leq 2\pi$  the lower half of the small cardioid. The equation [\(4.11\)](#) describes for  $0 < \theta \leq \pi$  the right half of the circle in the upper half plane, and for  $\pi < \theta \leq 2\pi$  the right half of the circle in the lower half plane. With the use of the constant  $v$  the solution for the small cardioid can be written as

$$c = -\frac{21}{16} + \frac{1}{4}v + \left(-\frac{7}{8} - \frac{1}{2}v\right) e^{i\phi} + \left(\frac{7}{16} + \frac{1}{4}v\right) e^{2i\phi}. \quad (4.13)$$



By means of the variable

$$\chi = (7 + 4v)(1 - e^{i\phi})^2 \quad (4.14)$$

it can be written as

$$c = -\frac{7}{4} + \frac{1}{16}\chi, \quad (4.15)$$

The equation for the two circles then read

$$c = -\frac{1}{8} - \frac{1}{32}\chi \pm \frac{1}{32}\sqrt{-432 + 136\chi - 3\chi^2 - 16\sqrt{-\chi(\chi - 28)^2}}. \quad (4.16)$$

The relation between  $\phi$  and  $\theta$  is given by

$$e^{i\theta} = 1 + \frac{1}{4}\chi - \frac{1}{8}\sqrt{-\chi(\chi - 28)^2}. \quad (4.17)$$

Upon substitution of equation (4.14) for  $\chi$  and then equation (4.12) for  $v$  the relation becomes tedious.

For a period 4 cycle we have  $f(f(f(f(z)))) = z \rightarrow (c - z + z^2)(1 + c + z + z^2)(1 + 2c^2 + 3c^3 + 3c^4 + 3c^5 + c^6 + 2cz + c^2z + 2c^3z + c^4z + cz^2 + 5c^2z^2 + 6c^3z^2 + 12c^4z^2 + 6c^5z^2 + z^3 + 4c^2z^3 + 4c^3z^3 + 4cz^4 + 3c^2z^4 + 18c^3z^4 + 15c^4z^4 + 2cz^5 + 6c^2z^5 + z^6 + 12c^2z^6 + 20c^3z^6 + 4cz^7 + 3cz^8 + 15c^2z^8 + z^9 + 6cz^{10} + z^{12}) = 0$  and  $c^3z + 2c^4z + 3c^5z + 3c^6z + c^7z + c^2z^3 + 4c^3z^3 + 9c^4z^3 + 15c^5z^3 + 7c^6z^3 + 3c^2z^5 + 9c^3z^5 + 30c^4z^5 + 21c^5z^5 + cz^7 + 3c^2z^7 + 30c^3z^7 + 35c^4z^7 + 15c^2z^9 + 35c^3z^9 + 3cz^{11} + 21c^2z^{11} + 7cz^{13} + z^{15} = e^{i\theta}/16$ . Discarding the period 1 solution  $(c - z + z^2) = 0$ , the period 2 solution  $(1 + c + z + z^2)$  and eliminating  $z$  we obtain

$$4096c^6 + 12288c^5 + 256c^4(48 + e^{i\theta}) + 256c^3(48 + e^{i\theta}) + 16c^2(512 - 16e^{i\theta} - e^{2i\theta}) + (16 - e^{i\theta})^3 = 0. \quad (4.18)$$

The equation has 6 solutions which are determined numerically. The solutions correspond with the red shapes in figure 4.16. Two of the shapes are disks of which one touches the blue cardioid in  $(1/4, 1/2)$  and the other one in  $(1/4, -1/2)$ . Two other shapes are small disks in the neighbourhood of  $(-0.158, 1.034)$  and  $(-0.158, -1.034)$  respectively. The fifth shape is a disk which touches the cyan circle in  $(-5/4, 0)$ . The sixth shape is a very small cardioid (more than 1000 times smaller than the blue cardioid) and is situated around  $(-1.941, 0)$ .

For a period 5 cycle we obtain 15 solutions. They correspond with: 1 small cardioid with its cusp at  $(a, b) \approx (-1.98541, 0)$ , 1 small cardioid with its cusp at  $(a, b) \approx (-1.86049, 0)$ , 1 small cardioid with its cusp at  $(a, b) \approx (-1.6242, 0)$ , 2 small cardioids at  $(a, b) \approx (-1.256, \pm 0.380)$ , 2 small cardioids at  $(a, b) \approx (-0.1982, \pm 1.1002)$ , 2 small cardioids at  $(a, b) \approx (-0.044, \pm 0.987)$ , 2 small cardioids at  $(a, b) \approx (0.359, \pm 0.643)$ , 4 disks which touch the blue cardioid. These 15 shapes are drawn green in figure 4.16.

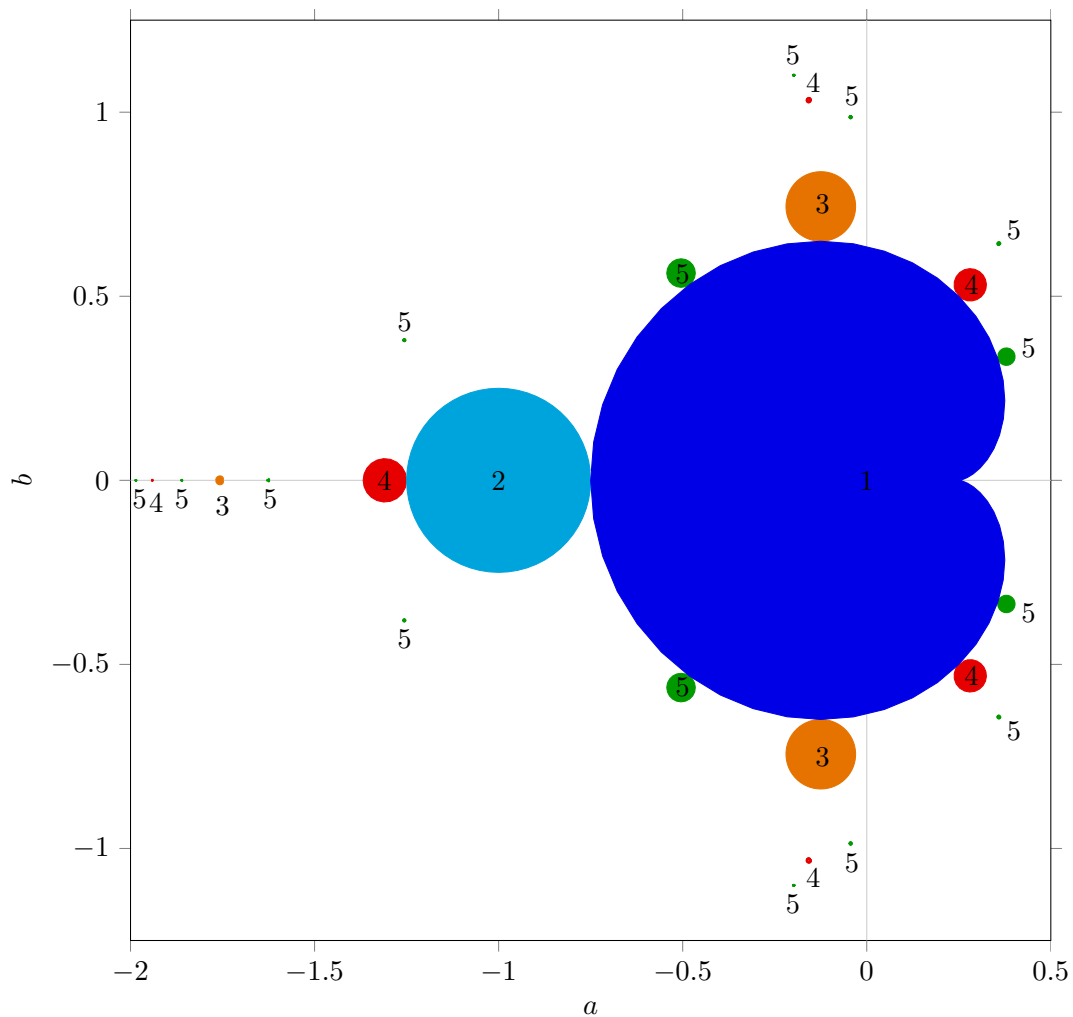


Figure 4.16: Analytical solutions for the border of the Mandelbrot set. The numbers inside or nearby a disk indicate the period of the limit cycle.

#### 4.7 Number of period $n$ solutions of the $z^2 + c$ map

Let us write the  $n$ -th iterate of  $z$  as  $z_{[n]}$ . The largest power of  $c$  in  $z_{[n]}$  is  $2^{n-1}$ . The period 1 solution was partly based on the condition  $z_{[1]} - z = 0$ ; the other part was  $\partial z_{[1]} = 1$ . The largest power of  $c$  in  $z_{[1]} - z$  is  $2^0 = 1$ . Therefore there is 1 period 1 solution. The period 2 solution was partly based on the condition  $(z_{[2]} - z)/(z_{[1]} - z) = 0$ ; the other part was  $\partial z_{[2]} = 1$ . The division by  $z_{[1]} - z$  is to exclude the period 1 solution. The largest power of  $c$  in  $(z_{[2]} - z)/(z_{[1]} - z)$  is  $2^1 - 2^0 = 1$ . Therefore there is 1 period 2 solution. The period 3 solution was partly based on the condition  $(z_{[3]} - z)/(z_{[1]} - z) = 0$ . The division by  $z_{[1]} - z$  is to exclude the period 1 solution. The largest power of  $c$  in  $(z_{[3]} - z)/(z_{[1]} - z)$  is  $2^2 - 2^0 = 3$ .

Therefore there are 3 period 3 solutions. The period 4 solution was partly based on the condition  $(z_{[4]} - z)/(z_{[2]} - z) = 0$ . The division by  $z_{[2]} - z$  is to exclude the period 2 solution. The largest power of  $c$  in  $(z_{[4]} - z)/(z_{[2]} - z)$  is  $2^3 - 2^1 = 6$ . Therefore there are 6 period 4 solutions. The period 5 solution was partly based on the condition  $(z_{[5]} - z)/(z_{[1]} - z) = 0$ . The division by  $z_{[1]} - z$  is to exclude the period 1 solution. The largest power of  $c$  in  $(z_{[5]} - z)/(z_{[1]} - z)$  is  $2^4 - 2^0 = 15$ . Therefore there are 15 period 5 solutions. The period 6 solution is based on the condition  $(z_{[6]} - z)/(z_{[3]} - z)/(z_{[2]} - z) * (z_{[1]} - z) = 0$ . The division by  $z_{[3]} - z$  and  $z_{[2]} - z$  is to exclude the period 3 and period 2 solution. Since both  $z_{[3]} - z$  and  $z_{[2]} - z$  contain the period 1 solution, we have divided by  $z_{[1]} - z$  one time too much. To repair it we multiply by  $z_{[1]} - z$ . The largest power of  $c$  in  $(z_{[6]} - z)/(z_{[3]} - z)/(z_{[2]} - z) * (z_{[1]} - z)$  is  $2^5 - 2^2 - 2^1 + 2^0 = 27$ . Therefore there are 27 period 6 solutions. Continuing this line of arguments we obtain the following series of numbers of period  $n$  solutions 1, 1, 3, 6, 15, 27, 63, 120, 252, .... The series is known as A000740 in OEIS [5].

For a period  $n$  solution we write  $n$  as its products of powers of distinct primes, the prime decomposition:  $n = \prod_{j=1}^k p_j^{m_j}$ . For instance, the prime decomposition of 30 is  $2^1 \cdot 3^1 \cdot 5^1$  and contains no squares and has three distinct primes. The prime composition of 84 is  $2^2 \cdot 3^1 \cdot 7^1$  and contains a square:  $2^2$ . The prime decomposition of 882 is  $2^1 \cdot 3^2 \cdot 7^3$  and contains three squares:  $3^2$ ,  $7^2$  and  $(3 \cdot 7)^2$ . The Möbius function  $\mu(n)$  is defined as

$$\mu(n) = \begin{cases} 1 & \text{if } n = 1; \\ 0 & \text{if } n \text{ contains one or more squares;} \\ (-1)^k & \text{if } n \text{ is a square free product of } k \text{ distinct primes.} \end{cases} \quad (4.19)$$

For instance,  $\mu(4) = 0$ ,  $\mu(5) = -1$ ,  $\mu(6) = 1$ ,  $\mu(12) = 0$  and  $\mu(30) = -1$ .

By means of the Möbius function the number  $s(n)$  of period  $n$  solutions is given by

$$s(n) = \sum_{d|n} \mu(n/d) 2^{d-1}. \quad (4.20)$$

where  $d|n$  are the numbers  $d$  which are a divisor of  $n$ . A recurrence relation for  $s(n)$  is

$$s(n) = 2^{n-1} - \sum_{d|n, d>1} s(n/d), \quad (4.21)$$

with  $s(1) = 1$  as initial value.

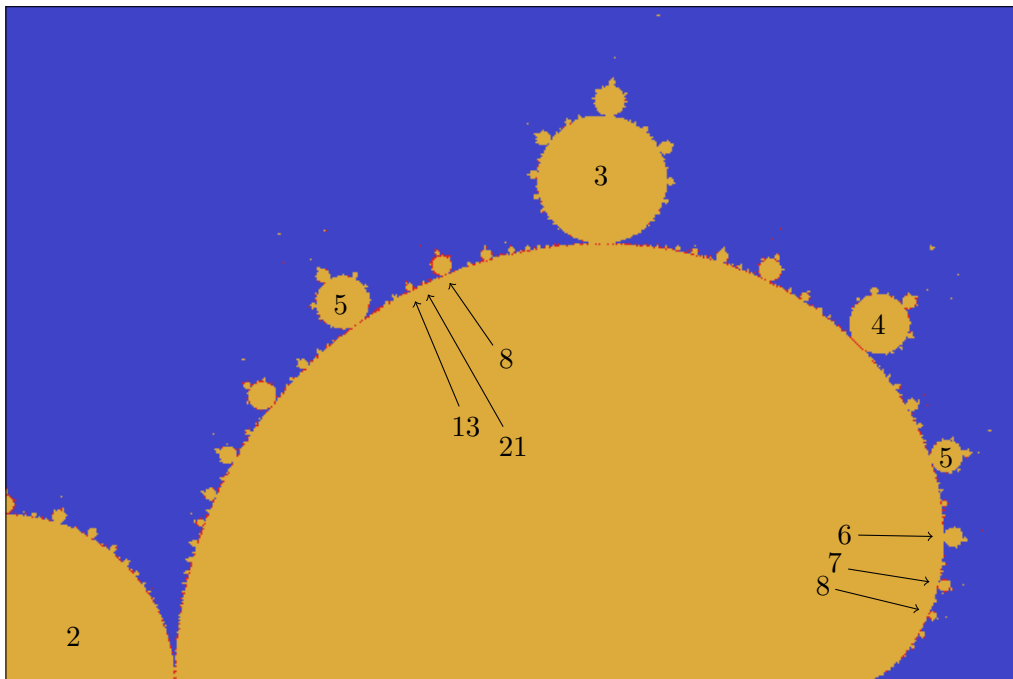
A property of  $s$  is  $\sum_{d|n} s(d) = 2^{n-1}$ .

## 4.8 Mandelbrot set and Fibonacci

If we follow the circumference of the main cardioid in figure [4.16](#), the largest object we meet is the cyan disk with number 2. Since the Mandelbrot set is symmetric with respect to the  $x$ -axis, we consider only the upper half plane from here. If we follow in the upper half of figure [4.16](#) the circumference of the main cardioid from the cyan disk with number 2 towards the cusp of the blue cardioid, then the largest object is an orange disk with number 3. From the orange disk with number 3 to the cusp the largest object is a red disk with number 4. The largest disk between the disk with number 4 and the cusp is a green disk with number 5. If we had plotted more disks, the next largest disk between 5 and the cusp would be a disk with number 6. Continuation of the procedure leads to the sequence: 1, 2, 3, 4, 5, 6, 7, 8, ...

The largest disk in figure [4.16](#) between the cyan disk with number 2 and the orange disk with number 3 is a green disk with number 5. If we had plotted more disks, the largest disk between the orange disk with number 3 and the green disk with number 5 would be a disk with number 8. The largest disk between number 5 and number 8 is a disk with number 13. The largest disk between 8 and 13 is a disk with number 21. Continuation of the procedure results in the Fibonacci sequence: 1, 2, 3, 5, 8, 13, 21, 34, 55, 89, 144, ....

The situation is illustrated in the figure below.

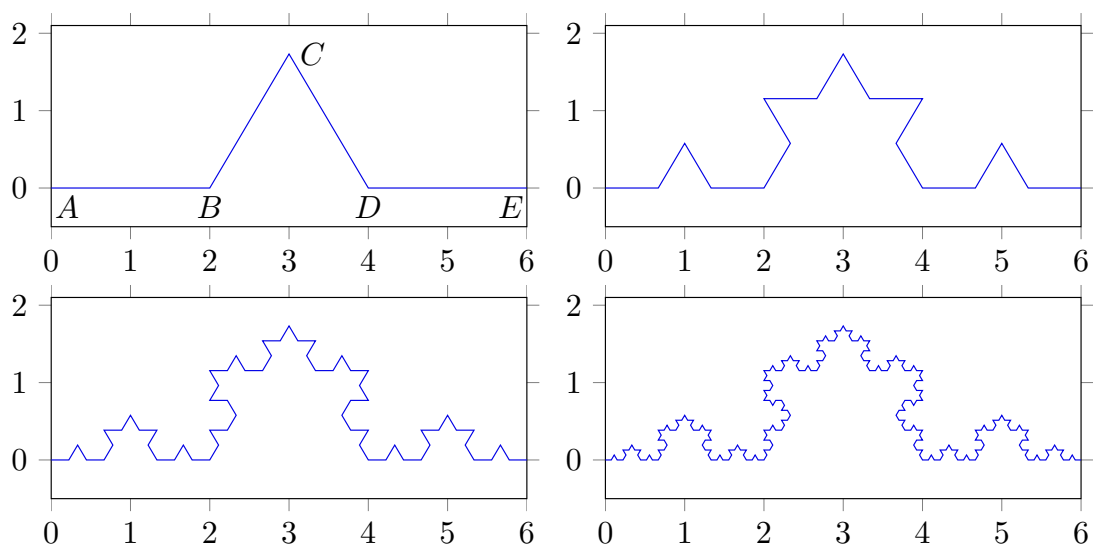


# Chapter 5

## Fractals

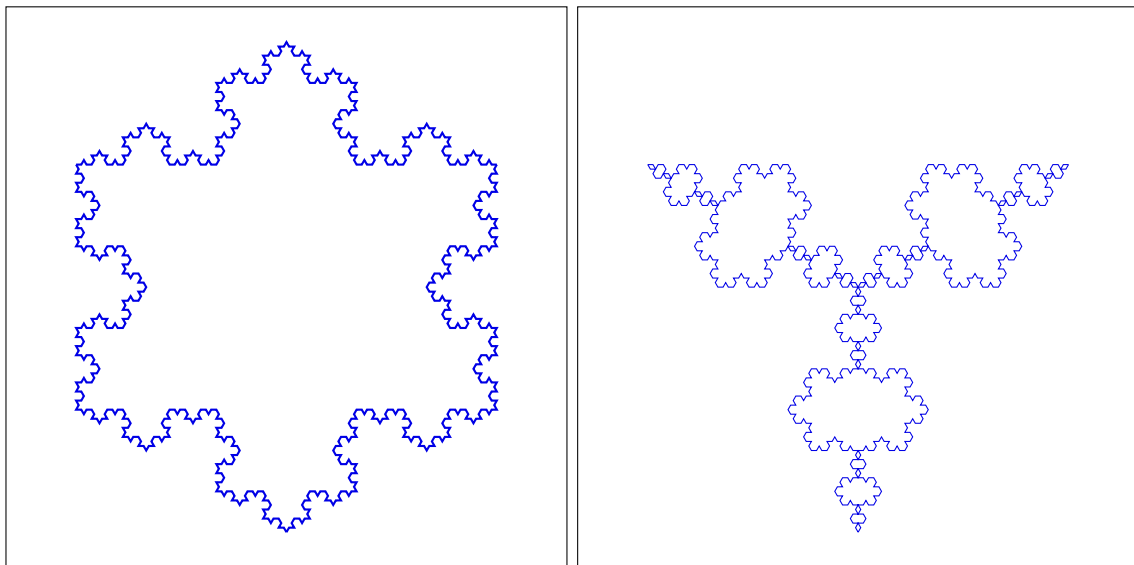
### 5.1 Koch snowflake

We start with five points  $A(0,0)$ ,  $B(2,0)$ ,  $C(3,\sqrt{3})$ ,  $D(4,0)$  and  $E(6,0)$ , and the four line segments  $AB$ ,  $BC$ ,  $CD$  and  $DE$ . The curve  $ABCDE$  is shown in the upper left panel of the next figure. Each of the four line segments has length 2. The distance between  $A$  and  $E$  is 6. The curve  $ABCDE$  is used as the building block of a structure with self-similarity. First every segment is replaced by a 3 times smaller version of  $ABCDE$ . The result is 16 line segments, see the upper right panel. Since every segments is 3 times smaller the length of the new segmented curve is  $32/3$ . Next every segment is replaced by a 9 times smaller version of  $ABCDE$ . The result is 64 line segments, see lower left panel. The length of the new segmented curve is  $128/9$ . Next every segment is replaced by a 27 times smaller version of  $ABCDE$ . The result is 256 line segments, see lower right panel. The length of the new segmented curve is  $512/27$ .



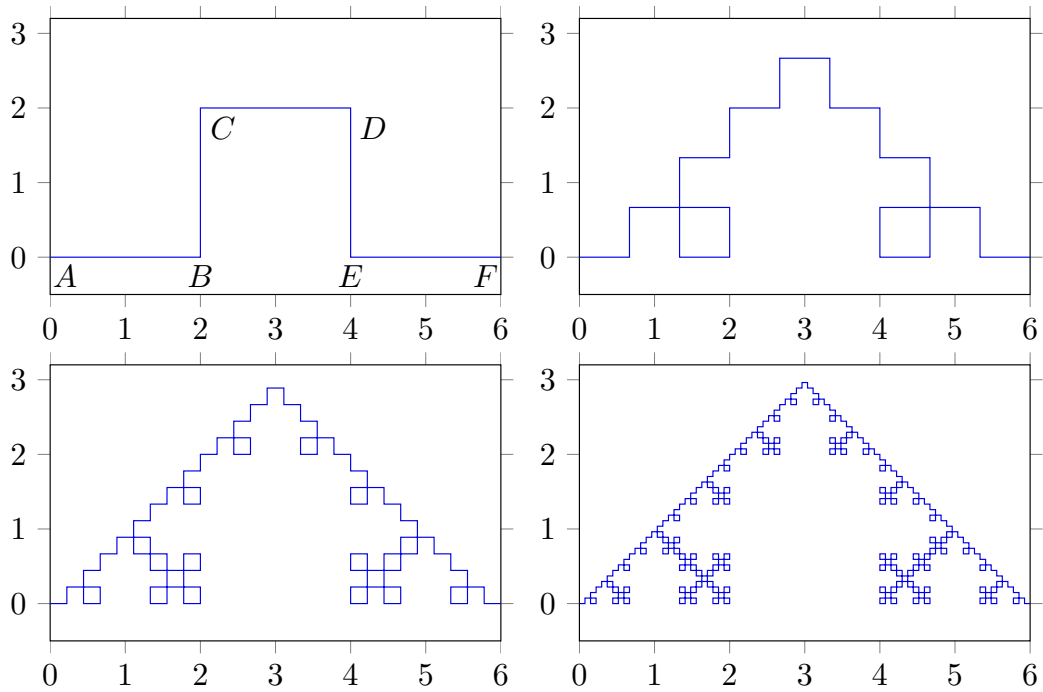
If the procedure is continued through infinity, the resulting figure has the following property: if one zooms in on a line segment, then it looks as the original figure. In other words, the resulting figure is self similar at all scales. Such a figure is called a *fractal*. In this case it is known as the Koch fractal.

If the procedure which leads to the Koch fractal is applied to the sides of an equilateral triangle in the outside direction, we obtain the so called Koch snowflake, see left panel of next figure. In the inside direction it is an anti-snowflake, see right panel of next figure.

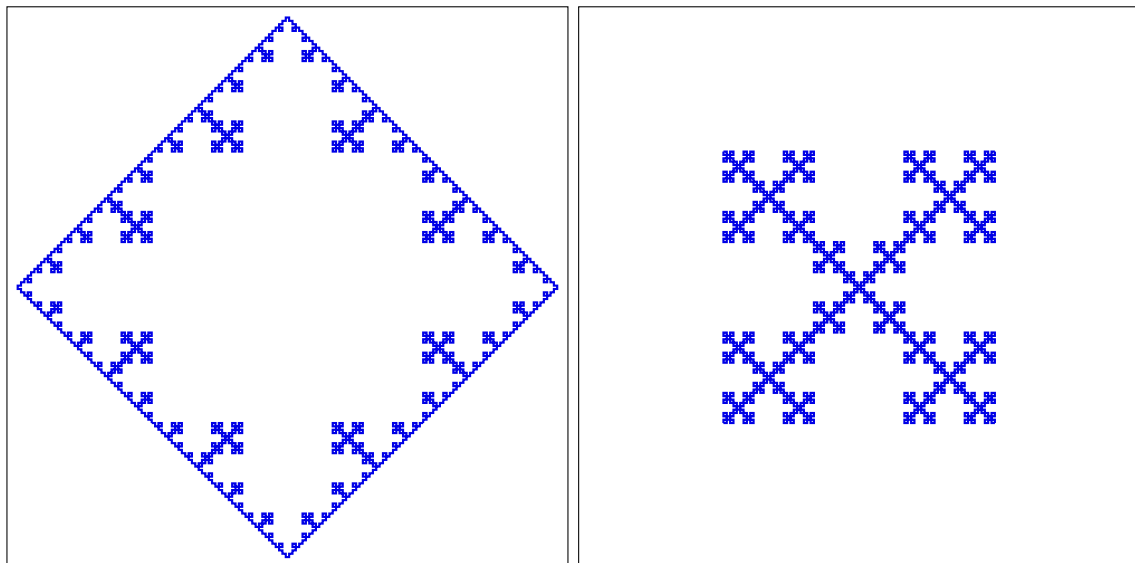


## 5.2 Designing fractals

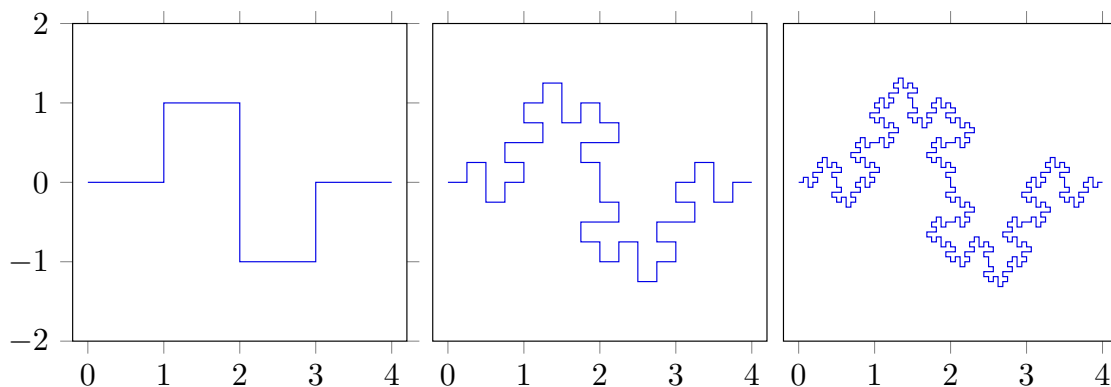
Here we consider another building block. We start with six points  $A(0,0)$ ,  $B(2,0)$ ,  $C(2,2)$ ,  $D(4,2)$ ,  $E(4,0)$  and  $F(6,0)$ , and the five line segments  $AB$ ,  $BC$ ,  $CD$ ,  $DE$  and  $EF$ . The curve  $ABCDEF$  is shown in the upper left panel of the next figure. Each of the five line segments has length 2. The distance between  $A$  and  $F$  is 6. Every segment is replaced by a 3 times smaller version of  $ABCDEF$ . The result is 25 line segments, see the upper right panel. Since every segment is 3 times smaller the length of the new segmented curve is  $50/3$ . Next every segment is replaced by a 9 times smaller version of  $ABCDEF$ . The result is 125 line segments, see lower left panel. The length of the new segmented curve is  $250/9$ . Next every segment is replaced by a 27 times smaller version of  $ABCDEF$ . The result is 625 line segments, see lower right panel. The length of the new segmented curve is  $1250/27$ .



If the procedure is repeated many times and applied to the sides of a square in the outside direction, we obtain a pattern as shown in the left panel of next figure. Application to the inside direction leads to the pattern shown in the right panel of next figure.

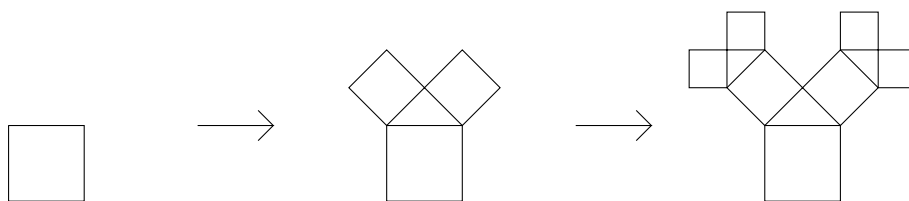


Next we consider another building block. We start with eight line segments connecting the nine points  $(0, 0)$ ,  $(1, 0)$ ,  $(1, 1)$ ,  $(2, 1)$ ,  $(2, 0)$ ,  $(2, -1)$ ,  $(3, -1)$ ,  $(3, 0)$  and  $(4, 0)$  as shown in the left panel of the next figure. Each of the line segments has length 1. The curve has length 8. Every segment is replaced by a 4 times smaller version of the initial building block. The result is 64 line segments, see the middle panel. Since every segment is 4 times smaller the length of the new segmented curve is 16. Repeating the procedure we obtain 512 line segments, see the right panel. The length of the new segmented curve is 32. Repeating the procedure leads to the so called Minkowski fractal. As for the previous fractals it can be applied to the sides of a triangle, a square or any polygon to obtain mathematical art figures.



### 5.3 Two dimensional fractals

We can also start with a two dimensional object and add smaller versions of the object. For instance, when we start with a square and add two smaller squares as shown below.



Taking more steps results in the *Pythagoras tree*, see the first figure on next page. Every branch is a smaller copy of the original tree. The self similarity is at all scales; the Pythagoras tree is a fractal. We can also make an asymmetric tree, see the second figure on next page.

Another example of a two dimensional fractal is obtained by starting with an isosceles triangle and place a smaller copy at the top of the original triangle with its base adjacent and perpendicular to one of the equal sides.



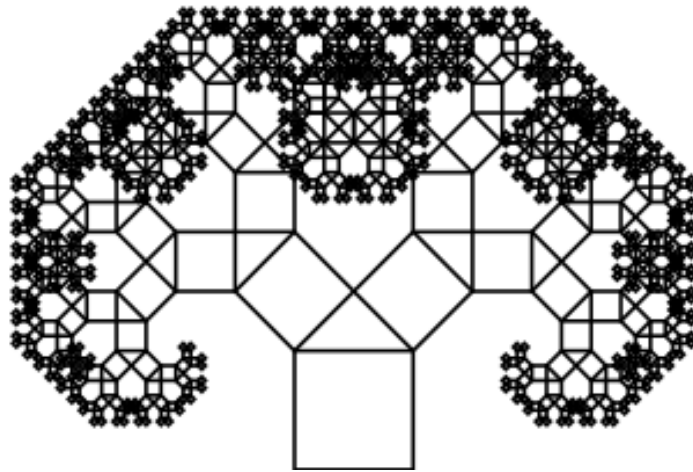


Figure 5.1: Pythagoras tree.

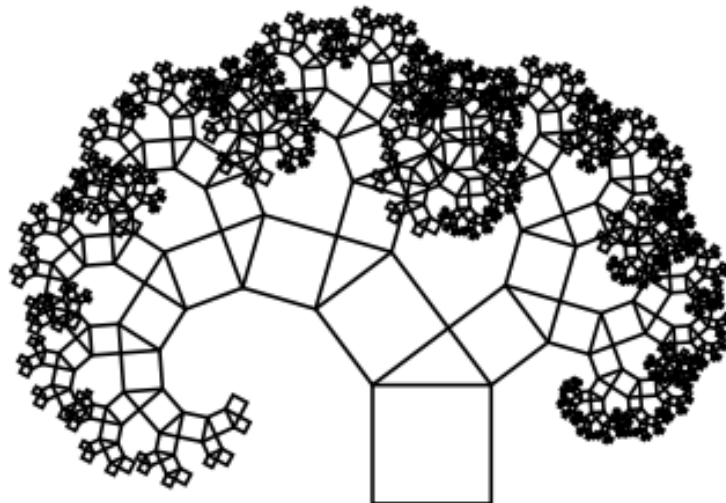
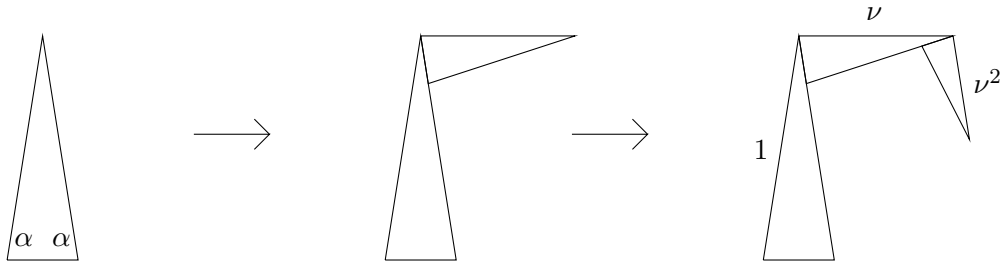
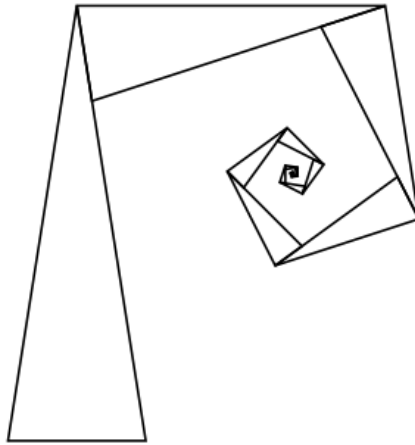


Figure 5.2: Pythagoras tree.

The two equal base angles are  $\alpha$ . After each step the triangle is a factor  $\nu$  smaller than the previous triangle. As a consequence each new triangle is rotated over an angle  $\alpha$  in clockwise direction. The next figure gives the first two steps.



After many steps a spiral is obtained, see the next figure.



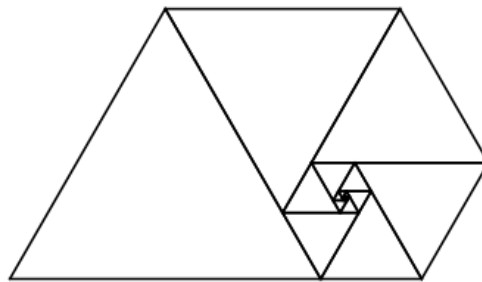
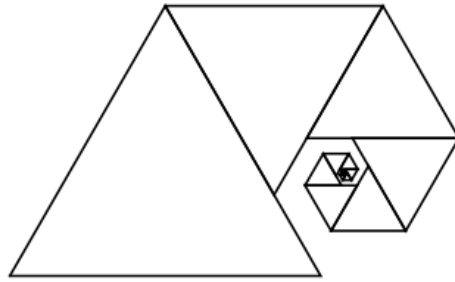
After  $n$  steps the left side of the triangle is parallel to the right side of the initial triangle if

$$\alpha = \frac{\pi}{n-2}. \quad (5.1)$$

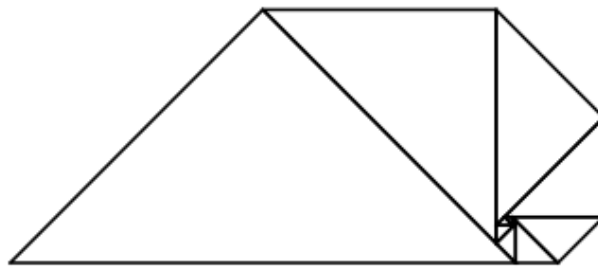
The first value of  $n$  for which  $\alpha < \pi/2$  is  $n = 5$ . Then  $\alpha = \pi/3$ ; the triangle is equilateral. For this situation the spiral is shown in the first figure on the next page. By increasing  $\nu$  we can obtain a situation where the spiral fills the inside area, see the second figure on next page.

For  $n = 5$  the spiral fills the area when  $\nu$  satisfies the equation  $\nu^2 + \nu^3 = 1$ . One of the three solutions is real:

$$\nu = \frac{1}{3} \left( -1 + \sqrt[3]{\frac{25 - 3\sqrt{69}}{2}} + \sqrt[3]{\frac{25 + 3\sqrt{69}}{2}} \right) \approx 0.754878. \quad (5.2)$$



For  $n = 6$  we have  $\alpha = \pi/4$ . An area-filling spiral then is obtained when  $\nu$  satisfies the equation  $\nu^2 + \sqrt{2}\nu^3 + \nu^4 = 1$ . One of the four solutions is real and positive:  $\nu \approx 0.652523$ . The situation is shown in the next figure.



For  $n = 7$  we have  $\alpha = \pi/5$ . For an area-filling spiral  $\nu$  has to satisfy the condition  $\nu^2 + \frac{1}{2}(1 + \sqrt{5})\nu^3 + \frac{1}{2}(1 + \sqrt{5})\nu^4 + \nu^5 = 1$ . One of the five solutions is real:  $\nu \approx 0.600610$ .

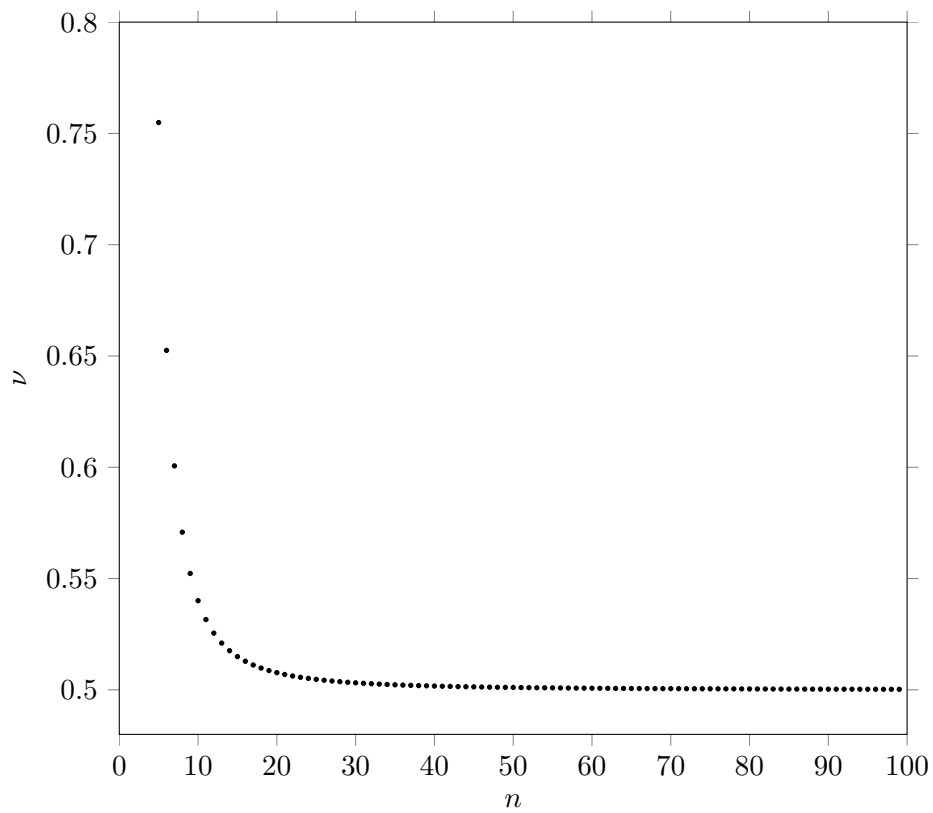
For  $n = 8$  we have  $\alpha = \pi/6$ . The area-filling condition is  $\nu^2 + \sqrt{3}\nu^3 + 2\nu^4 + \sqrt{3}\nu^5 + \nu^6 = 1$ . One of the six solutions is real and positive:  $\nu \approx 0.570841$ .

In general the area-filling condition is

$$\sum_{k=1}^{n-3} \sin\left(\frac{k\pi}{n-2}\right) \nu^{k+1} = \sin\left(\frac{\pi}{n-2}\right). \quad (5.3)$$

For  $n = 9, 10, 11, 13, 15, 16, \dots$  and most other values for  $n$  the latter equation does not lead to a polynomial in  $\nu$  with algebraic coefficients. A polynomial in  $\nu$  with algebraic coefficients only occur if the sine of  $\pi/(n-2)$  is algebraic, which is the case if  $n-2 \in \{2^m \cdot 3, 2^m \cdot 4, 2^m \cdot 5, 2^m \cdot 15\}$ , where  $m = 0, 1, 2, \dots$

The area-filling values for  $\nu$  are plotted against  $n$  in the next figure.



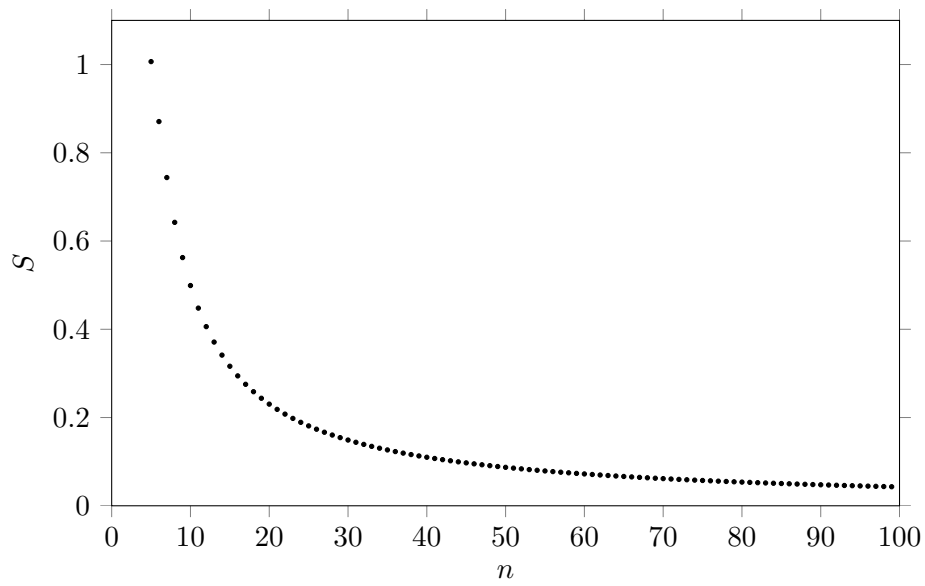
The total area  $S$  of a spiral of isosceles triangles is given by

$$S = \frac{\sin \alpha \cos \alpha}{1 - \nu^2}. \quad (5.4)$$

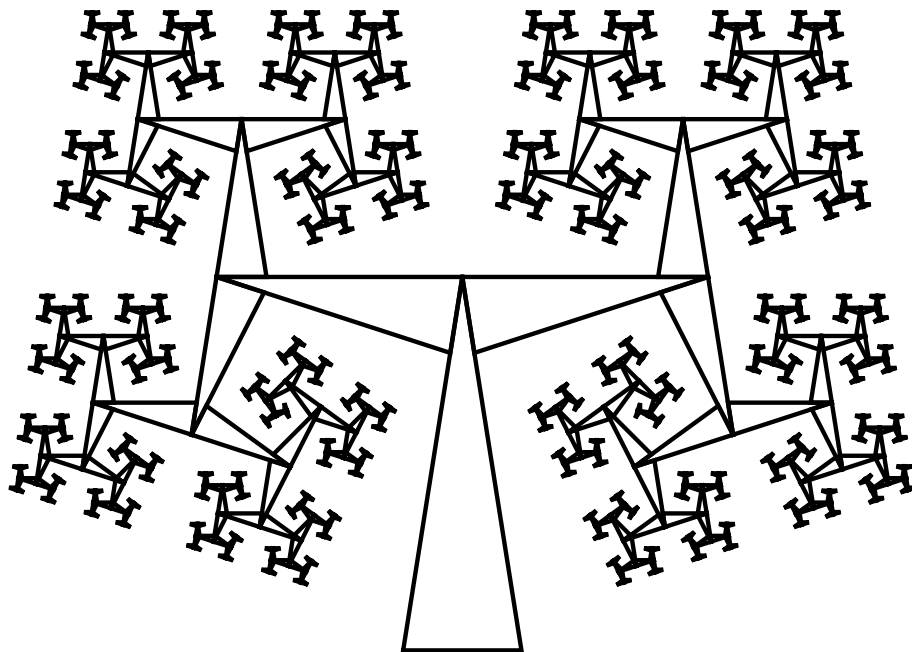
For area-filling spirals this is

$$S = \frac{1}{2 - 2\nu^2} \sin\left(\frac{2\pi}{n-2}\right), \quad (5.5)$$

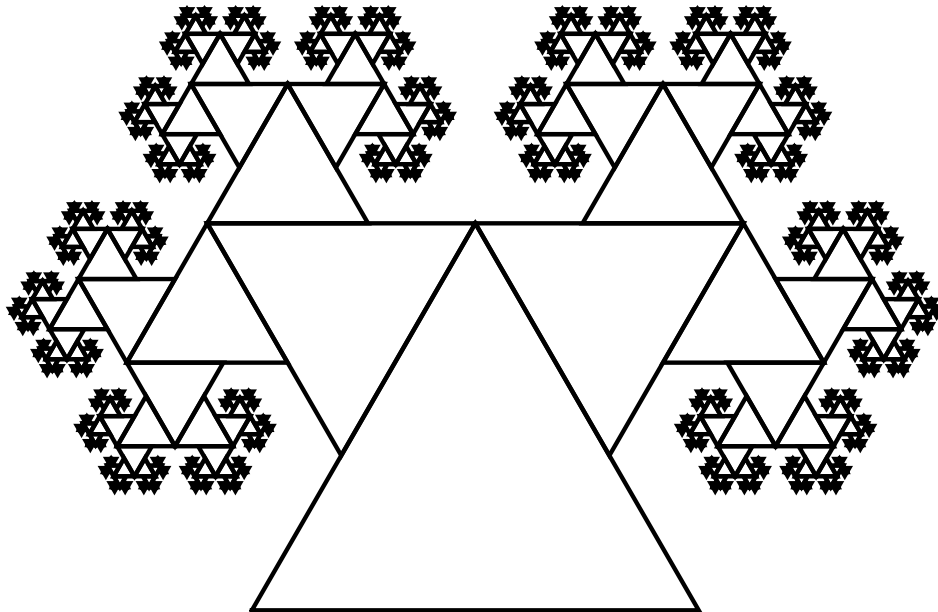
where  $\nu$  is the solution of equation (5.3). The areas for area-filling spirals are plotted against  $n$  in the next figure.



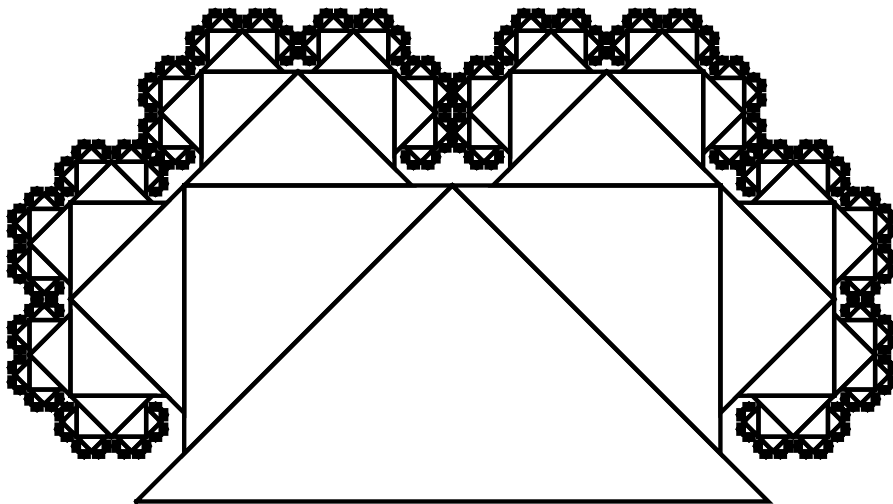
A two dimensional fractal with branches can be obtained by repeatedly placing two smaller copies at the top of the previous triangles with their base adjacent and perpendicular to the equal sides. The next figure gives an impression.



For  $\alpha = \pi/3$  and  $\nu = 0.6$  the tree is as follows.



For  $\alpha = \pi/4$  and  $\nu = 0.6$  the tree is as in the next figure.



## 5.4 Fractal dimension

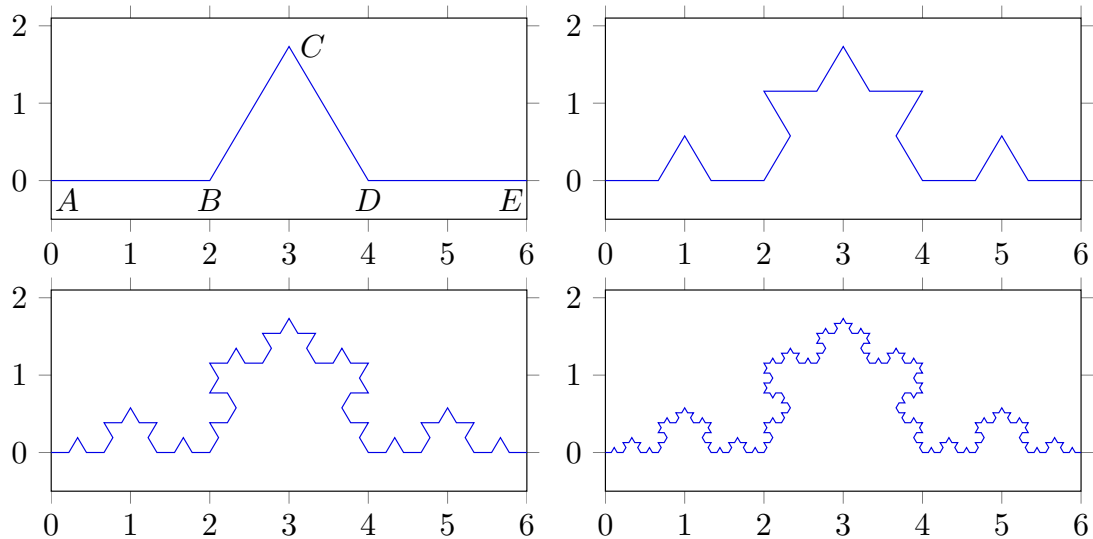
A stick with length  $l$  fits  $1/l$  times in a unit length. A square with side length  $l$  fits  $1/l^2$  in a unit square. A cube with edge length  $l$  fits  $1/l^3$  times in a unit cube. In general,  $N = 1/l^D$ , where  $N$  is the number of times a smaller copy fits in the object with unit sizes and where  $D$  is the dimension of the object. From the relation between  $N$  and  $l$  we can determine the dimension:

$$D = -\frac{\ln N(l)}{\ln l}. \quad (5.6)$$

For non-fractal objects as sticks, squares and cubes it does not matter how small we take the sizes. That is,

$$D = \lim_{l \rightarrow 0} -\frac{\ln N(l)}{\ln l} \quad (5.7)$$

leads to the same value for  $D$ . The situation changes for fractals. To this end we once more consider the construction of the Koch fractal:



If a stick has length 2, it would fit 4 times along the curve between  $A$  and  $E$ . If the length of the stick is  $2/3$  it would fit 16 times along the curve between  $A$  and  $E$ . Each time the length of the stick is decreased with a factor 3 the number of line segments that can be measured increases with a factor 4. If  $l$  is the length of the stick and  $N(l)$  the number of line segments that can be measured, then the fractal dimension  $D$  is defined as

$$D = \lim_{l \rightarrow 0} -\frac{\ln N(l)}{\ln l}. \quad (5.8)$$

If we start with a stick with length 6, that is  $l_0 = 6$ , then  $N_0 = 1$ . Next we take a stick with length 2, that is  $l_1 = 2$ , then  $N_1 = 4$ . In the next step we take a stick with length  $l_2 = 2/3$ , then  $N_2 = 4^2$ . For the  $n$ -th step we then have  $l_n = 6/3^n$  and  $N_n = 4^n$ . We thus find

$$-\frac{\ln N_n}{\ln l_n} = \frac{\ln 4^n}{\ln 6/3^n} = \frac{n \ln 4}{\ln 6 - n \ln 3}. \quad (5.9)$$

In the limit  $n \rightarrow \infty$ , which is equivalent to the limit  $l \rightarrow 0$ , the part  $\ln 6$  is negligible with respect to  $n \ln 3$ . For the fractal dimension of the Koch fractal we therefore obtain

$$D_{\text{Koch}} = \frac{\ln 4}{\ln 3}. \quad (5.10)$$

As another example we consider the Minkowski fractal. After each step of the construction of the Minkowski fractal the length of the line segments is 4 times smaller while the number of segments is 8 times larger. Hence

$$D_{\text{Minkowski}} = \frac{\ln 8}{\ln 4} = \frac{3 \ln 2}{2 \ln 2} = \frac{3}{2}. \quad (5.11)$$

For arithmetic fractals such as the Koch fractal and the Minkowski fractal an alternative definition is

$$D = \frac{\ln(N_{n+1}/N_n)}{\ln(l_n/l_{n+1})}. \quad (5.12)$$

The concept of a fractal dimension for one dimensional fractals can be generalized to two- and three dimensional fractals by replacing the length  $l$  by the square root of the area,  $\sqrt{A}$  and the cubic root of the volume,  $\sqrt[3]{V}$ , respectively. For instance, for two dimensional fractals the equation for the fractal dimension is

$$D = \lim_{A \rightarrow 0} -2 \frac{\ln N(A)}{\ln A} \quad (5.13)$$

or

$$D = 2 \frac{\ln(N_{n+1}/N_n)}{\ln(A_n/A_{n+1})}. \quad (5.14)$$

For the Pythagoras tree every square generates two squares, each with half the area of the generating square. Hence

$$D_{\text{Pythagoras tree}} = 2 \frac{\ln 2}{\ln 2} = 2. \quad (5.15)$$

An example of a three dimension fractal is the *Menger sponge*. The fractal dimension of the Menger sponge is

$$D_{\text{Menger sponge}} = 3 \frac{\ln 20}{\ln 27} = \frac{\ln 20}{\ln 3}. \quad (5.16)$$

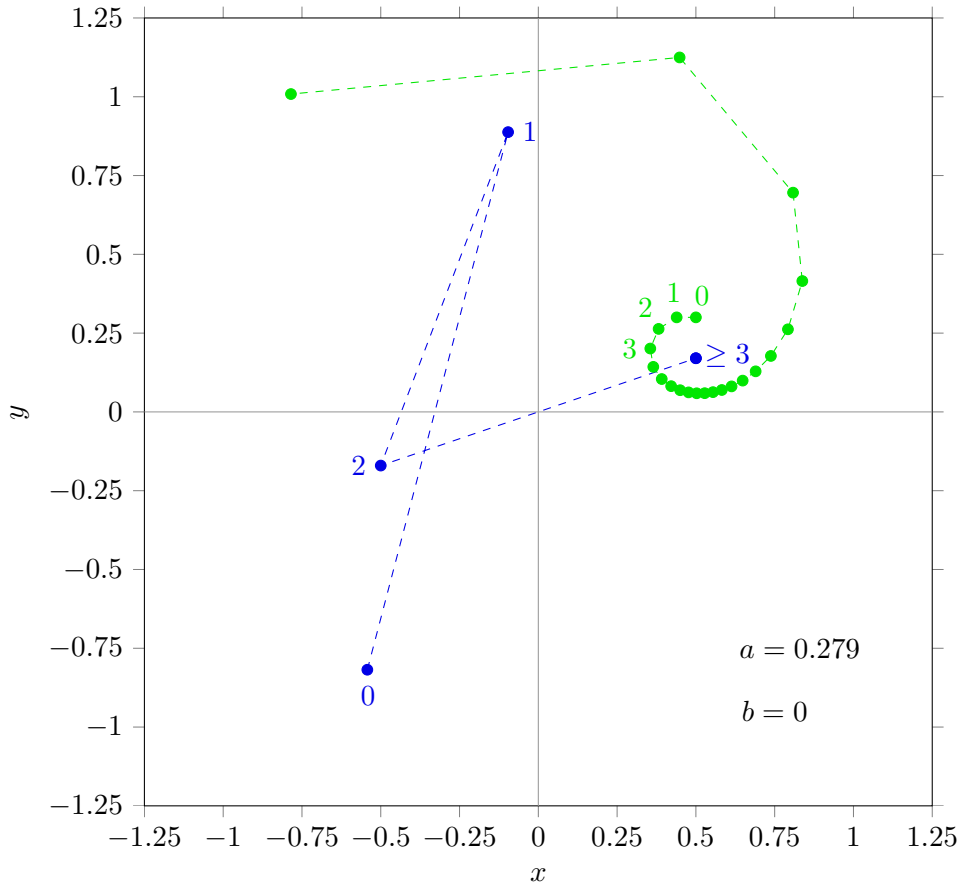
## 5.5 Julia fractals

Here we will consider once more the  $z^2 + c$  map:

$$\begin{aligned} x_{m+1} &= x_m^2 - y_m^2 + a \\ y_{m+1} &= 2x_m y_m + b. \end{aligned} \quad (5.17)$$



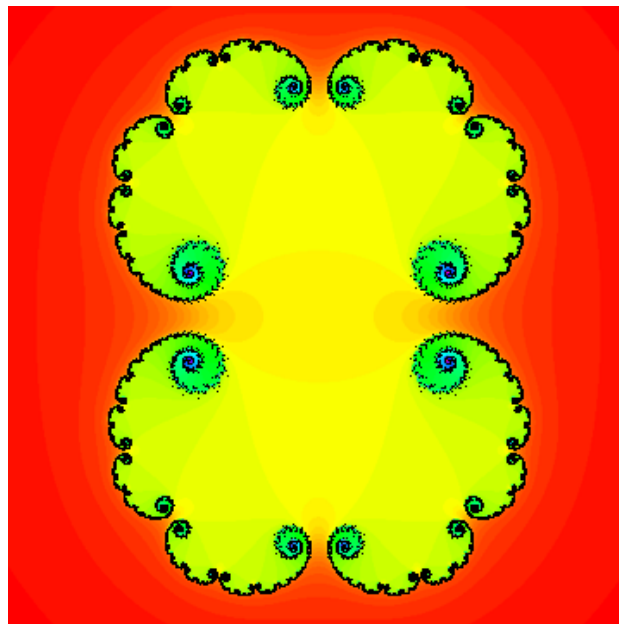
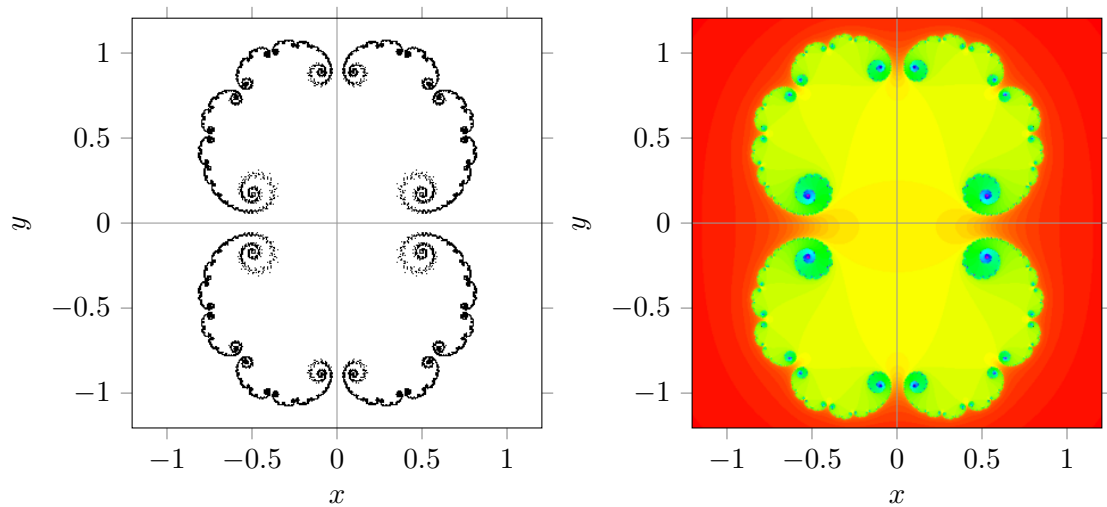
This time we focus on the orbit of points starting with  $(x_0, y_0)$ . As an example we consider the situation for  $a = 0.279$ ,  $b = 0$ . In the next figure the first few iterates are shown for  $(x_0, y_0) = (0.5, 0.3)$  (green) and  $(x_0, y_0) = (-0.54259166167\dots, -0.81811547324\dots)$  (blue).



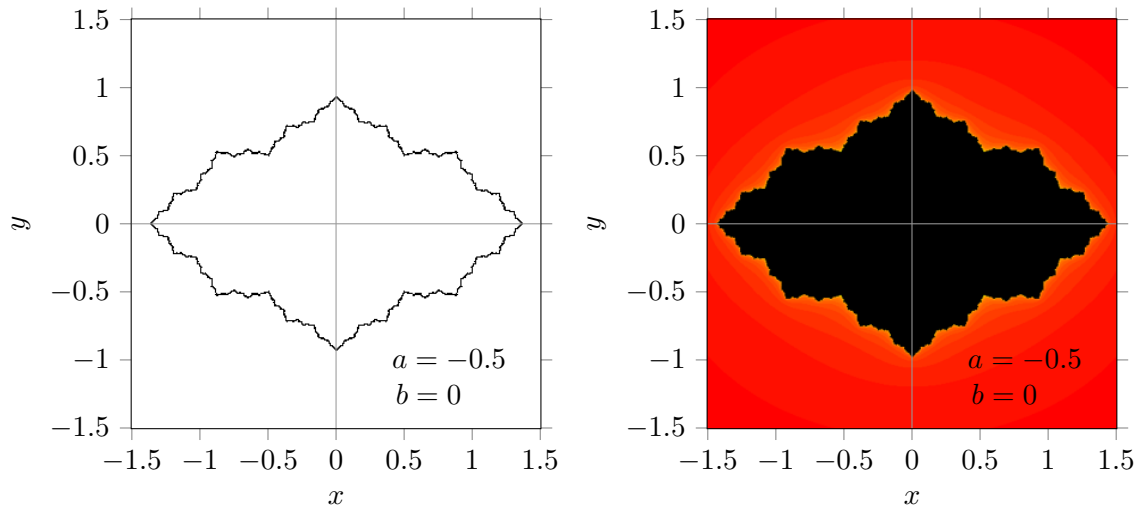
For  $(x_0, y_0) = (0.5, 0.3)$  the orbit spirals outwards; it diverges towards infinity.

For  $(x_0, y_0) = (-0.54259166167\dots, -0.81811547324\dots)$  the orbit ends after three iterations in point  $(0.5, 0.17029386365926\dots)$  and stays there;  $(0.5, 0.17029386365926\dots)$  is a fixed point. If one starts at a slightly different position the orbit diverges, after many iterates, to infinity. That is,  $(0.5, 0.17029386365926\dots)$  is an unstable fixed point. The set of all points which do not diverge to infinity is called the Julia set  $J(a, b)$ . The point  $(-0.54259166167\dots, -0.81811547324\dots)$  belongs to the Julia set  $J(0.279, 0)$  since it does not diverge to infinity. The same holds for the other blue points in the figure above. The point  $(-0.54259166167\dots, -0.81811547324\dots)$  is, as all the other blue points, a predecessor of  $(0.5, 0.17029386365926\dots)$ . All predecessors of unstable periodic cycles belong to the Julia set. The fixed point  $(0.5, -0.17029386365926\dots)$  is not a predecessor of  $(0.5, 0.17029386365926\dots)$ . So,  $(0.5, -0.17029386365926\dots)$  and its predecessors form a different set than  $(0.5, 0.17029386365926\dots)$  and its predecessors. The first is the mirror set of the latter with the  $y$ -axis as the mirror. Both sets belong to the Julia

set  $J(0.279, 0)$ . The complete Julia set  $J(0.279, 0)$  is a set of disconnected points. The Julia set  $J(0.279, 0)$  is shown in the left panel of the next figure. The Fatou set is the set of all points  $(x_0, y_0)$  which are not part of the Julia set. The iterates of the elements  $(x_0, y_0)$  of the Fatou set diverge to infinity. We can colour the pixel around  $(x_0, y_0)$  depending on the speed of divergence to infinity, see the right panel of the next figure. Yellow is for a slow divergence, green for an intermediate speed and red for a quick divergence to infinity. The Fatou set joined with the Julia set fill the  $x, y$ -plane. A complete picture is obtained by plotting the Julia set on top of the Fatou set, see the figure at the bottom of the page. It illustrates the Julia set to a certain extent the border between different coloured parts of the Fatou set.

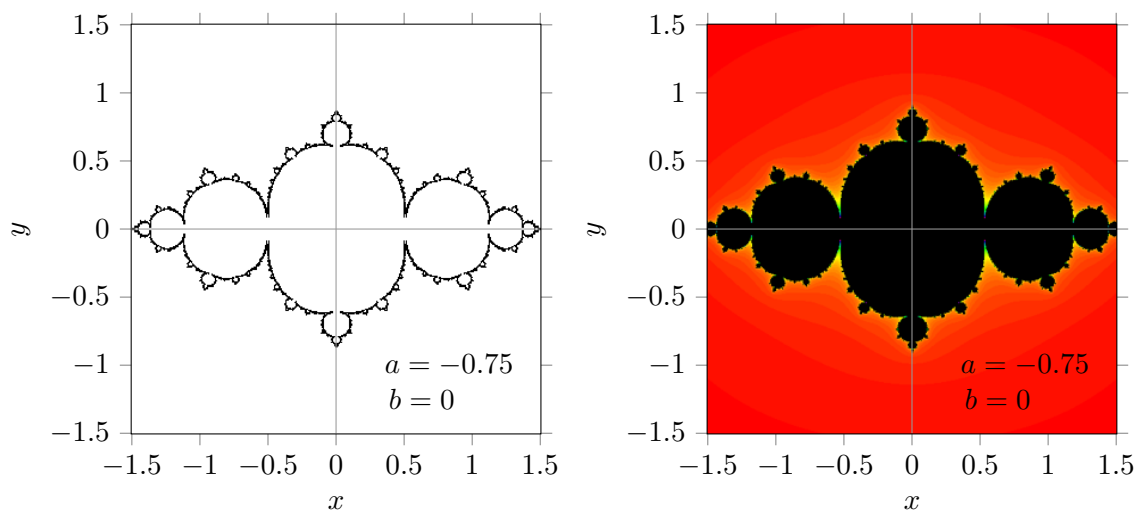


For other values of  $a$  and  $b$  we obtain other Julia and Fatou sets. In the figure below the sets  $J(-0.5, 0)$  (left panel) and  $F(-0.5, 0)$  (right panel) are shown.

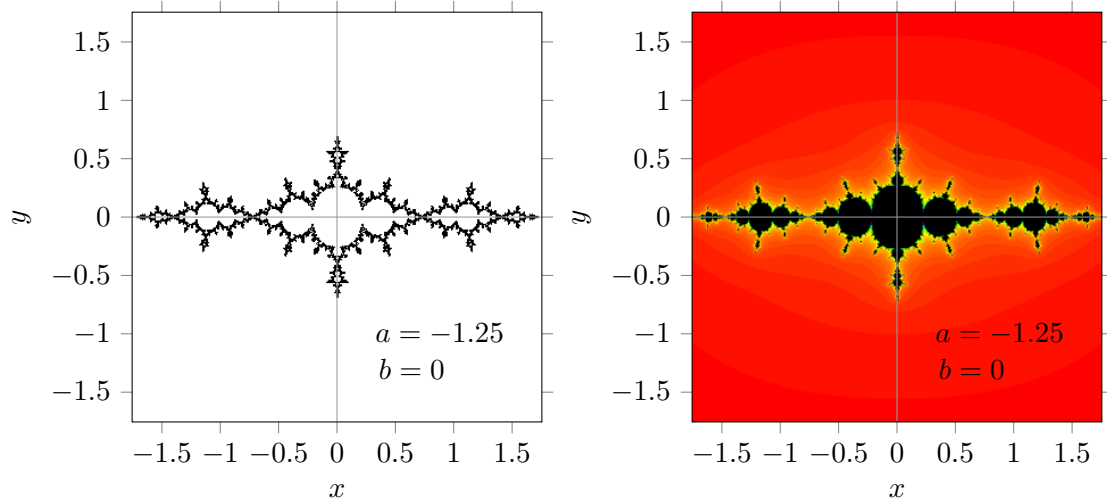


The Julia set  $J(-0.5, 0)$  is a set of connected points. The points outside the region enclosed by the Julia set  $J(-0.5, 0)$  diverge to infinity and are therefore coloured light. The points inside the region enclosed by the Julia set  $J(-0.5, 0)$  converge to the Julia set  $J(-0.5, 0)$ . They never come outside this region. In a way it can be regarded as if they tend to infinity in an extremely slow way. Therefore the region enclosed by the Julia set  $J(-0.5, 0)$  is coloured black in the Fatou set.

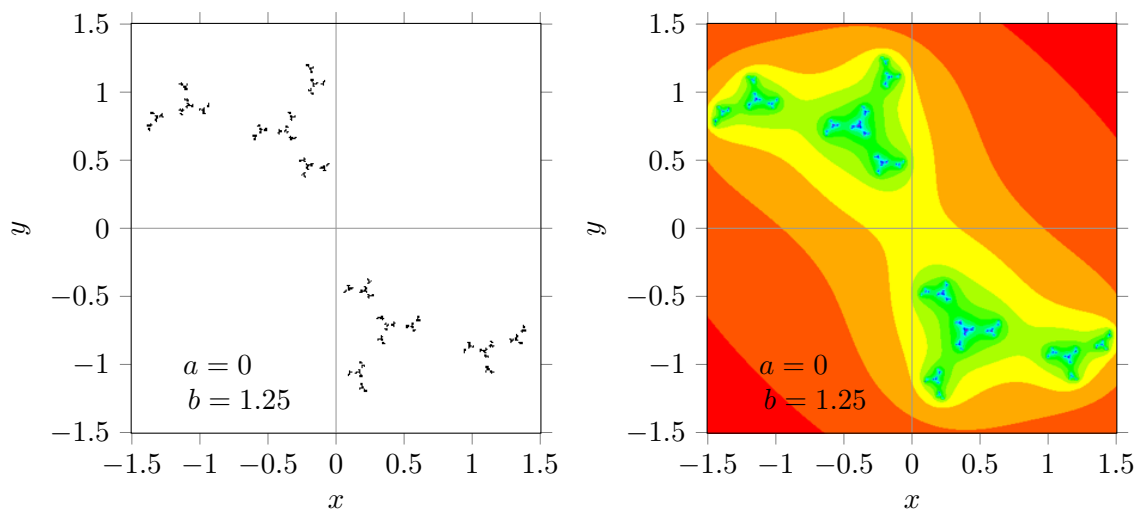
Julia sets are fractals. For  $a = -0.75$  and  $b = 0$  the Julia set  $J(-0.75, 0)$ , which is a connected set, is known as the San Marco fractal, see the figure below.



As another example with  $b = 0$  we show the Julia set and Fatou set for  $a = -1.25$ . The Julia fractal  $J(-1.25, 0)$  is connected.



Next we will consider Julia sets and fatou sets for  $b \neq 0$ . Below are shown the Julia set and Fatou set for  $a = 0$  and  $b = 1.25$ . The Julia fractal  $J(0, 1.25)$  is disconnected.



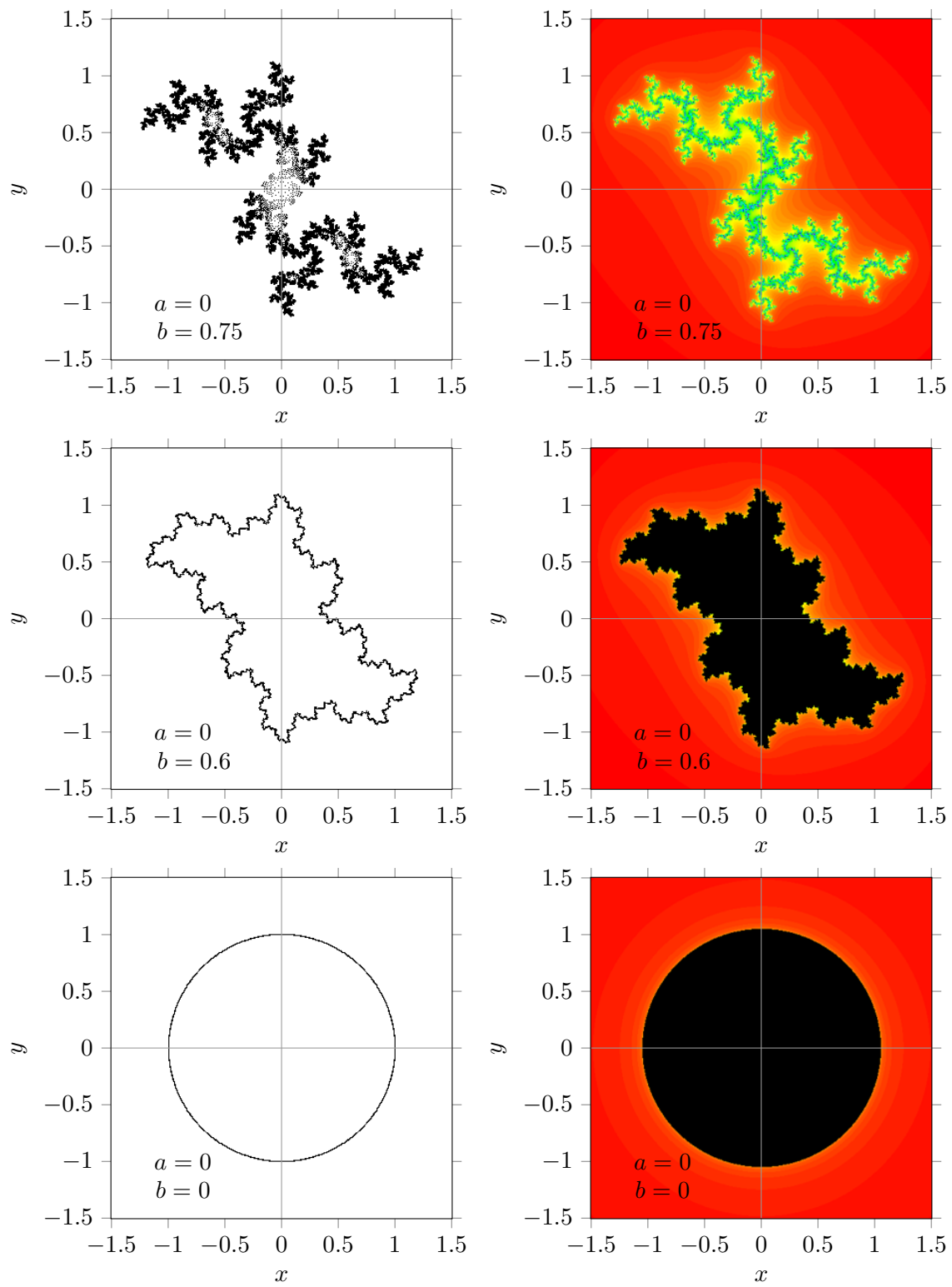
For  $b \neq 0$  the Julia set and Fatou set are point symmetric around the origin. The sets for  $-b$  are the mirror images of the sets for  $b$ , with the  $x$ -axis or the  $y$ -axis as the mirror axis.

Next are shown the Julia set and Fatou set for:

$a = 0$  and  $b = 0.75$ , the Julia fractal  $J(0, 0.75)$  is disconnected.

$a = 0$  and  $b = 0.6$ , the Julia fractal  $J(0, 0.6)$  is connected.

$a = 0$  and  $b = 0$ , the Julia fractal  $J(0, 0)$  is connected and is a circle with unit radius.



Finally we consider Julia and Fatou sets for the situation where both  $a \neq 0$  and  $b \neq 0$ .

Next are shown the Julia set and Fatou set for:

$a = 0.125$  and  $b = -0.75$ , the Julia fractal  $J(0.125, -0.75)$  is disconnected.

$a = 0.125$  and  $b = -0.625$ , the Julia fractal  $J(0.125, -0.625)$  is connected.

$a = -0.125$  and  $b = -1$ , the Julia fractal  $J(-0.125, 1)$  is disconnected.

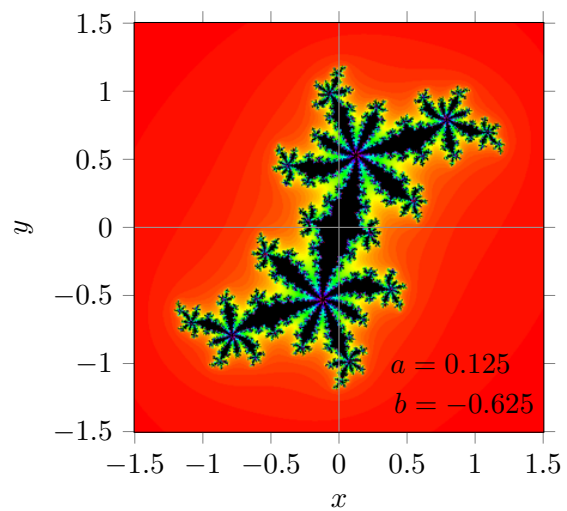
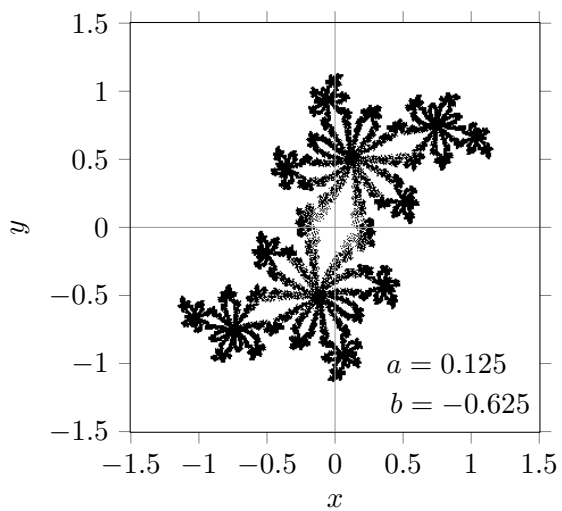
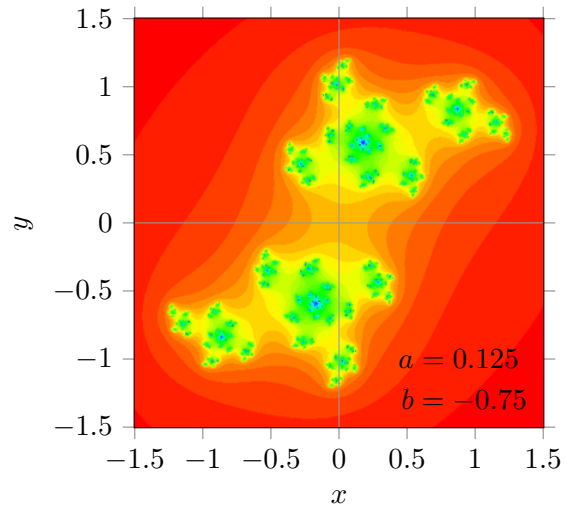
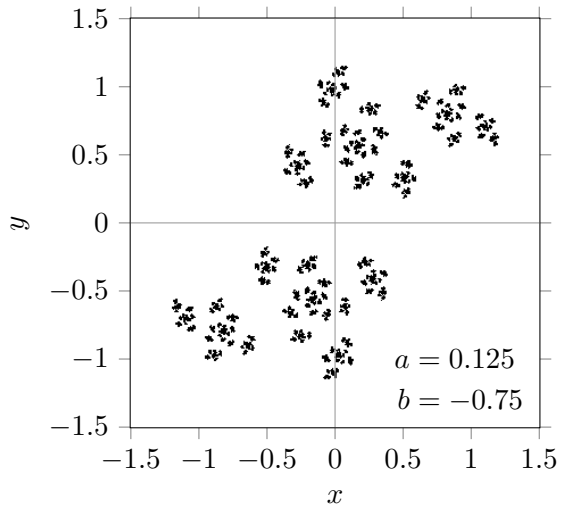
$a = -0.125$  and  $b = -0.85$ , the Julia fractal  $J(-0.125, -0.85)$  is connected.

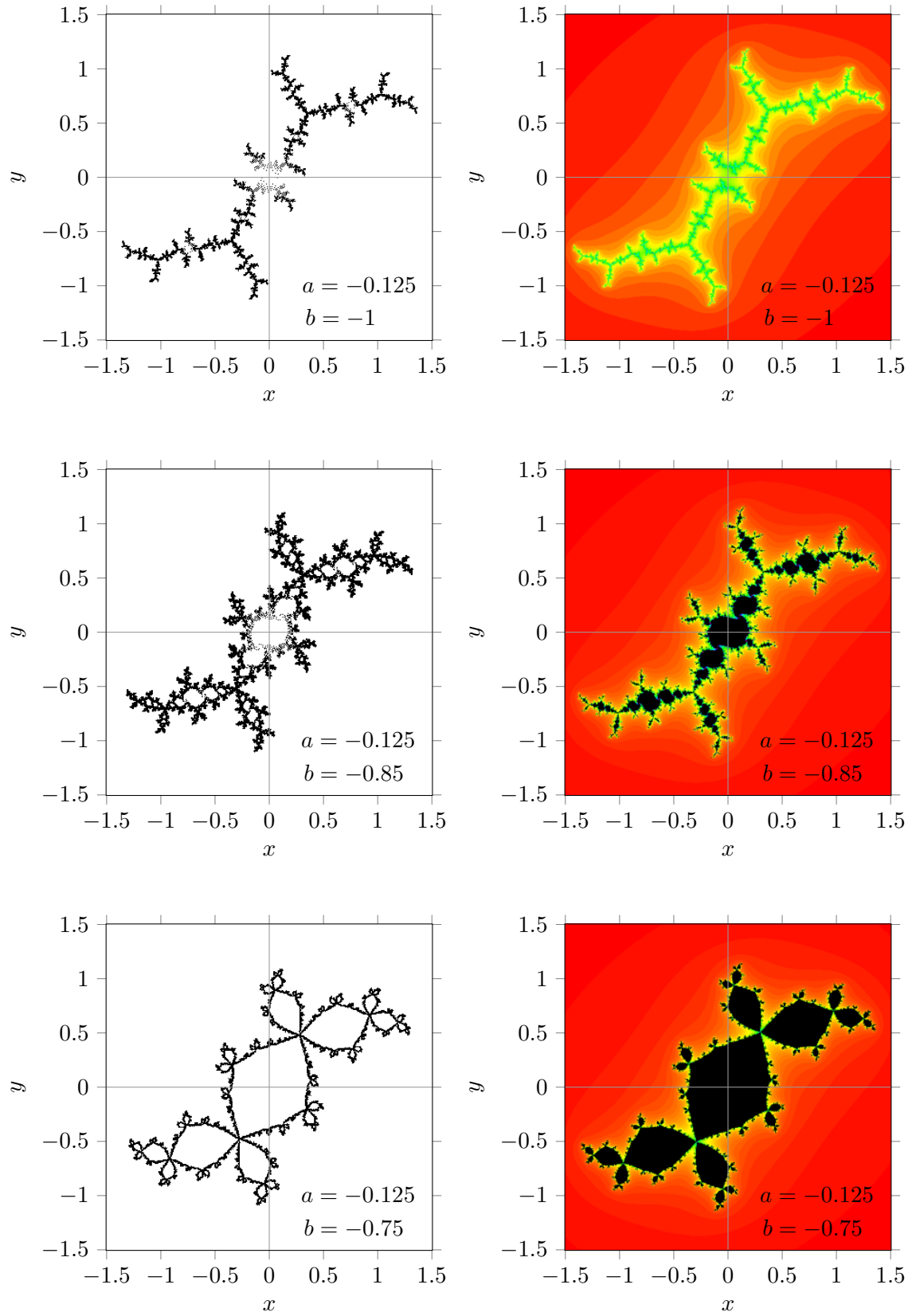
$a = -0.125$  and  $b = -0.75$ , the Julia fractal  $J(-0.125, -0.75)$  is connected.

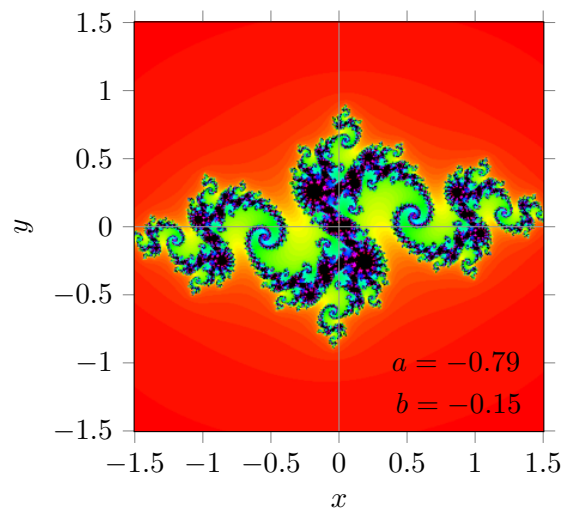
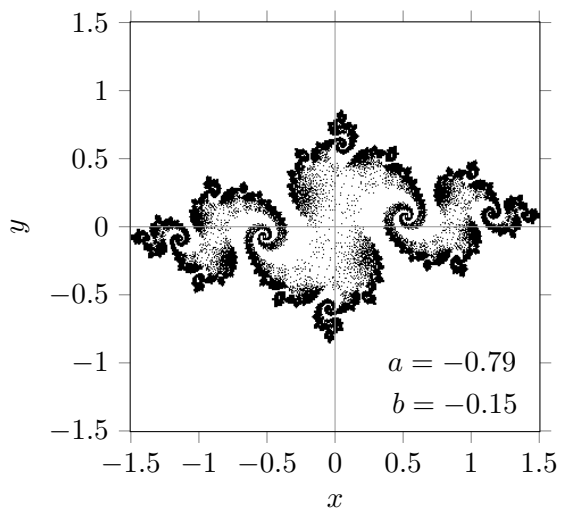
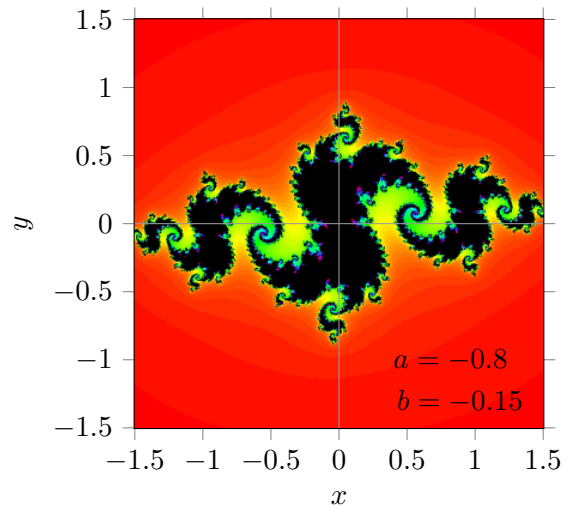
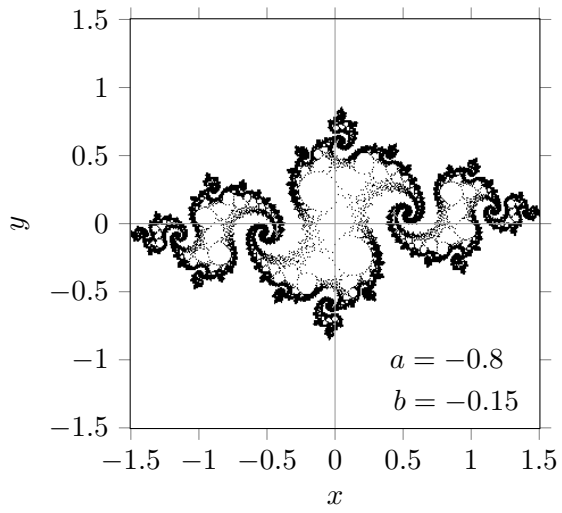
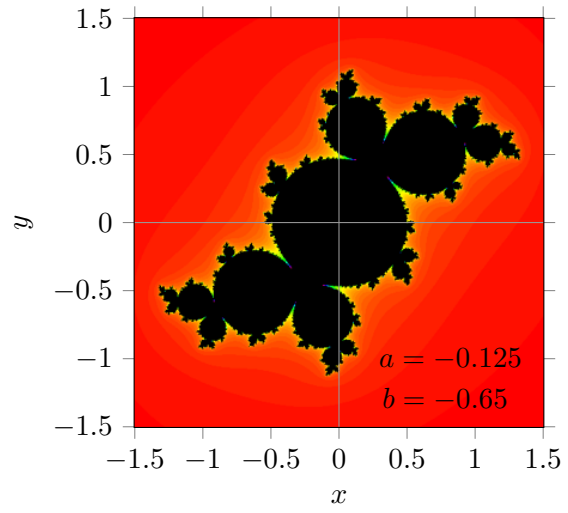
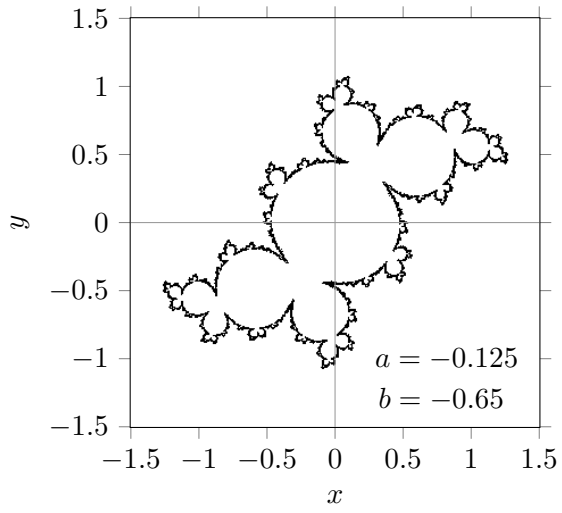
$a = -0.125$  and  $b = -0.65$ , the Julia fractal  $J(-0.125, -0.65)$  is connected.

$a = -0.8$  and  $b = -0.15$ , the Julia fractal  $J(-0.8, -0.15)$  is connected.

$a = -0.79$  and  $b = -0.15$ , the Julia fractal  $J(-0.79, -0.15)$  is disconnected.









If we blow up 100 times the right part of the latter Fatou set for  $a = -0.79$ ,  $b = -0.15$  we still see the same kind of shapes. No matter how much we blow up small sections, the fractal structure is present at every level.

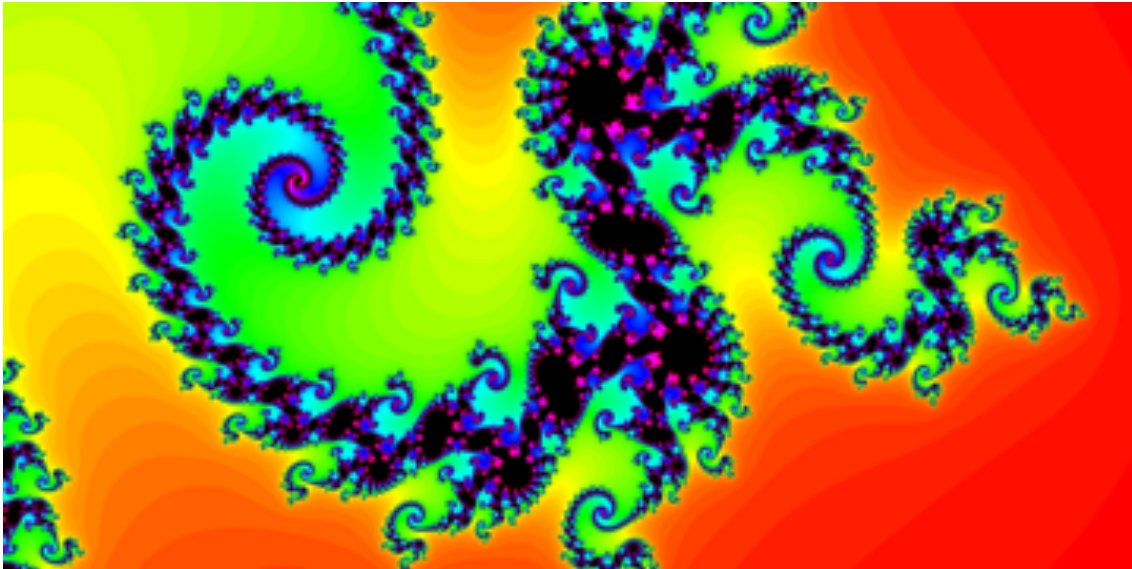
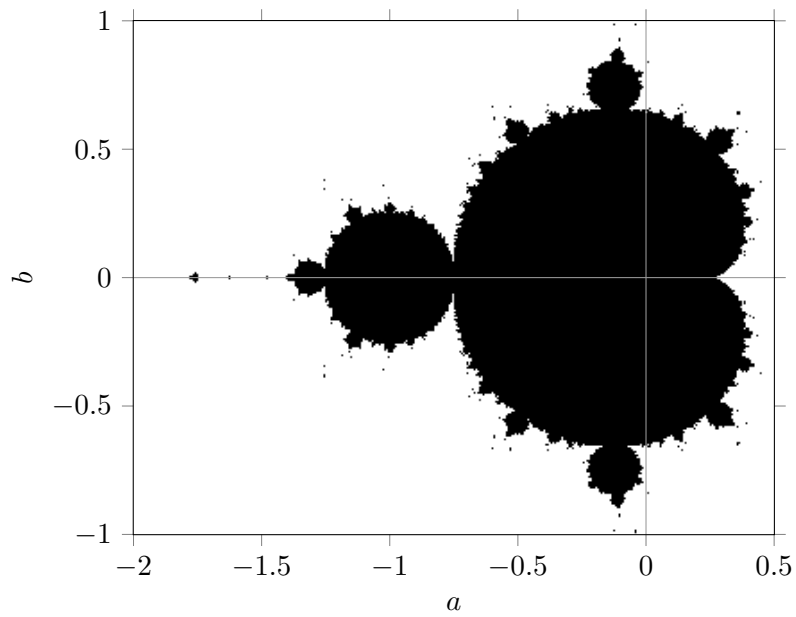


Figure 5.3: The  $1.465 \leq x \leq 1.525$  and  $0.06 \leq y \leq 0.09$  section of the Fatou set for  $a = -0.79$  and  $b = -0.15$ .

## 5.6 Mandelbrot fractal

From the figures of the previous section we see that Julia sets are point symmetric around  $(0, 0)$ . As a consequence, for connected Julia sets the point  $(0, 0)$  is inside the region enclosed by the Julia set. If we take  $(0, 0)$  as a starting point  $(x_0, y_0)$ , then  $(x_1, y_1) = (a, b)$ . Therefore the point  $(a, b)$  also is inside the region enclosed by the connected Julia set. As a consequence, there is an easy way to determine whether a Julia sets is connected or disconnected. Take the parameter values for  $a$  and  $b$  as the starting point, thus  $(x_0, y_0) = (a, b)$ . If the orbit  $(x_m, y_m)$  tends to infinity the Julia set  $J(a, b)$  is disconnected else the Julia set  $J(a, b)$  is connected.

For each pair  $(a, b)$  we place a black dot if  $J(a, b)$  is found to be connected. The result is shown in the next figure. We recognise the Mandelbrot set as we met it in the previous chapter. This is no surprise since in the previous chapter the Mandelbrot set was the set of pairs  $(a, b)$  for which  $(x_0, y_0) \approx (0, 0)$  leads to to a non diverging series  $(x_m, y_m)$ , while here the Mandelbrot set is the set of pairs  $(a, b)$  for which  $(x_0, y_0) \approx (a, b)$  leads to to a non diverging series  $(x_m, y_m)$ , and for the divergence test there is no difference between starting at a point very close to  $(0, 0)$  and starting at  $(a, b)$ .



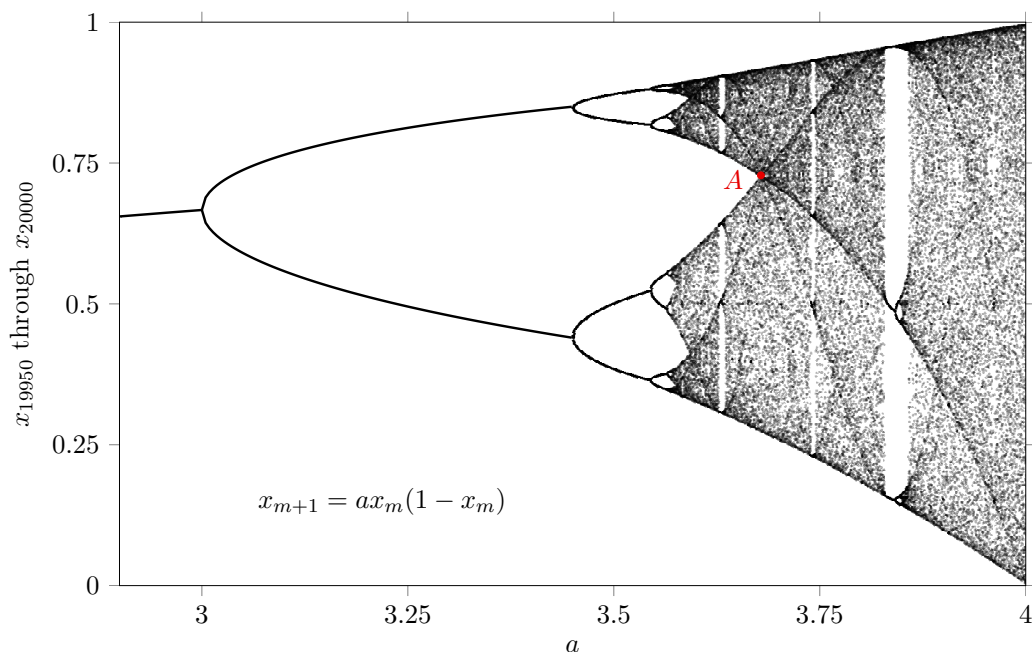
The Mandelbrot set is a fractal, the *Mandelbrot fractal*. Its fractal dimension is 2.

## Chapter 6

# Misiurewicz points

### 6.1 Polynomials for $x_0 = 1/2$

In the figure below the orbit diagram for the logistic equation  $x_{m+1} = ax_m(1 - x_m)$  is shown.

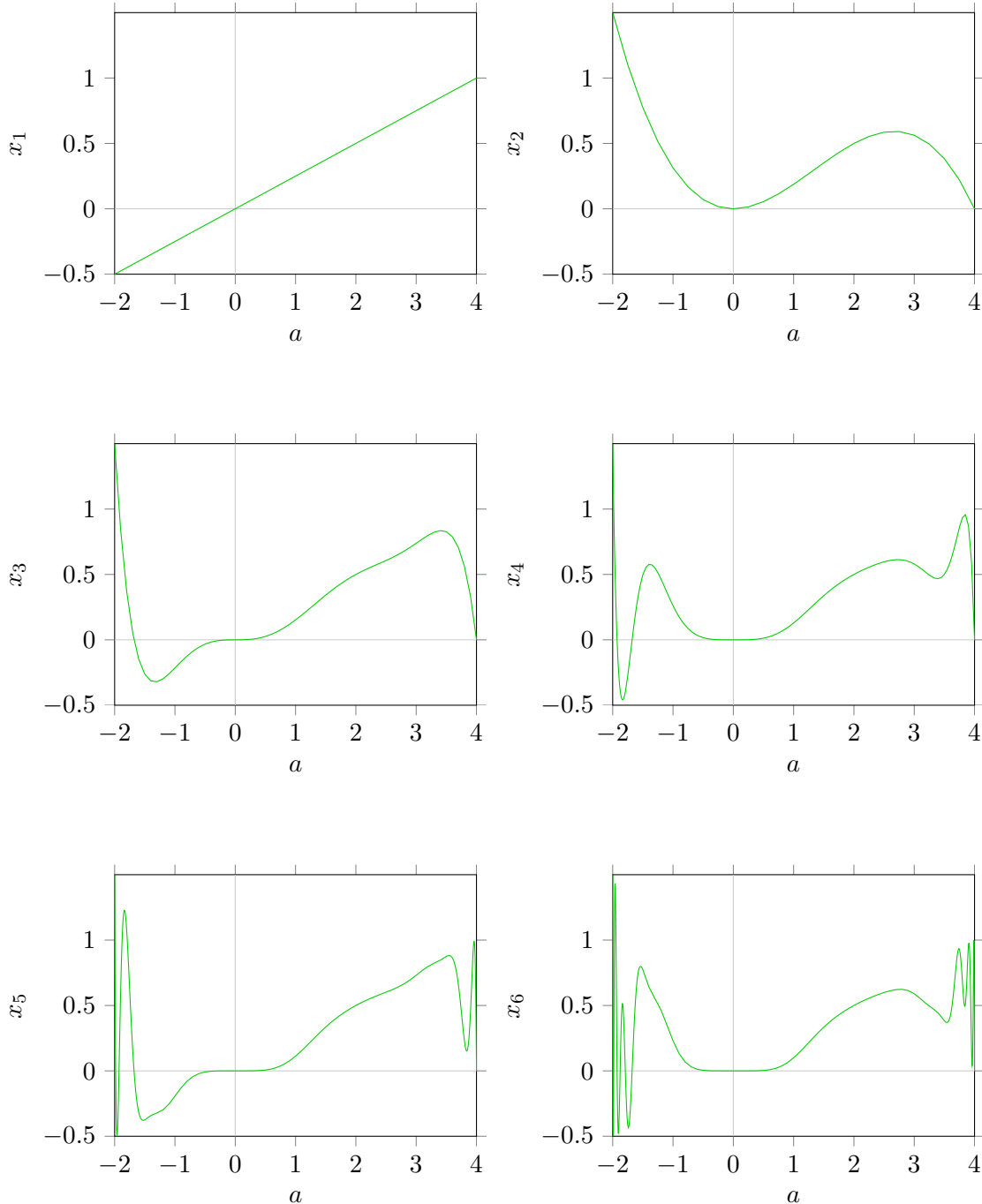


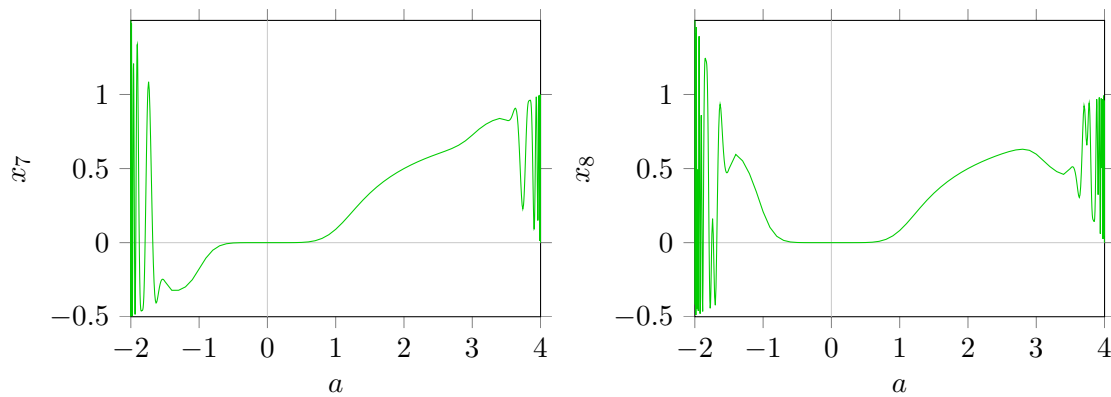
In the chaotic regions we clearly recognize dark curves. Point  $A$  is a point of intersection of such dark curves. It also is the most right point of the 'large void region', see the red point in the figure above. Since the curve of the function  $x(1 - x)$  is almost horizontal in the neighbourhood of  $x = 0.5$ , points near  $x = 0.5$  are mapped close  $a/4$  and thus close to each other. As a consequence, subsequent mappings will also be close to each other. Therefore the dark regions originate from orbits which pass near the critical point  $x = 0.5$ .

Because of the special role of the critical point we take  $x_0 = 1/2$  as a starting point and calculate some further  $x_k$ . It leads to polynomials in  $a$ :

$$x_1 = \frac{a}{4} \quad , \quad x_2 = \frac{a^2}{4} - \frac{a^3}{16} \quad , \quad x_3 = \frac{a^3}{4} - \frac{a^4}{16} - \frac{a^5}{16} + \frac{a^6}{32} - \frac{a^7}{256} \quad , \quad \text{and so on.}$$

In the next 8 figures the polynomials  $x_1$  through  $x_8$  are plotted against  $a$ .





In the next figure the foregoing 8 polynomials are plotted in a single diagram. The function  $x_0 = \frac{1}{2}$  is plotted in blue.

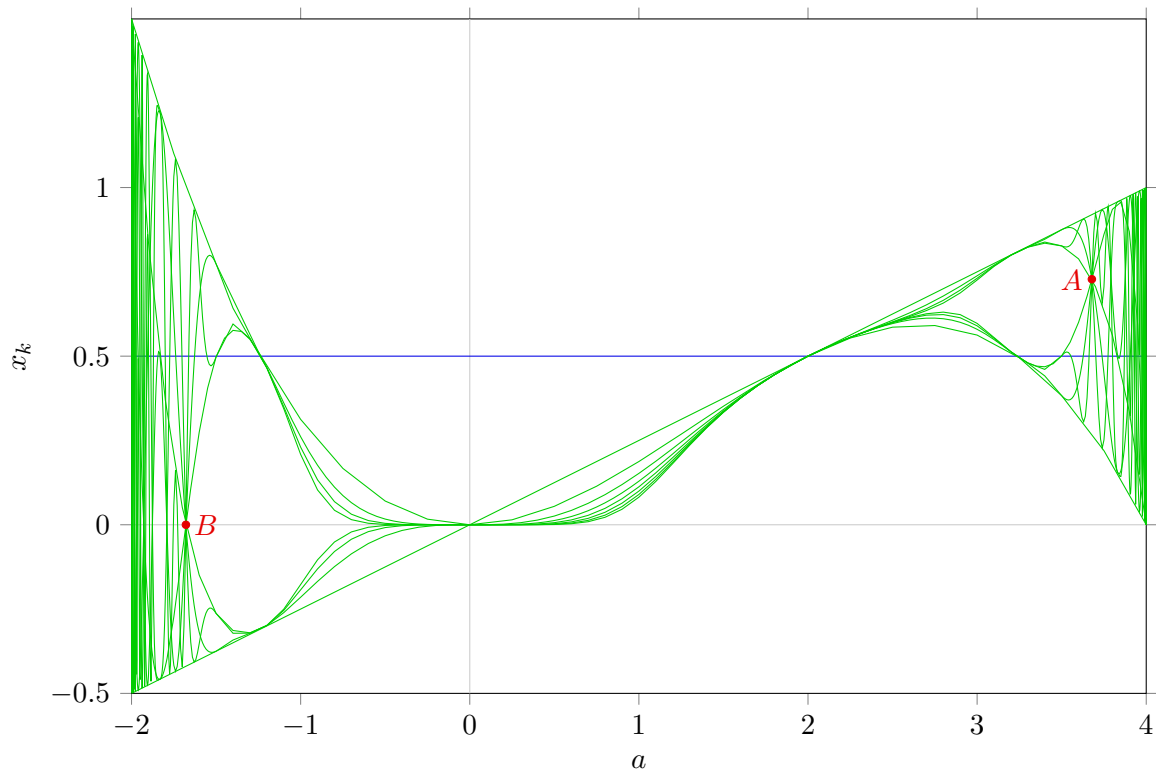


Figure 6.1: Polynomials  $x_k(a)$  for  $x_0 = 1/2$ .

Two points of intersection are indicated by red dots and the symbols  $A$  and  $B$ .

## 6.2 Points of intersection

For the points  $A$  and  $B$ :  $x_3 = x_4 = x_5 = \dots = x_k = \dots$ , while  $x_0 \neq x_3$ ,  $x_1 \neq x_3$ ,  $x_2 \neq x_3$ ,  $x_1 \neq x_0$ ,  $x_2 \neq x_0$  and  $x_2 \neq x_1$ . The fixed point condition  $x_4 = x_3$  is satisfied if either

$$ax_3(1 - x_3) = x_3 \quad \rightarrow \quad 1 - x_3 = \frac{1}{a} \quad \rightarrow \quad x_3 = \frac{a-1}{a}. \quad (6.1)$$

or  $x_3 = 0$ . The solution  $x_3 = x_4 = \dots = \frac{a-1}{a}$  corresponds to point  $A$ . In chapter 2 we already found that the fixed point solution  $x_k = \frac{a-1}{a}$  is only stable if  $1 \leq a \leq 3$ . The solution  $x_3 = x_4 = \dots = 0$  corresponds to point  $B$ . In chapter 2 we already found that the fixed point solution  $x_k = 0$  is only stable if  $-1 \leq a \leq 1$ . The points  $A$  and  $B$  are unstable fixed points. The periodicity sets in at  $x_3$ .

To find the predecessor  $x_2$  of point  $A$  we substitute  $x_3 = \frac{a-1}{a}$  in  $x_3 = ax_2(1 - x_2)$ :

$$ax_2(1 - x_2) = \frac{a-1}{a} \quad \rightarrow \quad ax_2^2 - ax_2 + \frac{a-1}{a} = 0 \quad \rightarrow \quad 2ax_2 = 1 \pm \sqrt{a^2 - 4(a-1)}. \quad (6.2)$$

The latter is reduced to

$$2ax_2 = 1 \pm (a-2). \quad (6.3)$$

For the  $+$  sign the solution is  $x_2 = \frac{a-1}{a}$ , which is ruled out by the condition  $x_2 \neq x_3$ . For the  $-$  sign the solution is  $x_2 = \frac{1}{a}$ . To find its predecessor  $x_1$  we substitute the latter into  $x_2 = ax_1(1 - x_1)$ :

$$\frac{1}{a} = ax_1(1 - x_1) \quad \rightarrow \quad x_1^2 - x_1 + \frac{1}{a^2} = 0 \quad \rightarrow \quad x_1 = \frac{a \pm \sqrt{a^2 - 4}}{2a}. \quad (6.4)$$

The substitution of the latter into  $x_1 = ax_0(1 - x_0)$  finally leads to the desired value for  $a$ :

$$\frac{a \pm \sqrt{a^2 - 4}}{2a^2} = x_0(1 - x_0). \quad (6.5)$$

For our point of interest,  $x_0 = \frac{1}{2}$ , this is

$$\frac{a \pm \sqrt{a^2 - 4}}{2a^2} = \frac{1}{4} \quad \rightarrow \quad a^4 - 4a^3 + 16 = 0 \quad \rightarrow \quad (a-2)(a^3 - 2a^2 - 4a - 8) = 0. \quad (6.6)$$

The solution  $a = 2$  implies  $x_3 = 1/2$  which is ruled out by the condition  $x_0 \neq x_3$ . Two of the three roots of  $a^3 - 2a^2 - 4a - 8$  are complex. An analytic expression for the real root is  $a = \frac{2}{3} \left( 1 + \sqrt[3]{19 - 3\sqrt{33}} + \sqrt[3]{19 + 3\sqrt{33}} \right)$ . Its numerical value, 3.67857351, is the  $a$  value of point  $A$  in figure [6.1](#). The  $x$  value of point  $A$  is approximately  $(3.67857351 - 1)/3.67857351 \approx 0.728155$ .

To find the predecessor  $x_2$  of point  $B$  we substitute  $x_3 = 0$  in  $x_3 = ax_2(1 - x_2)$ :

$$ax_2(1 - x_2) = 0. \quad (6.7)$$

One of its solutions,  $x_2 = 0$ , is ruled out by the condition  $x_2 \neq x_3$ . The other solution is  $x_2 = 1$ . For its predecessor  $x_1$  there necessarily holds  $1 = ax_1(1 - x_1)$ , which in turn leads to  $1 = a^2x_0(1 - x_0)(1 - ax_0(1 - x_0))$ . For  $x_0 = 1/2$  this is reduced to  $a^3 - 4a^2 + 16 = 0$ . Two of the three roots of  $a^3 - 4a^2 + 16 = 0$  are complex.

The real root,  $a = \frac{2}{3} \left( 2 - \sqrt[3]{19 + 3\sqrt{33}} - \sqrt[3]{19 - 3\sqrt{33}} \right) \approx -1.67857$ , is the  $a$  value of point  $B$  in figure [6.1](#). The  $x$  value of point  $B$  is 0.

In order to illustrate that our green polynomials are the dark curves of the orbit diagram, we have plotted the polynomials  $x_1$  through  $x_8$  on top of part of the orbit diagram, see next figure.

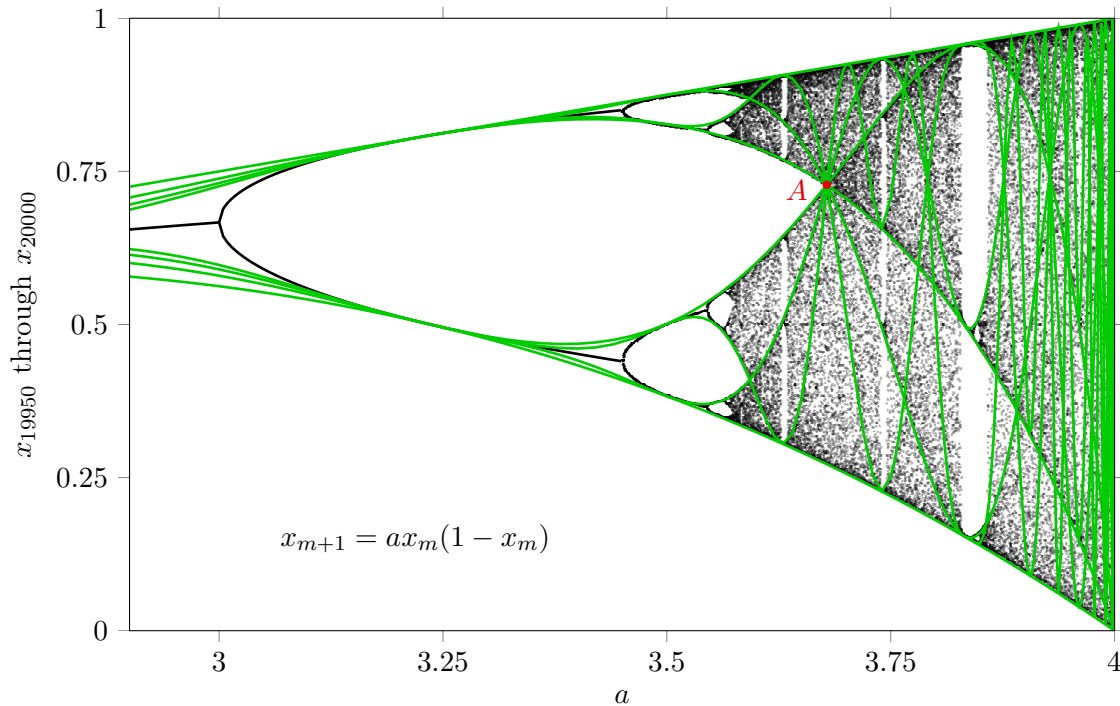


Figure 6.2: Polynomials  $x_k(a)$  for  $x_0 = 1/2$  on top of the orbit diagram for the logistic equation.

As mentioned before, the Fibonacci numbers are generated by  $u_{k+1} = u_k + u_{k-1}$  with  $u_0 = 0$  and  $u_1 = 1$ . In the limit where  $k \rightarrow \infty$  the ratio  $r$  between two successive Fibonacci numbers satisfies the equation  $r^2 - r - 1 = 0$ . Its positive root,  $\varphi = (1 + \sqrt{5})/2$ , is known as the

*golden ratio*. A generalisation of the Fibonacci recurrence relation is  $u_{k+1} = u_k + u_{k-1} + u_{k-2}$  with  $u_0 = 0$ ,  $u_1 = 0$  and  $u_2 = 1$ . The sequence of numbers are known as *tribonacci* numbers. The first few tribonacci numbers are 0, 0, 1, 1, 2, 4, 7, 13, 24, 44, 81, 149, ... In the limit where  $k \rightarrow \infty$  the ratio  $r$  between two successive tribonacci numbers satisfies the equation  $r^3 - r^2 - r - 1 = 0$ . Its real root,  $t = \frac{1}{3} \left( 1 + \sqrt[3]{19 - 3\sqrt{33}} + \sqrt[3]{19 + 3\sqrt{33}} \right) \approx 1.83929$ , happens to be half the  $a$  value for point  $A$ . Indeed  $t^3 - t^2 - t - 1 = 0$  is equal to  $a^3 - 2a^2 - 4a - 8 = 0$  for  $t = a/2$ .

### 6.3 Misiurewicz points

The parameter value(s) for which a periodic limit cycle has a critical point as a predecessor, is called a *Misiurewicz point*. For a map  $f(x)$  a point where  $df/dx = 0$  is a critical point. For the logistic function we have  $\frac{dax(1-x)}{dx} = a(1-2x) = 0$  if  $x = 1/2$ . Therefore, the point  $x_0 = 1/2$  is the only critical point. Taking  $a = \frac{2}{3} \left( 1 + \sqrt[3]{19 - 3\sqrt{33}} + \sqrt[3]{19 + 3\sqrt{33}} \right) \approx 3.67857$  and starting at  $x_0 = 0.5$  we obtain  $x_1 \approx 0.919643$ ,  $x_2 \approx 0.271845$ ,  $x_3 \approx 0.728155$ ,  $x_4 \approx 0.728155$ ,  $x_5 \approx 0.728155$ , etc. That is, starting at the critical point  $x_0 = 1/2$  we arrive after 3 steps at the single fixed point  $A$ . Let us denote Misiurewicz points for the logistic map as  $a_{k,n}$  where  $k$  and  $n$  are positive integers. The integer  $k$  is the number of steps it takes from the critical point to arrive at a periodic cycle and the integer  $n$  is the period of the cycle. For instance, the parameter value  $a = \frac{2}{3} \left( 1 + \sqrt[3]{19 - 3\sqrt{33}} + \sqrt[3]{19 + 3\sqrt{33}} \right) \approx 3.678573510428322265$  is a Misiurewicz point. Since it takes 3 steps from  $x_0 = 1/2$  to arrive at a cycle with period 1, it is denoted as  $a_{3,1}$ :  $a_{3,1} \approx 3.678573510428322265$ .

In the first figure on the next page we have indicated two points which are part of a period 2 cycle and which have  $x_0 = 1/2$  as a predecessor. The  $a$  value for these two red points is approximately 3.592572184106978649. It takes 5 steps from  $x_0 = 1/2$  to arrive at the period 2 cycle. We therefore write  $a_{5,2} \approx 3.592572184106978649$ .

In the second figure on the next page we have indicated four points which are part of a period 4 cycle and which have  $x_0 = 1/2$  as a predecessor. The  $a$  value for these four red points is approximately 3.5748049387592. It takes 9 steps from  $x_0 = 1/2$  to arrive at the period 4 cycle. We therefore write  $a_{9,4} \approx 3.5748049387592$ . Continuation of the procedure leads to  $a_{17,8} \approx 3.57098594034161$ ,  $a_{33,16} \approx 3.570168472496375$ ,  $a_{65,32} \approx 3.56999338855913$ , and so on.

In the limit  $m \rightarrow \infty$  the sequence  $a_{2^{m+1}+1,2^m}$  converges to 3.56994567187, which is the same value for  $a$  where the period doubling series  $2^m$  ends at the  $2^\infty$  limit cycle [8].



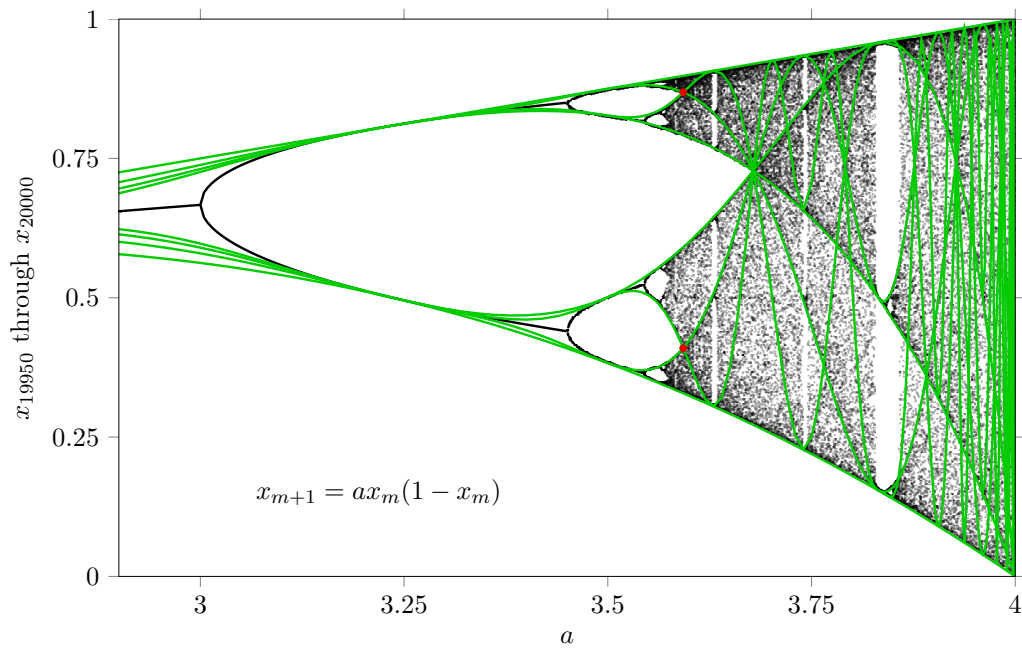


Figure 6.3: Polynomials  $x_k(a)$  for  $x_0 = 1/2$  on top of the orbit diagram for the logistic equation. The two red points are part of an (unstable) period 2 cycle.

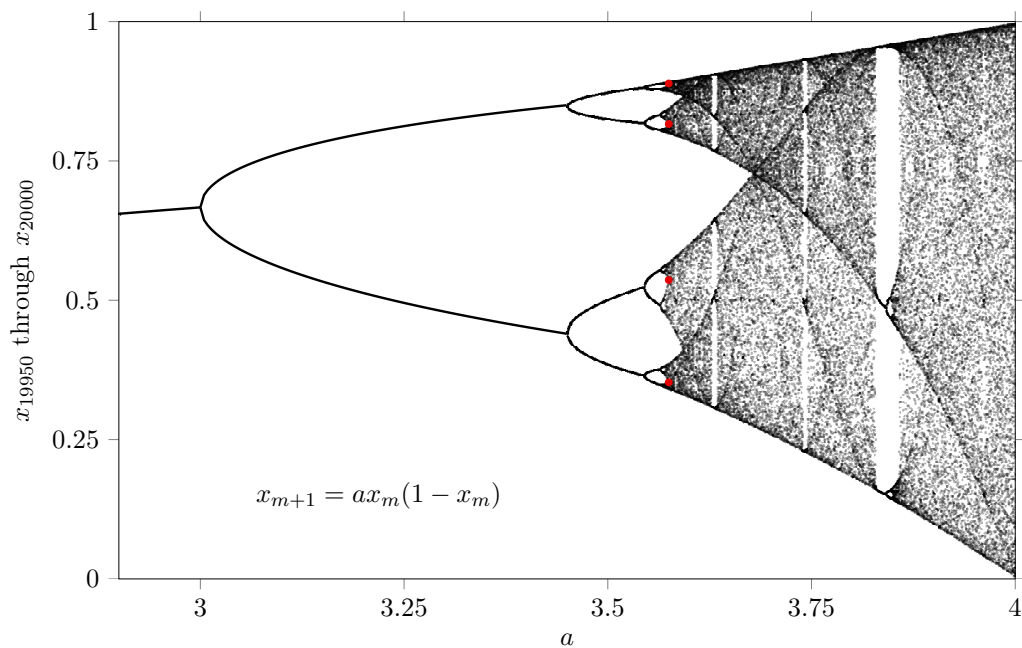


Figure 6.4: The orbit diagram for the logistic equation. The four red points are part of an (unstable) period 4 cycle.

For the ratio of the distances between the first few Misiurewicz points we obtain:

$$\frac{a_{3,1} - a_{5,2}}{a_{5,2} - a_{9,4}} \approx 4.840442, \quad \frac{a_{5,2} - a_{9,4}}{a_{9,4} - a_{17,8}} \approx 4.652331, \quad \frac{a_{9,4} - a_{17,8}}{a_{17,8} - a_{33,16}} \approx 4.671741,$$

$$\frac{a_{17,8} - a_{33,16}}{a_{33,16} - a_{65,32}} \approx 4.669005, \text{ and so on.}$$

In the limit  $m \rightarrow \infty$  the ratio  $\frac{a_{2^{m+1}+1, 2^m} - a_{2^{m+2}+1, 2^{m+1}}}{a_{2^{m+2}+1, 2^{m+1}} - a_{2^{m+3}+1, 2^{m+2}}}$  converges to the Feigenbaum constant 4.669201609... [8].

## 6.4 Misiurewicz points for the $z^2 + c$ map

For the complex function  $f(z) = z^2 + c$  we have  $\frac{df}{dz} = 2z = 0$  if  $z = 0$ . Therefore, the point  $z_0 = 0$  is the only critical point. A complex parameter  $c$  is a Misiurewicz point  $M_{k,n}$  if it takes  $k$  steps from the starting point  $z_0 = 0$  to arrive at a cycle with period  $n$ . Let us start with  $z_0 = 0$  and look at the first few  $z_m$ :

$$z_1 = c, \quad z_2 = c + c^2, \quad z_3 = c + c^2 + 2c^3 + c^4, \\ z_4 = c + c^2 + 2c^3 + 5c^4 + 6c^5 + 6c^6 + 4c^7 + c^8, \text{ and so on.}$$

Let us see if a Misiurewicz point  $M_{1,1}$  exists. The requirements are  $z_2 = z_1$  and  $z_1 \neq z_0$ . The first requirement gives  $c^2 + c = c$ . Its solution,  $c = 0$ , is ruled out by the second requirement. A point  $M_{1,1}$  therefore does not exist.

Next we try  $M_{2,1}$ . Then the requirements are  $z_3 = z_2$ ,  $z_2 \neq z_1$ ,  $z_2 \neq z_0$  and  $z_1 \neq z_0$ . The condition  $z_3 = z_2$  leads to  $c^3(c+2) = 0$ . The first solution,  $c = 0$ , is ruled out by  $z_1 \neq z_0$ . The second solution,  $c = -2$ , is a Misiurewicz point:  $M_{2,1} = -2$ . It leads to the sequence  $\{0, -2, 2, 2, 2, \dots\}$  for the  $z_m$ .

For  $M_{1,2}$  the requirements are  $z_3 = z_1$ ,  $z_2 \neq z_1$ ,  $z_2 \neq z_0$  and  $z_1 \neq z_0$ . The condition  $z_3 = z_1$  leads to  $c^2(c+1)^2 = 0$ . The first solution,  $c = 0$ , is ruled out by  $z_1 \neq z_0$ . The second solution,  $c = -1$ , is ruled out by  $z_2 \neq z_0$ . In fact,  $M_{1,n}$  does not exist for all (positive integer)  $n$ . If it would exist the condition  $z_{n+1} = z_1$  together with the equalities  $z_{n+1} = z_n^2 + c$  and  $z_1 = c$  would imply  $z_n = 0$ , which is ruled out by  $z_n \neq z_0$ .

Points  $M_{3,1}$  are roots of  $c^3 + 2c^2 + 2c + 2$ . For the real root this is

$$M_{3,1} = \frac{1}{3} \left( -2 - \sqrt[3]{17 + 3\sqrt{33}} + \sqrt[3]{-17 + 3\sqrt{33}} \right) \approx -1.543689.$$

It leads to the sequence  $\{0, -1.54369, 0.839287, -0.839287, -0.839287, \dots\}$ .

For the complex roots we get

$$M_{3,1} = \frac{1}{3} \left( -2 + \frac{1 + i\sqrt{3}}{2} \sqrt[3]{17 + 3\sqrt{33}} - \frac{1 - i\sqrt{3}}{2} \sqrt[3]{-17 + 3\sqrt{33}} \right) \approx -0.228155 + 1.11514i$$

with sequence  $\{0, -0.228155 + 1.11514i, -1.41964 + 0.606291i, 1.41964 - 0.606291i, 1.41964 - 0.606291i, \dots\}$  and

$$M_{3,1} = \frac{1}{3} \left( -2 + \frac{1 - i\sqrt{3}}{2} \sqrt[3]{17 + 3\sqrt{33}} - \frac{1 + i\sqrt{3}}{2} \sqrt[3]{-17 + 3\sqrt{33}} \right) \approx -0.228155 - 1.11514i$$

with sequence  $\{0, -0.228155 - 1.11514i, -1.41964 - 0.606291i, 1.41964 + 0.606291i, 1.41964 + 0.606291i, \dots\}$ .

Points  $M_{2,2}$  are roots of  $c^2 + 1$ . The two imaginary roots are  $M_{2,2} = -i$  and  $M_{2,2} = i$ . They lead to the sequences  $\{0, -i, -1-i, i, -1-i, i, -1-i, i, \dots\}$  and  $\{0, i, -1+i, -i, -1+i, -i, -1+i, -i, \dots\}$  respectively.

Points  $M_{4,1}$  are roots of  $c^7 + 4c^6 + 6c^5 + 6c^4 + 6c^3 + 4c^2 + 2c + 2$ . The real root is  $M_{4,1} \approx -1.89291$  with sequence  $\{0, -1.89291, 1.6902, 0.963869, -0.963869, -0.963869, \dots\}$ . For the complex roots:  $M_{4,1} \approx -1.29636 \pm 0.441852i$ ,  $M_{4,1} \approx -0.101096 \pm 0.956287i$  and  $M_{4,1} \approx 0.343907 \pm 0.70062i$ .

Points  $M_{3,2}$  are roots of  $c^3 + c^2 - c + 1$ . The real root is minus the tribonacci constant:

$$M_{3,2} = \frac{1}{3} \left( -1 - \sqrt[3]{19 + 3\sqrt{33}} - \sqrt[3]{19 - 3\sqrt{33}} \right) \approx -1.83929.$$

It leads to the sequence  $\{0, -1.83929, 1.54369, 0.543689, -1.54369, 0.543689, -1.54369, \dots\}$ .

For the complex roots we get

$$M_{3,2} = \frac{1}{3} \left( -1 + \frac{1 + i\sqrt{3}}{2} \sqrt[3]{19 + 3\sqrt{33}} + \frac{1 - i\sqrt{3}}{2} \sqrt[3]{19 - 3\sqrt{33}} \right) \approx 0.419643 + 0.606291i$$

with sequence  $\{0, 0.419643 + 0.606291i, 0.228155 + 1.11514i, -0.771845 + 1.11514i, -0.228155 - 1.11514i, -0.771845 + 1.11514i, -0.228155 - 1.11514i, \dots\}$  and

$$M_{3,2} = \frac{1}{3} \left( -1 + \frac{1 - i\sqrt{3}}{2} \sqrt[3]{19 + 3\sqrt{33}} + \frac{1 + i\sqrt{3}}{2} \sqrt[3]{19 - 3\sqrt{33}} \right) \approx 0.419643 - 0.606291i$$

with sequence  $\{0, 0.419643 - 0.606291i, 0.228155 - 1.11514i, -0.771845 - 1.11514i, -0.228155 + 1.11514i, -0.771845 - 1.11514i, -0.228155 + 1.11514i, \dots\}$ .

Points  $M_{2,3}$  are roots of  $c^6 + 2c^5 + 2c^4 + 2c^3 + c^2 + 1$ . The 6 complex roots are  $M_{4,1} \approx -1.23923 \pm 0.412602i$ ,  $M_{4,1} \approx -0.155788 \pm 1.11222i$  and  $M_{4,1} \approx 0.395014 \pm 0.555625i$ .

In summary, we found 1 Misiurewicz point  $M_{2,1}$ , 3 points  $M_{3,1}$  and 2 points  $M_{2,2}$ , 7 points  $M_{4,1}$ , 3 points  $M_{3,2}$  and 6 points  $M_{2,3}$ . That is a total of 22 Misiurewicz points for which the sum of the indices is smaller than 6. In the figure on the next page we have plotted the 22 Misiurewicz points we obtained so far.

The number  $N_{k,n}$  of Misiurewicz points  $M_{k,n}$  is given by

$$N_{k,n} = s_n \left( 2^{k-1} - t_{k,n} \right), \quad (6.8)$$

where  $t_{k,1} = 1$  and

$$t_{k,n>1} = \begin{cases} 1 & \text{if } k \bmod n = 1 \\ 0 & \text{if } k \bmod n \neq 1 \end{cases} \quad (6.9)$$

and where  $s_n$  is the same function as we found in chapter 4 for the number of period  $n$  solutions of the Mandelbrot set:

$$s_n = \sum_{d|n} \mu(n/d) \cdot 2^{d-1}, \quad (6.10)$$

with  $\mu$  the Mobius function. The equation (6.8) gives a relation between the number  $N_{k,n}$  of Misiurewicz points  $M_{k,n}$  and the number of period  $n$  solutions of the Mandelbrot set.

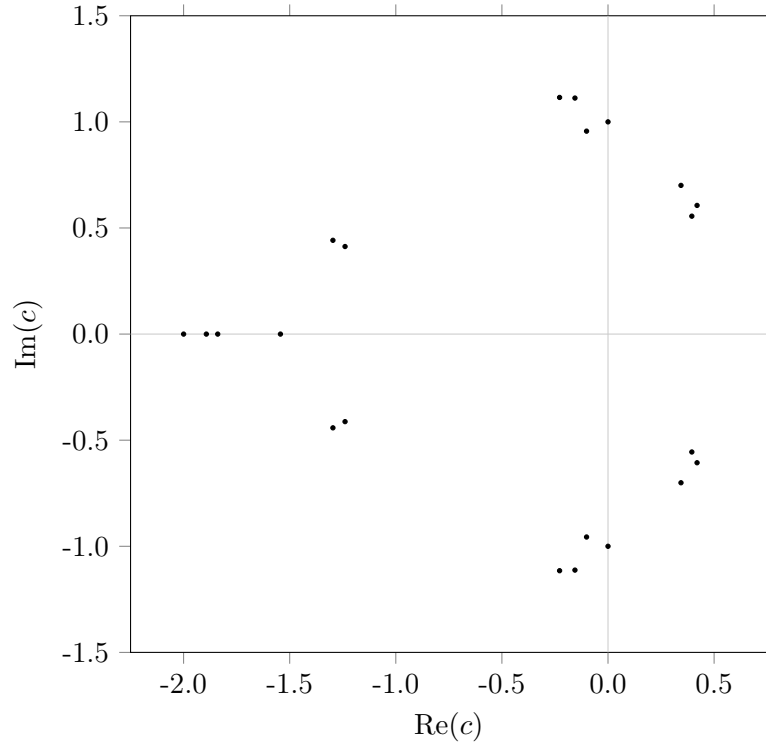


Figure 6.5: Misiurewicz points  $M_{2,1}$ ,  $M_{3,1}$ ,  $M_{2,2}$ ,  $M_{4,1}$ ,  $M_{3,2}$  and  $M_{2,3}$  for the map  $z^2 + c$ .

We give some explicit calculations for the calculation of  $N_{k,n}$ :

$$N_{2,3} = s_3 (2^{2-1} - t_{2,3}) = 3 (2^1 - 0) = 6, \quad (6.11)$$

$$N_{3,2} = s_2 (2^{3-1} - t_{3,2}) = 1 (2^2 - 1) = 3, \quad (6.12)$$

$$N_{4,1} = s_1 (2^{4-1} - t_{4,1}) = 1 (2^3 - 1) = 7, \quad (6.13)$$

$$N_{4,2} = s_2 (2^{4-1} - t_{4,2}) = 1 (2^3 - 0) = 8, \quad (6.14)$$

$$N_{4,3} = s_3 (2^{4-1} - t_{4,3}) = 3 (2^3 - 1) = 21. \quad (6.15)$$

The number  $N_{k,n}$  of Misiurewicz points  $M_{k,n}$  are tabulated in next table.

$k+n \backslash k$	1	2	3	4	5	6	7	8	9	10	11	12	13	14	$S$
2	0														0
3	0	1													1
4	0	2	3												5
5	0	6	3	7											16
6	0	12	12	8	15										47
7	0	30	24	21	15	31									121
8	0	54	60	48	48	32	63								305
9	0	126	108	120	90	96	63	127							730
10	0	240	252	216	240	192	189	128	255						1712
11	0	504	480	504	432	465	384	384	255	511					3919
12	0	990	1008	960	1008	864	960	768	768	512	1023				8861
13	0	2046	1980	2016	1920	2016	1701	1920	1530	1533	1023	2047			19732
14	0	4020	4092	3960	4032	3840	4032	3456	3840	3072	3072	2048	4095		43559
15	0	8190	8040	8184	7920	8064	7680	8001	6912	7680	6144	6144	4095	8191	95245

In the final row is the sum of numbers of Misiurewicz points for which  $k+n$  is a constant, say

$$m. \text{ That is, } S = \sum_{k=2}^{m-1} N_{k,m-k}.$$

Their cumulative sums are shown in the next table.

$t$	3	4	5	6	7	8	9	10	11	12	13	14	15
$\sum_{m=3}^t \sum_{k=2}^{m-1} N_{k,m-k}$	1	6	22	69	190	495	1225	2937	6856	15717	35449	79008	174253

In the final figure the 15717 Misiurewicz points have been plotted for which the sum of the indices is 12 or smaller. The Mandelbrot set is also shown in order to illustrate that the Misiurewicz points form an ‘envelope’ of the Mandelbrot set.

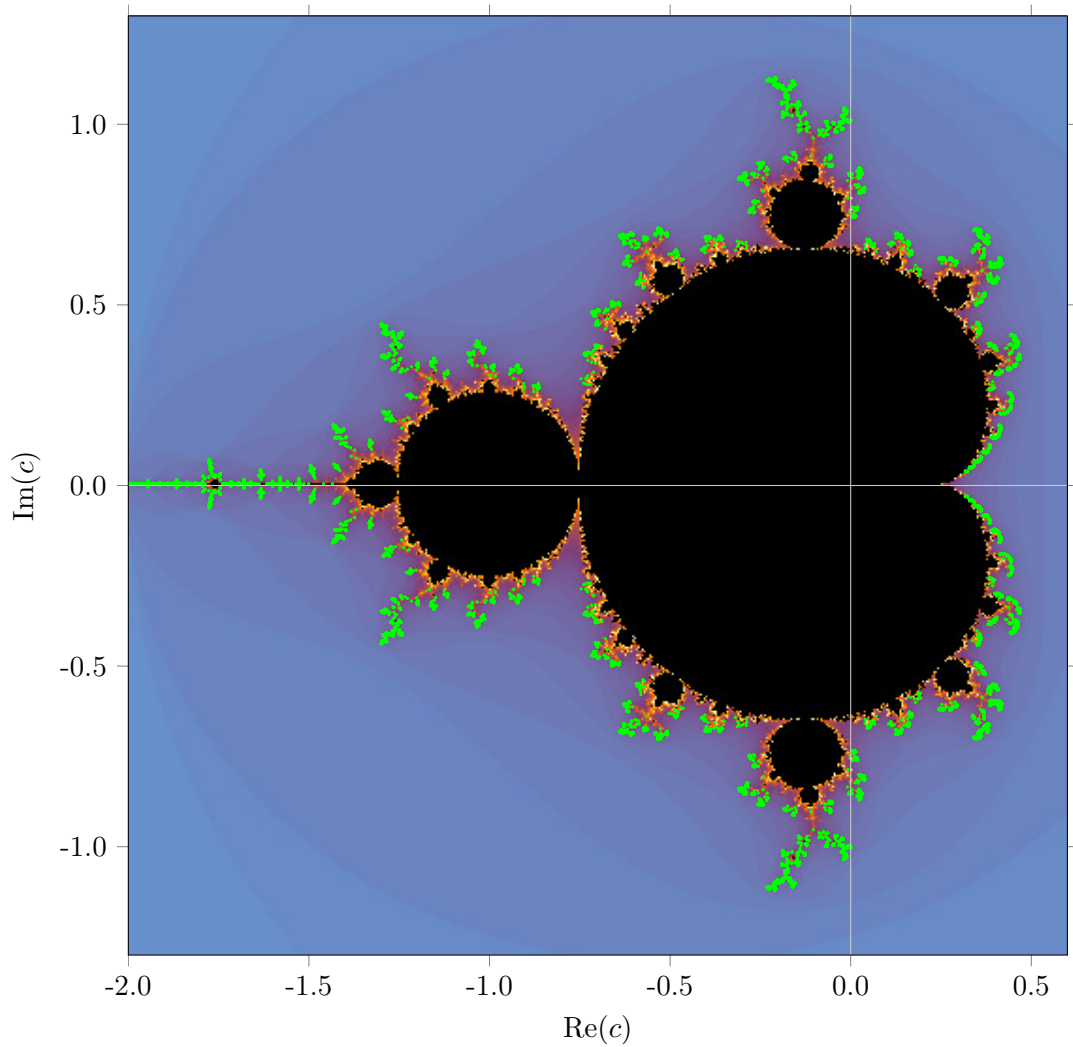


Figure 6.6: The 15717 Misiurewicz points  $M_{k,n}$  (green) for which  $k+n \leq 12$  and the Mandelbrot set (black). Close to the Mandelbrot set the divergence to infinity is slow (orange) and further away from the Mandelbrot set the divergence is faster (blue).

## Appendix A

### A series solution

In this appendix we derive a recursion formula of the type  $v_{n+1} = av_n + bv_{n-1}$  with  $v_0$  and  $v_1$  as initial values. For  $n \geq 2$  we successively obtain

$$v_2 = av_1 + bv_0,$$

$$v_3 = av_2 + bv_1 = (a^2 + b)v_1 + abv_0,$$

$$v_4 = av_3 + bv_2 = (a^3 + 2ab)v_1 + (a^2 + b)bv_0, \text{ etc.}$$

For  $n \geq 2$  this is

$$v_n = v_1 \sum_{k=0}^{\lfloor n/2-1/2 \rfloor} \binom{n-1-k}{k} a^{n-1-2k} b^k + bv_0 \sum_{k=0}^{\lfloor n/2-1 \rfloor} \binom{n-2-k}{k} a^{n-2-2k} b^k. \quad (\text{A.1})$$

The latter will be proven below by induction. We have to distinguish between  $n$  is even and  $n$  is odd. For even  $n$  we write  $n = 2m$ . Then the equation (A.1) reads

$$v_{2m} = v_1 \sum_{k=0}^{m-1} \binom{2m-1-k}{k} a^{2m-1-2k} b^k + bv_0 \sum_{k=0}^{m-1} \binom{2m-2-k}{k} a^{2m-2-2k} b^k. \quad (\text{A.2})$$

For odd  $n$  we write  $n = 2m + 1$ . Then equation (A.1) reads

$$v_{2m+1} = v_1 \sum_{k=0}^m \binom{2m-k}{k} a^{2m-2k} b^k + bv_0 \sum_{k=0}^{m-1} \binom{2m-1-k}{k} a^{2m-1-2k} b^k. \quad (\text{A.3})$$

Assuming the equations to be true for  $n = 2m$  and  $n = 2m + 1$  we will show it to be true for  $n = 2m + 2$ . That is we will derive

$$v_{2m+2} = v_1 \sum_{k=0}^m \binom{2m+1-k}{k} a^{2m+1-2k} b^k + bv_0 \sum_{k=0}^m \binom{2m-k}{k} a^{2m-2k} b^k. \quad (\text{A.4})$$

Assuming the equations to be true for  $n = 2m + 1$  and  $n = 2m + 2$  we will show it to be true for  $n = 2m + 3$ . That is we will derive

$$v_{2m+3} = v_1 \sum_{k=0}^{m+1} \binom{2m+2-k}{k} a^{2m+2-2k} b^k + bv_0 \sum_{k=0}^m \binom{2m+1-k}{k} a^{2m+1-2k} b^k. \quad (\text{A.5})$$

For  $n = 2$  the equation (A.2) indeed gives

$$v_2 = v_1 \sum_{k=0}^0 \binom{1-k}{k} a^{1-2k} b^k + bv_0 \sum_{k=0}^0 \binom{-k}{k} a^{-2k} b^k = av_1 + bv_0. \quad (\text{A.6})$$

For  $n = 3$  the equation (A.3) indeed gives

$$v_3 = v_1 \sum_{k=0}^1 \binom{2-k}{k} a^{2-2k} b^k + bv_0 \sum_{k=0}^0 \binom{1-k}{k} a^{1-2k} b^k = (a^2 + b)v_1 + av_0. \quad (\text{A.7})$$

For the induction we substitute the equations (A.2) and (A.3) into the recurrence relation  $v_{n+1} = av_n + bv_{n-1}$ . For  $n = 2m + 1$  this is

$$\begin{aligned} v_{2m+2} &= av_{2m+1} + bv_{2m} \\ &= av_1 \sum_{k=0}^m \binom{2m-k}{k} a^{2m-2k} b^k + abv_0 \sum_{k=0}^{m-1} \binom{2m-1-k}{k} a^{2m-1-2k} b^k + \\ &\quad + bv_1 \sum_{k=0}^{m-1} \binom{2m-1-k}{k} a^{2m-1-2k} b^k + b^2 v_0 \sum_{k=0}^{m-1} \binom{2m-2-k}{k} a^{2m-2-2k} b^k \\ &= v_1 \left[ \sum_{k=0}^m \binom{2m-k}{k} a^{2m+1-2k} b^k + \sum_{k=0}^{m-1} \binom{2m-1-k}{k} a^{2m-1-2k} b^{k+1} \right] + \\ &\quad + bv_0 \left[ \sum_{k=0}^{m-1} \binom{2m-1-k}{k} a^{2m-2k} b^k + \sum_{k=0}^{m-1} \binom{2m-2-k}{k} a^{2m-2-2k} b^{k+1} \right] \\ &= v_1 \left[ a^{2m+1} + \sum_{k=1}^m \binom{2m-k}{k} a^{2m+1-2k} b^k + \sum_{k=0}^{m-1} \binom{2m-1-k}{k} a^{2m-1-2k} b^{k+1} \right] + \\ &\quad + bv_0 \left[ a^{2m} + \sum_{k=1}^{m-1} \binom{2m-1-k}{k} a^{2m-2k} b^k + b^m + \sum_{k=0}^{m-2} \binom{2m-2-k}{k} a^{2m-2-2k} b^{k+1} \right] \\ &= v_1 \left[ a^{2m+1} + \sum_{k=1}^m \binom{2m-k}{k} a^{2m+1-2k} b^k + \sum_{j=1}^m \binom{2m-j}{j-1} a^{2m+1-2j} b^j \right] + \\ &\quad + bv_0 \left[ a^{2m} + \sum_{k=1}^{m-1} \binom{2m-1-k}{k} a^{2m-2k} b^k + b^m + \sum_{j=1}^{m-1} \binom{2m-1-j}{j-1} a^{2m-2j} b^j \right] \\ &= v_1 \left[ a^{2m+1} + \sum_{k=1}^m \left( \binom{2m-k}{k} + \binom{2m-k}{k-1} \right) a^{2m+1-2k} b^k \right] + \\ &\quad + bv_0 \left[ a^{2m} + b^m + \sum_{k=1}^{m-1} \left( \binom{2m-1-k}{k} + \binom{2m-1-k}{k-1} \right) a^{2m-2k} b^k \right] \end{aligned} \quad (\text{A.8})$$

By means of *Pascal's rule*,

$$\binom{r}{k} + \binom{r}{k-1} = \binom{r+1}{k}, \quad (\text{A.9})$$



it is further reduced to

$$\begin{aligned}
v_{2m+2} &= v_1 \left[ a^{2m+1} + \sum_{k=1}^m \binom{2m+1-k}{k} a^{2m+1-2k} b^k \right] + \\
&\quad + bv_0 \left[ a^{2m} + b^m + \sum_{k=1}^{m-1} \binom{2m-k}{k} a^{2m-2k} b^k \right] \\
&= v_1 \sum_{k=0}^m \binom{2m+1-k}{k} a^{2m+1-2k} b^k + bv_0 \sum_{k=0}^m \binom{2m-k}{k} a^{2m-2k} b^k.
\end{aligned} \tag{A.10}$$

Indeed the latter is equal to the equation [\(A.4\)](#).

For  $n = 2m + 2$  we get

$$\begin{aligned}
v_{2m+3} &= av_{2m+2} + bv_{2m+1} \\
&= av_1 \sum_{k=0}^m \binom{2m+1-k}{k} a^{2m+1-2k} b^k + abv_0 \sum_{k=0}^m \binom{2m-k}{k} a^{2m-2k} b^k + \\
&\quad + bv_1 \sum_{k=0}^m \binom{2m-k}{k} a^{2m-2k} b^k + b^2v_0 \sum_{k=0}^{m-1} \binom{2m-1-k}{k} a^{2m-1-2k} b^k \\
&= v_1 \left[ \sum_{k=0}^m \binom{2m+1-k}{k} a^{2m+2-2k} b^k + \sum_{k=0}^m \binom{2m-k}{k} a^{2m-2k} b^{k+1} \right] + \\
&\quad + bv_0 \left[ \sum_{k=0}^m \binom{2m-k}{k} a^{2m+1-2k} b^k + \sum_{k=0}^{m-1} \binom{2m-1-k}{k} a^{2m-1-2k} b^{k+1} \right] \\
&= v_1 \left[ a^{2m+2} + \sum_{k=1}^m \binom{2m+1-k}{k} a^{2m+2-2k} b^k + b^{m+1} + \sum_{k=0}^{m-1} \binom{2m-k}{k} a^{2m-2k} b^{k+1} \right] + \\
&\quad + bv_0 \left[ a^{2m+1} + \sum_{k=1}^m \binom{2m-k}{k} a^{2m+1-2k} b^k + mab^m + \sum_{k=0}^{m-2} \binom{2m-1-k}{k} a^{2m-1-2k} b^{k+1} \right] \\
&= v_1 \left[ a^{2m+2} + \sum_{k=1}^m \binom{2m+1-k}{k} a^{2m+2-2k} b^k + b^{m+1} + \sum_{j=1}^m \binom{2m+1-j}{j-1} a^{2m+2-2j} b^j \right] + \\
&\quad + bv_0 \left[ a^{2m+1} + ab^m + \sum_{k=1}^{m-1} \binom{2m-k}{k} a^{2m+1-2k} b^k + mab^m + \sum_{j=1}^{m-1} \binom{2m-j}{j-1} a^{2m+1-2j} b^j \right] \\
&= v_1 \left[ a^{2m+2} + b^{m+1} + \sum_{k=1}^m \left( \binom{2m+1-k}{k} + \binom{2m+1-k}{k-1} \right) a^{2m+2-2k} b^k \right] + \\
&\quad + bv_0 \left[ a^{2m+1} + (m+1)ab^m + \sum_{k=1}^{m-1} \left( \binom{2m-k}{k} + \binom{2m-k}{k-1} \right) a^{2m+1-2k} b^k \right]
\end{aligned} \tag{A.11}$$

By means of Pascal's rule it is further reduced to

$$\begin{aligned}
v_{2m+3} &= v_1 \left[ a^{2m+2} + b^{m+1} + \sum_{k=1}^m \binom{2m+2-k}{k} a^{2m+2-2k} b^k \right] + \\
&\quad + bv_0 \left[ a^{2m+1} + (m+1)ab^m + \sum_{k=1}^{m-1} \binom{2m+1-k}{k} a^{2m+1-2k} b^k \right] \\
&= v_1 \sum_{k=0}^{m+1} \binom{2m+2-k}{k} a^{2m+2-2k} b^k + bv_0 \sum_{k=0}^m \binom{2m+1-k}{k} a^{2m+1-2k} b^k.
\end{aligned} \tag{A.12}$$

Indeed the latter is equal to the equation (A.5). This completes the proof.

## Appendix B

### A binomial identity

In this appendix it will be shown by induction that for  $a^2 + 4b \neq 0$  the equation [\(1.34\)](#),

$$v_n = v_1 \sum_{k=0}^{\lfloor n/2-1/2 \rfloor} \binom{n-1-k}{k} a^{n-1-2k} b^k + bv_0 \sum_{k=0}^{\lfloor n/2-1 \rfloor} \binom{n-2-k}{k} a^{n-2-2k} b^k, \quad (\text{B.1})$$

is identical to the equation [\(1.37\)](#),

$$v_n = \frac{v_0 g_+ - v_1}{g_+ - g_-} g_-^n - \frac{v_0 g_- - v_1}{g_+ - g_-} g_+^n, \quad (\text{B.2})$$

where  $g$  is a root of the equation  $g^2 - ag - b = 0$ .

First we take  $n = 0$ . Then the equation [\(B.2\)](#) gives

$$v_0 = \frac{v_0 g_+ - v_1}{g_+ - g_-} - \frac{v_0 g_- - v_1}{g_+ - g_-} = \frac{v_0 g_+ - v_0 g_-}{g_+ - g_-} = v_0. \quad (\text{B.3})$$

For  $n = 1$  the equation [\(B.2\)](#) gives

$$v_1 = \frac{v_0 g_+ - v_1}{g_+ - g_-} g_- - \frac{v_0 g_- - v_1}{g_+ - g_-} g_+ = \frac{v_0 g_+ g_- - v_0 g_- g_+}{g_+ - g_-} - \frac{v_1 g_- - v_1 g_+}{g_+ - g_-} = v_1. \quad (\text{B.4})$$

For  $n = 2$  the equation [\(B.2\)](#) gives

$$\begin{aligned} v_2 &= \frac{v_0 g_+ - v_1}{g_+ - g_-} g_-^2 - \frac{v_0 g_- - v_1}{g_+ - g_-} g_+^2 = \frac{v_0 g_+ g_-^2 - v_0 g_- g_+^2}{g_+ - g_-} - \frac{v_1 g_-^2 - v_1 g_+^2}{g_+ - g_-} \\ &= -v_0 g_- g_+ + v_1 (g_+ + g_-) = bv_0 + av_1. \end{aligned} \quad (\text{B.5})$$

For  $n = 3$  the equation [\(B.2\)](#) gives

$$\begin{aligned} v_3 &= \frac{v_0 g_+ - v_1}{g_+ - g_-} g_-^3 - \frac{v_0 g_- - v_1}{g_+ - g_-} g_+^3 = \frac{v_0 g_+ g_-^3 - v_0 g_- g_+^3}{g_+ - g_-} - \frac{v_1 g_-^3 - v_1 g_+^3}{g_+ - g_-} \\ &= -v_0 g_- g_+ \frac{g_+^2 - g_-^2}{g_+ - g_-} + v_1 \frac{g_+^3 - g_-^3}{g_+ - g_-} \\ &= -v_0 g_- g_+ (g_+ + g_-) + v_1 (g_+^2 + g_+ g_- + g_-^2) = av_0 + (a^2 + b)v_1. \end{aligned} \quad (\text{B.6})$$

Now we will show that equation (B.2) equals equation (B.1) for any  $n \geq 2$ .

If  $n$  is an even number,  $n = 2m$ , the equation (B.1) reads

$$v_{2m} = v_1 \sum_{k=0}^{m-1} \binom{2m-1-k}{k} a^{2m-1-2k} b^k + bv_0 \sum_{k=0}^{m-1} \binom{2m-2-k}{k} a^{2m-2-2k} b^k, \quad (\text{B.7})$$

while the equation (B.2) becomes

$$v_{2m} = \frac{v_0 g_+ - v_1}{g_+ - g_-} g_-^{2m} - \frac{v_0 g_- - v_1}{g_+ - g_-} g_+^{2m} = bv_0 \frac{g_+^{2m-1} - g_-^{2m-1}}{g_+ - g_-} + v_1 \frac{g_+^{2m} - g_-^{2m}}{g_+ - g_-}. \quad (\text{B.8})$$

The latter is equal to equation (B.7) if both

$$\frac{g_+^{2m-1} - g_-^{2m-1}}{g_+ - g_-} = \sum_{k=0}^{m-1} \binom{2m-2-k}{k} a^{2m-2-2k} b^k \quad (\text{B.9})$$

and

$$\frac{g_+^{2m} - g_-^{2m}}{g_+ - g_-} = \sum_{k=0}^{m-1} \binom{2m-1-k}{k} a^{2m-1-2k} b^k \quad (\text{B.10})$$

are true identities.

If  $n$  is an odd number,  $n = 2m + 1$ , the equation (B.1) reads

$$v_{2m+1} = v_1 \sum_{k=0}^m \binom{2m-k}{k} a^{2m-2k} b^k + bv_0 \sum_{k=0}^{m-1} \binom{2m-1-k}{k} a^{2m-1-2k} b^k, \quad (\text{B.11})$$

while the equation (B.2) becomes

$$v_{2m+1} = \frac{v_0 g_+ - v_1}{g_+ - g_-} g_-^{2m+1} - \frac{v_0 g_- - v_1}{g_+ - g_-} g_+^{2m+1} = bv_0 \frac{g_+^{2m} - g_-^{2m}}{g_+ - g_-} + v_1 \frac{g_+^{2m+1} - g_-^{2m+1}}{g_+ - g_-}. \quad (\text{B.12})$$

The latter is equal to equation (B.11) if both

$$\frac{g_+^{2m} - g_-^{2m}}{g_+ - g_-} = \sum_{k=0}^{m-1} \binom{2m-1-k}{k} a^{2m-1-2k} b^k \quad (\text{B.13})$$

and

$$\frac{g_+^{2m+1} - g_-^{2m+1}}{g_+ - g_-} = \sum_{k=0}^m \binom{2m-k}{k} a^{2m-2k} b^k \quad (\text{B.14})$$

are true identities. Identity (B.13) is equal to identity (B.10) and identity (B.14) is identity (B.9) with  $m$  replaced by  $m + 1$ .

For the induction step we multiply  $g_+^{2m} - g_-^{2m}$  by  $g_+ + g_-$ . The result is

$$(g_+^{2m} - g_-^{2m})(g_+ + g_-) = g_+^{2m+1} - g_-^{2m+1} + g_- g_+ (g_+^{2m-1} - g_-^{2m-1}). \quad (\text{B.15})$$

Hence,

$$\frac{g_+^{2m+1} - g_-^{2m+1}}{g_+ - g_-} = a \frac{g_+^{2m} - g_-^{2m}}{g_+ - g_-} + b \frac{g_+^{2m-1} - g_-^{2m-1}}{g_+ - g_-}. \quad (\text{B.16})$$

Assuming the two identities (B.9) and (B.10) are true, we obtain

$$\frac{g_+^{2m+1} - g_-^{2m+1}}{g_+ - g_-} = a \sum_{k=0}^{m-1} \binom{2m-1-k}{k} a^{2m-1-2k} b^k + b \sum_{k=0}^{m-1} \binom{2m-2-k}{k} a^{2m-2-2k} b^k. \quad (\text{B.17})$$

This can be elaborated to

$$\begin{aligned} \frac{g_+^{2m+1} - g_-^{2m+1}}{g_+ - g_-} &= \sum_{k=0}^{m-1} \binom{2m-1-k}{k} a^{2m-2k} b^k + \sum_{k=0}^{m-1} \binom{2m-2-k}{k} a^{2m-2-2k} b^{k+1} \\ &= a^{2m} + b^m + \sum_{k=1}^{m-1} \binom{2m-1-k}{k} a^{2m-2k} b^k + \sum_{k=0}^{m-2} \binom{2m-2-k}{k} a^{2m-2-2k} b^{k+1} \\ &= a^{2m} + b^m + \sum_{k=1}^{m-1} \binom{2m-1-k}{k} a^{2m-2k} b^k + \sum_{j=1}^{m-1} \binom{2m-1-j}{j-1} a^{2m-2j} b^j \\ &= a^{2m} + b^m + \sum_{k=1}^{m-1} \binom{2m-1-k}{k} a^{2m-2k} b^k + \sum_{k=1}^{m-1} \binom{2m-1-k}{k-1} a^{2m-2k} b^k. \end{aligned} \quad (\text{B.18})$$

By means of Pascal's rule,

$$\binom{r}{k} + \binom{r}{k-1} = \binom{r+1}{k}, \quad (\text{B.19})$$

it is further reduced to

$$\frac{g_+^{2m+1} - g_-^{2m+1}}{g_+ - g_-} = a^{2m} + b^m + \sum_{k=1}^{m-1} \binom{2m-k}{k} a^{2m-2k} b^k = \sum_{k=0}^m \binom{2m-k}{k} a^{2m-2k} b^k. \quad (\text{B.20})$$

That is, assuming the identities to be true for the powers  $2m-1$  and  $2m$  of  $g_+$  and  $g_-$  we find the first identity to be true for the power  $2m+1$ .

Next we multiply  $g_+^{2m+1} - g_-^{2m+1}$  by  $g_+ + g_-$  and elaborate the result to

$$\frac{g_+^{2m+2} - g_-^{2m+2}}{g_+ - g_-} = a \frac{g_+^{2m+1} - g_-^{2m+1}}{g_+ - g_-} + b \frac{g_+^{2m} - g_-^{2m}}{g_+ - g_-}. \quad (\text{B.21})$$

Assuming the identities (B.13) and (B.14) are true, we obtain

$$\begin{aligned}
\frac{g_+^{2m+2} - g_-^{2m+2}}{g_+ - g_-} &= a \sum_{k=0}^m \binom{2m-k}{k} a^{2m-2k} b^k + b \sum_{k=0}^{m-1} \binom{2m-1-k}{k} a^{2m-1-2k} b^k \\
&= \sum_{k=0}^m \binom{2m-k}{k} a^{2m+1-2k} b^k + \sum_{k=0}^{m-1} \binom{2m-1-k}{k} a^{2m-1-2k} b^{k+1} \\
&= a^{2m+1} + mab^m + \sum_{k=1}^m \binom{2m-k}{k} a^{2m+1-2k} b^k + \sum_{k=0}^{m-2} \binom{2m-1-k}{k} a^{2m-1-2k} b^{k+1} \\
&= a^{2m+1} + mab^m + \sum_{k=1}^m \binom{2m-k}{k} a^{2m+1-2k} b^k + \sum_{j=1}^{m-1} \binom{2m-j}{j-1} a^{2m+1-2j} b^j \\
&= a^{2m+1} + mab^m + ab^m + \sum_{k=1}^{m-1} \binom{2m-k}{k} a^{2m+1-2k} b^k + \sum_{k=1}^{m-1} \binom{2m-k}{k-1} a^{2m+1-2k} b^k.
\end{aligned} \tag{B.22}$$

By means of Pascal's rule it further reduces to

$$\begin{aligned}
\frac{g_+^{2m+1} - g_-^{2m+1}}{g_+ - g_-} &= a^{2m+1} + (m+1)ab^m + \sum_{k=1}^{m-1} \binom{2m+1-k}{k} a^{2m+1-2k} b^k \\
&= \sum_{k=0}^m \binom{2m+1-k}{k} a^{2m+1-2k} b^k.
\end{aligned} \tag{B.23}$$

That is, assuming the identities to be true for the powers  $2m$  and  $2m+1$  of  $g_+$  and  $g_-$  we find the identity to be true for  $2m+2$ . This completes the proof.

## Appendix C

### Another binomial identity

In this appendix it will be shown by induction that for  $a^2 + 4b = 0$  the equation [\(1.34\)](#),

$$v_n = v_1 \sum_{k=0}^{\lfloor n/2-1/2 \rfloor} \binom{n-1-k}{k} a^{n-1-2k} b^k + bv_0 \sum_{k=0}^{\lfloor n/2-1 \rfloor} \binom{n-2-k}{k} a^{n-2-2k} b^k, \quad (\text{C.1})$$

is identical to the equation [\(1.38\)](#),

$$v_n = nv_1 g^{n-1} - (n-1)v_0 g^n, \quad (\text{C.2})$$

where  $g$  is a root of the equation  $g^2 - ag - b = 0$ .

First we take  $n = 0$ . Then the equation [\(C.2\)](#) gives

$$v_0 = 0 - -v_0 g^0 = v_0. \quad (\text{C.3})$$

For  $n = 1$  the equation [\(C.2\)](#) gives

$$v_1 = v_1 g^0 - 0 = v_1. \quad (\text{C.4})$$

For  $n = 2$  the equation [\(C.2\)](#) gives

$$v_2 = 2v_1 g - v_0 g^2 = av_1 - \frac{a^2}{4}v_0 = bv_0 + av_1. \quad (\text{C.5})$$

Now we show by means of induction that equation [\(C.2\)](#) equals equation [\(C.1\)](#) for any  $n \geq 2$ .

If  $n$  is an even number,  $n = 2m$ , the equation (C.1) reads

$$\begin{aligned}
v_{2m} &= v_1 \sum_{k=0}^{m-1} \binom{2m-1-k}{k} a^{2m-1-2k} b^k + bv_0 \sum_{k=0}^{m-1} \binom{2m-2-k}{k} a^{2m-2-2k} b^k \\
&= av_1 \sum_{k=0}^{m-1} \binom{2m-1-k}{k} a^{2m-2-2k} b^k + bv_0 \sum_{k=0}^{m-1} \binom{2m-2-k}{k} a^{2m-2-2k} b^k \\
&= av_1 \sum_{k=0}^{m-1} \binom{2m-1-k}{k} (a^2)^{m-1-k} b^k + bv_0 \sum_{k=0}^{m-1} \binom{2m-2-k}{k} (a^2)^{m-1-k} b^k \\
&= av_1 \sum_{k=0}^{m-1} \binom{2m-1-k}{k} (-4b)^{m-1-k} b^k + bv_0 \sum_{k=0}^{m-1} \binom{2m-2-k}{k} (-4b)^{m-1-k} b^k \\
&= av_1 \sum_{k=0}^{m-1} \binom{2m-1-k}{k} (-4)^{m-1-k} b^{m-1} + bv_0 \sum_{k=0}^{m-1} \binom{2m-2-k}{k} (-4)^{m-1-k} b^{m-1} \\
&= ab^{m-1} v_1 \sum_{k=0}^{m-1} \binom{2m-1-k}{k} (-4)^{m-1-k} + b^m v_0 \sum_{k=0}^{m-1} \binom{2m-2-k}{k} (-4)^{m-1-k},
\end{aligned} \tag{C.6}$$

while the equation (C.2) becomes

$$\begin{aligned}
v_{2m} &= 2mv_1 g g^{2m-2} - (2m-1)v_0 g^{2m} = mav_1 (g^2)^{m-1} - (2m-1)v_0 (g^2)^m \\
&= mab^{m-1} v_1 (-1)^{m-1} - (2m-1)b^m v_0 (-1)^m.
\end{aligned} \tag{C.7}$$

The latter is equal to equation (C.6) if both

$$(2m-1)(-1)^{m-1} = \sum_{k=0}^{m-1} \binom{2m-2-k}{k} (-4)^{m-1-k} \tag{C.8}$$

and

$$m(-1)^{m-1} = \sum_{k=0}^{m-1} \binom{2m-1-k}{k} (-4)^{m-1-k} \tag{C.9}$$

are true identities.

If  $n$  is an odd number,  $n = 2m + 1$ , the equation (1.34) reads

$$\begin{aligned}
v_{2m+1} &= v_1 \sum_{k=0}^m \binom{2m-k}{k} a^{2m-2k} b^k + bv_0 \sum_{k=0}^{m-1} \binom{2m-1-k}{k} a^{2m-1-2k} b^k \\
&= v_1 \sum_{k=0}^m \binom{2m-k}{k} a^{2m-2k} b^k + abv_0 \sum_{k=0}^{m-1} \binom{2m-1-k}{k} a^{2m-2-2k} b^k \\
&= v_1 \sum_{k=0}^m \binom{2m-k}{k} (a^2)^{m-k} b^k + abv_0 \sum_{k=0}^{m-1} \binom{2m-1-k}{k} (a^2)^{m-1-k} b^k \\
&= v_1 \sum_{k=0}^m \binom{2m-k}{k} (-4b)^{m-k} b^k + abv_0 \sum_{k=0}^{m-1} \binom{2m-1-k}{k} (-4b)^{m-1-k} b^k \\
&= b^m v_1 \sum_{k=0}^m \binom{2m-k}{k} (-4)^{m-k} + ab^m v_0 \sum_{k=0}^{m-1} \binom{2m-1-k}{k} (-4)^{m-1-k},
\end{aligned} \tag{C.10}$$



while the equation (C.2) becomes

$$\begin{aligned} v_{2m+1} &= (2m+1)v_1g^{2m} - 2mv_0g^{2m+1} = (2m+1)v_1(g^2)^m - 2mv_0g(g^2)^m \\ &= (2m+1)b^m v_1(-1)^m + mab^m v_0(-1)^{m-1}. \end{aligned} \quad (\text{C.11})$$

The latter is equal to equation (C.10) if both

$$m(-1)^{m-1} = \sum_{k=0}^{m-1} \binom{2m-1-k}{k} (-4)^{m-1-k} \quad (\text{C.12})$$

and

$$(2m+1)(-1)^m = \sum_{k=0}^m \binom{2m-k}{k} (-4)^{m-k} \quad (\text{C.13})$$

are true identities. Identity (C.12) is equal to identity (C.9) and identity (C.13) is identity (C.8) with  $m$  replaced by  $m+1$ .

For the induction step we consider the expression

$$\sum_{k=0}^m \binom{2m-k}{k} (-4)^{m-k} = 1 + \sum_{k=0}^{m-1} \binom{2m-k}{k} (-4)^{m-k}. \quad (\text{C.14})$$

Assuming the identities (C.8) and (C.9) are true, we obtain

$$\begin{aligned} &\sum_{k=0}^m \binom{2m-k}{k} (-4)^{m-k} \\ &= 1 - 4m(-1)^{m-1} + \sum_{k=0}^{m-1} \binom{2m-k}{k} (-4)^{m-k} + 4 \sum_{k=0}^{m-1} \binom{2m-1-k}{k} (-4)^{m-1-k} \\ &= 1 - 4m(-1)^{m-1} + \sum_{k=1}^{m-1} \binom{2m-k}{k} (-4)^{m-k} - \sum_{k=1}^{m-1} \binom{2m-1-k}{k} (-4)^{m-k} \\ &= 1 - 4m(-1)^{m-1} + \sum_{k=1}^{m-1} \left\{ \binom{2m-k}{k} - \binom{2m-1-k}{k} \right\} (-4)^{m-k}. \end{aligned} \quad (\text{C.15})$$

By means of Pascal's rule, it is further reduced to

$$\begin{aligned} &\sum_{k=0}^m \binom{2m-k}{k} (-4)^{m-k} = 1 - 4m(-1)^{m-1} + \sum_{k=1}^{m-1} \binom{2m-1-k}{k-1} (-4)^{m-k} \\ &= 1 - 4m(-1)^{m-1} + \sum_{j=0}^{m-2} \binom{2m-2-j}{j} (-4)^{m-1-j} \\ &= -4m(-1)^{m-1} + \sum_{j=0}^{m-1} \binom{2m-2-j}{j} (-4)^{m-1-j} \\ &= -4m(-1)^{m-1} + (2m-1)(-1)^{m-1} = (-2m-1)(-1)^{m-1} = (2m+1)(-1)^m. \end{aligned} \quad (\text{C.16})$$

That is, if identity (C.8) is true for  $m$  then it is also true for  $m + 1$ .

Next we consider the expression

$$\sum_{k=0}^m \binom{2m+1-k}{k} (-4)^{m-k}. \quad (\text{C.17})$$

Assuming the identities (C.12) and (C.13) are true, we obtain

$$\begin{aligned} & \sum_{k=0}^m \binom{2m+1-k}{k} (-4)^{m-k} \\ &= (2m+1)(-1)^m + \sum_{k=0}^m \binom{2m+1-k}{k} (-4)^{m-k} - \sum_{k=0}^m \binom{2m-k}{k} (-4)^{m-k} \\ &= (2m+1)(-1)^m + \sum_{k=0}^m \left\{ \binom{2m+1-k}{k} - \binom{2m-k}{k} \right\} (-4)^{m-k} \\ &= (2m+1)(-1)^m + \sum_{k=1}^m \left\{ \binom{2m+1-k}{k} - \binom{2m-k}{k} \right\} (-4)^{m-k}. \end{aligned} \quad (\text{C.18})$$

By means of Pascal's rule, it is further reduced to

$$\begin{aligned} & \sum_{k=0}^m \binom{2m+1-k}{k} (-4)^{m-k} = (2m+1)(-1)^m + \sum_{k=1}^m \binom{2m-k}{k-1} (-4)^{m-k} \\ &= (2m+1)(-1)^m + \sum_{j=0}^{m-1} \binom{2m-1-j}{j} (-4)^{m-1-j} \\ &= (2m+1)(-1)^m + m(-1)^{m-1} = (2m+1)(-1)^m - m(-1)^m = (m+1)(-1)^m. \end{aligned} \quad (\text{C.19})$$

That is, if identity (C.12) is true for  $m$  then it is also true for  $m + 1$ . This completes the proof.

## Appendix D

### A Hénon eigenvalue inequality

The goal is to show for  $4a > -(1-b)^2$  that  $\lambda_4 > 1$ , where

$$\lambda_4 = -aL_- + \sqrt{a^2L_-^2 + b}, \quad (\text{D.1})$$

and

$$L_- = \frac{b-1 - \sqrt{(1-b)^2 + 4a}}{2a}. \quad (\text{D.2})$$

By means of  $w := \sqrt{(1-b)^2 + 4a}$  the latter equation can be written as

$$2aL_- = b-1-w. \quad (\text{D.3})$$

For  $\lambda_4$  we then obtain

$$\begin{aligned} 2\lambda_4 &= -2aL_- + \sqrt{4a^2L_-^2 + 4b} \\ &= 1-b+w + \sqrt{(1-b+w)^2 + 4b} \\ &= 1-b+w + \sqrt{(1-b)^2 + 2(1-b)w + w^2 + 4b} \\ &= 1-b+w + \sqrt{(1+b)^2 + 2(1-b)w + w^2} \\ &= 1-b+w + \sqrt{(1+b)^2 - 2bw + 2w + w^2} \\ &= 1-b+w + \sqrt{(1+b)^2 - 2(1+b)w + 4w + w^2} \\ &= 1-b+w + \sqrt{(1+b-w)^2 + 4w}. \end{aligned} \quad (\text{D.4})$$

For  $4a > -(1-b)^2$  we have  $w > 0$ . As a consequence

$$\begin{aligned} 2\lambda_4 &> 1-b+w + \sqrt{(1+b-w)^2} \\ 2\lambda_4 &> 1-b+w + 1+b-w \\ 2\lambda_4 &> 2 \\ \lambda_4 &> 1. \end{aligned} \quad (\text{D.5})$$

This completes the proof.



# Bibliography

- [1] A. J. Lotka, Analytical Note on Certain Rhythmic Relations in Organic Systems, Proc. Natl. Acad. Sci. USA, **6**, 410-415 (1920)
- [2] V. Volterra, Variazioni e fluttuazioni del numero d'individui in specie animali conviventi, Mem. Acad. Lincei Roma, **2**, 31-113 (1926)
- [3] W. Tucker, *In search for the Hénon attractor*,  
[https://www.math.uu.se/digitalAssets/562/c\\_562622-1\\_1k\\_tucker\\_slides.pdf](https://www.math.uu.se/digitalAssets/562/c_562622-1_1k_tucker_slides.pdf)
- [4] D. Cross, *Algebraic solution of mandelbrot orbital boundaries*,  
[http://cosinekitty.com/mandel\\_orbits\\_analysis.html](http://cosinekitty.com/mandel_orbits_analysis.html)
- [5] N.J.A. Sloane, *The Online Encyclopedia of Integer Sequences*,  
<https://oeis.org>
- [6] M. Markus and B. Hess, Lyapunov exponents of the logistic map with periodic forcing, *Comput. and Graphics*, **13**, 553-558 (1989)
- [7] M. Markus, Chaos in Maps with Continuous and Discontinuous Maxima, *Comput. in Phys.*, 481-493, (1990)
- [8] H.K. Sarmah and T.K. Baishya, Period Doubling Route in the Periodic and Chaotic region of the Logistic Map, *Int. J. Appl. Math. Stat. Sci.*, **2**, 49-62, (2013)